

# Non-contact Methods for Detecting Hot-mix Asphalt Nonuniformity

Edgar David de León Izeppi

Dissertation submitted to the faculty of the Virginia Polytechnic Institute and State  
University in partial fulfillment of the requirements for the degree of

Doctor of Philosophy  
In  
Civil and Environmental Engineering

Gerardo W. Flintsch, Chairman  
A. Lynn Abbott  
Imad L. Al-Qadi  
Amara Loulizi  
Dusan Teodorovic

September 21, 2006  
Blacksburg, Virginia

Keywords: hot-mix asphalt, quality assurance, segregation, macrotexture, digital imaging

# Non-contact Methods for Detecting Hot-mix Asphalt Nonuniformity

Edgar David de León Izeppi

## ABSTRACT

Segregation, or non-uniformity, in Hot Mix Asphalt (HMA) induces accelerated pavement distress(es) that can reduce a pavement's service life up to 50%. Quality Assurance procedures should detect and quantify the presence of this problem in newly constructed pavements. Current practices are usually based on visual inspections that identify non-uniform surface texture areas. An automatic process that reduces subjectivity would improve the quality-assurance procedures of HMA pavements.

Virginia has undertaken a focused research effort to improve the uniformity of hot-mix asphalt (HMA) pavements. A method using a dynamic (laser-based) surface macrotexture instrument showed great promise, but it revealed that it may actually miss significant segregated areas because they only measure very thin longitudinal lines. The main objective of this research is to develop a non-contact system for the detection of segregated HMA areas and for the identification of the locations of these areas along a road for HMA quality assurance purposes.

The developed system uses relatively low cost components and innovative image processing and analysis software. It computes the gray level co-occurrence matrix (GLCM) of images of newly constructed pavements to find various parameters that are commonly used in visual texture analysis. Using principal component analysis to integrate multivariable data into a single classifier, Hotelling's  $T^2$  statistic, the system then creates a list of the location of possible nonuniformities that require closer inspection.

Field evaluations of the system at the Virginia Smart Road proved that it is capable of discriminating between different pavement surfaces. Verification of the system was conducted through a series of field tests to evaluate the uniformity of newly constructed pavements. A total of 18 continuous road segments of recently paved roads were tested and analyzed with the system. Tables and plots to be used by inspection personnel in the field were developed. The results of these field tests confirmed the capability of the system to detect potential nonuniformities of recently completed pavements. The system proved its potential as a useful tool in the final inspection process.

## ACKNOWLEDGMENTS

I would like to acknowledge the assistance of all the members of my committee, Gerardo Flintsch, Lynn Abbott, Imad Al-Qadi, Amara Loulizi, and Dusan Teodorovic, in helping me to complete this dissertation. The role that my advisor, Gerardo Flintsch, has played in this stage of my life is invaluable. He has always provided me with all the support and encouragement that I have needed allowing me to complete my doctoral studies. Lynn Abbott gave me the opportunity to embark in this adventure with knowledge that goes far beyond the scope of the normal Civil Engineering studies I have acquired, allowing me to find an innovative approach into the inspection of asphalt pavements. Imad Al-Qadi and Dusan Teodorovic will always be appreciated for their wise advice and lessons given in the classrooms that I will undoubtedly put to practice in my professional work. Finally, Amara Loulizi, more than a colleague, was a friend and an unconditional source of information in times of despair, helping me solve all kinds of problems. I feel I am indebted to all of you for helping me finish this adventure.

I would also like to express my deepest gratitude to Samer Lahouar, whose programming expertise proved invaluable with the frame grabber software used to acquire all of the digital images used in my research. I will never forget all our adventures collecting data on the roads in Virginia, where the ideas for this dissertation started. I am now proud to say those ideas have been completed and have resulted in this work.

Thanks also to all the members of the Road Infrastructure Group, past and present, that I have had the pleasure of sharing my time with this second time around at Virginia Tech. I will always remember you as part of my big Hokie family. I will never forget the times we had together. Special thanks are also due to all the members of the Virginia Tech Transportation Institute who participated with their special skills in the implementation of hardware for the vehicle used in this research.

Finally, this dissertation is dedicated to my family, my friends, Guatemala, and to my new home, the Commonwealth of Virginia.

## TABLE OF CONTENTS

<b>Acknowledgments</b>	<b>iii</b>
<b>List of Tables</b>	<b>vii</b>
<b>List of Figures</b>	<b>viii</b>

### Introduction

BACKGROUND	1
The origins of Road Construction	1
Hot-mix Asphalt (HMA) Road Construction	2
Hot-mix Asphalt (HMA) Segregation	2
Types of Segregation	2
Measuring and Detecting Segregation	3
DISSERTATION OVERVIEW	4
Problem Statement	4
Research Objectives	4
Organization of the Dissertation	4
Expected Results and Significance	6
REFERENCES	6

### Pavement Surface Macrotexture Measurement and Applications

ABSTRACT	8
INTRODUCTION	8
PAVEMENT SURFACE TEXTURE	9
Macrotexture Measurements	9
Microtexture Measurements	10
MACROTEXTURE MEASUREMENTS CORRELATION	10
CTMeter versus Sand Patch Correlation	11
Laser Profiler versus Sand Patch Correlation	11
EFFECT OF PAVEMENT MACROTEXTURE ON SKID RESISTANCE	11
International Friction Index	11
IFI Speed Constant Equation Validation	13
MACROTEXTURE FOR HMA SEGREGATION DETECTION AND MEASUREMENT	13
SUMMARY AND CONCLUSIONS	15
ACKNOWLEDGEMENTS	15
REFERENCES	15

## **Field Validation of Macrotexture-Based Hot-Mix Asphalt Segregation Detection Methods**

Abstract	30
Introduction	31
<i>Use of Macrotexture to Detect and Measure Segregation</i>	32
<i>Prediction of Non-segregated Macrotexture</i>	32
<i>NCHRP 441 Model</i>	32
<i>Alternative Model</i>	33
PURPOSE AND SCOPE	34
METHODS	34
<i>Field Data Collection</i>	35
<i>Predicting Non-segregated/Target Pavement Surface Texture</i>	37
FINDINGS AND DISCUSSION	38
<i>Field HMA Properties</i>	38
<i>Relating Macrotexture to Traditional Measures of Segregation</i>	41
<i>Macrotexture Measurements</i>	42
CONCLUSIONS AND RECOMMENDATIONS	49
REFERENCES	50

## **Measuring the Uniformity of Hot Mix Asphalt Pavements with Digital Image Technology**

ABSTRACT	53
INTRODUCTION	54
OBJECTIVE	54
COMPUTER VISION	54
SYSTEM FRAMEWORK	55
Hardware Design	55
Digital Images	57
Image Processing	59
Image Analysis	59
FIELD TESTING	62
CONCLUSIONS AND RECOMMENDATIONS	65
REFERENCES	66

## **Application of Digital Image Technology to Measure Hot Mix Asphalt Homogeneity**

Abstract	67
Introduction	68
<i>Background</i>	68
<i>Problem Statement</i>	69
<i>Approach</i>	69
<i>Objectives and Scope</i>	70
Methods	70

<i>Visual Texture Analysis Results</i>	70
<i>Principal Component Analysis</i>	71
<i>Visualizing the Results of the Principal Component Analysis</i>	72
<i>Hotelling's <math>T^2</math> Statistic</i>	73
<i>Uniformity Profile with Hotelling's <math>T^2</math> Statistic</i>	74
FINDINGS AND DISCUSSION	76
CONCLUSIONS AND RECOMMENDATIONS	80
REFERENCES	81

## **High-Speed, Noncontact Digital Imaging System for Inspection of Hot-Mix Asphalt Pavements**

Abstract	82
Introduction	83
Objective	84
System Design	84
<i>Hardware</i>	84
<i>Images Processing and Analysis</i>	84
<i>Principal Component Analysis</i>	86
<i>Visualization of the Results of the Principal Component Analysis</i>	86
<i>Hotelling's <math>T^2</math> Statistic</i>	86
<i>System Validation</i>	87
System Verification	88
<i>Continuous and Homogenous Road Segments</i>	88
<i>Effect of Traffic</i>	89
<i>Different Quality Control Procedures and the Dispersion of Non-uniformities</i>	89
Conclusions and Recommendations	90
REFERENCES	91

## **Summary, Findings, Conclusions and Recommendations for Future Research**

FINDINGS	103
CONCLUSIONS	103
RECOMMENDATIONS AND SUGGESTIONS FOR FUTURE RESEARCH	104
<b>Appendix A</b> Hotelling's $T^2$ Plots	105
<b>Appendix B</b> Scatter Plots of PCA components in 2-D	132

## LIST OF TABLES

### **Pavement Surface Macrotexture Measurement and Applications**

List of Tables and Figures	18
TABLE 1. Texture Classifications	19
TABLE 2. Laboratory Measured Properties of the Wearing Surface HMA	20

### **Field Validation of Macrotexture-Based Hot-Mix Asphalt Segregation Detection Methods**

TABLE 1. Average Non-Segregated HMA Aggregate Properties	39
TABLE 2. Average Non-Segregated HMA Volumetric Properties	39
TABLE 3. Extreme Mix Properties and Expected Levels of Segregation	40
TABLE 4. Segregation Level Distribution (%) on the Left Wheel Path (LWP)	46
TABLE 5. Segregation Level Distribution (%) on the Lane Center (BWP)	47

### **Measuring the Uniformity of Hot Mix Asphalt Pavements with Digital Image Technology**

TABLE 1. Smart Road Mix Types	63
-------------------------------	----

### **Application of Digital Image Technology to Measure Hot Mix Asphalt Homogeneity**

TABLE 1. Principal component coefficients and % variability	72
TABLE 2. Hotelling's $T^2$ statistical data with location	74

### **High-Speed, Noncontact Digital Imaging System for Inspection of Hot-Mix Asphalt Pavements**

Table 1. Paving Sites Analyzed	92
Table 2. Location of significant visual difference	93

### **Summary, Finding, Conclusions and Recommendations for Future Research**

Table 1. Paving Sites Analyzed	102
--------------------------------	-----

## LIST OF FIGURES

### **Pavement Surface Macrotexture Measurement and Applications**

FIGURE 1. Microtexture and Macrotexture Illustration	21
FIGURE 2. Schematic of Mean Profile Depth Computation	22
FIGURE 3. Circular Track Meter and Sand Patch Correlation	23
FIGURE 4. Sand Patch and Laser Macrotexture Correlation	24
FIGURE 5. Example of Frictional Properties of Surfaces with Various Degrees of Friction and Macrotexture	25
FIGURE 6. Macrotexture Measurements (ICCTEX) for all Sections (a) Instrumented Lane, (b) Non-Instrumented Lane	26
FIGURE 7. Variation of the Average Percent Normalized Gradient over Time (a) Smooth Tire, (b) Ribbed Tire	27
FIGURE 8. Sp (100/PNG) - Macrotexture Relationship	28
FIGURE 9. Measured versus Predicted Macrotexture (NCHRP 441 Model)	29

### **Field Validation of Macrotexture-Based Hot-Mix Asphalt Segregation Detection Methods**

Figure 1. Test Site Layout	36
Figure 2. Example of (a) Non-segregated and (b) Segregated Areas (project 02-1079)	40
Figure 3. Correlation of Macrotexture with Asphalt Content	41
Figure 4. Correlation of Macrotexture with Voids in the Total Mix	42
Figure 5. Correlation of Macrotexture Measurements with (a) AC Content (Pb %), (b) Voids in the Total Mix (VTM) and (c) Voids in the Mineral Aggregate (VMA)	43
Figure 6. Example Segregation Analysis Using NCHRP 441 Model with (a) Converted ICCTEC Data and (b) Converted CTM Data	44
Figure 7. Example Segregation Analysis Using Alternative Model	45
Figure 8. Example Segregation Analysis for a Coarse 25.0-mm Mix (Project 02-1026)	48
Figure 9. Example Segregation Analysis for a Fine 9.5-mm Mix (Project 02-1043)	49

### **Measuring the Uniformity of Hot Mix Asphalt Pavements with Digital Image Technology**

FIGURE 1. GPR-Digital Imaging System	55
FIGURE 2. Shadows and Illumination Problems	56
FIGURE 3. Different lenses available for tests	57
FIGURE 4. Example of True Color, Bayer 8 Indexed, and Grayscale Digital Images	58
FIGURE 5. Raw image pixel values and processed pixel values resulting from interpolations	60
FIGURE 6. Un-segregated and segregated pavements	61
FIGURE 7. Smart Road Profiler Texture Plot	64



## **Application of Digital Image Technology to Measure Hot Mix Asphalt Homogeneity**

FIGURE 1. GLCM Plot for Project 11-06-19	71
FIGURE 2. Two dimensional principal component data plot	73
FIGURE 3. Non-uniformity plot at different confidence levels	75
FIGURE 4. System image captured at night, station 760	76
FIGURE 5. Day image captured during inspection, station 760	77
FIGURE 6. Day images of Non-uniform area	78
FIGURE 7. Station 2900 night image	79
FIGURE 8. Station 2900 day picture	79

## **High-Speed, Noncontact Digital Imaging System for Inspection of Hot-Mix Asphalt Pavements**

Figure 1. System framework and sample image	94
Figure 2. Hotelling's $T^2$ plots for Project SM East a) complete and b) paved segment only	95
Figure 3. Highest $T^2$ locations in SM East (all)	96
Figure 4. Images from intersections and adjacent dirt lots	97
Figure 5. Combined scatter 2-D principal component plot for Projects 3 and 7	98
Figure 6. Hotelling's $T^2$ plots for Projects 3 and 7	99
Figure 7. Examples of non-uniformities from Project 7 (nighttime)	100
Figure 8. Examples of non-uniformities from Project 7 (daytime)	101

# Introduction

## BACKGROUND

### The origins of Road Construction

Roads have been built since man started to have a repetitive need to travel between two places. Hunting would not qualify in this category of travel need because it did not have a consistent direction. The origin of roads can be traced back to the beginnings of the Bronze Age, when man developed the necessary tools that allowed early civilizations to flourish. With these tools, permanent dwellings developed. The tools and permanent dwellings also permitted the invention of agriculture, which allowed man to grow the crops he needed to feed his family and became sedentary. Shortly after, road constructions must have started when man had to travel repetitively to marketplaces for trading purposes.

Two other events further increased road construction efforts: the invention of the wheel and the domestication of the horse. Horse-pulled carts created a need for roads with uniform hard surfaces. The heavy concentrated loads of the carts destroyed roads faster wherever the underlying materials could not support them. In order to improve the paths used until then, the ground on the surface was first leveled and any holes still present, filled. To prevent the damage caused by rain and ground moisture, extra soil materials were obtained by digging ditches on the sides of the road and used to raise the level of the road by putting it in the center. Hence the name “highway”, or higher road, came to exist. Credit for starting this process of artificial road building for men travel needs is given to the Sumerians somewhere in Mesopotamia around 3,000 BC (1).

After this, there is ample evidence of other civilizations that built road systems in their empires, i.e. in India, Egypt, Persia, South America, etc. Their methods varied and evidence of these older roads still remains. However, because of the excellence and durability of their roads, a product of the methods and materials employed, it has been recognized that the first scientific road builders were the Romans (2). They established a system of stone-paved highways primarily for military and administrative use, but open to all kinds of traffic, which separates them from previous civilizations that usually restricted their use for state-only purposes. Their use of surveying instruments and the refined construction techniques separate them from the other civilizations. Since then, road construction has evolved tremendously, and after the 19th century, it could be argued that it parallels economic development in industrialized countries (3).

Unfortunately, roads are built on top of soils that are composed of many different materials and have been exposed to different weather effects and telluric movements throughout the ages. This creates non-uniform conditions that affect the final pavement structure. Even with recent advances achieved by geotechnical engineers to determine the behavior of soils, there is still a very limited knowledge of soil conditions on road projects because they are usually designed based on a small sample of these soils along the length of the road. Furthermore, practical construction and economic considerations do not allow design changes every time soil conditions change, so variability is an imbedded inherent factor in the road building process.

## Hot-mix Asphalt (HMA) Road Construction

Modern life made our travel and freight patterns dependant on roads, which now have to provide not only an appropriate travel surface under all-weather conditions, but also one that meets the safety and comfort expectations of the users. For this reason, road engineers are constantly devising ways to improve road construction. Some of the early improvements included the use of asphalt and concrete as construction materials. For example, Hot Mix Asphalt (HMA) pavements are designed considering a myriad of different factors, such as environmental conditions, amount of traffic and the magnitude of their load, specific characteristics of the available materials, and local construction practices, among others. These factors combine to introduce a series of elaborate intricacies that add to the non-uniform conditions that are involved in road construction.

Road building is now one of the largest construction industries in the world. As such, its construction methods have evolved during the years but the ultimate goal is still to build roads that are durable, safe, comfortable, adequately drained, etc. To achieve this, the industry is constantly improving the construction methods, testing new materials, implementing high quality controls in their operations, and complying with the specifications required in the contracting documents. Agencies, on the other hand, make sure that contractors deliver the specified quality of the roads through quality assurance procedures that are verified in the field through rigorous inspections.

## Hot-mix Asphalt (HMA) Segregation

Road construction methods involve many potential variability sources that could result in an unacceptable end product quality. This variability found in the production of HMA is responsible for creating segregation. Segregation is found if the HMA constituents present signs of non-uniformity in the in-place constituents. It is a serious problem because it leads to accelerated pavement distress(es) (4). According to the Asphalt Institute: "...of a number of potentially damaging problems that can occur in the design, production and placement of hot mix paving mixtures...perhaps the most serious is segregation"(5). A segregated mix does not conform to the original job-mix formula in gradation and/or asphalt content. This nonconformity affects the density and air void content of the mix. The resulting non-uniform composition of aggregates, asphalt binder, and/or air voids results in uneven aggregate distribution in the surface.

Many studies and agencies have tried to develop reliable and independent methods to define, detect, and quantify segregation, but none have eliminated the need for the visual inspections. The reduction in pavement performance life due to segregation can be up to 50% (6, 7). Considering that the industry produces more than 500 million tons of asphalt a year (8), great savings could be expected if more accurate means to detect segregation problems could be developed.

## Types of Segregation

A recent study (4) identified three different types of HMA segregation: Gradation Segregation, Temperature Segregation and Asphalt-Aggregate Segregation. Gradation Segregation is the non-uniform distribution of coarse and fine aggregate materials in the finished HMA mat, which are introduced during HMA production, hauling, and placement operations. Coarse Aggregate Segregation usually has high air voids and low asphalt content, which allow these areas to cool faster. This causes moisture damage, as well as durability-related distresses such as fatigue

cracking, pothole formation and raveling. Fine Aggregate Segregation usually has low air voids and high asphalt content. This makes it susceptible to rutting and flushing.

Temperature segregation, often referred in the literature as temperature differential damage (TDD), is the result of the cooling of portions of the mix that are not compacted satisfactorily when laid down. The difference in temperature introduces the damage to the mix. The cooling down of the mix can be caused for two reasons. The first one happens during the hauling from the plant to the site and the augers are incapable of remixing appropriately on the paver before going through the screed and being laid down. This creates portions of cool mix that can be intermittently incorporated into the paving material creating cooler areas that will not compact adequately resulting in lower density areas with higher air voids.

The second reason for mix cool down happens immediately behind the screed during normal paving operations when a paver is stopped waiting for a haul truck or adjusting its equipment. This portion of the mix in the mat will cool down and the compacting equipment will not be able to compact it properly after the paver moves on, resulting in a localized transversal region of low density.

The introduction of Stone Matrix Asphalt (SMA) mixes from Europe has sprouted a new type of segregation that is being referred as Asphalt-Aggregate Segregation. Because these mixes are very rich in asphalt content, a draindown process of the mix is possible. In this process, the asphalt binder is separated from the aggregates in the mix. It is not specifically associated with any size of aggregate in particular.

#### Measuring and Detecting Segregation

Most state DOT base their segregation detection on visual identification by their construction inspectors, followed by density measurements to define boundaries of the segregated area. Upon its detection and delimitation, the usual action taken is to completely remove and replace the segregated area for the full depth of the course. Sometimes, depending on the nature of the problem, even an overlay is required (9). Since the extra work is to be done at no additional expense to the owner, angry disputes usually spark with contractors.

NCHRP Report 441 (4) investigated state-of-the-art technologies for detecting segregation (visual identification, sand patch texture measurement, and nuclear density gauges) and measuring segregation (permeability, nuclear density/moisture content gauges, and destructive testing). It also investigated the use of new technologies that held promise in this respect, such as infrared thermography, ground penetration radar, thin-lift nuclear asphalt content/density gauges, dynamic (laser-based) surface macrotexture measurement devices, and seismic pavement analyzers. Because infrared thermography can only be used during the laydown process while the mix is hot, this method was recommended for quality control. Macrotexture measurements were recommended for quality assurance purposes.

Recent work performed in Virginia, confirmed that macrotexture measurements could be used for quality assurance purposes after construction is done, preferably before the road is open to traffic. However, the models used to predict non-segregated macrotexture did not worked for all of the projects evaluated, and although this approach holds promise, it was also recommended the

exploration of other approaches, such as the use of digital imaging to identify and quantify segregation (10).

## DISSERTATION OVERVIEW

### Problem statement

Segregation, or non-uniformity, in Hot Mix Asphalt induces accelerated pavement distress(es) that can reduce the pavement service life up to 50%. Therefore, it is imperative to include HMA Quality Assurance procedures that can detect and quantify the presence of this problem in newly constructed pavements. Presently, this is done based on visual inspections that identify these non-uniform surface texture areas. An automatic process that reduces subjectivity is necessary.

### Research objectives

The main objective of this research is to develop a non-contact system for the detection of segregated HMA areas and for the identification of the locations of these areas along a road for HMA quality assurance purposes. The proposed system will use relatively low cost off-the-shelf components for capturing images of new pavements and develop innovative image processing and analysis software for detecting and quantifying segregated areas.

To achieve the objective of this study, an extensive testing plan was planned. The plan would combine preliminary field measurements, hardware and software development, and laboratory and field calibrations, resulting in a novel method to detect and quantify segregation. In order to achieve the main objective of the investigation, the following specific objectives were proposed:

- To evaluate the effectiveness of the dynamic laser-based macrotexture approach to detect and quantify HMA segregation.
- To compare traditional segregation measurements with the dynamic laser-based macrotexture based approach for detecting and measuring segregation.
- To develop a prototype digital imaging system, to capture digital images of finished pavements and apply Image Processing and Analysis Methods to automatically detect changes in the surface textural appearance due to segregation.
- To evaluate preliminary results by testing the system at the Virginia Tech Smart Road with the available different road surfaces.
- To test, calibrate, and validate the system from field experimental data collection and analysis of recently paved projects.

### Organization of the Dissertation

Complying with the Graduate School's guidelines that encourage publication of research results, this dissertation follows a manuscript format which includes five manuscripts. Each manuscript is used as an individual chapter of the dissertation. They represent the research work in which the author was involved at Virginia Tech during the duration of the doctoral studies. The first chapter of the dissertation is this introduction, which provides an outline for the rest of the document. The following five chapters are introduced following.

Chapter 2: *Pavement Surface Macrotexture Measurement and Applications*. This paper, published in the Journal of the Transportation Research Board, No. 1860, by the National Academies in 2,003, contains an extensive literature review covering segregation and the macrotexture based methods used to detect segregation. It also contains the theoretical background and models used by this method as it was developed at the Virginia Smart Road.

Chapter 3: *Field Validation of Macrotexture-Based Hot-Mix Asphalt Segregation Detection Methods*. This paper, published in the 74<sup>th</sup> Journal of the Association of Asphalt Paving Technologists in 2,005, presents a complete review of all the fieldwork performed to test the uniformity of typical VDOT paving mixtures with the models developed in Chapter 2. Although this method showed great promise in controlled experimentations, the results presented several shortcomings in the field. The greatest problem encountered was that profilers measure very thin longitudinal lines and may miss significant segregated areas. To overcome this limitation, a recommendation was made to explore the use of an area based method such as digital image analysis.

Chapter 4: *Measuring the Uniformity of Hot Mix Asphalt Pavements with Digital Image Technology*. Based on the recommendations from chapters 2 and 3, a digital imaging system was developed, including the hardware and software, which was able to identify different pavement surfaces, after testing was performed at the Virginia Smart Road. The system computes the gray-level co-occurrence matrix (GLCM) of each image, to obtain various parameters commonly used in visual texture analysis.

Chapter 5: *Application of Digital Image Technology to Measure Hot Mix Asphalt Homogeneity*. This paper presents an example of the analysis procedure developed for the digital video system that was developed at Virginia Tech to evaluate the uniformity of newly constructed pavements. The methodology developed in chapter 4 was expanded, applying principal component analysis to integrate multi variable data into a single classifier, Hotelling's  $T^2$  statistic, to create a list indicating the location of possible non-uniformities that require closer inspection.

Chapter 6: *High-Speed, Non-Contact Digital Imaging System for Inspection of Hot-Mix Asphalt Pavements*. This paper discusses the use of the new system using digital video images in the inspection of several recently constructed asphalt pavements. The system uses the single classifier presented in chapter 5, to distinguish different pavement textures automatically, providing inspection personnel the exact location of possible non-uniformities that require closer inspection. A total of 18 continuous road segments of recently paved roads were analyzed. More testing is suggested to completely evaluate its capacity under working conditions.

The first two manuscripts represent work where the author was deeply involved in the data analysis and provided the groundwork on which the digital imaging system was developed. A copy of the necessary permissions has been obtained to include each of these chapters. The last three manuscripts constitute the original work and contribution of the author. All of them have recently been submitted for consideration for publication at the time of the defense of this dissertation. They represent the results of the new approach proposed by the author to detect and quantify HMA segregation using an area-based imaging method.

## Expected Results and Significance

This research produced a system that is capable of detecting nonuniformities usually associated with segregated HMA areas through the identification of visual textural properties of captured digital images, with the exact identification of the location of these areas along a road for HMA quality assurance purposes. The use of the system may help improve the quality of the HMA layers and enhance pavement performance of newly paved road work.

Making a conservative estimate, if 1 out of every 1,000 tons (0.1%) of the 500 million tons of asphalt that are placed in this country every year have some degree of segregation that could be detected with the proposed system, significant savings ( $\pm$ \$15 million, assuming \$30/ton) in direct mix costs could be achieved. In addition, there would be even higher savings because of the extension of the pavement service life and the consequent reductions in down time and repair work that could result from the reduction of the segregation problem.

## REFERENCES

- 1) Hindley, Geoffrey. *A History of Roads*. The Chaucer Press, London, 1971.
- 2) Rose, Albert. *Public Roads of the Past*. American Association of State Highway Officials, Washington, D.C., 1952.
- 3) Hudson, Ronald, Haas, Ralph, and Uddin, Waheed. *Infrastructure Management*. McGraw-Hill, New York, 1997.
- 4) Stroup-Gardiner, M. and E. R. Brown. *NCHRP Report 441, Segregation of Hot-Mix Asphalt Pavements*. TRB, National Research Council. Washington, DC, 2000.
- 5) Sherockman, J. *Segregation: causes and cures*. Asphalt Institute/NAPA, Washington, 1997. 25 pp.
- 6) Brock, J.D. and Jakob, H. *Temperature Segregation/Temperature Differential Damage*. Astec Industries, Inc., Technical Paper T-134. Chattanooga, TN, 1996.
- 7) Wilson, R.L. *Commentary on Special Provision Concerning HMAC Segregation*. Texas: Texas Department of Transportation, 1999.
- 8) Acott, Mike. *How the U.S. Asphalt Industry is affected by HS&E Regulations, and how it is responding to SHRP developments*. 2<sup>nd</sup> Eurasphalt & Eurobitume Congress, Barcelona, 2000.
- 9) Information provided by Merrill Zwanka, State Materials Engineer, South Carolina Department of Transportation, June 28, 2002, and Ken Fults from Texas Dot on June 10, 2002.
- 10) McGhee, K.K., Flintsch, G.W., de León, E., “*Using High-Speed Texture Measurement to Improve the Uniformity of Hot-Mix Asphalt*”, VTRC 03-R12, Virginia Transportation Research Council and Federal Highway Administration, May 2003. 23 pp.

# *Pavement Surface Macrotexture Measurement and Applications*

Gerardo W. Flintsch

Assistant Professor, The Via Department of Civil and Environmental Engineering  
Transportation Fellow, Virginia Tech Transportation Institute  
200 Patton Hall, Virginia Polytechnic Institute and State University  
Blacksburg, VA 24061-0105  
voice (540) 231 9748, fax (540) 231 7532  
email: [flintsch@vt.edu](mailto:flintsch@vt.edu)

Edgar de León

Graduate Research Assistant, Virginia Tech Transportation Institute  
3500 Transportation Research Plaza  
Blacksburg, VA 24061-0105  
voice (540) 231 1568, fax (540) 231 1555  
email: [edeleoni@vt.edu](mailto:edeleoni@vt.edu)

Kevin K. McGhee

Senior Research Scientist, Virginia Transportation Research Council  
530 Edgemont Road  
Charlottesville, VA 22903  
voice (434) 293-1956, fax (434) 293-1990  
email: [McGheeKK@vdot.state.va.us](mailto:McGheeKK@vdot.state.va.us)

Imad L. Al-Qadi

Charles E. Via, Jr., Professor of Civil and Environmental Engineering  
Leader, Roadway Infrastructure Group, Virginia Tech Transportation Institute  
200 Patton Hall, Virginia Polytechnic Institute and State University  
Blacksburg, VA 24061-0105  
voice (540) 231 5262, fax (540) 231 7532  
email: [alqadi@vt.edu](mailto:alqadi@vt.edu)

**Virginia Tech Transportation Institute**

**Virginia Tech**

**Blacksburg, VA**



# Pavement Surface Macrotexture Measurement and Applications

## ABSTRACT

Different techniques for measuring pavement surface macrotexture and their application in pavement management are discussed. The main applications of surface macrotexture are to measure the frictional properties of the pavement surface and to detect hot mix asphalt (HMA) construction segregation or non-uniformity. Since surface macrotexture can be measured quite efficiently using non-contact technologies and provides important information regarding pavement safety and HMA construction quality, this parameter may be included in the quality assurance or control procedures.

Correlations between different measuring devices were investigated utilizing different HMA wearing surfaces. Excellent correlation was found between the CTMeter and the sand patch measurements. In addition, the macrotexture determined using a laser profiler correlates well with the sand patch measurements.

Consistent with previous studies, it was found that the skid number gradient with speed is inversely proportional to the pavement macrotexture. However, there was a noticeable difference in speed dependency when smooth and ribbed tires were used. Oscillations in the percent normalized gradient with time due to seasonal variations were also observed.

Macrotexture measurements hold great promise as tools to detect and quantify segregation for quality assurance purposes. A standard construction specification has been proposed in a recent NCHRP study. However, the equation proposed for computing the non-segregated ETD could not be applied to the mixes studied. An alternative equation has been proposed, which estimates the surface macrotexture using the mix nominal maximum size and voids in the mineral aggregate. The study was based on the mixes used at the Virginia Smart Road. Further investigation using other mixes is recommended.

## INTRODUCTION

The current trend towards mechanistic flexible pavement design and analysis procedures has placed a great deal of emphasis on integrated pavement and hot-mix-asphalt (HMA) systems design. Within this scheme, HMA is designed to be strong and resilient to withstand traffic and environmental conditions expected for a particular roadway section over its design life. Traditional HMA construction quality control and assurance procedures reflect this approach and focus on ensuring the required strength and durability of the material.

Since the main function of the pavement is to provide a safe and smooth ride to the drivers, or “clients” of the facility, functional characteristics such as ride quality, safety, and noise must also be optimized, especially for the wearing surface mixes. Construction specifications for smoothness have been implemented by several states (1, 2). HMA safety-related texture and skid properties are not yet quantitatively included in most specifications. Since surface macrotexture can be measured quite efficiently using non-contact technologies and since it provides important information regarding pavement safety and HMA construction quality (uniformity), this parameter could be efficiently included in the quality control procedures.

Several authors have discussed the incorporation of pavement-related safety considerations into the pavement management process. Tighe et al. (3) identified the main pavement engineering relationships associated with road safety and related to pavement management. Researchers also proposed a systematic approach for coordinating pavement maintenance programs with road safety improvements. This integration has recently proved more important with the advent of the transportation asset management philosophy. The two most promising applications of surface macrotexture measurements include pavement safety assessment and segregation detection.

Surface macrotexture is a predominant contributor to wet-pavement safety (4, 5). The safety of a pavement surface is related to both the surface friction and texture of the pavement. It is imperative that pavement surfaces provide adequate friction and drainage ability to minimize the number of accidents that occur as a result of frictional deficiencies. These frictional properties of pavement surfaces are determined by the surface condition (porosity, wear, etc.), HMA properties (aggregate type and gradation), and environmental conditions (6, 7). Designing and maintaining HMA wearing surfaces that provide adequate skid resistance and texture may decrease wet weather accidents.

Continuous macrotexture measurements can also be used to detect HMA construction segregation or non-uniformity (8). Traditionally, visually identified areas of non-uniform surface texture have been subjectively classified as segregated mix and, consequently, bad construction. The result has been disputes between contractors and highway agencies. Many studies have attempted to develop reliable and independent methods to define, detect, and quantify segregation, but none have eliminated the need for visual inspections prior to measuring the identified areas. An objective quantitative macrotexture-based method has been proposed (8).

The different techniques for measuring pavement surface macrotexture and its application in pavement management are discussed. Also presented are correlations between different macrotexture measuring devices utilizing different HMA wearing surfaces at the Virginia Smart Road. The effect of macrotexture on skid resistance and the possibility of predicting “non-segregated” macrotexture based on HMA design and production properties are investigated.

## **PAVEMENT SURFACE TEXTURE**

Pavement surface characteristics are important for both the safety and comfort of drivers. Pavement surfaces should provide adequate friction and maintain a good level of ride quality to ensure satisfaction of the driving public. The combination of good friction, low levels of roughness, and low levels of noise is important in the design of a pavement wearing surface.

Pavement texture is the feature of the road surface that ultimately determines most tire-road interactions such as wet friction, noise, splash and spray, rolling resistance, and tire wear. Pavement texture has been categorized into three ranges based on the wavelength of its components: microtexture, macrotexture, and megatexture (Table 1). Wavelengths longer than the upper limit of megatexture are defined as roughness, smoothness, or evenness (9).

The resistance to skidding on a road surface is largely affected by both microtexture and macrotexture. Figure 1 illustrates the two concepts. Pavement macrotexture provides the hysteresis component of the friction and allows for the rapid drainage of water from the pavement. Enhanced drainage improves the contact between the tire and the pavement surface and helps reduce the probability of hydroplaning. Microtexture provides direct tire-pavement contact and contributes to the adhesion component of the friction (9).

Increasing the texture of in-service or new pavement surfaces would increase the skid resistance levels of the pavement. This increased texture may sometimes increase the level of discomfort for vehicle occupants and adjacent property owners because of increased interior and exterior noise, vibration, fuel consumption, and tire wear (10). However, the negative aspects of increasing pavement friction are outweighed by the potential decrease in the number of accidents due to inadequate pavement friction (11).

### **Macrotexture Measurements**

The macrotexture of a pavement surface results from the large aggregate particles in the mixture. A detailed list of different devices currently in use for measuring pavement surface texture is provided elsewhere (9). Macrotexture measurements can be divided into two main classes: static measurements and dynamic measurements. Common static macrotexture measurement methods include the sand patch method, the outflow meter, and the circular texture meter (CTMeter). The sand patch method, ASTM E-

965, is a volumetric approach of measuring pavement macrotexture. A known volume of sand (or glass beads) is spread properly on a pavement surface to form a circle, thus filling the surface voids up with sand. The diameter of the circle on which the sand material has been spread is measured and used to calculate Mean Texture Depth (MTD). Because of operator dependency, the test results have poor repeatability (9). This volumetric test is still used as the reference ground-truth standard throughout the word because of the availability of significant earlier research results.

The outflow meter indirectly estimates pavement texture based on the time for a fixed volume of water to escape from a measured cylinder with a rubber bottom. The CTMeter has a laser displacement sensor mounted on an arm that rotates on a circumference with a 142-mm radius and measures the texture with a sampling interval of approximately 0.9mm.

Vehicle-mounted laser devices are typically used to measure macrotexture without disrupting traffic flow. A standard method for determining the mean profile depth (MPD) of the pavement macrotexture from a pavement profile is provided in ASTM Standard E-1845. The MPD is a two-dimensional estimate of the three-dimensional MTD. Some equipment manufacturers also use the Root Mean Square (RMS) of the profile after filtering to remove wavelengths longer than 100 mm. However, area-based measures, such as the MPD, correlate better with the volumetric patch method and with friction (12).

According to ASTM E-1845, the measured profile of the pavement macrotexture is divided for analysis purposes into segments, each having a base-length of 100 mm. The slope, if any, of each segment is suppressed by subtracting a linear regression of the segment. The segment is divided in half and the highest peak in each half segment is determined. The difference between the resulting height and the average level of the segment is calculated for each half segment and the average of both halves computed. The average peak value of both segments is reported as MPD (Figure 2). When MPD is used to estimate the MTD by means of a transformation equation, the computed value is called estimated (mean) texture depth (ETD).

### **Microtexture Measurements**

Microtexture is defined as a surface-roughness quality on the sub-visible or microscopic level. A function of the aggregate particle properties, microtexture is not measured directly in the field. Microtexture levels are commonly estimated using low-speed friction measurement devices such as the British Portable Tester (BPT), the Dynamic Friction Tester (DF Tester), and the locked wheel skid trailer when testing is performed at low speeds (13). Earlier research indicated that skid trailer measurements conducted using a ribbed tire (ASTM E-501) are more sensitive to the microtexture properties of the pavement surface than to macrotexture; thus, they are good estimators of pavement microtexture (14).

### **MACROTEXTURE MEASUREMENTS CORRELATION**

Two laser macrotexture measuring devices owned by the Virginia Transportation Research Council (VTRC) were compared and referenced to ground-truth sand patch tests. The laser devices evaluated include a CTMeter (manufactured by Sunny Koken) and a laser inertial road profiler (manufactured by the International Cybernetics Corporation).

All the measurements were conducted at the Virginia Smart Road, which is a controlled traffic facility with seven different HMA wearing surfaces. These wearing surfaces include different Superpave mixtures, a 12.5-mm stone mastic asphalt (SMA), and a 12.5-mm open-graded friction course (OGFC). Limited tests were also conducted on a texturized, continuously reinforced concrete section. Measurements were taken the same day at three locations within each section studied both in the left wheel path and in-between wheel paths. The profiler was run three times for each lane and the average macrotexture (ICCTEX) for a 1.5m (5ft) section centered on the selected location was used for the

comparisons. The average of the three runs was used to partially compensate for lateral variability. Sand patch tests (using Ottawa sand) were conducted after the CTMeter measurements in the same location.

### **CTMeter versus Sand Patch Correlation**

The correlation between the CTMeter and the sand patch measurements was excellent, as shown in Figure 3. Using all points, an almost one-to-one relationship was obtained with a coefficient of determination ( $R^2$ ) of 0.943. These results are consistent with those reported elsewhere (15), and indicate that the sand patch test can be substituted by the more objective CTMeter test with a high degree of accuracy.

### **Laser Profiler versus Sand Patch Correlation**

Figure 4 compares the measurements taken with the laser profiler to those taken with the sand patch tests. Both linear and exponential regression equations are superimposed to the experimental data. The linear equation indicates a slightly weaker correlation ( $R^2=0.884$ ) than in the case of the CTMeter. Figure 4a indicates that the relationship may be different from the one used by ASTM E-1845, which is as follows:

$$ETD = 0.2 + 0.8MPD \quad (1)$$

Equation 1 is formed by rounding the relationship obtained from comparing the equations used in the International Friction Index (IFI) (13) to compute the speed constant ( $S_p$ ). Equation 2 is obtained by combining the  $S_p$  equations using MPD and MTD:

$$ETD = 0.227 + 0.79MPD \quad (2)$$

The relationship obtained in this study is approximately parallel to that used in ASTM E-1845, which may indicate a possible bias in the laser profiler used for this investigation. The discrepancy could also be due to possible differences in the algorithm used to compute the MPD between the profiler used for this study and that used in ASTM E-1845. Furthermore, some researchers believe that macrotexture measurements on open graded surfaces are questionable because the laser profiler cannot detect some of the voids that are filled with sand. The placement on the chart of the different surfaces studied is displayed graphically in Figure 4b.

## **EFFECT OF PAVEMENT MACROTEXTURE ON SKID RESISTANCE**

The effect of pavement texture on pavement skid resistance was reported on in early skid resistance studies (16-18). The complete frictional characteristics of the road can be found if both the microtexture and macrotexture are known. It was established early that good microtexture is important at low speeds and good macrotexture is important at high speeds (19). However, some researchers believe that the microtexture of the aggregate is important at all speeds (20). The effect of texture on water drainage into the pavement-tire contact and its effect on skid resistance and hydroplaning are discussed elsewhere (21).

### **International Friction Index**

The recently proposed IFI formally incorporates pavement macrotexture. The IFI was developed as a common reference scale for quantifying the pavement surface frictional properties (13). To calculate the IFI, it is necessary to have at least one friction measurement and one macrotexture measurement. The IFI is reported in two parameters: the normalized wet friction value at 60 km/h ( $F_{60}$ ) and a speed constant ( $S_p$ ). A transformation equation has also been established to allow for calculation of the wet friction value at speeds other than 60 km/h.

The importance of good macrotexture is depicted in Figure 5. In addition to reducing the chances of hydroplaning (22), high macrotexture reduces the gradient of skid resistance with speed; thus improving skid resistance at high speeds. This observation implies that the gradient is inversely proportional to the pavement macrotexture. Previous research indicates that the skid number is highly

dependent upon the test speed (14, 23, 24) following the exponential model known as the Penn State University model:

$$SN = SN_0 * e^{\left(\frac{PNG}{100} * v\right)} \quad (3)$$

where

SN = calculated skid number,  
 SN<sub>0</sub> = skid number at zero speed (indicator of microtexture),  
 PNG = percent normalized gradient (indicator of macrotexture), and  
 v = velocity (mph).

Equation 3 was used for developing the IFI speed correction formula, in which the term PNG was replaced by 100/S<sub>p</sub>. Thus, S<sub>p</sub>, which depicts the change of friction with speed, is proportional to macrotexture and can be computed as follows:

$$S_p = a + b * TX \quad (4)$$

where TX is the macrotexture parameter in millimeters and a, b are calibration constants dependent on the method used for determining TX; a=14.2 and b=89.7 if TX is expressed as MPD, according to ASTM E-1845.

The speed at which the friction parameters are measured is adjusted to the required 60 km/h using the speed constant and the measured friction values as follows:

$$FR60 = FRS * e^{\frac{S-60}{S_p}} \quad (5)$$

where,

FR60 = adjusted friction value to 60 km/h,  
 FRS = friction measured by the equipment at the slip speed S,  
 S = slip speed (km/h), and  
 S<sub>p</sub> = speed constant (km/h).

If the measurements are conducted using a ribbed tire, which is relatively insensitive to macrotexture properties of the surface (13), the macrotexture measurement is also used to correct the normalized wet friction value at 60 km/h (F60). The adjusted friction value and the texture measurement are used to calculate the value for F60:

$$F60 = A + B * FR60 + C * TX \quad (6)$$

where

F60 = normalized friction value,  
 A, B, C = calibration constants dependent on measurement equipment used (if ASTM E-274 skid trailer is used: A=0.045, B=0.925, and C=0 for the smooth tire; A= -0.023, B=0.607, and C=0.098 for the ribbed tire),  
 FR60 = Value calculated using Equation 5; and  
 TX = Macrotexture measurement (mm).

## **IFI Speed Constant Equation Validation**

The validity of the relationships between skid number speed gradient and macrotexture was investigated using friction and texture measurements. These tests were conducted over a 3-year period on the seven HMA mixes at the Virginia Smart Road. The effect of testing condition on the relationship was also investigated. The *ICCTEX* of each section was recorded at 3-month intervals. The profiler used estimated macrotexture using an RMS calculation on the filtered high-definition surface profile. Measurements were obtained on the left wheelpath (LWP) and in between wheelpaths (BWP). The macrotexture measurements for all sections throughout the study period are shown in Figure 6. The measurements did not vary significantly over time. The first set of test data was excluded from the following analysis because of some difficulty in distinguishing section breaks in the measurement data.

Skid resistance testing of the different surfaces was also periodically performed on both lanes in both directions. Both ASTM standard tires (ribbed and smooth) were used. Tests were performed at three speeds: 32, 64, and 80km/h. Three replicates in each lane and direction were used for each tire. The Penn State University exponential model coefficients were determined using regression analysis for each section, lane, direction, and testing date. The average  $R^2$  considering all of the experimental data was approximately 0.90.

Changes in the *PNG* (determined using regression analysis) with time are presented in Figure 7. There is a noticeable difference in speed dependency between the two tires. Measurements conducted using the smooth tire show a higher dependency on speed than measurements taken with the ribbed tire. Furthermore, Figure 7 shows oscillations in the *PNG* with time, which are believed to be due to seasonal variations.

Figure 8 shows the measured and computed skid number speed gradients for the Virginia Smart Road HMA mixes. The graph suggests that the coefficients used to compute  $S_p$  based on MPD measurements may not be applicable to the equipment and mixes considered in the study. The lack of agreement could be due to the algorithm used to compute the profiler to compute the macrotexture or to the types of mixes considered. The profiler used in this study does not provide a standard MPD value according to ASTM E-1845. Furthermore, the experimental  $S_p$  is not consistent for the smooth and ribbed tires.

## **MACROTEXTURE FOR HMA SEGREGATION DETECTION AND MEASUREMENT**

The use of macrotexture measurements as a mean to detect and measure HMA construction segregation has been proposed in a National Cooperative Highway Research Program (NCHRP) study (8). Segregation may be defined as a lack of homogeneity (uniformity) in the HMA constituents of the in-place mat of such magnitude that there is reasonable expectation of accelerated pavement distress or distresses. A segregated mix does not conform to the original job mix formula in gradation or asphalt content, or both, which also creates a difference in the expected density and air void content of the mix. Research has shown that when this nonconformity occurs, there is a loss of pavement service life because of diminished stiffness, tensile strength, and fatigue properties, which all result in accelerated pavement distresses such as raveling, longitudinal cracking, fatigue cracking, and rutting (8, 25-27).

The aforementioned study (8) investigated available technologies for detecting segregation (visual identification, sand patch, and nuclear density gauges) and measuring segregation (permeability, nuclear density and moisture content gauges, and destructive testing). Many developing technologies were also evaluated such as infrared thermography, ground penetration radar, thin-lift nuclear asphalt content and density gauges, laser surface texture measurement devices, and seismic pavement analyzers. The criteria used to evaluate the methods and technologies included the ability to measure and detect mixture properties that would change because of segregation, and the availability of equipment that can be used in a rapid, repeatable, and nondestructive manner preferably at normal highway speed. The study recommended infrared thermography and laser surface texture measurements as the most promising

technologies. A draft construction specification designed to identify and measure segregation was proposed.

Further evaluation of these technologies suggested that infrared thermography has good potential for quality control purposes because it can be used during paving operations. However, laser profiling appears to be the most practical mean for detecting and quantifying segregation for quality assurance purposes. Based on the information available about ongoing research at the time this paper was prepared, at least four state departments of transportation (Kansas, New Jersey, Texas, and Virginia) are considering the use of laser profiling for segregation detection and measurement. However, before judgments regarding the varying degrees of segregation can be made, an objective estimate of non-segregated texture is first required.

Past studies demonstrated that aggregate type and structure significantly influence microtexture and macrotexture (28). Other HMA properties, such as asphalt content and void content, also affect macrotexture. A model for predicting the [estimate of the MTD computed using road surface analyzer (ROSAN) laser measurements] using wearing surface mix properties has been proposed. The model was developed based on a limited assortment of HMA mixes. According to the study, the non-segregated ETD of an HMA could be computed (8):

$$ETD = 0.01980 * MS - 0.004984 * P_{4.75} + 0.1038 * C_c - 0.004861 * C_u \quad (7)$$

where,

$MS$  = maximum size of the aggregate (mm),  
 $P_{4.75}$  = percentage passing 4.75-mm sieve,  
 $C_c$  = coefficient of curvature =  $(D_{30})^2 / (D_{10}D_{60})$ ,  
 $C_u$  = coefficient of uniformity =  $D_{60}/D_{10}$ ,  
 $D_{10}$  = the sieve size associated with 10% passing (mm),  
 $D_{30}$  = the sieve size associated with 30% passing (mm), and  
 $D_{60}$  = the sieve size associated with 60% passing (mm).

The values computed based on the measured mix properties for some of the HMA mixes studied are compared with the corresponding average sand patch measurements in Figure 9. The average mix properties obtained from field cores are presented in Table 2. Figure 9 suggests that the equation cannot appropriately predict the macrotexture for the mixes studied (especially for the SMA and OGFC mixes). No visual segregation was detected in any of the mixes.

A study of the Virginia Smart Road mixes (29) also investigated the possibility of predicting non-segregated field macrotexture based on mix properties determined on laboratory-compacted specimens. Loose samples were taken during placement of the wearing surface from which specimens were prepared in the laboratory in accordance with the Virginia Department of Transportation (VDOT) mixture design practices. This study concluded that the surface macrotexture could be predicted using the aggregate nominal maximum size (NMS) and voids in the mineral aggregate (VMA). The developed regression model to compute the *ICCTEX* is as follows ( $R^2 = 0.965$  and RMS error = 0.123 mm):

$$ICCTEX = -2.896 + 0.2993 * NMS + 0.0698 * VMA \quad (8)$$

where *NMS* is the nominal maximum size in millimeters and *VMA* is the percentage of voids in the mineral aggregate.

A continuation of this study is currently looking into calibrating the equation to use actual as-constructed mix properties determined for the same mixes from cores extracted from the pavement soon after construction. A validation effort using a wider range of mixes and locations is also underway.

## SUMMARY AND CONCLUSIONS

The main applications of surface macrotexture for pavement management are to measure the frictional properties of the pavement surface and to detect HMA construction segregation or non-uniformity. Since surface macrotexture can be measured quite efficiently using non-contact technologies and can provide important information regarding pavement safety and HMA construction quality, this parameter may be included in the quality assurance or control procedures.

Correlations among different macrotexture measuring methods and devices were investigated on the basis of measurements determined from seven different HMA wearing surfaces. The correlation between the CTMeter and the sand patch measurements was excellent ( $R^2=0.94$ ). The correlation between the profile-based macrotexture and the sand patch was also strong ( $R^2=0.88$ ). However, the correlation is not in agreement with the one presented in ASTM E-1845. This finding suggests a possible bias in the laser profiler used for this investigation or a difference in the algorithm used to compute the macrotexture.

Consistent with previous studies, it was found that the skid number gradient with speed is inversely proportional to the pavement macrotexture. In addition, there was a noticeable difference in speed dependency when smooth and ribbed tires were used. Measurements conducted using the smooth tire showed a higher dependency on speed than those measurements conducted with the ribbed tire. The analysis suggested that the coefficients used to compute  $S_p$  (based on MPD measurements) may not be applicable to the equipment and mixes considered in the study. The lack of agreement could be due to the algorithm used to compute the average macrotexture utilized by the profiler. Oscillations in the  $PNG$  with time due to seasonal variations were also observed.

Macrotexture measurements hold great promise as tools to detect and quantify segregation for quality assurance purposes. A standard construction specification was proposed in a recent NCHRP study; however, the equation proposed for computing the non-segregated ETD could not be applied to the mixes tested in this study. An alternative equation has been proposed that estimates the surface macrotexture using the mix NMS and VMA. Further investigation using other mixes is recommended.

## ACKNOWLEDGEMENTS

The construction and instrumentation of the Virginia Smart Road project has been made possible through a cooperative effort of the Virginia Department of Transportation (VDOT), the Virginia Transportation Research Council (VTRC), Virginia's Center for Innovative Technologies (CIT), the Federal Highway Administration (FHWA) and Virginia Tech. Special thanks to Robert Honeywell of VDOT; L. E. (Buddy) Wood, Arthur Wagner, Linda De Grasse, and Brian D. Prowell of VTRC; and Amara Loulizi, Mohammad Rahman, Robin Davis, and Jeff Kuttesch of Virginia Tech for collaborating in the data collection and analysis.

## REFERENCES

- (1) Smith, K. L., K. D. Smith, L. D. Evans, T. E. Hoerner, M. I. Darter, and J. H. Woodstrom. *Smoothness Specifications for Pavements*. NCHRP Program 1-31 Unpublished Report, 1977.
- (2) McGhee, K. K. *Measuring, Achieving, and Promoting Smoothness of Virginia's Asphalt Overlays*. Virginia Transportation Research Council, Research Report, Charlottesville, VA, 1999.



- (3) Tighe, S., N. Li, L. C. Falls, and R. Haas. Incorporating Road Safety into Pavement Management. In *Transportation Research Record 1669*, TRB, National Research Council, Washington, DC, 2000, pp. 1-10.
- (4) Mahone, D. C. *An Evaluation of the Effects of Tread Depth, Pavement Texture, and Water Film Thickness on Skid Number–Speed Gradients*. Virginia Highway and Transportation Research Council, Charlottesville, VA, 1975.
- (5) Anderson, D. A., R.S., Huebner, J.R. Reed, J.C. Warner, and J.J. Henry. *Improved Surface Drainage of Pavements*. NCHRP Web Document 16 (Project 1-29), TRB, National Research Council, Washington, DC, 1998.
- (6) Panagouli, O. K. and A. B. Kokkalis. Skid Resistance and Fractal Structure of Pavement Surface. *Chaos Solutions and Fractals*, Vol. 9, No. 3, 1998, pp. 493-505.
- (7) Haas, R., R. W. Hudson, and J. Zaniewski. *Modern Pavement Management*. Krieger Publishing Company, Florida, 1994.
- (8) Stroup-Gardiner, M. and E. R. Brown. *NCHRP Report 441, Segregation of Hot-Mix Asphalt Pavements*. TRB, National Research Council. Washington, DC, 2000.
- (9) Henry, J. J. *NCHRP Synthesis 291, Evaluation of Pavement Friction Characteristics*, TRB, National Research Council, Washington, DC, 2000.
- (10) Ivey, D. L., L. I. Griffin, III, J. R. Lock, and D. L. Bullard. *Texas Skid Initiated Accident Reduction Program: Final Report*. Report 910-1F, TTI: 2-18-89/910, TX-92/910-1F, TXDOT, Austin, TX, 1992.
- (11) Ivey, D. L. and W. F. McFarland. Economic Factors Related to Raising Levels of Skid Resistance and Texture. In *Transportation Research Record 836*, TRB, National Research Council, Washington, DC, 1981, pp. 83-86.
- (12) Sandberg, U. Development of an International Standard for Measurement of Pavement Macrotecture. Paper presented at the *20th World Road Conference*, Montreal, Canada, September, 1995.
- (13) Wambold, J. C., C. E. Antle, J. J. Henry, and Z. Rado. *International PIARC Experiment to Compare and Harmonize Texture and Skid Resistance Measurements*. Final Report submitted to the Permanent International Association of Road Congresses (PIARC), State College, PA, 1995.
- (14) Leu, M. C. and J. J. Henry. Prediction of Skid Resistance as a Function of Speed from Pavement Texture. In *Transportation Research Record 666*, TRB, National Research Council. Washington, DC, 1978. pp. 7-13.
- (15) Abe, H., A. Tamai, J. J. Henry, and J. Wambold. Measurement of Pavement Macrotecture with Circular Texture Meter. In *Transportation Research Record 1764*, TRB, National Research Council. Washington, DC, 2001, pp. 201-209.
- (16) Moore, A. B. and J. B. Humphreys. High Speed Skid Resistance and the Effects of Surface Texture on the Accident Rate. In *Skid Resistance of Highway Pavements, ASTM STP 530*. American Society of Testing and Materials, Philadelphia, PA, 1972, pp. 91-100.
- (17) Rose, J. C., J. W. Hutchinson, and B. M. Gallaway. Summary and Analysis of the Attributes of Methods of Surface Texture Measurement. In *Skid Resistance of Highway Pavements, ASTM STP 530*. American Society of Testing and Materials, Philadelphia, PA, 1972, pp. 60-77.
- (18) Yager, T. J. and F. Bühlmann. Macrotecture and Drainage on a Variety of Concrete and Asphalt Surfaces. In *Pavement Surface Characteristics and Materials, ASTM STP 763*. American Society of Testing and Materials, Philadelphia, PA, 1980, pp. 16-30.

- (19) AASHTO Task Force for Pavement Design. *Guidelines for Skid Resistant Pavement Design*. American Association of State Highway and Transportation Officials, Washington, DC, 1976.
- (20) Dupont, P. and Y. Ganga. Skid Resistance and Texture Measurement of Road Surfaces on Difficult Sites. Paper presented at the *20th World Road Conference*, Montreal, Canada, September, 1995.
- (21) Horne, W. B. *Elements Affecting Runway Traction*. SAE Paper 740496, 1974.
- (22) Balmer, G. G. and B. M. Gallaway. Pavement Design and Controls for Minimizing Automotive Hydroplaning and Increasing Traction. In *Frictional Interaction of Tire and Pavement, ASTM STP 793*. American Society of Testing and Materials, Philadelphia, PA, 1983, pp. 167-190.
- (23) Wambold, J. C. Obtaining the Skid Number at Any Speed from a Test at Single Speed. In *Transportation Research Record 1196*, TRB, National Research Council. Washington, DC, 1998, pp. 300-305.
- (24) Henry, J. J. and K. Saito. Skid Resistance Measurements with Blank and Ribbed Test Tires and Their Relationship to Pavement Texture. In *Transportation Research Record 946*, TRB, National Research Council. Washington, DC, 1983, pp. 38-43.
- (25) Cross, S. A. and E. R. Brown. Effect of Segregation on Performance of Hot-Mix Asphalt. In *Transportation Research Record 1417*, TRB, National Research Council. Washington, DC, 1993, pp. 117-126.
- (26) Khedaywi, T. S. and T. D. White. Effect of Segregation on Fatigue Performance of Asphalt Paving Mixtures. In *Transportation Research Record 1543*, TRB, National Research Council. Washington, DC, 1996, pp. 63-70.
- (27) Elliot, R. P., M. C. Ford, Jr., M. Ghanim, and Y. F. Tu. Effect of Aggregate Gradation Variation on Asphalt Concrete Mix Properties. In *Transportation Research Record 1317*, TRB, National Research Council. Washington, DC, 1992, pp. 52-60.
- (28) Beaton, J. L. Providing Skid Resistant Pavements. In *Transportation Research Record 622*, TRB, National Research Council. Washington, DC, 1976, pp. 39-50.
- (29) Davis, R., G. F. Flintsch, I. L. Al-Qadi, and K. K. McGhee. Effect of Wearing Surface Characteristics on Measured Pavement Skid Resistance and Texture, Preprint, Presented at the *81st Annual Meeting of the Transportation Research Board*, Washington, DC, January 13-17, 2002.

## **LIST OF TABLES AND FIGURES**

- Table 1. Texture Classifications
- Table 2. Laboratory Measured Properties of the Wearing Surface HMA
- 
- Figure 1. Microtexture and Macrotecture Illustration
- Figure 2. Schematic of Mean Profile Depth Computation
- Figure 3. Circular Track Meter and Sand Patch Correlation
- Figure 4. Sand Patch and Laser Macrotecture Correlation
- Figure 5. Example of Frictional Properties of Surfaces with Various Degrees of Friction and Macrotecture
- Figure 6. Macrotecture Measurements for all Sections  
(a) Instrumented Lane, (b) Non-Instrumented Lane
- Figure 7. Variation of the Average Percent Normalized Gradient over Time  
(a) Smooth Tire, (b) Ribbed Tire
- Figure 8. Sp (100/PNG) - Macrotecture Relationship
- Figure 9. Measured versus Predicted Macrotecture (NCHRP 441 Model)

**TABLE 1. Texture Classifications**

<b>Texture Classification</b>	<b>Relative Wavelengths</b>
Microtexture	$\lambda < 0.5 \text{ mm}$
Macrottexture	$0.5 \text{ mm} < \lambda < 50 \text{ mm}$
Megattexture	$50 \text{ mm} < \lambda < 500 \text{ mm}$
Roughness/Smoothness	$0.5 \text{ m} < \lambda < 50 \text{ m}$

**TABLE 2. Laboratory Measured Properties of the Wearing Surface HMA**

<b>Section</b>	<b>Mix</b>	<b>Binder</b>	<b>NMS</b>	<b>MS</b>	<b>Pb</b>	<b>PP 9.5</b>	<b>PP 4.75</b>	<b>PP 2.36</b>	<b>PP 1.18</b>	<b>PP 0.6</b>
A	SM-12.5D	PG 70-22	9.5	12.5	5.9	97.3	81.9	46.0	34.2	26.3
E -H	SM-9.5D	PG 70-22	9.5	12.5	5.9	93.8	61.6	41.4	29.2	20.1
J	SM-9.5D	PG 70-22	9.5	12.5	4.9	92.3	53.5	36.5	25.8	18.0
K	OGFC	PG 76-22	12.5	19	5.5	80.8	13.6	1.8	1.4	1.3
L	SMA-12.5D	PG 70-22	12.5	19	6.8	86.0	36.5	24.6	21.1	18.4

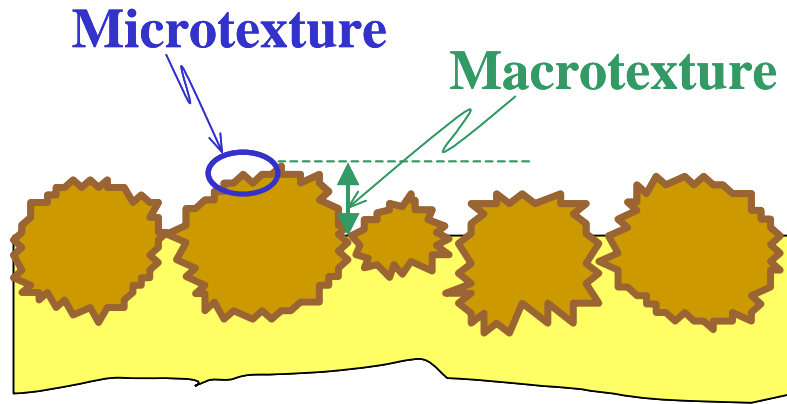


**FIGURE 1. Microtexture and Macrottexture Illustration**

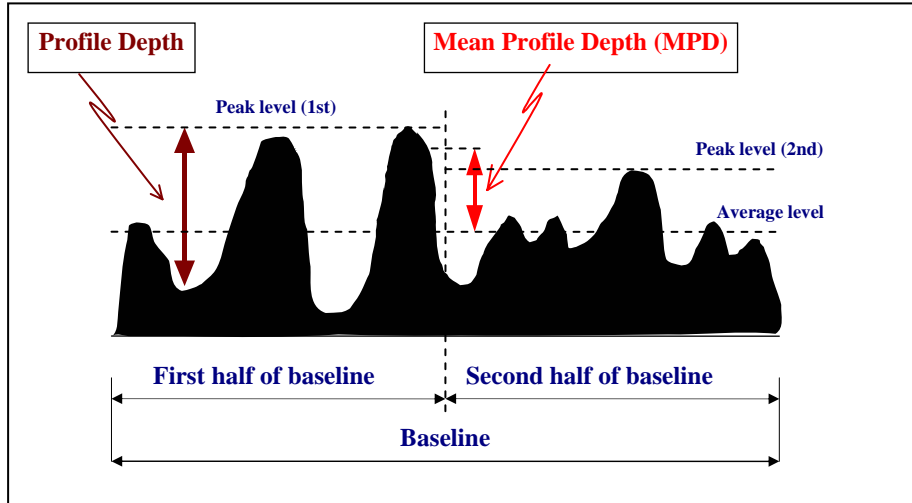


**FIGURE 2. Schematic of Mean Profile Depth Computation**

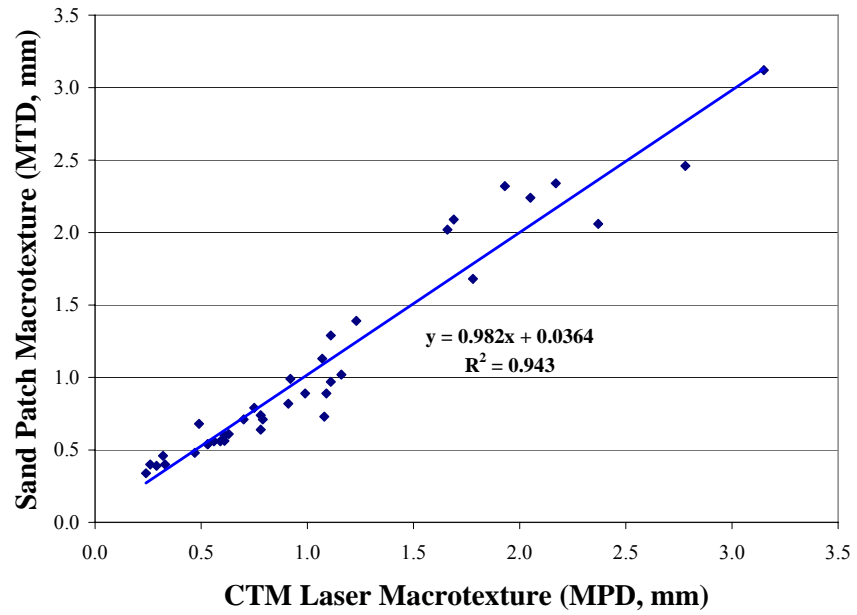


**FIGURE 3. Circular Track Meter and Sand Patch Correlation**



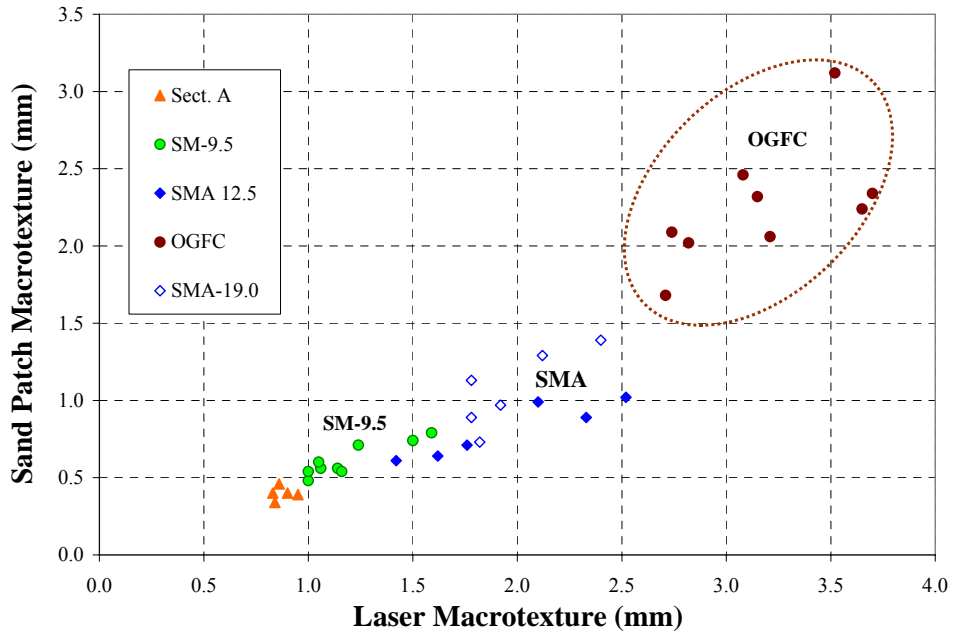
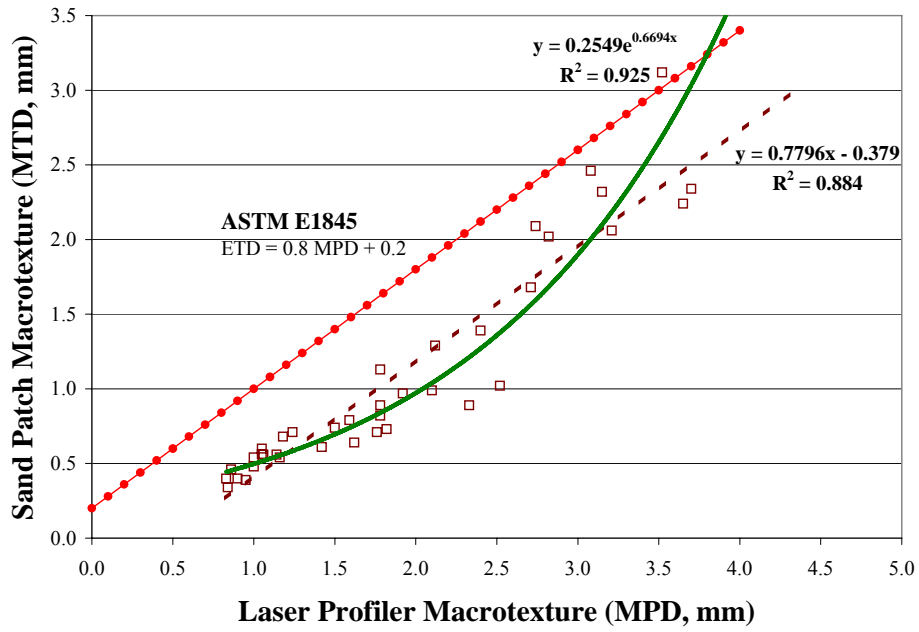


**FIGURE 4. Sand Patch and Laser Macrotexture Correlation**

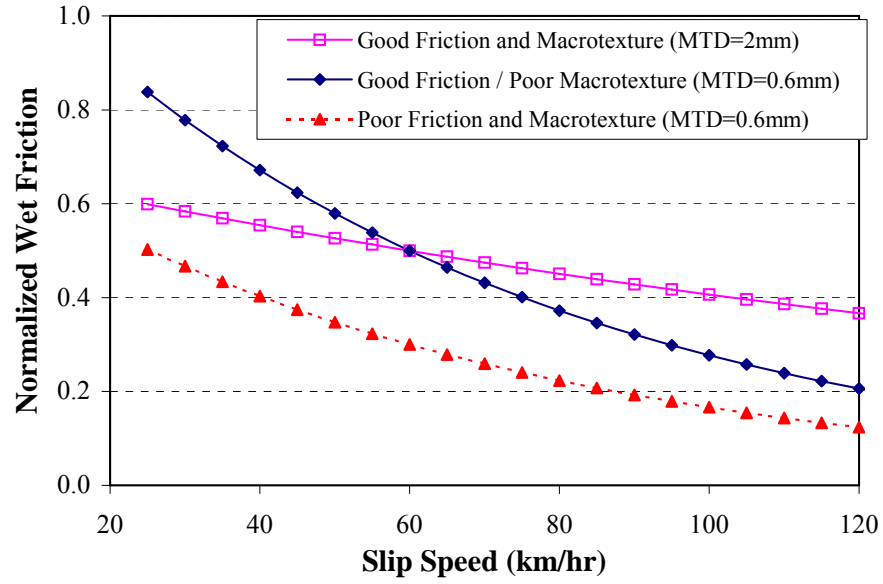


**FIGURE 5. Example of Frictional Properties of Surfaces with Various Degrees of Friction and Macrotexture**

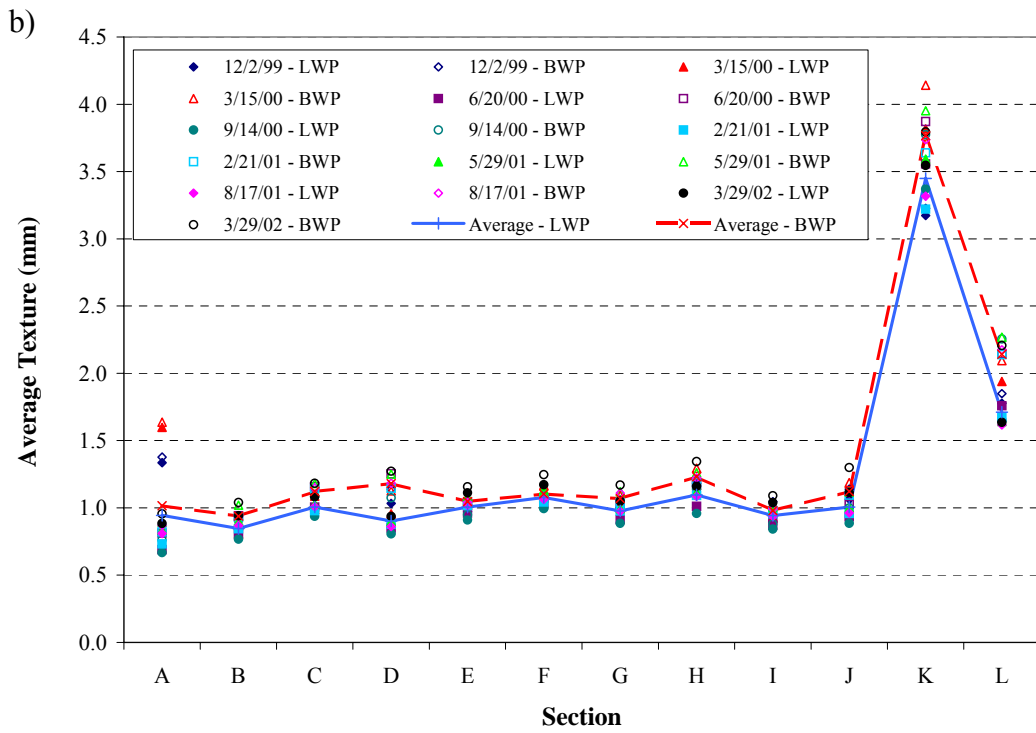
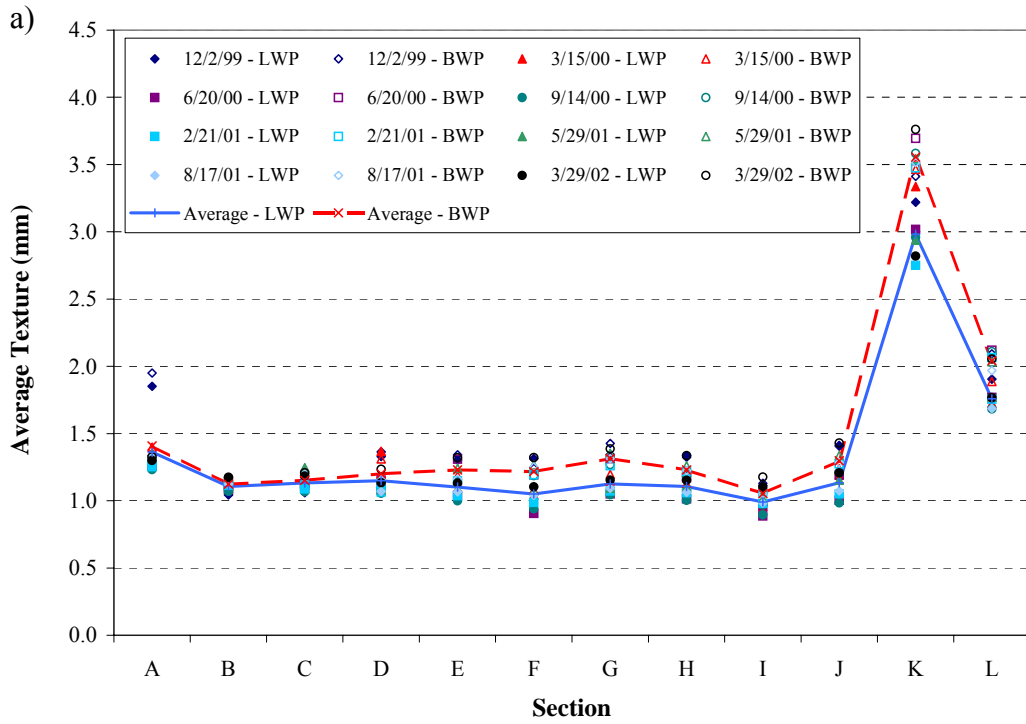


**FIGURE 6. Macrotexture Measurements (ICCTEX) for all Sections  
(a) Instrumented Lane, (b) Non-Instrumented Lane**

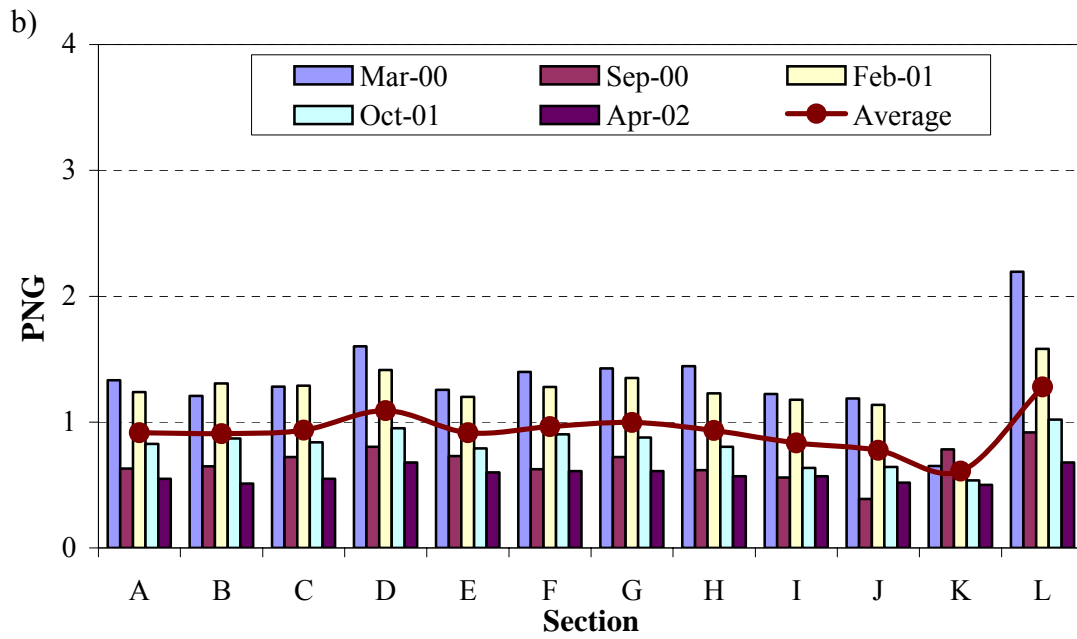
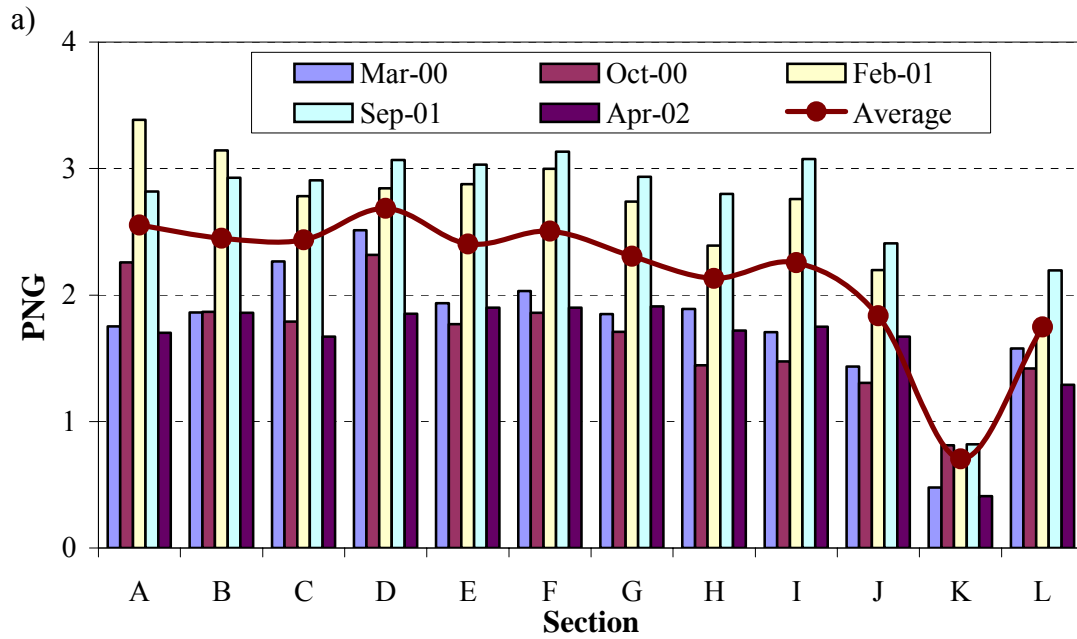


**FIGURE 7. Variation of the Average Percent Normalized Gradient over Time**  
**(a) Smooth Tire, (b) Ribbed Tire**

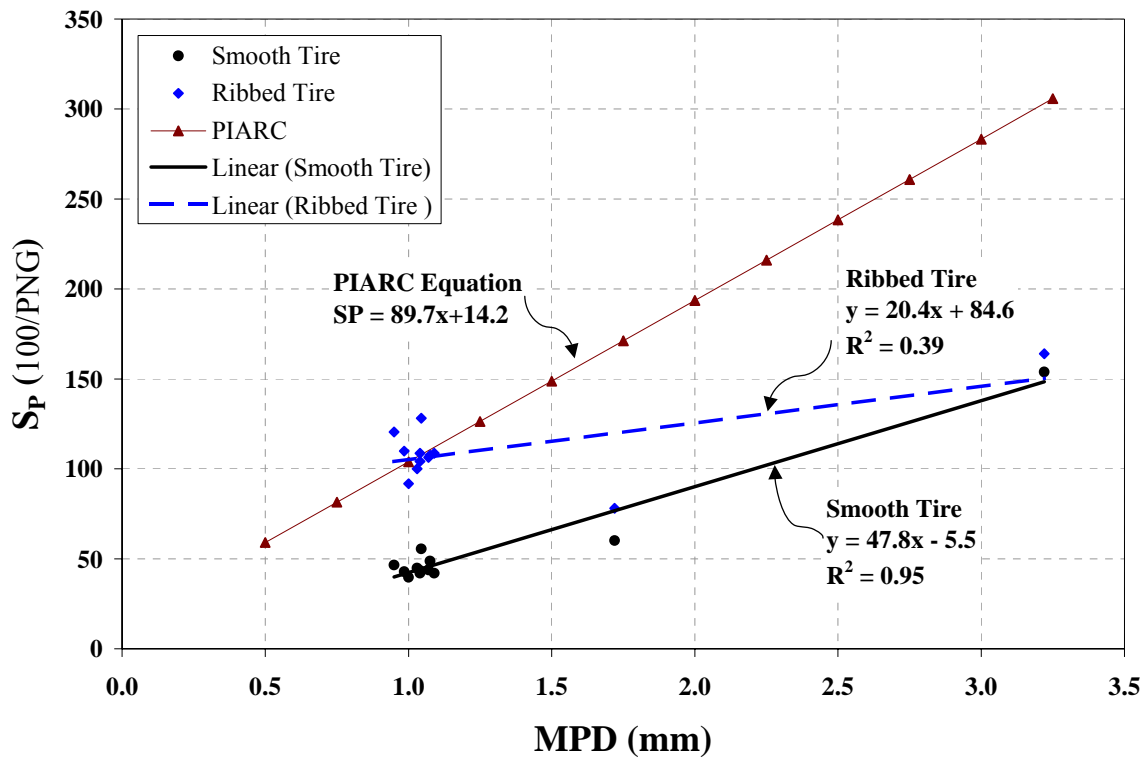
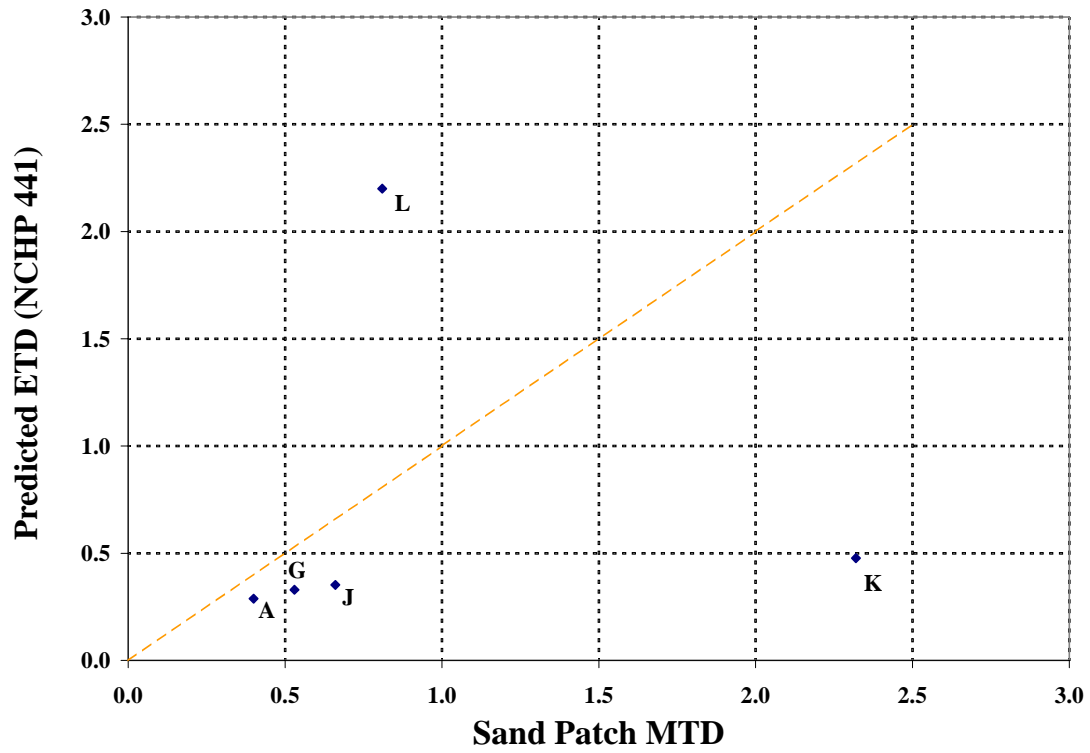


FIGURE 8.  $S_P$  (100/PNG) - Macrotexture Relationship



**FIGURE 9. Measured versus Predicted Macrotexture (NCHRP 441 Model)**

## **Field Validation of Macrotexture-Based Hot-Mix Asphalt Segregation Detection Methods**

By Gerardo W. Flintsch<sup>1</sup>, Kevin K. McGhee<sup>2</sup>, and Edgar de León<sup>3</sup>

### **Abstract**

This paper discusses the efforts carried out in Virginia to validate the use of macrotexture measurements for identifying and measuring hot-mix asphalt (HMA) segregation as detected by more conventional laboratory procedures. The foundation of this project was a series of field experiments designed to sample the uniformity of typical VDOT paving mixtures and to test the validity of available equations to predict target macrotexture values. Eight HMA mixes with variable maximum aggregate size and volumetric properties were considered. At each location, the research team conducted dynamic macrotexture measurements and selected the areas to conduct static tests based on those measurements. The static tests included the following: static macrotexture using a Circular Track Meter, density using nuclear and electromagnetic devices, and core extraction and testing. The laboratory tests performed on the cores included: core height (mm), Specific Gravity, void content, laboratory permeability, asphalt content, and gradation. The researchers demonstrated that macrotexture measurement holds great promise as a tool to detect and quantify segregation for quality-assurance purposes. Correlations of texture with void level/density and asphalt content (traditional measures of segregation) are strong, especially for mixes with moderately-sized aggregates.

**Key Words:** Hot-mix asphalt, segregation, macrotexture

<sup>1</sup> Associate Professor and <sup>3</sup> Graduate research Assistant, Virginia Tech

<sup>2</sup> Senior Research Scientist, Virginia Transportation Research Council

Reproduced with permission from the 74<sup>th</sup> volume of the Journal of the Association of Asphalt Paving Technologists, St. Louis, MO, 2005, pp.1-21.

## Introduction

Segregation has long been one of the major problems in the production and placement of hot-mix asphalt (HMA). A segregated mix does not conform to the specifications in the original job mix formula in gradation and/or asphalt content, creating a difference in the expected density and air void content of the mix. Research has shown that when this happens, the service life of the pavement decreases because of diminished stiffness, tensile strength, and fatigue life, resulting in accelerated pavement distresses, such as raveling, longitudinal cracking, fatigue cracking, and rutting (1, 2). Recent National Cooperative Highway Research Program (NCHRP) research suggests that the agency costs for segregation range from 10% to as much as 50% of the original cost of the pavement (3).

Traditionally, segregated pavement is first identified through a highly subjective visual assessment. Too frequently, however, this technique results in disputes between contractors and highway agencies. Researchers (1, 4) have attempted to develop reliable and independent methods to define, detect, and quantify segregation, but few have offered a feasible alternative to the initial visual inspection.

The study presented in NCHRP Report 441 (3) investigated a variety of commonly available technologies for detecting segregation (visual identification, “sand patch” texture measurement, and nuclear density gauges) and measuring segregation (permeability, nuclear density/moisture content gauges, and destructive testing). Many developing technologies, such as infrared thermography, ground penetration radar, thin-lift nuclear asphalt content/density gauges, dynamic (laser-based) surface texture measurement devices, and seismic pavement analyzers were also evaluated. The researchers recommended infrared thermography and dynamic texture measurements as the most promising technologies. The NCHRP 441 report further suggests that infrared thermography has good potential for quality-control purposes because it can be used during paving operations. On the other hand, dynamic texture measurement appears to be the most practical means for detecting and quantifying segregation for quality-assurance purposes.



### ***Use of Macrotexture to Detect and Measure Segregation***

The connection between HMA mix segregation and observable changes in surface macrotexture has been studied for some time. Earlier research at Auburn University (1) and the University of Kansas (5) identified this relationship. The significance of an objective measure of texture is likewise recognized through its presence in particular construction specifications (4).

The significant advancement made by the work reported in NCHRP Report 441 (3) involves the method used to measure texture. Although the earlier texture measurements were made using volumetric techniques (e.g., the sand patch method, ASTM E-965 [6]), this latest work applied high-speed laser-based equipment to collect semi-continuous measurements of pavement surface texture. The obvious advantages include the ability to take measurements at highway speeds and the ability to collect a practically continuous stream of texture estimates, a “texture profile,” to observe how it varies (or does not vary) along a pavement mat.

### ***Prediction of Non-segregated Macrotexture***

The texture-based approach proposed in NCHRP Report 441 (3) builds on the presumption that an “ideal” texture exists for every mix and that this ideal texture can be predicted using various properties of the original job-mix formula. Given this ideal as a target, actual texture measurements can be obtained and compared to the target to assess if and where, within a new surface, the mix has departed from the original formula. Through the use of a limited assortment of HMA mixes, a model for predicting ideal texture was developed; this model is referred to as the NCHRP 441 model in the current study.

#### ***NCHRP 441 Model***

According to the NCHRP report, the non-segregated texture of an HMA surface could be computed based on Equation 1 ( $R^2 = 0.65$ ):

$$ETD = 0.01980 * MAS - 0.004984 * P_{4.75} + 0.1038 * C_c + 0.004861 * C_u \quad (1)$$

where,

$ETD$  = estimated mean texture depth (a function of the Mean Profile Depth [MPD] provided in ASTM E-1845 [6]),  
 $MAS$  = maximum size of the aggregate (mm),  
 $P_{4.75}$  = percentage passing the 4.75-mm sieve,  
 $C_c$  = coefficient of curvature =  $(D_{30})^2 / (D_{10}D_{60})$ ,  
 $C_u$  = coefficient of uniformity =  $D_{60} / D_{10}$  (*Note*: The sign of  $C_u$  was changed from (-) to (+) after discussion with the authors; apparently, there was a typographical error in the report.),  
 $D_{10}$  = the sieve size associated with 10% passing (mm),  
 $D_{30}$  = the sieve size associated with 30% passing (mm), and  
 $D_{60}$  = the sieve size associated with 60% passing (mm).

This formula was tested using the average mix properties derived from field cores taken from various HMA mixes at the Virginia Smart Road in Blacksburg, Virginia. The  $ETD$  values computed (with equation 1) using these measured mix properties were compared with corresponding average sand patch (MTD) measurements. The comparison showed that the equation yields a good estimate of the macrotexture for the finer mixes but cannot appropriately predict the macrotexture for the coarser stone mastic asphalt (SMA) and open graded friction course (OGFC) mixes. No visual segregation was detected in any of these mixes (7).

#### *Alternative Model*

Related work at Virginia Tech (8) investigated the possibility of predicting non-segregated field macrotexture based on mix properties determined from laboratory-compacted specimens. The study reported that the surface macrotexture could be predicted using the nominal maximum aggregate size (NMAS) and voids in the mineral aggregate (VMA) and provided the regression Equation 2 to compute an estimated texture (Alternative model). The model had an  $R^2$  value of 0.965 and a root mean squared error (RMSE) of 0.123 mm.

$$ICCTEX = -2.896 + 0.2993 * NMAS + 0.0698 * VMA \quad (2)$$

where,

$ICCTEX$  = proprietary high-speed macrotexture estimate provided by the International Cybernetics Corporation (ICC) laser-based macrotexture measuring device (mm),

*NMAS* = nominal maximum aggregate size (mm), and  
*VMA* = voids in the mineral aggregate (%).

This model predicted macrotexture values similar to those predicted by the NCHRP 441 model for the fine mixes but performed better for the nontraditional coarser mixes. However, the alternative model also presented problems when used to predict the macrotexture of mixes other than the ones used for developing the model (7).

## **PURPOSE AND SCOPE**

The approach proposed in NCHRP Report 441 (3) represents a very appealing alternative for detecting and measuring segregation in HMA pavements. However, the dynamic texture measuring technology used operationally in Virginia (discussed in more depth elsewhere in [9]) is different from that used in the NCHRP 441 study and thus, its applicability must be carefully studied.

The over-arching purpose of the research project discussed in this paper was to support the development of a mechanism to promote maximum uniformity in Virginia's HMA pavements. The paper focuses on the efforts carried out in Virginia to validate the use of macrotexture measurements for identifying and measuring HMA segregation as detected by more conventional laboratory procedures.

## **METHODS**

Following an extensive review of relevant literature and current practice, the project moved into a series of field experiments designed to gather key information on segregation (or uniformity) for mixes typically used in Virginia. The ability to predict non-segregated macrotexture as a basis for assessing segregation was examined using measured macrotexture (dynamically and with a static reference) combined with the various mix properties determined from cores. A complete discussion of pavement

texture and texture-measuring devices can be found elsewhere (10).

### ***Field Data Collection***

In the selection of the test sites for the field experiments, an effort was made to represent typical mixes from across the state while targeting mixes with evidence of segregation. Eight projects were selected, which included five surface mixes, two base mixes, and an intermediate mix. For surface mixes, the potential candidates were drawn primarily from VDOT's active maintenance resurfacing schedule. Two ongoing new-construction projects provided candidates for intermediate and base-mix testing.

Upon selection of a candidate project, the site was "scouted" with a high-speed laser macrotexture measuring device installed in the Virginia Transportation Research Center (VTRC) pavement-evaluation vehicle. A single test run with the dynamic texture system (set to the highest resolution) was conducted. Next, a report that provided texture estimates every 2 ft for the length of the project was generated and reviewed to identify areas where the texture was most pronounced or actively fluctuating. The research team then traveled to those locations to visually assess their suitability for further tests.

Provided that the dynamic texture data and visual review suggested an identifiable non-uniformity in the mat, the lane(s) was closed (as required) and a test site was established. Figure 1 (11) illustrates the layout of a typical test site. Since the dynamic texture data were available from only the left and center laser sensors of the pavement-evaluation vehicle (see close-up of sensor configuration in Figure 1), corresponding static tests were confined to those locations. The entire test site was 120 ft in length (one site was 150 ft in length) and centered on the most pronounced (visually determined) area of non-uniformity. Once a test site was selected, the limits of the site were identified and traffic cones (outfitted with highly reflective striping) were placed at each end. Before any further layout work took place, two further dynamic texture-measuring passes were made using an automatic triggering system (triggered by the tape on the cones) to ensure that any static measurements could be matched closely with data from the dynamic equipment. The results from these two passes were averaged to provide the texture profile data for further analysis.

Once this step was completed, the remainder of the layout and testing took place.

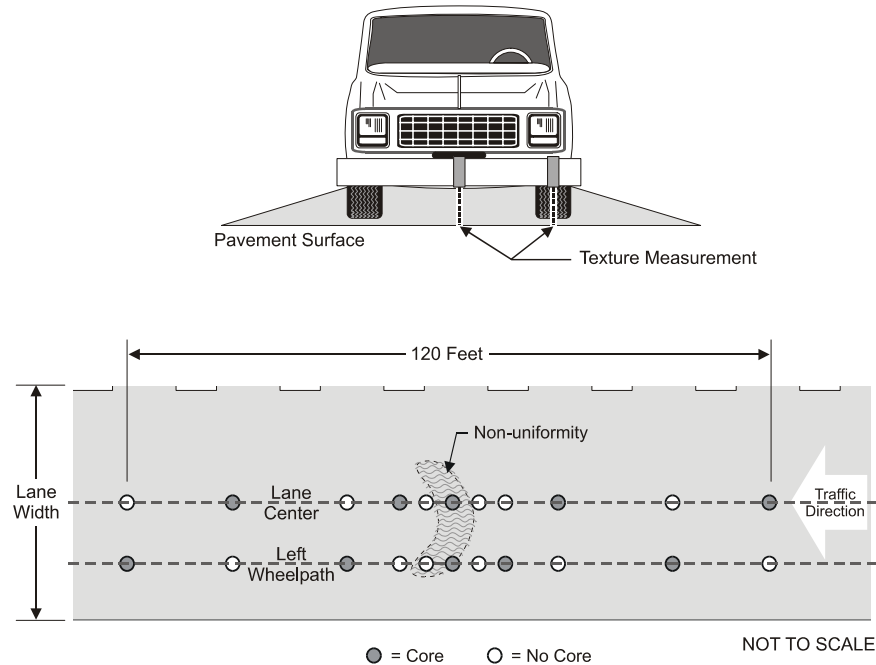


Figure 1 Test Site Layout.

Note: The circles depict locations where static tests were performed. At the center of the test site, the measurements were made at 5-ft intervals. After the first two series of tests, the spacing was expanded to 10 and then 20 ft. Following completion of static tests, cores were taken at the locations indicated with shaded circles.

After completing the dynamic testing and site layout, a series of non-destructive static tests were conducted, followed by the extraction of up to ten 6-in. cores. The non-destructive tests used and the corresponding American Society of Testing and Materials (ASTM [6]) or Virginia Test Method (VTM [12]) designation include the following:

- Circular Track Texture Meter (CTM): mean profile depth (MPD, ASTM E-1845/E-2157),
- Nuclear gauge: density (VTM 76, VTM 81), and

- Electromagnetic pavement quality indicator (PQI): density, surface temperature, and water content (%).

This series of static tests was performed at each location depicted by a circle in Figure 1 (one test per location). The CTM is essentially a modern laser-based surrogate for the volumetric (sand patch) texture measurement. The nuclear and PQI density measurements were conducted to assess relative compaction levels throughout a test section. Since many of these test sections had been in place for several weeks (some with recent rains) and no attempt was made to calibrate the devices to known densities, the output reflected relative density only.

The ten cores were distributed in an attempt to measure as much of the as-built variability as possible (within a test section). It was important that data be gathered from both segregated and non-segregated areas (as determined by visual inspection). The laboratory tests performed on the cores include: core height (mm), Specific Gravity (SSD, AASHTO T 166 [13]), void content (AASHTO T 269 [13]), laboratory permeability (VTM 120 [12]), asphalt content (AASHTO T 308 [13]), and gradation (AASHTO T 11 and T 27 [13]). As was the case with non-destructive field density measurements, the requirements of particular lab testing procedures were “compromised” to ensure the fullest characterization of mix properties throughout a test section. For example, a full gradation analysis requires a larger sample than was possible with a single 6-in. core. Instead of combining material from several cores to comply with the AASHTO T 11 test procedures (13), the analyses were conducted with a smaller amount of separate material.

### ***Predicting Non-segregated/Target Pavement Surface Texture***

The majority of each section was observed to be relatively uniform, with corresponding test results that confirmed no measurable segregation. The mix properties for these non-segregated areas (derived from cores) were used to generate “target” ETD (NCHRP 1441 model) and ICCTEX (alternative model) values using the models depicted by equations 1 and 2, respectively. Since the alternative model had been developed using the texture data from the ICC system (ICCTEX), it was possible to compare its results with the dynamic macrotexure measurements directly. For the NCHRP 441 model, however, it

was first necessary to convert the field measurements to ETD based on transfer functions given in equations 3 and 4 (14).

$$ETD = 0.78ICCTEX - 0.38 \quad (3)$$

$$ETD = 0.98MPD_{CTM} + 0.04 \quad (4)$$

where

*ETD* = estimate of *mean* texture depth (mm),

*ICCTEX* = estimate of macrotexture as computed by a proprietary algorithm (mm), and

*MPD<sub>CTM</sub>* = mean profile depth computed by the CTM (mm).

Once the target texture values were calculated, it was possible to review the texture profiles for a test section to characterize estimated levels of segregation. This step applied the procedures presented in Appendix J of NCHRP Report 441, which estimate the level of segregation by comparing measured texture and expected texture (3).

## FINDINGS AND DISCUSSION

### *Field HMA Properties*

Six of the projects evaluated were part of VDOT's annual maintenance resurfacing program, and two of the test sections were new construction work. There were two test sites for every mix designation, with the exception of the 19-mm mixes --for which one site was an intermediate mix and the other was a surface mix. With each mix pairing, one of the sites was considered (subjectively at least) to be part of a typical-to-good project and the other was considered to be "non-uniform" (i.e., at least moderate segregation was observed).

The average properties of the mixes tested are summarized in Tables 1 and 2. Only the values obtained for the cores extracted from the *non-segregated* areas were included for computing the average results. Figure 2 shows examples of a non-segregated area and a segregated area for a 19-mm surface mix.

**TABLE 1 AVERAGE NON-SEGREGATED HMA  
AGGREGATE PROPERTIES**

<b>Project</b>	<b>Mix</b>	<b>MAS (mm)</b>	<b>NMAS (mm)</b>	<b>P4.75 (%)</b>	<b>Cc</b>	<b>Cu</b>
02-1039	SM-9.5D	12.5	9.5	0.57	2.61	31.0
02-1043	SM-9.5	12.5	9.5	0.61	1.41	33.9
02-1041	SM-12.5	19.0	12.5	0.48	5.31	48.8
02-1068	SM-12.5A	19.0	12.5	0.54	2.23	31.8
02-1056	IM-19.0	25.0	19.0	0.51	1.52	33.1
02-1079	SM-19.0	25.0	19.0	0.57	3.48	48.0
02-1026	BM-25	37.5	25.0	0.39	3.78	47.7
02-1050	BM-25	37.5	25.0	0.43	2.37	56.6

MAS = maximum aggregate size, NMAS = nominal maximum aggregate size ,  
PP = percent passing , C<sub>c</sub> = coefficient of curvature, C<sub>u</sub> = coefficient of  
uniformity.

**TABLE 2 AVERAGE NON-SEGREGATED HMA  
VOLUMETRIC PROPERTIES**

<b>Project</b>	<b>Mix</b>	<b>Pb (%)</b>	<b>VMA (%)</b>	<b>VTM (%)</b>
02-1039	SM-9.5D	5.56	20.2	6.4
02-1043	SM-9.5	5.64	19.6	7.2
02-1041	SM-12.5	5.19	22.4	10.9
02-1068	SM-12.5A	6.05	21.5	9.8
02-1056	IM-19.0	5.35	19.0	7.5
02-1079	SM-19.0	4.80	13.6	5.3
02-1026	BM-25	4.97	19.4	8.0
02-1050	BM-25	4.72	17.0	6.1

P<sub>b</sub> = percent binder VMA = voids in mineral aggregate , VTM = voids in the  
total mix.



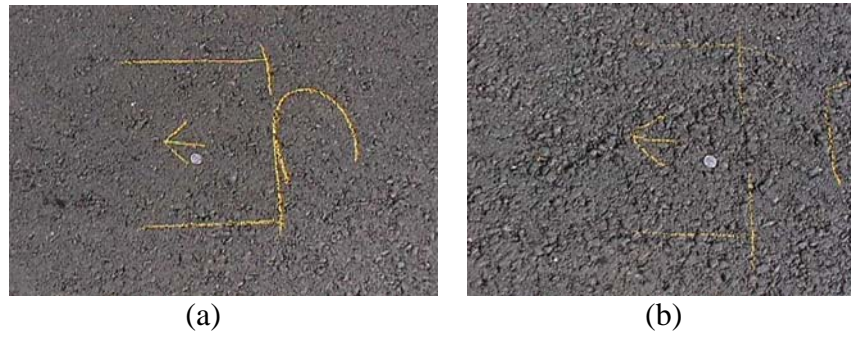


Figure 2 Example of (a) Non-segregated and (b) Segregated Area (project 02-1079).

The texture-based method for estimating segregation was compared with the more traditional (destructive) methods for confirming mix segregation. Table 3 provides additional measures from the test sections described in Tables 1 and 2. Instead of reporting the “average” measured properties, Table 3 highlights extremes in measured voids (VTM) and percent binder content ( $P_b$ ). The differences ( $\Delta$  %) between the average and extreme properties have been shown to correlate well with segregation (3).

TABLE 3 EXTREME MIX PROPERTIES AND EXPECTED LEVELS OF SEGREGATION

Project	$P_b$ (min %)	$P_b$ ( $\Delta$ %)	Segr. Level	VTM (max %)	VTM ( $\Delta$ %)	Segreg. Level
02-1039	5.38	-0.18	None	8.9	2.5	Low
02-1043	4.9	-0.74	Low	12.6	5.4	High
02-1041	5.04	-0.15	None	15.9	5.0	Med./high
02-1068	4.38	-1.67	High	13.8	4.0	Low/med.
02-1056	4.77	-0.58	Low	11.7	2.4	Low
02-1079	4.28	-0.52	Low	11.1	5.8	Med./high
02-1026	3.56	-1.41	High	9.9	1.9	None/low
02-1050	4.37	-0.35	Low	7.8	1.7	None/low

$P_b$  = percent binder , VTM = voids in the total mix.

Using ranges recommended in NCHRP Report 441 (3), the table further reports the maximum degree of segregation within these test sections. It is clear that the two criteria do not produce consistent results. However, in general, the assessment matches the visual subjective evaluation of the research team. This was somehow expected because even among these destructive measures of segregation, complete agreement rarely exists. The disagreement may simply be due to sample and testing variability. It may also relate, however, to *temperature* segregation effects (explained elsewhere [3]), which would explain low densities but acceptable binder content.

***Relating Macrotexture to Traditional Measures of Segregation***

Since static and dynamic macrotexture measurements exist for each core location, it is possible to take the approach introduced by Table 3 to another level and to review the response of macrotexture to changes in binder and voids/density on a core-by-core basis. Figures 3 and 4 present plots of  $P_b$  and VTM for the 12.5-mm NMAS mix classification, respectively. Although an identifiable trend and a reasonable correlation exists for the macrotexture and VTM data, only a very slight trend is observed with the  $P_b$  data.

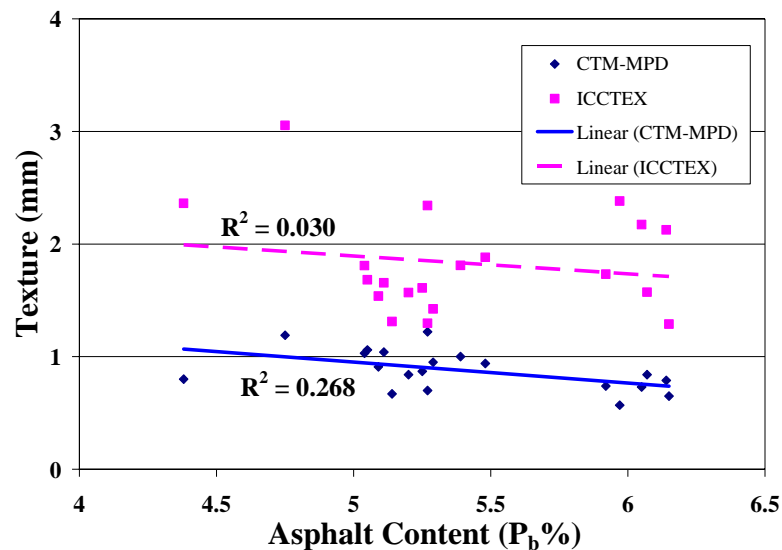


Figure 3 Correlation of Macrotexture with Asphalt Content

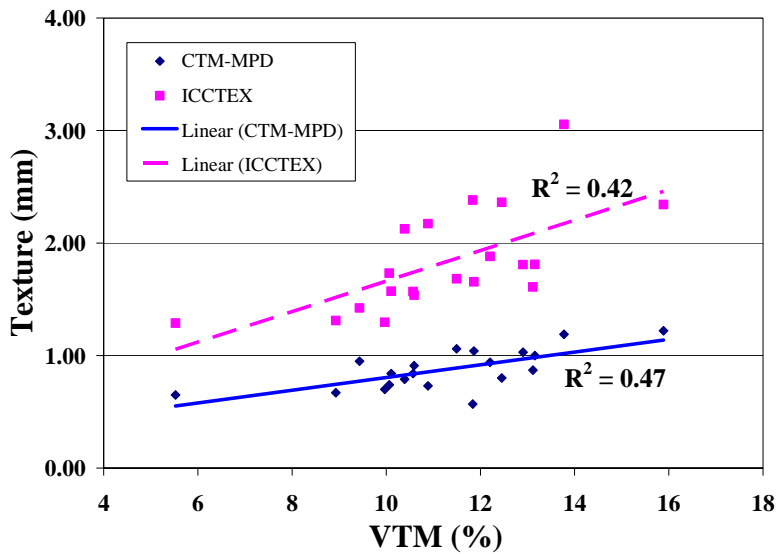


Figure 4 Correlation of Macrotexture with Voids in Total Mix.

Figure 5 summarizes the results of a simple correlation analysis for all four mix classifications. There is a negative correlation between texture and binder content, as well as a consistent positive correlation with void level and VMA. For most mixes, the correlations are good (greater than 0.4), although the correlation between macrotexture and VTM is much better than that observed for  $P_b$ . There seems to be a problem with the characterization of segregation on the finer mixes.

### ***Macrotexture Measurements***

Figure 6 illustrates the various texture measurements (including conversion as necessary) on the left-wheel path (LWP) and on the lane center or between-wheel paths (BWP) for one of the test sites (Project 02-1068). Plotted with the texture measurements are the estimated ranges of texture that define segregation according to the ratios provided elsewhere in (3). For Figure 6, the estimated values were computed using the NCHRP 441 model (equation 1), and the field measurements (ICCTEX and  $CTM_{MPD}$ ) were converted to ETD values.

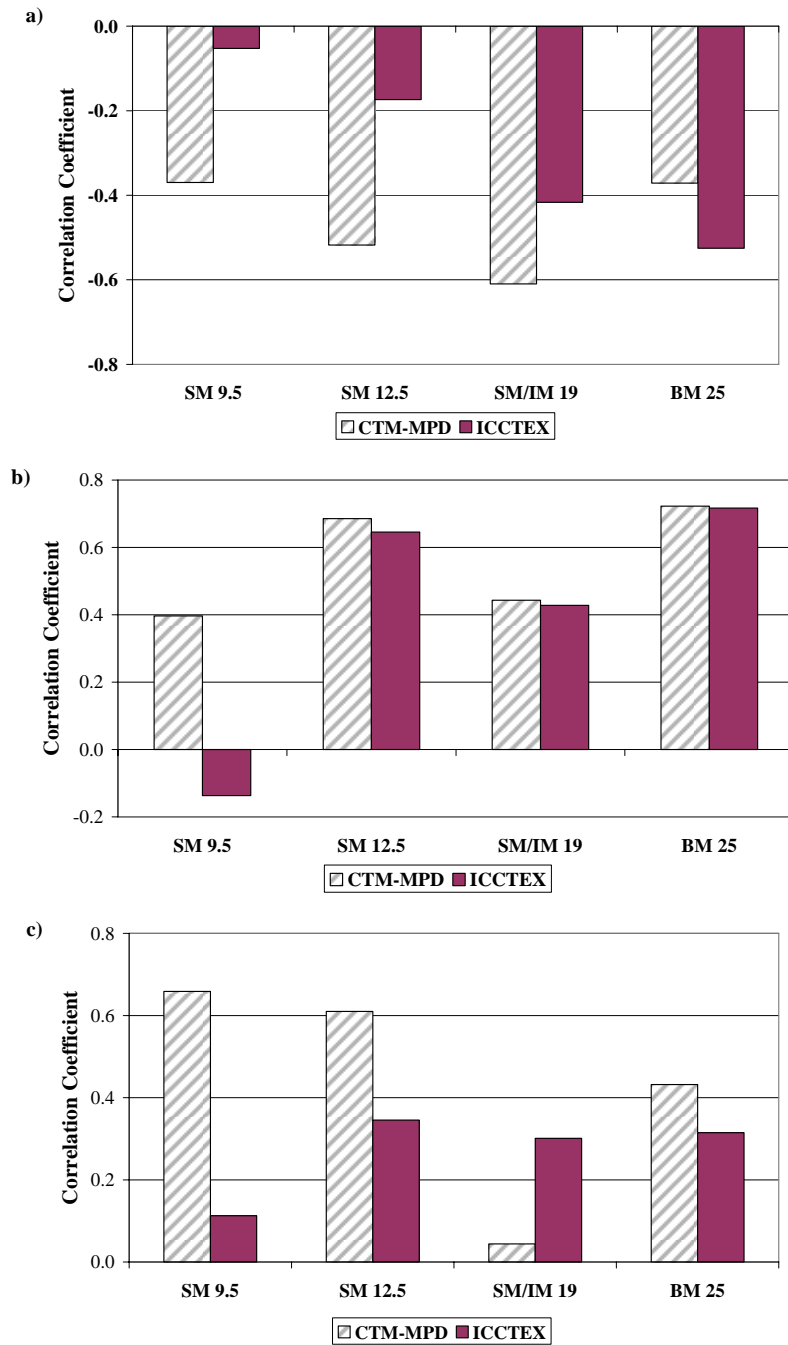
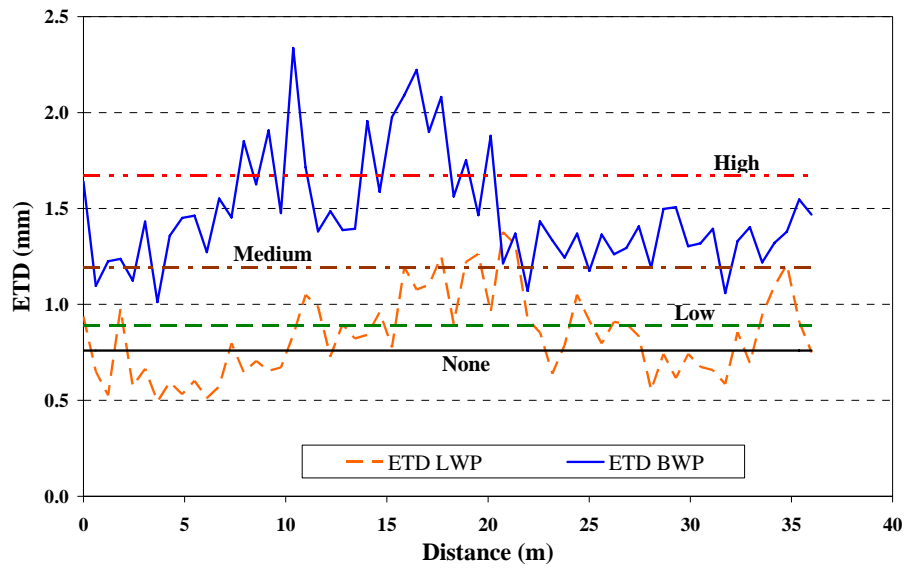
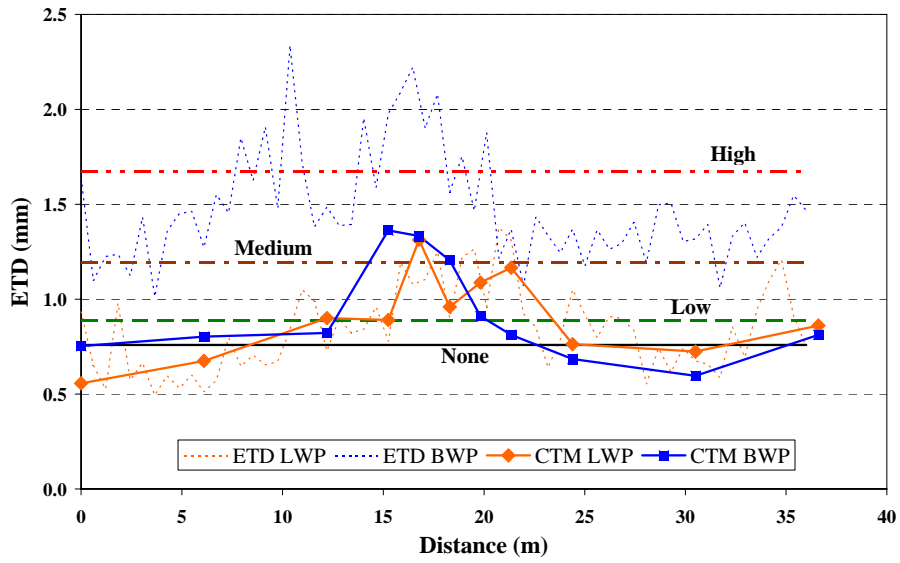


Figure 5 Correlation of Macrotexture Measurements with (a) AC Content (Pb%), (b) Voids in Total Mix (VTM), and (c) Voids in the Mineral Aggregate (VMA).



(a)



(b)

Figure 6 Example Segregation Analysis Using NCHRP 441 Model with (a) Converted ICCTEX Data and (b) Converted CTM Data.

In Figure 7, the estimated target texture was generated using the alternative model (equation 2). Although Figures 6 and 7 represent the same test section, the estimated levels of segregation according to the different models and measuring equipment differ considerably. Similar results were observed for the other mixes.

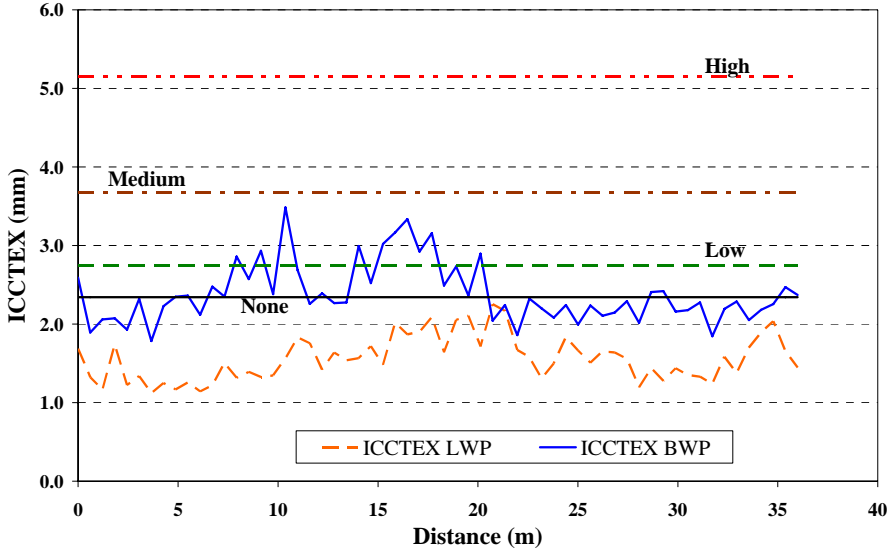


Figure 7 Example Segregation Analysis Using Alternative Model.

Tables 4 and 5 summarize the application of the target texture approach (illustrated by Figures 6 and 7) to all eight test sections using the information collected on the LWP and BWP, respectively. It reports the percentage of each section that exhibited various levels of segregation. The results are organized by texture model used and texture-measuring device.

Although both models produce reasonable results in most cases, they both tend to overestimate the segregated areas for at least some of the projects studied. For example, in Project 02-1026 most of the BWP (71%) and part of the LWP (14%) are segregated based on the CTM measurements and the NCHRP 441 model. However, only the central part of the project was visually segregated. On the other hand, the alternative model predicted such high expected texture values for this project that it failed to detect any significant segregation. The macrotexture plot for this project is presented in Figure 8.

**TABLE 4 SEGREGATION LEVEL DISTRIBUTION (%) ON  
THE LEFT WHEELPATH (LWP)**

Mix	Project	Segregation Level	LWP		
			Altern.	NCHRP 441	
				ICC	CTM
SM-9.5	02-1039 <sup>a</sup>	None	77	73	0
		Low	13	13	9
		Medium	10	13	55
		High	0	0	36
SM-9.5	02-1043	None	95	92	73
		Low	5	3	18
		Medium	0	5	9
		High	0	0	0
SM-12.5	02-1041	None	98	92	100
		Low	2	7	0
		Medium	0	2	0
		High	0	0	0
SM-12.5	02-1068 <sup>a</sup>	None	100	42	27
		Low	0	17	18
		Medium	0	30	45
		High	0	12	9
IM-19.0	02-1056	None	100	23	82
		Low	0	35	9
		Medium	0	33	9
		High	0	8	0
SM-19.0	02-1079 <sup>a</sup>	None	100	75	64
		Low	0	3	9
		Medium	0	15	18
		High	0	7	9
BM-25	02-1026 <sup>a</sup>	None	100	74	86
		Low	0	8	0
		Medium	0	8	0
		High	0	11	14
BM-25	02-1050	None	100	42	73
		Low	0	20	27
		Medium	0	32	0
		High	0	7	0

LWP = left wheelpath; ICC = International Cybernetics Corporation laser texture device; CTM = circular track texture meter.

<sup>a</sup> Areas of segregated mix were evident.

**TABLE 5 SEGREGATION LEVEL DISTRIBUTION (%) ON  
THE LANE CENTER (BWP)**

Mix	Project	Segregation Level	BWP		
			Altern.	NCHRP 441	
				ICC	CTM
SM-9.5	02-1039 <sup>a</sup>	None	42	33	0
		Low	52	40	27
		Medium	7	27	45
		High	0	0	27
SM-9.5	02-1043	None	92	82	36
		Low	8	10	18
		Medium	0	8	45
		High	0	0	0
SM-12.5	02-1041	None	100	90	91
		Low	0	10	9
		Medium	0	0	0
		High	0	0	0
SM-12.5	02-1068 <sup>a</sup>	None	55	0	27
		Low	28	0	36
		Medium	17	12	9
		High	0	88	27
IM-19.0	02-1056	None	100	43	100
		Low	0	28	0
		Medium	0	22	0
		High	0	7	0
SM-19.0	02-1079 <sup>a</sup>	None	100	90	100
		Low	0	5	0
		Medium	0	5	0
		High	0	0	0
BM-25	02-1026 <sup>a</sup>	None	99	3	29
		Low	0	14	29
		Medium	1	30	29
		High	0	53	14
BM-25	02-1050	None	100	98	100
		Low	0	2	0
		Medium	0	0	0
		High	0	0	0

BWP = lane center (between wheelpaths); ICC = International Cybernetics Corporation laser texture device; CTM = circular track texture meter.

<sup>a</sup> Areas of segregated mix were evident.



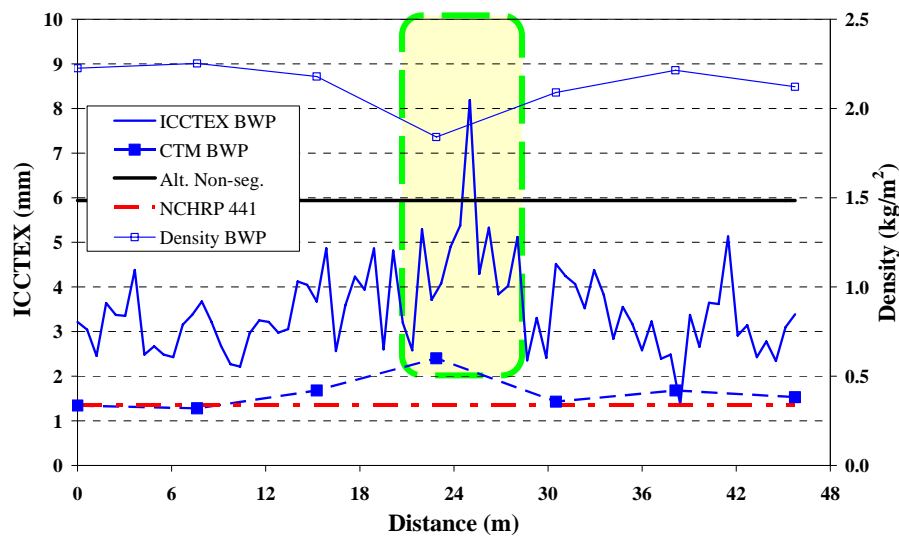


Figure 8 Example Segregation Analysis for a Coarse 25.0-mm Mix (Project 02-1026).

It is interesting to note that in this analysis, the dynamically measured texture appears to reasonably reflect segregation levels in the smaller-stone mixes. For example, Figure 9 presents one of the 9.5-mm sections with the target macrotexture values for the alternative model. This is in spite of the difficulty achieving good correlations with  $P_b$  or VTM in the previous discussion (Figures 3 and 4). This observation suggests that either these predictive equations produce good results by accident or that the semi-continuous measurement of texture is absolutely necessary to fully characterize uniformity of smaller-stone mixes.

In addition, Figure 9 appears to indicate some difficulties coupling the dynamically collected data with core locations from at least one of the sites with 9.5 mm mixes. The peaks in texture do not correspond exactly with the valleys in the density plots.

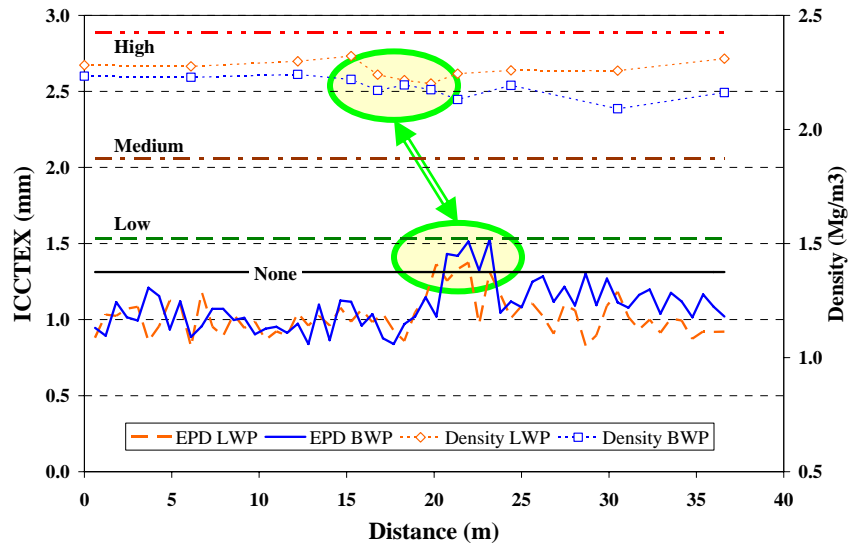


Figure 9 Example Segregation Analysis for a Fine 9.5-mm Mix (Project 02-1043).

## CONCLUSIONS AND RECOMMENDATIONS

The findings from this study support the hypothesis that high-speed macrotexture measurement shows great promise as a tool for detecting and measuring HMA segregation. Correlations of texture with void level/density and asphalt content (traditional measures of segregation) are strong, especially for mixes with moderately-sized aggregates.

More research is required before the ICC dynamic texture measuring systems should be applied to characterize segregation of smaller-stone HMA. Results relating to segregation measurement of smaller-stone mixes appear to conflict. Poor correlation with traditional (and destructive) methods to measure segregation is countered by very good subjective performance.

## REFERENCES

1. Cross, S.A., and Brown, E.R. Effect of Segregation on Performance of Hot-Mix Asphalt. In *Transportation Research Record 1417*,. TRB, National Research Council, Washington, DC., 1993, pp. 117-126.
2. Khedaywi, T.S., and White, T.D. Effect of Segregation on Fatigue Performance of Asphalt Paving Mixture. In *Transportation Research Record 1543*, TRB, National Research Council, Washington, D.C., 1996, pp. 63-70.
3. Stroup-Gardiner, M., and Brown, E.R. *Segregation in Hot-Mix Asphalt Pavements*. NCHRP Report 441. Transportation Research Board, Washington, DC., 2000.
4. Ministry of Ontario. *OPSS 313 Special Provision, Specification 103S38*. Ontario Provincial Standards Section, Ontario, Canada, 1999.
5. Cross, S.A., Hainin, M.R., and Adu-Osei, A. *Effect of Segregation on Mix Properties of Hot Mix Asphalt*. Report No. K-Tran:KU-96-6. University of Kansas Center for Research, Inc., 1997.
6. ASTM International. *Annual Book of ASTM Standards*, Vol. 4.03. West Conshohocken, PA, 2002.
7. Davis, R., Flintsch, G. W., Al-Qadi, I. L., and McGhee, K. K., Effect of Wearing Surface Characteristics on Measured Pavement Skid Resistance and Texture, preprint 02-2403, *81st Annual Meeting of the Transportation Research Board*, Washington, DC, January, 2002 (CD-ROM).
8. McGhee, K.K., and Flintsch, G.W. *High-Speed Texture Measurement of Pavements*. VTRC 03-R9. Virginia Transportation Research Council, Charlottesville, 2003.
9. Flintsch, G.W., McGhee, K.K., and de León, E., Use of Surface Macrotexure Measurements to Detect Segregation. *International Conference on Highway Pavement Data, Analysis, and Mechanistic Design Applications*, Columbus, OH, September 7-10, 2003.
10. Henry, J.J. *Evaluation of Pavement Friction Characteristics*. NCHRP Synthesis 291. Transportation Research Board, Washington, DC, 2000.

11. McGhee, K.K., Flintsch, G.W., de León, E., *Using High-Speed Texture Measurement to Improve the Uniformity of Hot-Mix Asphalt*, Final Report, VTRC 03-R12, Virginia Transportation Research Council and Federal Highway Administration, May 2003. 23 p.
12. Virginia Department of Transportation. *Virginia Test Methods*. Richmond, VA.
13. American Association of State Highway and Transportation Officials. *Standard Specifications for Transportation Materials and Methods of Sampling and Testing (Parts 2A and 2B: Tests)*. Washington, D.C., 2002.
14. Flintsch, G.W., de León, E., McGhee, K.K., and Al-Qadi, I.L. Pavement Surface Macrotecture: Measurement and Application. In *Transportation Research Record*. Transportation Research Board, Washington, D.C. In press for December 2003.

# *Measuring the Uniformity of Hot Mix Asphalt Pavements with Digital Image Technology*

Edgar D. de León Izeppi  
Graduate Research Assistant, Virginia Tech Transportation Institute  
3500 Transportation Research Plaza  
Blacksburg, VA 24061-0105  
voice (540) 231 1021, fax (540) 231 1555  
email: [edeleoni@vt.edu](mailto:edeleoni@vt.edu)

Gerardo W. Flintsch, Ph.D., P.E.  
Associate Professor, The Via Department of Civil and Environmental Engineering  
Director, Center for Safe and Sustainable Transportation Infrastructure,  
Virginia Tech Transportation Institute  
3500 Transportation Research Plaza, Virginia Polytechnic Institute and State University  
Blacksburg, VA 24061-0105  
voice (540) 231 9748, fax (540) 231 7532  
email: [flintsch@vt.edu](mailto:flintsch@vt.edu)

A. Lynn Abbott, Ph.D.  
Associate Professor, The Bradley Department of Electrical and Computer Engineering  
339 Durham Hall, Virginia Polytechnic Institute and State University  
Blacksburg, VA 24061-0105  
voice (540) 231 4472, fax (540) 231 3362  
email: [abbott@vt.edu](mailto:abbott@vt.edu)

Words	5,231
Figures 7*250	1,750
Tables 1*250	<u>250</u>
Total	7,231

## **ABSTRACT**

This paper discusses the application of imaging techniques in a system for assessing the uniformity of newly constructed pavements. The developed system is designed to be used for the detection of segregated Hot Mix Asphalt (HMA) areas and identification of these areas along a road for HMA quality assurance purposes. The system uses relatively low cost off-the-shelf components for capturing images of new pavements and applies innovative image processing and analysis software for detecting and quantifying segregated areas. The development has included the design of the hardware component of the system as well as the development of the necessary image processing and analysis software. Challenges in the hardware design included the positioning of the camera on a moving vehicle and development of an appropriate illumination system. The image processing module uses a Gray Level Co-occurrence Matrix (GLCM), commonly used in visual texture analysis, to compute various different parameters that characterize surface texture. Measures of contrast, correlation, energy, and homogeneity are used to discriminate areas having different visual texture characteristics in the pavement surface. Testing of the system has been conducted at the Virginia Smart Road. The outputs of the system appear to be well suited for automatic identification of several different types of pavement surfaces. If the system can identify non-uniformities on new construction projects properly, then the use of such a system can help improve the quality of the HMA layers and enhance pavement performance, increasing pavement service life with the consequent reductions in down time from repair work.

## **INTRODUCTION**

Hot Mix Asphalt (HMA) is used today in most road construction and maintenance operations. HMA manufacturing starts at specialized facilities using different aggregates that are bonded with asphalt binder cement. Sometimes HMA uses certain additives and/or modifiers which enhance different properties for different applications. Aggregates used to be obtained exclusively from quarry operations, but because of increases in costs and environmental reasons, it is normal now to use recycled material obtained from milling of existing pavements.

Regardless of the mix design methodology used, HMA has to be proportioned, blended, and heated in an asphalt plant before it is transported to the site, laid down and compacted on the roadway. All of these operations are performed following strict specifications that should control the quality of the finished product. The performance of the pavement will depend on this quality. In other words, if the contractor can achieve the level of quality that is required by the design, the expected years of service will equal the assumed service life period.

However, as in most manufacturing processes, certain uncontrollable events can create non-uniformities in the manufacturing process. These non-uniformities are referred to as HMA Segregation and have been defined previously, along with their role in shortening the life of a pavement (1). Segregation can exhibit different characteristics inherent to its specific cause, but usually appear as spots where it is apparent that the aggregate particles have either become dislodged or are intricately closer than the ones in neighboring places. The human eye can detect these non-uniformities by observing the texture of the mix in these areas and comparing it with a normal area. Experienced state highway personnel effectively perform this process. However, in difficult situations, human subjectivity, eye fatigue, and environmental factors can adversely affect the observations.

Today, most state DOT Quality Assurance programs base segregation detection on visual identification by their construction inspectors. If detected, density measurements are made to define the boundaries of the segregated area and then the usual action taken is to completely remove and replace the segregated area for the full depth of the course. Sometimes, depending on the nature of the problem, even an overlay is required (2). Since the extra work is to be done at no additional expense, angry disputes usually spark with contractors.

## **OBJECTIVE**

The main objective of this paper is to introduce a new imaging system that has been developed for the detection of segregated HMA areas. The paper discusses the application of automatic image analysis techniques that have the potential to identify these areas along a road for HMA quality assurance purposes. The proposed system uses relatively low cost off-the-shelf components for capturing images of new pavements and applies innovative image processing and analysis software for detecting and quantifying segregated areas.

## **COMPUTER VISION**

Regardless of all the technological methods now available, human pavement inspectors still play a vital role in the supervision of all highway construction projects. Visual inspections have been the baseline against which any quantitative approach used to detect and measure segregation is tested and compared (3, 4). No automatic method has been completely successful, and it seems fair to state that visual inspections will continue to be used for a long time. For this reason it was deemed necessary to start a research experiment to explore the use of computer vision techniques to try to automate the visual inspection process.

The field of computer vision is concerned with the automatic interpretation of pictorial information. "Automatic" is, however, a long-term goal for most applications. The problem of using a two dimensional visual image to infer information from three-dimensional objects is very complicated. In spite of the difficulties, the human visual system performs extremely well and seemingly with very little effort. Human vision can analyze shapes and recognize many objects automatically, and it has the advantage of using two

eyes which allow it to detect depth (stereo vision). Although machine vision systems may not perform as well for sophisticated tasks, they offer other advantages in certain applications. For example, machine vision systems can help eliminate some problems associated with the subjectivity of human visual inspections, fatigue, inconsistencies, repeatability, etc. Although there are challenges associated with the capture of digital images that will be explained later, the application of the approach proposed herein provides a more objective quality assurance methodology.

Typically in computer vision systems, an image-processing phase is followed by a higher-level image analysis phase. Image processing commonly modifies the pictorial appearance of the image and deals with noise removal, edge detections, or contrast improvements of an image. Image analysis can then extract information from this “improved” image more efficiently. Common applications of this second phase deal with problems involving object recognition, distance estimation, statistical analysis, etc. Both of these phases are used in this research.

Digital imaging has been used in various highway related applications, including pavement crack detection, aggregate shape properties, aggregate shape characterization, and pavement distress surveys. In Virginia, Clemeña and Howe (5) studied the feasibility of using digital image analysis to evaluate pavement distresses. In Texas, image analysis was used to quantify the surface condition of seal coated pavements utilizing a two-dimensional Fourier Transform to compare images of the different pavements analyzed (6).

## SYSTEM FRAMEWORK

Development of the framework for the system started from a previous project (7) in which ground penetration radar was utilized to make longitudinal vertical scans of the different pavements layers. It was deemed convenient to use visible-light images of the pavement surface in conjunction with the radar data to view possible distresses that could explain some of the findings in the radar scan. The imaging system consists of a digital camera, which was mounted in front of the vehicle (see Figure 1), a distance measuring device (DMI), and a computer to control the acquisition rate and store the images.



**FIGURE 1 GPR-Digital Imaging System**

The camera has a resolution of 640 x 480 pixels (picture elements) and a capability of recording up to 80 frames per second. This allows the frame grabber software system to record images up to every foot at highway speeds of 55 mph. The volume of images used can be adjusted by increasing/decreasing the data collection frequency.

## Hardware Design

Although this system was useful for assessing GPR performance, the experience revealed the fact that there were several problems associated with it for pavement assessment purposes. First, during the day, shadows of trees, clouds, wire lines, vehicles, etc. potentially block part of the images (see figure 2). Other sources of variability included different light intensities depending on the position of the sun, cloudy skies, etc. Such variations in illumination can cause large difficulties in the development of image analysis algorithms and



software. It was then concluded that it would be better to focus on collecting the data at night, to allow for greater control of illumination of the pavement. Although this would eliminate some problems, it created others. For example, searching for the adequate light source proved a very challenging task. Ideally, uniform illumination should be used, but most vehicles utilize lights that illuminate the road with a central beam. This was discovered in some of the early attempts with different lights tested at the Virginia Tech Transportation Institute (VTTI).

Several tests were made with diffuser lenses, different off-road lights (such as tractor flood lights, Xenon lights, and halogen lights). Even though more expensive and brighter lights can be installed, the illumination used was sufficient for the purposes of taking adequate images at night driving at highway speeds. The criterion used to define this is that the exposure time (which controls the camera shutter speed) is the same as if the images were being taken in daylight.

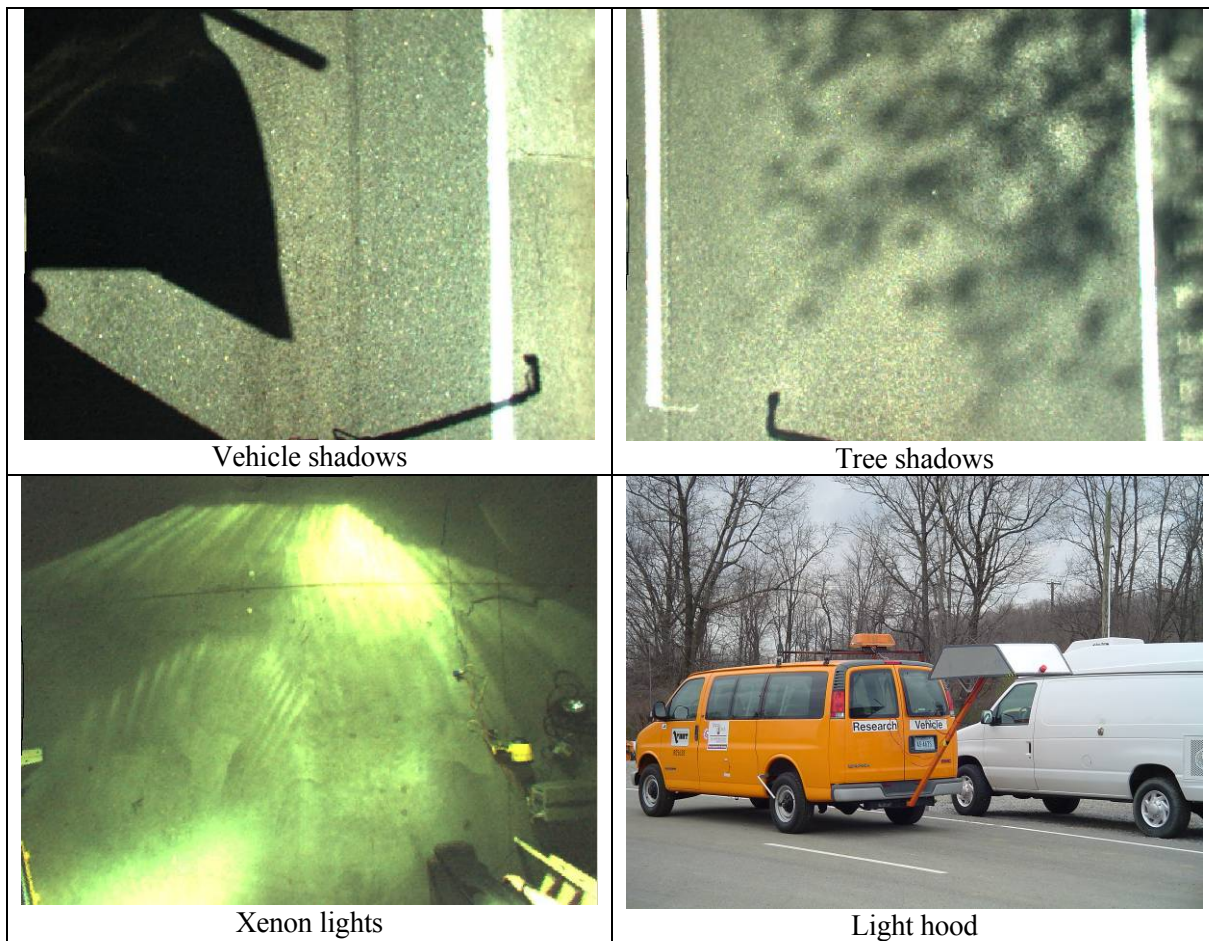


**FIGURE 2 Shadows and illumination problems**

When an adequate light source was found, its original location at the front of the van proved an obstacle for driving at night. The position of the camera and the light source had to be relocated to the back of the vehicle. This relocation caused interference to vehicles following the van, so a hood was added to cover up these lights in the back.

The development of the system also involved experimenting with different lenses for the camera. Quality Assurance (QA) specifications use methods such as random sampling to know if the operations are producing an acceptable product. In order to do this, it was deemed appropriate to experiment with different focal lengths in order to decide the optimum field of view for this application. Figure 3 illustrates the sizes of the fields of view that can be obtained using four lenses that are available for this study. The field of view of the 4.5 mm lens is too large to be properly illuminated; the 12.5 mm lens is currently being used to

capture the images by the system. The size of the rectangular area captured by the 12.5 mm lens is roughly 104 cm by 79 cm. This means that each pixel has 1.7 mm per side in the pavement images being captured. Whole lane images will be possible with wider illumination arrangements.

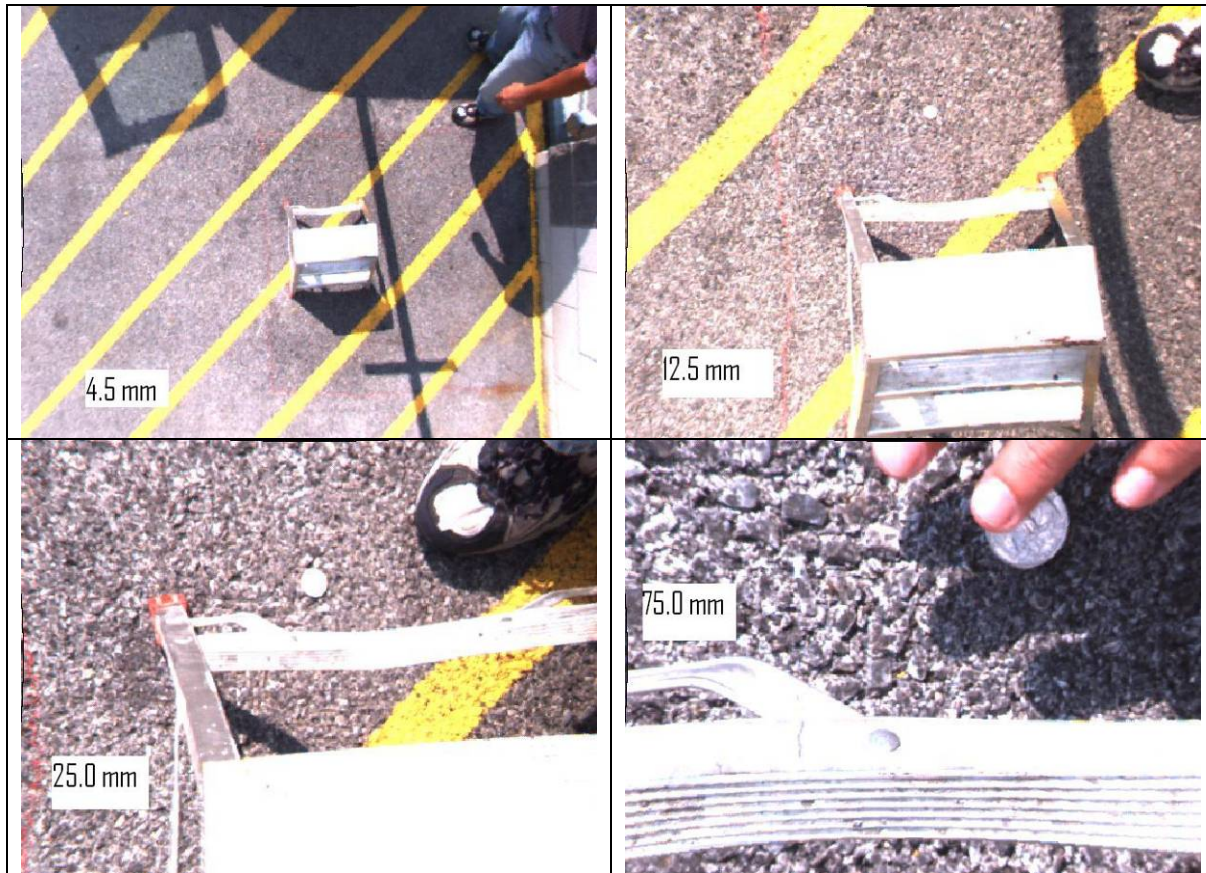


**FIGURE 3 Different lenses available for tests**

### **Digital Images**

A digital image comprises an array of pixels, with spatial coordinates in the two dimensions facing the camera. The array forms a matrix that has an (x, y) configuration with a color code or a brightness level in each of the cells of the matrix. Digital cameras can take black and white (or binary), grayscale, and color images. Black and white images use only 0 as black and 1 as white; thus the name binary. Grayscale or intensity images contain a brightness number for each pixel, commonly in the range 0 to 255. Typically this represents 254 shades of gray in between 0 (black) and 255 (white). Color images can be indexed (pseudocolor) or true color, where every pixel contains information about three different colors, but are stored in slightly different formats.

The camera used in this research is a Basler A-311fc color camera, which is equipped with an additive color separation filter known as a Bayer filter (8). Each pixel in the camera is covered with a micro-lens which allows light of only one color (red, green, or blue) to strike each pixel. The first pixel in the first row records only red light intensity. The second pixel in the first row and the first pixel in the second row represent only green light. Finally, the second pixel in the second row records only blue light. Using twice as many green elements as red or blue is a combination that mimics the human eye's greater resolving power with green light. This pattern repeats itself throughout the whole sensor of the A-311fc with the same configuration, or RRGB for short.

The camera is set to record the data for the images in a mode of operation known as Bayer 8, in which the camera outputs the raw data for each pixel, using 8 bits per pixel. This mode of operation is



Because grayscale images of pavements, such as the ones used in this research, are usually very dark and uniform, a more colorful picture is used to illustrate these concepts. Figure 4 shows a parking lot with some vehicles and two traffic cones with a white car as background. To analyze an equivalent area of interest notice the rectangles on top of the right traffic cone on each image. They show the position of a close up window whose pixel contents are shown to the right of each image type, with a magnification of one individual pixel for each type of image.

We can see three digital images, each with  $m = 480$  rows by  $n = 640$  columns. The first image, known as a true-color RGB image, is composed of 3  $m$ -by- $n$  matrices, each matrix containing data for red, green and blue color levels in each pixel of the color image. This image shows the frame under analysis in real color.

The second image is an indexed “raw” image as stored by the camera’s Bayer filter, just like the ones obtained in this research, where every pixel has recorded the intensity level of only one of the three colors, two thirds of the color data missing from each pixel. To obtain full color, a demosaicing algorithm is used to interpolate a set of complete red, green and blue values for each pixel to obtain a resulting color image as shown in the first image. “Raw” image data allow a user to perform color interpolations or other processing algorithms on pixel data that has not been manipulated. The camera manufacturers recommend, in its user’s manual (8), the following formulas, where  $Y$  gives the values of luminance and  $U$  and  $V$  the chrominance, respectively, for the color conversions:

$$Y = 0.257R + 0.504G + 0.098B + 16 \quad (1)$$

$$U = -0.148R - 0.291G + 0.439B + 128 \quad (2)$$

$$V = 0.439R - 0.368G - 0.071B + 128 \quad (3)$$

Finally, the last image, commonly known as a grayscale or intensity image, is also obtained by interpolating the “raw” image data. This is usually done using only equation (1) above which yields the luminance value, or grayscale information of the image. This last type is the type of images that will be analyzed in this research.

### **Image Processing**

The demosaicing process is illustrated in figure 5 using a part of an actual pavement frame. The first picture represents the first five pixels in the first three rows of a “raw” image. The second one contains the interpolated grayscale values for the same pixels in the new converted image after the interpolation. The pixels in the first picture have been framed in color to help understand the configuration pattern of the Bayer filter, as part of an indexed image with the RGGB configuration as was explained earlier. It is important to emphasize that the interpolation for each pixel is done in groups of four pixels, always taking two green, one red and one blue. The target pixel is always the first pixel in the group, i.e. the one in the upper left corner of the group of four. Because there are two green pixels, the green value will be averaged to substitute for  $G$  in the interpolation conversion formula, or equation (1) above.

Depending on what characteristics of an image need to be enhanced, corrected, or amplified for the analysis, further image processing can be performed. Some filters help emphasize or remove certain features using smoothing, sharpening or edge enhancement operators. Other transformations can be used to de-blur, enhance, compress or detect certain features in images. Morphological operations change images using different shape operators that achieve contrast enhancements, noise removal, thinning, skeletonization, fillings or segmentations (9, 10). No further processing was done on the images after the demosaicing.

### **Image Analysis**

The MATLAB Image Processing Toolbox® (9) was used for both the pre-processing and the analysis of the digital images obtained. The software included in the toolbox allows reading each frame from a concatenated video file in .avi format obtained from the grabber software. These videos contain the raw images recorded with camera using the Bayer 8 filter mentioned above.

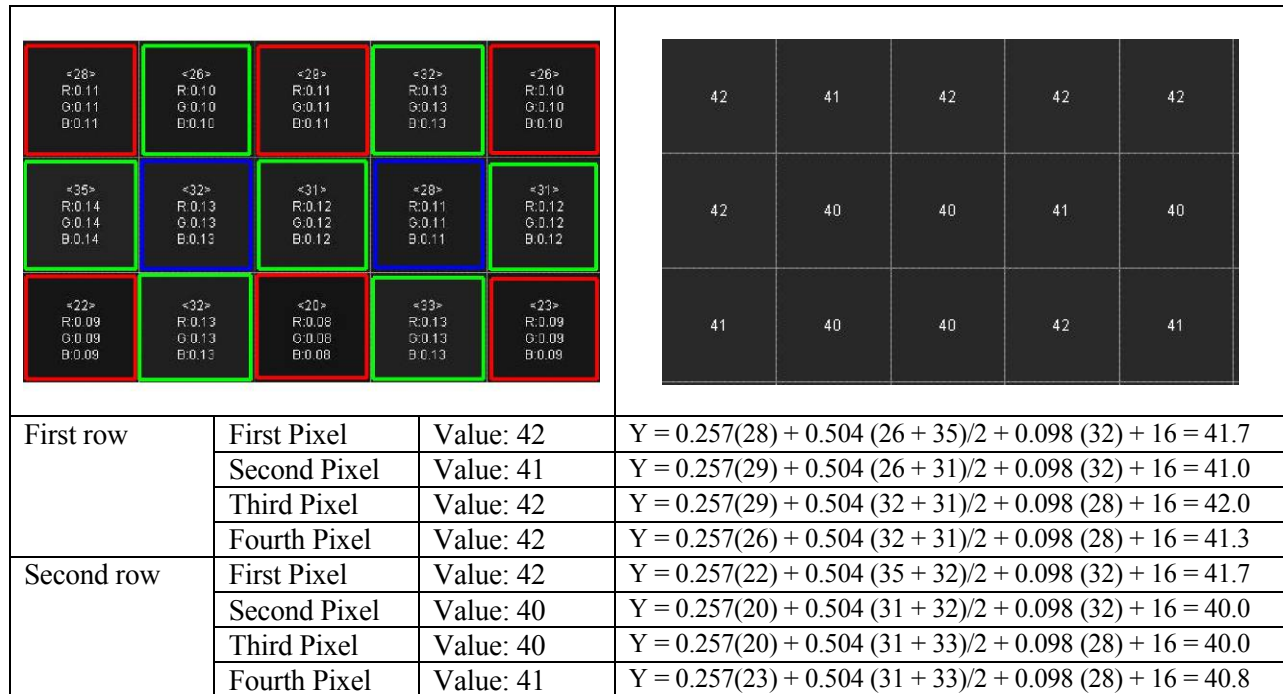


**FIGURE 5 Raw image pixel values and processed pixel values resulting from interpolations**

With this software, a histogram of pixel values of a digital image can be obtained and it is often possible to obtain some useful image properties through fast statistical analysis of this. For example, figure 6 shows two pictures taken with a hand held digital camera at a test site where segregation was found. The brightness histogram of the segregated pavement appears skewed, it has a lower maximum at its peak, and it has a wider base of intensity values than the one for the non-segregated pavement, which seems closer to a normal distribution. It could probably be inferred from this information that the picture of the pavement to the right is of lesser quality than that on the left. However, one limitation of a standard histogram analysis is that spatial information is ignored. In other words, the relative placement of image constituents is not used in the creation of the histogram.

An alternative to standard histogram analysis is to make use of a Gray Level Co-occurrence Matrix (GLCM), which is commonly used in visual texture analysis (10). This two-dimensional matrix captures statistical information, similar to that of a histogram, based on the relative locations of pixel values in the image. The distribution of values within the GLCM depends on the level of coarseness of the visual texture. Various parameters can be derived from the distributions of the different gray levels contained inside the matrix.

Human perception of texture is typically qualitative, and people often use terms such as coarse, fine, regular, irregular, granular, etc. The relationship between texture and image intensity is complex, but a quantitative analysis can be done by identifying texture primitives (texels) and describing the spatial relationships between them. Pixel values can be assessed using first-order statistics like marginal probability:

$$P_i = \Pr(I(r, c) = i) \quad (4)$$

Images can also be assessed using second-order statistics, similar to the following joint probability:

$$P_{ij} = \Pr(I(r, c) = i \cap I(r + \Delta r, c + \Delta c) = j) \quad (5)$$

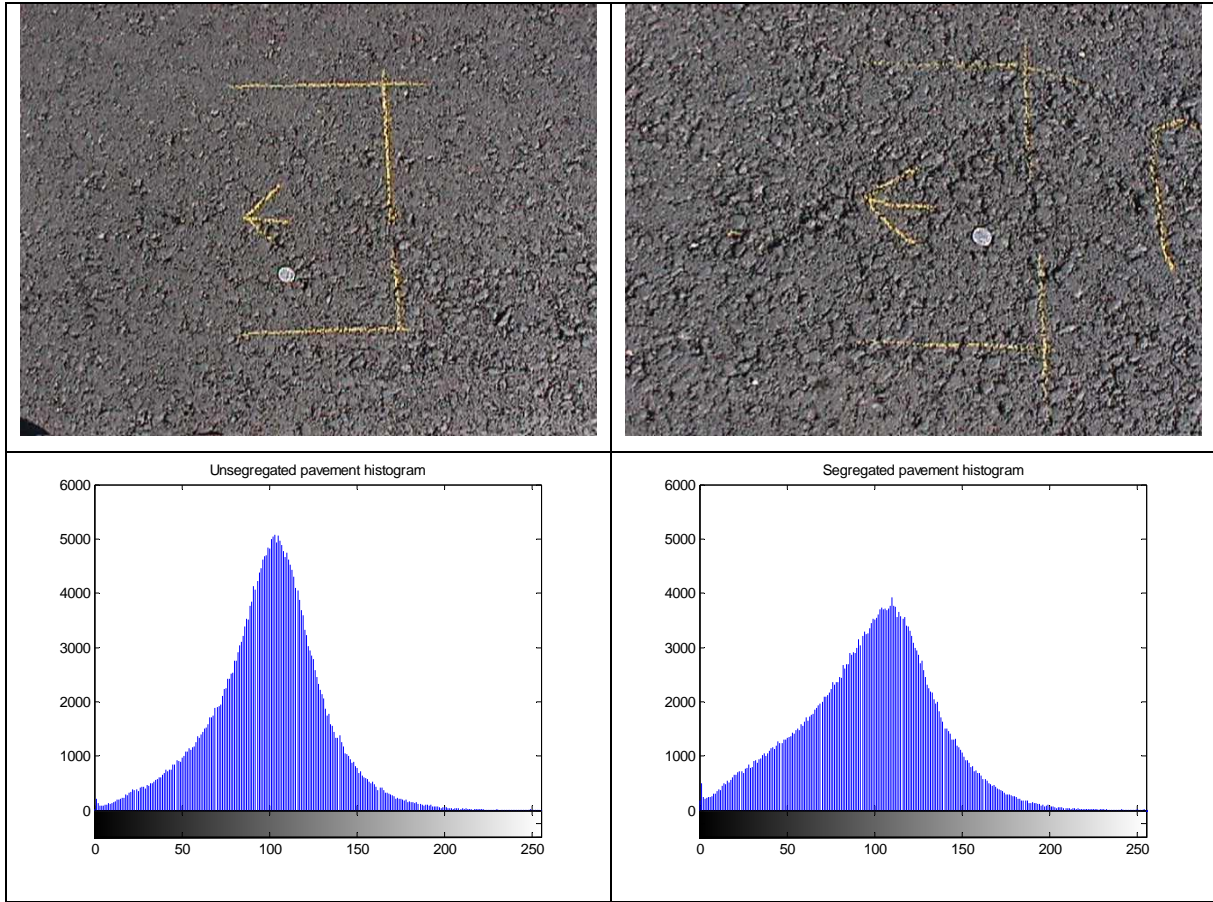


**FIGURE 6 Un-segregated and segregated pavements**

This concept is used in the Gray-level Co-occurrence Matrix (GLCM), which gives intensity information in pixel “pairs”, with a displacement vector  $d = (\Delta r, \Delta c)$ . The GLCM is equal to

$$C(i, j) = \frac{1}{M} [a_{i,j}] \quad (6)$$

where

$i$  = intensity value of the pixel in row “ $r$ ” and column “ $c$ ”

$j$  = intensity value of the pixel in row “ $r+\Delta r$ ” and column “ $c+\Delta c$ ”

$C$  = co-occurrence matrix

$M$  = # different pixel pairs and

$a_{i,j}$  is the number of times  $I(r,c)=i$  and  $I(r+\Delta r, c+\Delta c)=j$

Coarse textures result in GLCM arrays with large values along the diagonal, whereas fine textures tend to cause GLCM values to be spread out from the diagonal. Using the GLCM results, parameters such as contrast, correlation, energy and homogeneity, among others, have been derived by machine vision researchers and have been used in many areas. Example application areas include aerial imagery, where it is useful to discriminate areas having natural vegetation, urban areas, and roads. GLCM-based analysis has also been used in the analysis of photomicrographs for the identification of identify different types of tissues and cells in medical investigations. Those principles are now being applied here to help us identify different surface types in newly constructed pavements to reach the objectives stated earlier. The formulas for these parameters are the following:

$$\text{Contrast} = \sum_{ij} P_{ij}^2 \quad (7)$$

$$\text{Energy} = \sum_{ij} |i - j|^2 P_{ij} \quad (8)$$

$$\text{Correlation} = \sum_{ij} \frac{(i - \mu)(j - \mu)P_{ij}}{\sigma^2} \quad (9)$$

$$\text{Homogeneity} = \sum_{ij} \frac{P_{ij}}{1 + |i - j|} \quad (10)$$

where

$\mu$  = gray level mean  
 $\sigma^2$  = gray level variance

The process used to calculate these parameters has to be simplified by the use of a scaled image. This is done by default in MATLAB to an eight level scaled image, and it also uses a spatial relationship of the pixel of interest, the pixel immediately to the right, also known as the displacement vector:

$$\vec{d} = (0,1) \quad (11)$$

When evaluating different processing alternatives, one of the parameters tested to understand the effectiveness of the filters included the effect of the separation of the spatial relationship, or displacement vector of the GLCM texture parameters. No significant difference was found in increasing this value, so all four of the textural parameters were computed with this vector to help discriminate between the different visual texture characteristics of pavement surfaces.

## FIELD TESTING

Testing of the system was conducted at the Virginia Smart Road, which is a controlled traffic facility with seven different variations of surface textures in twelve asphalt pavement sections. These surface types include five different SUPERPAVE mixtures, a 12.5 mm stone mastic asphalt (SMA), and a 12.5 mm open-graded friction course (OGFC). Additionally, there are three other different pavement surfaces on this test road without mix properties: the first one referred to as “the Loop”, a Portland Cement Concrete (PCC) bridge where the road goes over Janelle Road between sections D and E, and at end of the asphalt sections, a continuously reinforced concrete pavement (CRCP) section that has a texturized surface.

Table 1 presents some of the mix properties of the different HMA surface types of all the sections in the Smart Road. The table shows the differences in mixes, aggregate size, binder type, and in one case, section I, higher (h) compaction was applied. Other mix characteristics listed are the asphalt content (Pb), air voids (VTM) and voids in the mineral aggregate (VMA). All of these properties indicate different mix characteristics in between most sections, even those with the same mix type, as in the case for sections B, E, F, G, H, and J; all under a SM-9.5D mix classification. Even though the aggregate sizes are the same, the asphalt content, and percent air voids and VMA are different.

Previous research performed (11, 12, 13 and 14) investigated the use of a laser inertial road profiler macrotexture measuring device to test its capability to detect and measure segregation as proposed by an NCHRP study (3). A direct comparison of both methods is now possible by comparing their results at the Smart Road. The macrotexture measurements consist of scans obtained every 5 feet in the left wheel path (LWP) and between wheel paths (BWP), while the visual measurements are the result calculating the four texture parameters (contrast, correlation, energy and homogeneity) resulting from the GLCM calculations,

for every frame on a run with the 12.5 mm lens capturing digital images every 10 feet. These results were plotted in the first plot of Figure 7, with the visual texture scale on the left side and the macrotexture scale in millimeters on the right side.

**TABLE 1 Smart Road Mix Types**

Section	Mix	Binder	NMS	MS	Pb	VTM	VMA
Loop	SMA-19/12.5						
A	SM-12.5D	PG 70-22	9.5	12.5	5.9	5.8	17.9
B	<b>SM-9.5D</b>	PG 70-22	9.5	12.5	6.7	8.6	17.1
C	SM-9.5E	PG 76-22	9.5	12.5	8.4	5.9	18.0
D	SM-9.5A	PG 64-22	9.5	12.5	8.6	1.9	15.5
Bridge	PCC						
E -H	<b>SM-9.5D</b>	PG 70-22	9.5	12.5	5.9	4.8	16.2
I	SM-9.5A(h)	PG 64-22	9.5	12.5	5.4	1.1	12.8
J	<b>SM-9.5D</b>	PG 70-22	9.5	12.5	4.9	10.6	19.7
K	OGFC	PG 76-22	12.5	19	5.5	22.4	34.4
L	SMA-12.5D	PG 70-22	12.5	19	6.8	7.3	21.1
CRCP	PCC						

While both methods measure visible differences between the different pavement section surfaces, it is not very clear with macrotexture measurements where the different sections begin or end. In contrast, the digital image method presented here clearly shows abrupt “breaks” in its parameters, especially in correlation and energy, allowing a clearer distinction of the boundaries between the different types of pavement surfaces. This is also very apparent when reviewing the individual frames of adjacent sections through the camera viewer. The macrotexture method has marked differences found in the texture on the wheel path and that in between wheel paths due to the densification under traffic (see sections C and D on the plot).

On the second plot, the digital image results were taken separately and vertical lines were drawn to separate the different sections, with their appropriate labeling. Clear-cut differences are seen between the loop, sections A, B, C, D and the bridge. Starting with section E through H, the parameters calculated fail to discern clearly between the different sections, as is to be expected, because there are no construction joints or change in the surface mix type. After the start of section I, it is again obvious by the sharp cuts in the parameters, that there are more differences between sections I, J, K, L and the final concrete section.

These empirical results have demonstrated the applicability of the method. The task at hand is to utilize these texture measures in the design of a classifier that can distinguish different pavement types automatically (or semi-automatically). Decision boundaries can be found in a feature space that depends directly on acceptable values of contrast, correlation, energy and homogeneity. By carefully tuning these boundaries, it should be possible to use this system effectively in the identification of non-uniformity or segregation in recently paved projects. With the start of the 2006 paving season, possible research sites have been identified and data logging is being done on them to test these ideas to reach the ultimate goal. Real paving projects will allow the assessment that is needed to refine the system for eventual use as a quality assurance tool.



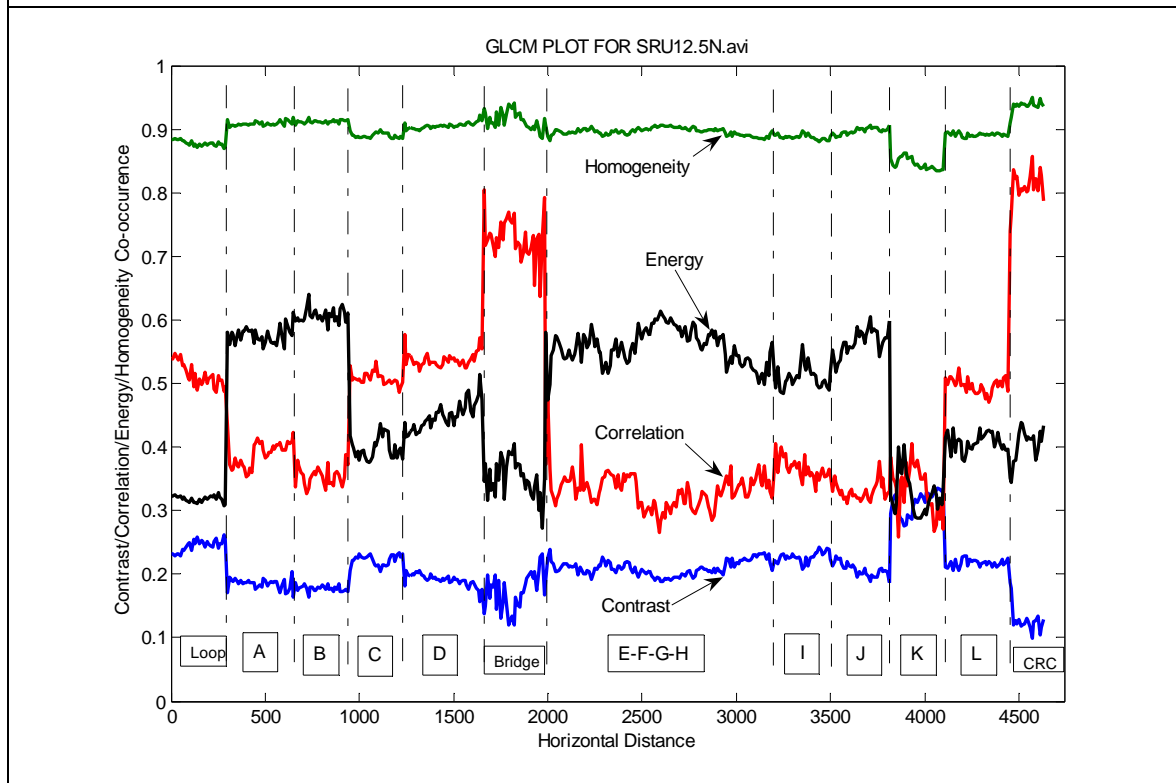
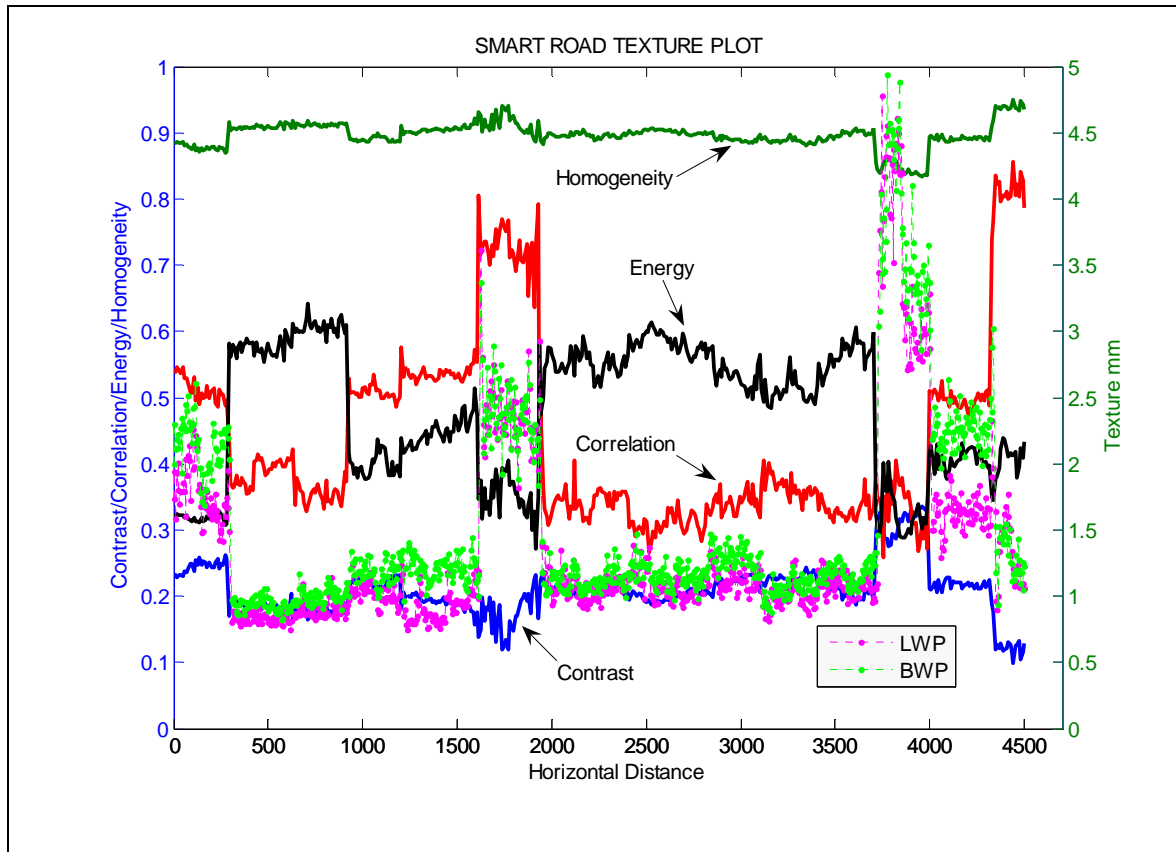


Figure 7 Smart Road Profiler Texture Plot

## **CONCLUSIONS AND RECOMMENDATIONS**

A system has been developed which uses digital visible-light image technology to detect non-uniformities in HMA. Ultimately, this system should make it possible to discriminate areas where segregation is suspected, and to identify these areas along a road for HMA quality assurance purposes. The system uses relatively low cost off-the-shelf components for capturing images of new pavements and applies innovative image processing and analysis software for detecting and quantifying segregated areas. The image analysis uses a Gray Level Co-occurrence Matrix (GLCM), commonly used in visual texture analysis, to compute various different parameters that characterize surface texture. Measures of contrast, correlation, energy, and homogeneity, are used to discriminate areas having different texture characteristics in the pavement surface.

Testing of the system at the Virginia Smart Road has demonstrated that the system has the potential to identify different types of pavement surfaces better than the inertial laser profiler method tested previously. Tests on a number of new construction projects are currently in progress. These will indicate whether the system can also identify non-uniformities on new construction projects. If segregation can be detected properly, the use of such a system can help improve the quality of the HMA layers and enhance pavement performance, increasing pavement service life and reduce down time from repair work.

## REFERENCES

1. Flintsch, G.W., McGhee, K.K., and de León, E., Field Validation of Macrotexture-Based Hot Mix Asphalt Segregation Detection Methods, *Journal of Association of Asphalt Paving Technologists*, Volume 74, 2005, pp 1-21.
2. Information provided by Merrill Zwanka, State Materials Engineer, South Carolina Department of Transportation, June 28, 2002, and Ken Fults from Texas DOT on June 10, 2002.
3. Stroup-Gardiner, M. and E. R. Brown. *NCHRP Report 441, Segregation of Hot-Mix Asphalt Pavements*. TRB, National Research Council. Washington, DC, 2000.
4. Khedaywi, T. S. and T. D. White. Effect of Segregation on Fatigue Performance of Asphalt Paving Mixtures. In *Transportation Research Record: Journal of the Transportation Research Board, No. 1543*, TRB, National Research Council. Washington, DC, 1996, pp. 63-70.
5. Clemeña, G. and Howe, R. An Assessment of the Feasibility of Developing and Implementing an Automated Pavement Distress Survey System Incorporating Digital Image Processing. Virginia Transportation Research Council Research Report No. VTRC 98-R1, Charlottesville, VA, 1998.
6. Gransberg, D.D., Karaca, I., and Burkett, W.R. Quantifying Seal Coat Surface Condition Using Digital Image Processing Based on Information Theory. In *International Journal of Pavement Engineering*. Taylor and Francis, London, UK, 2003, Vol. 3, No. 4/25, pp. 197-205.
7. Al-Qadi, I. L. and Lahouar, S., Use of GPR for thickness measurements and quality control of flexible pavements, *Journal of Association of Asphalt Paving Technologists*, Volume 73, 2004, pp 657-687.
8. *Basler A 310f User's Manual*, Basler Vision Technologies, Exton, Pa., 2004, pp 3-23.
9. MATLAB Image Processing Toolbox (2005), The Math Works, Inc., Natick, Massachusetts.
10. Haralick, Robert, and Shapiro, Linda. *Computer and Robot Vision, Volume 1*. Addison-Wesley Publishing Company, Inc., Reading, Massachusetts, 1992.
11. Flintsch, G.W., de León, E., McGhee, K.K., and Al-Qadi, I.L. Pavement Surface Macrotexture: Measurement and Application. In *Transportation Research Record: Journal of the Transportation Research Board, No. 1860*, TRB, National Research Council, Washington, D.C. 2003, pp. 168-177.
12. McGhee, K.K., Flintsch, G.W., de León, E., "Using High-Speed Texture Measurement to Improve the Uniformity of Hot-Mix Asphalt", Technical Report VTRC 03-R12, Virginia Transportation Research Council and Federal Highway Administration, May 2003. 23 pp.
13. McGhee, K.K., Flintsch, G.W., and de León, E., Detecting and Measuring Hot-Mix Asphalt Segregation using High-Speed Texture Measurement. Paper 04-3827 in *Transportation Research Board 83<sup>rd</sup> Annual Meeting*. CD-ROM. Transportation Research Board of the National Academies, Washington, DC., 2004.
14. Flintsch, G.W., McGhee, K.K., and de León, E., 2003, Use of Surface Macrotexture Measurements to Detect Segregation. In *International Conference on Highway Pavement (IHP) Data, Analysis and Mechanistic Design Applications*. CD-ROM, September 8-10, 2003.

# Application of Digital Image Technology to Measure Hot Mix Asphalt Homogeneity

By Edgar de León Izeppi<sup>1</sup> and Gerardo W. Flintsch<sup>2</sup>

## Abstract

This paper describes the analysis procedure developed for a digital video system that has been developed at Virginia Tech for evaluating uniformity of newly constructed pavements. The system consist of a single classifier that can distinguish different pavement textures automatically (or semi-automatically) to provide inspection personnel the exact location of possible non-uniformities that require closer inspection.

The video system uses image analysis with a Gray Level Co-occurrence Matrix (GLCM), commonly used in visual texture analysis, to compute the various parameters that characterize surface texture. However, a translation was needed to provide field personnel a clear output, based on multivariate analysis, as to the exact location and degree of non-uniformity that could be expected at different points in the road.

Because night operations are becoming increasingly popular to perform most of the road work, the system had already been designed to work at night. The design of the classifier also needed to be efficient and fast to allow the inspection immediately after the capturing of the images.

The developed procedure uses multivariate statistics, with Principal Component Analysis, to integrate and visualize the multi variable data. Principal Components made from a linear combination of the original variables are combined into a single parameter, Hotelling's  $T^2$  statistic, to create a single statistic that can be more easily interpreted and understood.

**Key Words:** Hot-mix asphalt, Surface texture, multivariate analysis, segregation, quality assurance.

<sup>1</sup> Graduate Research Assistant, and <sup>2</sup>Associate Professor, Virginia Tech

## **Introduction**

### ***Background***

One of the most challenging aspects for the agencies responsible of road maintenance and construction operations is the need to evaluate a contractor's final product for payment purposes. In house or contracted personnel, with different levels of experience, evaluate the pavement's final quality in accordance to the construction specifications governing the contracted work. Due to the high traffic volumes on the roads, there exists a lot of pressure by the users on these facilities to perform the necessary work as soon as possible, preferably at night, to minimize delays and interruptions.

Paving Contractors that manufacture Hot Mix Asphalt (HMA) follow a very specialized process that can be affected by changes in temperature, weather, traffic and other uncontrollable events that can interrupt its continuity, which may introduce non-uniformities in the process. Commonly referred to as HMA segregation, these non-uniformities are usually associated to varying degrees of negative pavement performance, and can exhibit different characteristics inherent to its specific cause, but usually appear as spots on the road where it is apparent that the aggregate particles have either become dislodged or are intricately closer than the ones in neighboring places. During the inspection process, experienced highway personnel can detect these non-uniformities by observing the texture of the mix in these areas and comparing it with a normal area. However, in difficult situations as the ones encountered in high volume roads or during night construction, human subjectivity, eye fatigue, and environmental factors can adversely affect the observations.

A new imaging system has been developed to help inspectors detect non-uniform HMA areas. The system uses relatively off-the-shelf components for capturing images of new pavements and applies innovative image processing and analysis software for detecting and quantifying areas where non-uniformities are present and require further closer inspection. The system also has the advantage of providing a permanent record of captured images of the final pavement condition, which if needed, could also be

evaluated later and compared to images obtained from the same pavement at later stages in its life.

### ***Problem Statement***

A digital imaging system that captures images of newly constructed pavements has been developed and testing of it at the Virginia Smart Road has demonstrated that the system has the potential to identify different types of pavement surfaces better than the inertial laser profiler method currently in use (1). The image analysis uses a Gray Level Co-occurrence Matrix (GLCM), commonly used in visual texture analysis, to compute various different parameters that characterize surface texture (2). Measures of contrast, correlation, energy, and homogeneity, can be used to discriminate areas having different texture characteristics in the pavement surface. However, for field personnel implementation purposes, it required the design of a single classifier that could distinguish different pavement types automatically (or semi-automatically) and provide clearly defined boundaries to alert inspection personnel to the exact location of possible non-uniformities that required closer inspection. By carefully tuning these boundaries, this system can be used effectively in the identification of non-uniformity or segregation in recently paved projects. The system could also eventually be incorporated in performance-based specifications.

### ***Approach***

During the 2006 paving season, research sites were identified and digital images were collected from real paving projects. The recorded data allowed testing the system capabilities and the derivation of a method to conjugate one single parameter to evaluate non-uniformity. The method uses Principal Component Analysis, which is commonly used in multivariate statistical work to visualize data that has many variables. The single classifier used is Hotelling's  $T^2$  statistic. This statistic is used to develop a road profile that can be used in the final inspection process, to identify possible locations of non-uniformities along a road segment. The profile developed outputs different levels of probability of finding non-uniformities, by comparing the totality of the images under analysis. The user of the system can therefore define the level of significance that he wants to use in his analysis.

### ***Objectives and Scope***

The objective of the study was to develop a profile of a single classifier that clearly defined the possible location of the different levels of non-uniformities along a project. This classifier was to be based on Principal Component Analysis of the four parameters obtained from the digital image texture analysis. This profile had to be able to convey information useful for quality assurance purposes, fast and efficiently during night time operations.

### **Methods**

#### ***Visual Texture Analysis Results***

The study captured digital images at highway speeds along a series of recently paved projects in Montgomery County, Virginia, during the beginning of the 2006 paving season. A series of recently paved projects was selected to develop and test the methodology. The results of the analysis of the visual textural properties calculated from digital images recorded by the system were adapted to support the road construction inspection process. The developed process is illustrated with an example that is presented throughout the paper. All the images were collected after sundown to eliminate incorporating non-uniformities that could affect the quality of the images due to shadows, etc.

The system captures an area for analysis in each frame of about 41 by 31 inches. The camera has a resolution of 640 x 480 pixels (picture elements) and a capability of recording up to 80 frames per second. This allows the frame grabber software system to record images up to every foot at highway speeds of 55 mph. The volume of images used can be adjusted by increasing/decreasing the data collection frequency as needed.

After collecting the images, the system analyzes each frame and computes four visual texture parameters: homogeneity, energy, correlation, and contrast. This creates a problem for a user when he tries to visualize data with so many variables and very different magnitudes, even though the data is all in the same range of zero to one. One solution is to plot all the variables in one figure, as they vary in the project as shown in FIGURE 1.

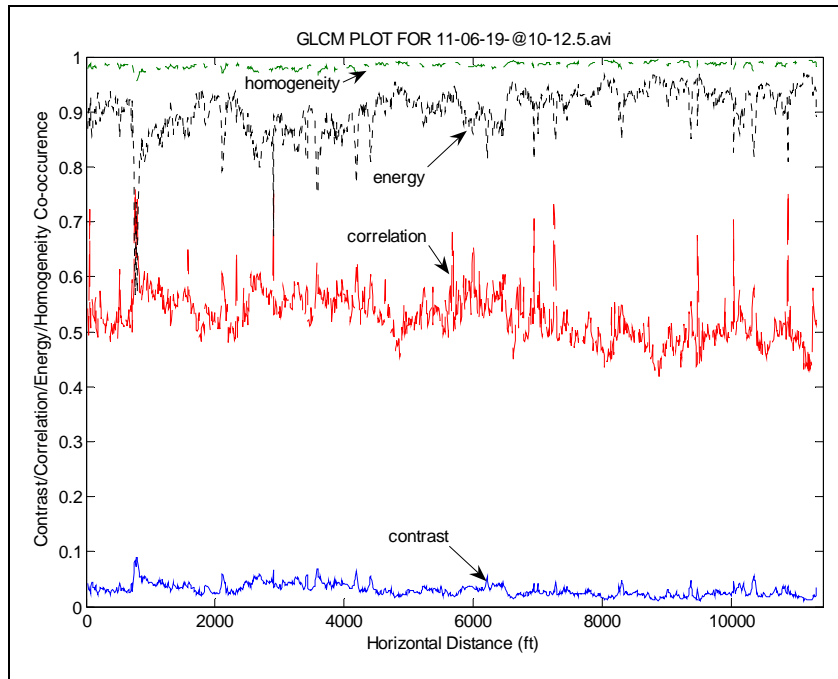


**FIGURE 1 GLCM Plot for Project 11-06-19**

For the example, the system collected 1,130 images every 10 feet; the analysis was done in less than 15 minutes. Several very noticeable “non-uniform” segments can be subjectively identified by the peaks in the plotted values of the parameters, especially at the beginning and the end of the plot, and around the 800 and the 2,900 feet mark. However, upon further scrutiny, it can be noticed that there are several other locations of smaller peaks where it is not so clear if they warrant closer inspection. Analyzing all the variables at once becomes very difficult, especially since the values of these measurements are not easy to understand.

***Principal Component Analysis***

Multivariate statistics make use of Principal Component Analysis as a method to better understand and visualize data that have many variables. This is possible because usually several of the multiple variables are dependent and measure the same behavioral characteristic of the system. Principal Component Analysis generates a new set of variables called *principal components* made from a linear combination of the original



variables. Finding a least-squares solution and using orthogonal components reduces unnecessary dimensions of a problem (3).

The size of the full set of principal components is the same as the number of original variables, but because the variance for each new variable is the maximum possible for all possible choices in each new axis, possible eliminations can be performed, allowing the variability of the data to be effectively visualized with only the first few components. TABLE 1 shows the coefficients obtained for each of the variables and the percent of the variability explained by each new component obtained for our example after computing the principal component analysis. Notice that there is more than 99.8 % of the variability explained with just the first two components.

**TABLE 1 Principal component coefficients and % variability**

	1 <sup>st</sup> comp	2 <sup>nd</sup> comp	3 <sup>rd</sup> comp	4 <sup>th</sup> comp
Contrast	-0.1683	0.2121	-0.8525	-0.4472
Correlation	-0.7161	-0.6973	-0.0321	0.0000
Energy	0.6722	-0.6764	-0.3010	0.0000
Homogeneity	0.0841	-0.1060	0.4262	-0.8944
% Variability	91.8 %	8.1 %	0.1 %	0.0 %

***Visualizing the Results of the Principal Component Analysis***

When multiplying each of the values of the original variables by the corresponding computed coefficient of each of the principal components, we obtain the original data mapped into a new coordinate system defined by the principal components. As explained before, a two dimensional plot (FIGURE 2) can now let us visualize more than 99.8% of the variability of the data.

The first principal component is the horizontal axis and the second principal component is the vertical axis. Each of the 1,130 data points are shown in this plot. The new values obtained with the computed coefficients have a mean of zero in each of the principal components, so the farther away from the origin that a data point is, the more variability it has and therefore is a possible source of non-uniformity in the pavement. If all points would fall in the origin, we would have a perfectly homogenous pavement with no visual variability; hardly the case found in HMA pavements.

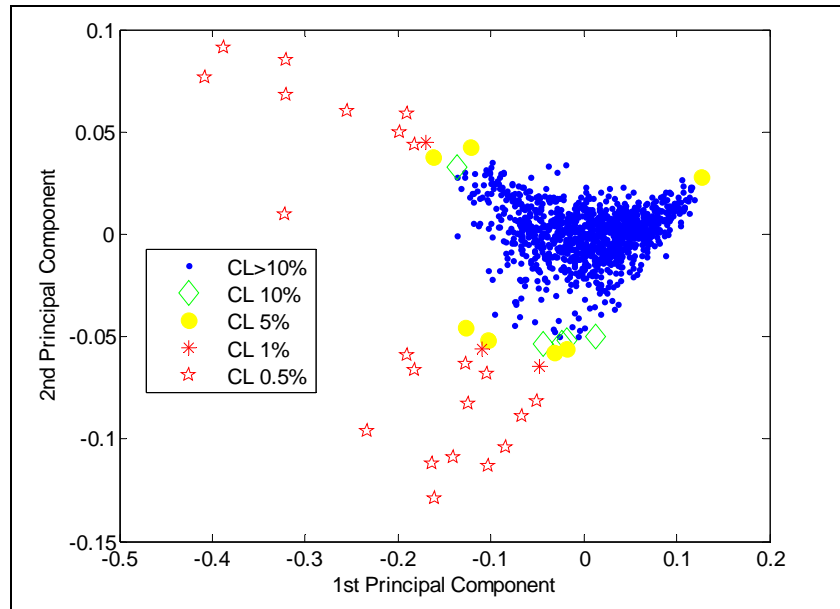


**FIGURE 2 Two dimensional principal component data plot**

### *Hotelling's $T^2$ Statistic*

A new computation is now required to try to scale the variability of the observed data points, relative to each other. A Hotelling's  $T^2$  chart is the most widely used multivariate procedure to control changes in the mean vector of  $p$  correlated quality characteristics (4). Hotelling's  $T^2$  is a statistical measure of the multivariate distance of each observation from the center of the data set. It is an analytical method to find the most extreme points in the data set (5).

Hotelling's  $T^2$  statistic is used to differentiate the individual data points where 4 different parameters converged before into a new single objective "score" that could identify non-uniformity in the pavement images. In FIGURE 2, the different confidence levels shown in different colors were obtained by comparing the computed Hotelling's  $T^2$  values to Chi-square values with 4 degrees of freedom for  $\alpha$  value for 0.005, 0.01, 0.05 and 0.10 confidence levels. The red marks indicate clearly non-uniform locations. However, this plot is still not very helpful for road inspection personnel to locate the non-uniform areas in the field. Tabulating the information proved more useful.

***“Uniformity” Profile with Hotelling’s T<sup>2</sup> Statistic***

The specific location of the non-uniformities along the road segment is very important to alert inspection personnel when performing quality assurance tests required by the specifications. TABLE 2 the various locations where there is a high degree of probably (confidence level) of having a non-uniform area.

**TABLE 2 Hotelling’s T<sup>2</sup> statistical data with location**

<b>Station</b>	<b>Hotelling’s T<sup>2</sup></b>	<b>Confidence Level</b>
<b>50</b>	<b>52.5</b>	<b>99.5</b>
740	10.2	95
<b>750</b>	<b>41.7</b>	<b>99.5</b>
<b>760</b>	<b>333.6</b>	<b>99.5</b>
<b>770</b>	<b>19.4</b>	<b>99.5</b>
<b>780</b>	<b>99.9</b>	<b>99.5</b>
<b>790</b>	<b>241.7</b>	<b>99.5</b>
<b>800</b>	<b>102.5</b>	<b>99.5</b>
<b>810</b>	<b>20.2</b>	<b>99.5</b>
820	8.2	90
1580	12.0	95
<b>2330</b>	<b>17.8</b>	<b>99.5</b>
<b>2900</b>	<b>143.9</b>	<b>99.5</b>
<b>3580</b>	<b>15.0</b>	<b>99.5</b>
3590	13.8	99
4190	11.2	95
<b>5670</b>	<b>42.5</b>	<b>99.5</b>
<b>5680</b>	<b>25.2</b>	<b>99.5</b>
<b>5690</b>	<b>35.2</b>	<b>99.5</b>
5740	10.3	95
<b>6000</b>	<b>18.4</b>	<b>99.5</b>
6010	11.4	95
6690	8.1	90
6720	13.3	99
6780	8.5	90
<b>6940</b>	<b>33.6</b>	<b>99.5</b>
7030	9.1	90
<b>7250</b>	<b>63.4</b>	<b>99.5</b>
<b>7260</b>	<b>45.1</b>	<b>99.5</b>
7270	13.7	99
8200	7.7	90
8880	9.8	95
<b>9480</b>	<b>26.6</b>	<b>99.5</b>
<b>9490</b>	<b>21.0</b>	<b>99.5</b>
<b>10040</b>	<b>22.1</b>	<b>99.5</b>
<b>10880</b>	<b>81.4</b>	<b>99.5</b>
11260	9.6	95

The table suggest that it would be important to check various road segments, as well as individual locations, where the confidence level is presumed very high, indicating a high probability of finding non-uniformities in the pavement. The specific questionable locations are between the following stations:

- 750-810
- 5670-5690
- 7250-7260
- 9480-9490

FIGURE 3 shows a plot that illustrates the data listed on TABLE 2. It has the advantage that it is easily understood because it has minimized the multivariate data (reduced to one value) and shows possible locations of non-uniformities.

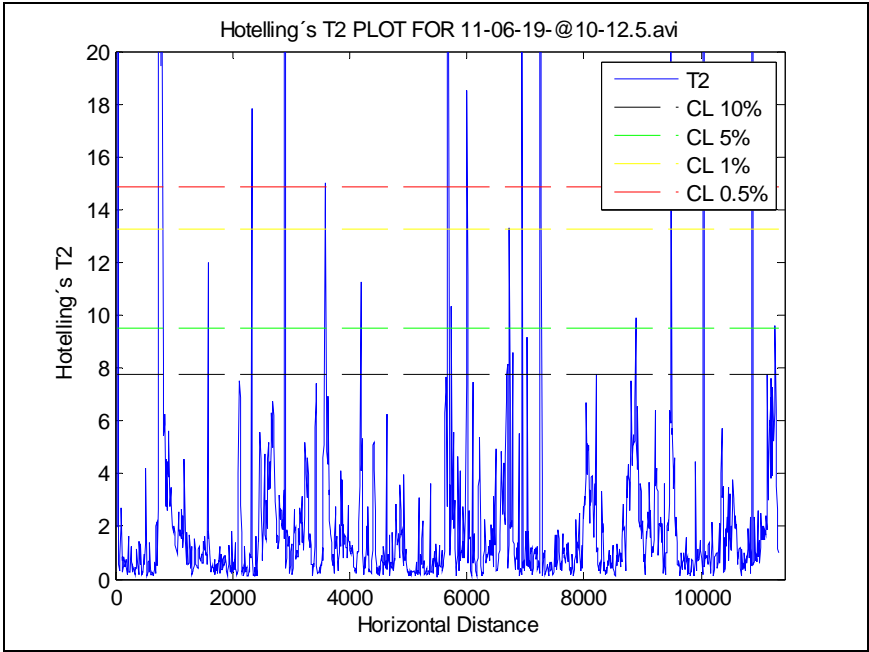


**Figure 3 Non-uniformity plot at different confidence levels**

After processing and analyzing the collected images, the inspection personnel have a list of locations, associated with a certain confidence level, where they can expect that there is a certain probability that non-uniformities might be present. The second part of the analysis takes less than one minute.

## FINDINGS AND DISCUSSION

### *Field Inspection Results*

With the previously computed data and plots, a detailed visual inspection was carried out during the day to verify the condition of the locations indicated by the system output. The following images illustrate some of the results found.

#### *Stations 750-810*

This segment of the project had the highest  $T^2$  statistics computed. Referring to FIGURE 4, upon close inspection of the video image, a different texture pattern was found. It is not very clear in the captured image because the light conditions make it difficult, but it became very evident during the day inspection, as can be seen on FIGURE 5.

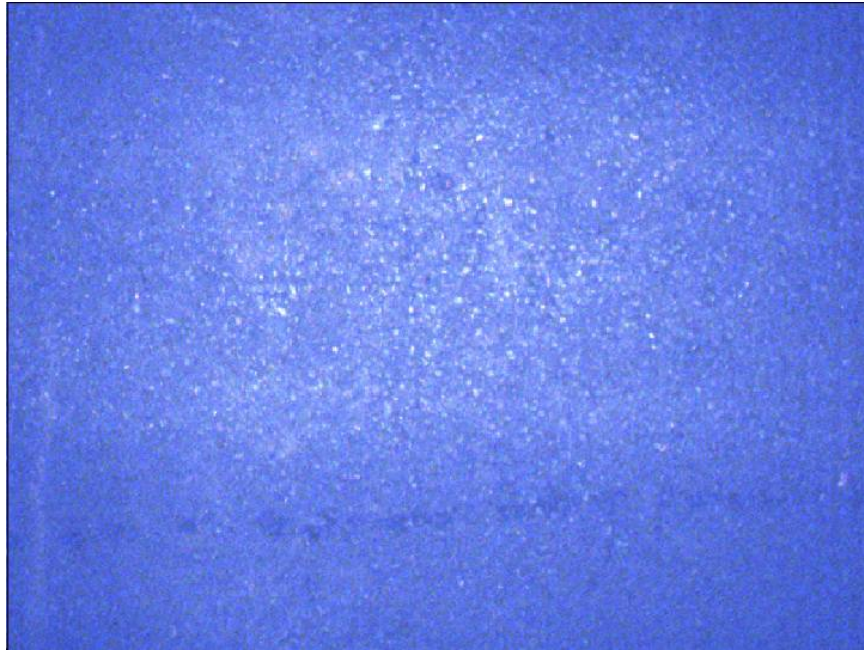


**FIGURE 4 System image captured at night, station 760**



**FIGURE 5 Day image captured during inspection, station 760**

FIGURE 5 clearly shows a difference in the texture, probably caused in the compaction process, being distinctly different from surrounding mat. There are also some noticeable long brighter markings. FIGURE 6 illustrate two other of these long markings found in the same area.

*Station 2900*

FIGURES 7 and 8 show similar images at station 2900, where a large segregated area can be observed. At these locations, inspection personnel would have had to perform density and other tests to determine the severity of the segregation and order the corrective measures, if needed, that the contractor had to perform before payment.

*Final Remarks*

In general, most locations listed on TABLE 2 had different visual conditions that made them different from the other images taken. Some evidenced clear non-uniformity conditions that clearly deserved major attention by the inspecting personnel, as was probably the case.



**FIGURE 6 Day images of Non-uniform area**



**FIGURE 7 Station 2900 night image**



**FIGURE 8 Station 2900 day picture**



However, other locations simply had other non-critical conditions caused by other factors. Examples of this are locations where locations with dirt roads coming right to the edge of the pavement, where a vehicle coming on to the asphalt sometimes carries part of the dirt, usually of a clearer color than the pavement, triggering different values of visual texture. These areas are wrongly identified by the system as having a different texture. Thus, it is important to conduct the image acquisition phase as soon as possible after construction.

## **CONCLUSIONS AND RECOMMENDATIONS**

The findings from this study confirmed that the digital imaging system has great potential to identify non-uniformities on recently completed road maintenance and construction operations.

Although the number of projects on which the system was tested was very limited, the tests suggest that the system can help the inspection process, especially during night operations. The system also creates a permanent record that will allow maintaining the means to evaluate the condition of the pavement, for comparison purposes, during its service life after the initial work.

However, in some cases traffic and other factors, e.g., lane markings, can alter the initial visual conditions and modify the analysis flagging areas because of surface conditions that do not necessarily have an impact on the pavement's performance. Thus, it became evident that the image acquisition phase would be most effective if done as soon as possible after the construction operations are finished.

It is also strongly recommended to test the system with different pavement mixes and construction conditions. This would be beneficial to determine what can be done to the paving operations to eliminate some of the non-uniformities that have the potential to become areas with bad pavement performance.

## REFERENCES

1. Flintsch, G.W., McGhee, K.K., and de León, E., Field Validation of Macrottexture-Based Hot-Mix Asphalt Segregation Detection Methods, *Journal of the Association of Asphalt Pavement Technologists*, vol. 74, 2005, pp. 1-21.
2. de León, E., Flintsch, G.W., and Abbott, A.L., Measuring the Uniformity of Hot Mix Asphalt Pavements with Digital Image Technology, *paper #07-1613 submitted for publication for the 86<sup>th</sup> Meeting of the Transportation Research Board*, Washington, D.C., 2007.
3. Duda, R., Hart, P., and Stork, David. *Pattern Classification*. John Wiley and Sons, Inc., New York, 2001.
4. Aparisi, F and Haro, C., Hotelling's T2 control chart with variable sampling intervals, *International Journal of Production Research*, 2001, Volume 39, Number 14, pp 3127-3140.
5. MATLAB Statistics Toolbox (2005), The Math Works, Inc., Natick, Massachusetts.

# High-Speed, Noncontact Digital Imaging System for Inspection of Hot-Mix Asphalt Pavements

By Edgar de León Izeppi<sup>1</sup> and Gerardo W. Flintsch<sup>2</sup>

**Abstract:** This paper discusses the results of the field experimentation of a new system developed to help inspect the construction of asphalt pavements using digital video images. The system computes the gray level co-occurrence matrix (GLCM) of images of newly constructed pavements to find various parameters that are commonly used in visual texture analysis. Using principal component analysis to integrate multivariable data into a single classifier, Hotelling's  $T^2$  statistic, the system creates a list of the location of possible nonuniformities that require closer inspection.

A total of 18 continuous road segments of recently paved roads were tested and analyzed with the system. These road segments allowed the refinement of the methodology and the software needed to produce tables and plots that will be used by inspection personnel in the field. The results demonstrated the capability of the system for detecting potential nonuniformities of recently completed pavements that can be used in the final inspection process. More testing is recommended under actual construction conditions to verify the system's capabilities.

**Key Words:** hot-mix asphalt, surface texture, multivariate analysis, segregation, quality assurance.

<sup>1</sup> Graduate Research Assistant, Virginia Tech Transportation Institute, 3500 Transportation Research Boulevard, Blacksburg, VA 24061, Tel. (540) 231-1504, Fax (540) 231-1555, E-mail: [edeleoni@vt.edu](mailto:edeleoni@vt.edu)

<sup>2</sup> Associate Professor, Virginia Tech, 3500 Transportation Research Boulevard, Blacksburg, VA 24061, Tel. (540) 231-1569, Fax (540) 231-1555, E-mail: [flintsch@vtti.vt.edu](mailto:flintsch@vtti.vt.edu)

## Introduction

In recent years, urban population growth has catapulted travel and freight needs into a high level of dependency on automobiles and the roads over which they travel as hardly experienced before. It used to be common for working parents to drive only 10 to 15 minutes to get to work. Children would walk or use a bike to go to school, trips to the grocery store were usually made once a week, and most after-school and after-work activities would be relatively close to home. Today, this is usually not the case for most people living in rural or urban areas, where any of these activities can take place tens of miles away and it is not uncommon to spend several hours a day driving back and forth to accomplish them. These conditions have augmented the pressure that personnel responsible for highway operations are faced with every day.

According to the asphalt industry, more than 90% of the existing paved roads are built with asphalt, and hot-mix asphalt concrete, or HMA, is the paving material most used by the asphalt industry to construct and maintain these roads (Asphalt Education Partnership 2006). HMA pavements are designed and constructed to withstand the expected traffic and environmental conditions of a particular road section. The goal is to build roads that are durable, safe, and comfortable to ride. However, roads deteriorate with use and require appropriate maintenance to sustain the level of service expected by users. Since these users are paying the taxes that pay for the maintenance, they also exert a lot of pressure to make responsible agencies perform any necessary work as soon as possible and preferably at night to minimize delays and interruptions.

To achieve this, the paving industry has had to adapt to these changing conditions, and it is not unusual now for contractors in Virginia to perform nighttime paving operations, working very long night shifts, especially on heavily traveled roads, to get the job done in the few summer months when this work can be performed. Agencies, on the other hand, operate on fixed day shifts with equally fixed budgets; they usually resist paying for overtime. A trend can be observed in which the more experienced inspection personnel are moving to consulting companies that are not bound by overtime restrictions, allowing them to obtain greater compensation for the extra time required to perform the inspections and supervisory tasks involved in the paving operation. This phenomenon is creating a huge vacuum inside agencies when that experience acquired over the years is no longer staying in-house or being transferred to the new personnel, which in turn is forcing agencies to continue contracting the inspection work.

Compounding the problem is the fact that HMA road construction operations, just as in most industrial processes, involve many potential sources of variability that could result in unacceptable end product quality. Improper aggregate handling, storage, loading or paver operations are just some of the many possible sources of variability. They are responsible for creating a lack of homogeneity (uniformity) in the HMA components, commonly referred to as segregation, which lead to accelerated pavement distress (Stroup-Gardiner and Brown 2000). Depending on its specific cause, the indications of segregation will vary, but they will usually manifest themselves as spots on the road where it is apparent that the aggregate particles are either farther apart or much closer together than the ones in the neighboring areas. Experienced personnel can easily pinpoint these areas by comparing the texture of the mix with that in normal areas. However, paving operations are now usually performed in areas with very high traffic volumes, at night, and under precarious environmental conditions where human subjectivity and eye fatigue can adversely affect the observations. This situation is further complicated if the

personnel performing the inspections lacks the necessary experience. Because the nighttime work trend can only be expected to continue, inspection methods have to improve to properly assess the quality and performance of roads in the future.

This research is a continuation of Virginia's research efforts to improve the uniformity of hot-mix asphalt (HMA) pavements, which started with previous work that developed a macrotexture based method (Flintsch et al. 2003). Although this method showed great promise, the results highlighted shortcomings in the equipment capability, such as the fact that because profilers measure very thin longitudinal lines, they may actually miss significant segregated areas (Flintsch et al. 2005).

## **Objective**

The objective of this paper is to propose and assess the results of a new system, developed and tested at the Virginia Smart Road, which automatically captures and analyzes images of newly constructed pavements to be used in the final inspection process of asphalt pavements. The system processes the images to obtain various parameters that characterize visual texture and develop a road profile of possible locations of nonuniformities. The system identifies, with a user-defined confidence level, the location of the places in the road where possible nonuniformities exist, indicating the degree of variability found in the final product. This characteristic makes the system ideally suited to develop a performance-based specification.

## **System Design**

### ***Hardware***

Figure 1 shows a picture of the system and its field of view. The system consists of a camera controlled by a computer connected to a distance-measuring instrument (DMI). To operate the system, the operator selects the frequency rate at which the images will be captured, every 10 feet for example, and the computer will trigger the camera using a signal from the DMI. The camera has a resolution of 640 x 480 pixels and can record up to 80 frames per second, so it is able to record images every foot at highway speeds of up to 55 mph. The volume of images collected can be adjusted by increasing or decreasing the data collection frequency. The typical field of view currently used by the system is a rectangular area about 30 by 40 inches. Larger images will be possible with wider illumination arrangements (de León et al. 2007).

### ***Image Processing and Analysis***

The system uses MATLAB Image Processing Toolbox® (2005) to process and analyze the acquired images. The captured color images are converted to a grayscale image in which each pixel has spatial coordinates in the two dimensions facing the camera and an associated intensity level (0 to 255). The analysis is performed using the gray level co-occurrence matrix (GLCM), which is commonly used in visual texture analysis (Haralick and Shapiro 1992).

Calculated GLCM's consider spatial relationships between texture and image intensity. This process is simplified by the use of a scaled image; MATLAB uses by default an eight-level scaled image. The probability (Pr) of any individual pixel in row  $r$  and column  $c$  having intensity  $i$  is independent of other first-order statistics, like marginal probability, and can be represented as:

$$P_i = \Pr(I(r, c) = i) \quad (1)$$

Comparing pixel pairs, images have second-order statistics with the following joint probability, where  $j$  is the intensity value of the pixel in row  $r+\Delta r$  and column  $c+\Delta c$ :

$$P_{ij} = \Pr(I(r, c) = i \cap I(r + \Delta r, c + \Delta c) = j) \quad (2)$$

GLCMs give intensity information in pixel pairs separated by a vector  $d = (\Delta r, \Delta c)$ . The gray level co-occurrence matrix  $C$  can now be defined as the matrix of occurrences for the pairs of intensities such that:

$$C(i, j) = \frac{1}{M} [a_{i,j}] \quad (3)$$

where  $M$  is the number of different pixel pairs,  $a_{ij}$  is the number of times  $I(r, c) = i$ , and  $I(r+\Delta r, c+\Delta c) = j$ .

For this system, the displacement vector used was for the pixel immediately to the right, or:

$$\vec{d} = (0,1) \quad (4)$$

Using GLCM results, a variety of several different parameters have been derived by machine vision researchers for use in aerial imagery, identification of tissue and cells, and other applications (Haralick and Shapiro 1992). Those same principles were used to calculate these parameters to differentiate variations in the types of surfaces represented in the images of newly constructed pavements. These parameters are:

$$\text{Contrast} = \sum_{ij} P_{ij}^2 \quad (5)$$

$$\text{Energy} = \sum_{ij} |i - j|^2 P_{ij} \quad (6)$$

$$\text{Correlation} = \sum_{ij} \frac{(i - \mu)(j - \mu)P_{ij}}{\sigma^2} \quad (7)$$

$$\text{Homogeneity} = \sum_{ij} \frac{P_{ij}}{1 + |i - j|} \quad (8)$$

where  $\mu$  = gray level mean and  $\sigma^2$  = gray level variance.

### ***Principal Component Analysis***

Multivariate statistics make use of principal component analysis (PCA) to better understand and visualize data that have many variables. This is possible because several of the multiple variables are usually dependent and measure the same behavioral characteristic of a system. Principal component analysis generates a new set of variables called *principal components* made from a linear combination of the original variables. Finding a least-squares solution and using orthogonal components reduces unnecessary dimensions of a problem (Duda et al. 2001).

The size of the full set of principal components is the same as the number of original variables, but because the variance for each new variable is the maximum possible for all possible choices in each new axis, possible eliminations can be performed, allowing the variability of the data to be effectively visualized with only the first few components. The system uses the MATLAB Statistical Toolbox® (2005) to perform all PCA and statistical computations.

### ***Visualization of the Results of the Principal Component Analysis***

When multiplying each of the values of the original variables by the corresponding computed coefficient of each of the principal components, the original data can be mapped into a new coordinate system defined by the principal components. If all points fell on the origin of the multi-component space, it would be the result of a perfectly homogenous pavement with no visual variability. This is hardly ever the case, but fortunately plotting the first two or three principal components produces an adequate visualization representing the patterns that explain most of the variance of a system. The new values obtained with the computed coefficients have a mean of zero in each of the principal components. This means that the farther away from the origin a data point is, the more variability it has with respect to the rest of the observed points. Although this concept could be used to represent some of the possible nonuniformities found in the road segment, it would not incorporate all the possible sources of variation that could be present in any particular observation. For this purpose, it was deemed necessary to incorporate all the possible sources of nonuniformities into a single classifier whose variations could be plotted or listed along a road segment indicating the possible locations of nonuniformities. The system uses Hotelling's  $T^2$  statistic as this single classifier.

### ***Hotelling's $T^2$ Statistic***

Statisticians have developed several techniques for analyzing data. Most analyses are performed through the use of statistical inferences, or conclusions made for a population based on measurements from a sample. The most widely used inferences are those made from population means. The validity of these inferences is based on the probability that a specific test value  $u_o$  is equal to the mean value of the population  $u$ . To solve this problem, a test of two competing hypotheses is made, where  $H_o$  is the null hypothesis and  $H_l$  is the alternative hypothesis, or  $H_o: u = u_o$  and  $H_l: u \neq u_o$ . If  $X_n$  measurements are made from a normal population, the most common test statistic used to solve this problem is the following:

$$t = \frac{(\bar{X} - \mu_o)}{s/\sqrt{n}} \quad (9)$$

where  $\bar{X} = \frac{1}{n} \sum_{j=1}^n X$  and  $s^2 = \frac{1}{n-1} \sum_{j=1}^n (X_j - \bar{X})^2$ . The test statistic has a student's  $t$ -distribution with  $n-1$  degrees of freedom (df). The test value  $u_o$  is rejected if the observed  $|t|$  exceeds a specified percentage point of the  $t$ -distribution with  $n-1$  df. It can easily be proven that if  $H_o$  is rejected when  $|t|$  is large,  $H_o$  will also be rejected when its square is large,

$$t^2 = \frac{(\bar{X} - \mu_o)^2}{s^2/n} = n(\bar{X} - \mu_o)(s^2)^{-1}(\bar{X} - \mu_o) \quad (10)$$

The variable  $t^2$  is the squared distance from the sample mean  $\bar{X}$  to the test value  $u_o$ . In 1931, Harold Hotelling applied this concept in its multivariate analog (Johnson and Wichern 2002) using the following:

$$T^2 = (\bar{\bar{X}} - \bar{\mu}_o)' \left( \frac{1}{n} \bar{S} \right)^{-1} (\bar{\bar{X}} - \bar{\mu}_o) = n(\bar{\bar{X}} - \bar{\mu}_o)' \bar{S}^{-1} (\bar{\bar{X}} - \bar{\mu}_o) \quad (11)$$

where  $\bar{\bar{X}}_{(p \times 1)} = \frac{1}{n} \sum_{j=1}^n \bar{X}_j$ ,  $\bar{S}_{(p \times p)} = \frac{1}{n-1} \sum_{j=1}^n (\bar{X}_j - \bar{\bar{X}})(\bar{X}_j - \bar{\bar{X}})'$ , and  $\bar{\mu}_o_{(p \times 1)} = \begin{bmatrix} \mu_{10} \\ \mu_{20} \\ \vdots \\ \mu_{p0} \end{bmatrix}$ .

In this expression,  $\frac{1}{n} \bar{S}$  is the estimated covariance matrix of  $\bar{\bar{X}}$ . As was the case before, if  $T^2$  is too large, the null hypothesis  $H_o: \bar{\mu} = \bar{\mu}_o$  will also be rejected. For large samples ( $\geq 100$ ),  $T^2$  follows a chi square ( $\chi^2$ ) distribution with  $p$  degrees of freedom, where  $p$  is the same as the number of quality characteristics, or variables, measured (Johnson and Wichern 2002). The sample size taken during the inspection of any road segment can always be adjusted to meet this criterion.

Hotelling's  $T^2$  statistic is used to differentiate the individual data points where the four different visual texture parameters converted with the PCA are converged into a new single objective score that can completely identify the degree of nonuniformity in a pavement image. This statistic is being successfully used in various applications of multivariate analysis that control changes in the mean vector of  $p$  correlated quality characteristics (Aparisi and Haro 2001). Hotelling's  $T^2$  is a statistical measure of the multivariate distance of each observation from the center of the data set. It is an analytical method to find the most extreme points in a data set (MATLAB Statistics Toolbox 2005). Using  $T^2$  after the PCA allows the incorporation of all of the variability into one statistic.

### **System Validation**

Testing of the system was conducted at the Virginia Smart Road, a controlled-traffic test facility with seven different variations of surface textures in 12 asphalt pavement sections. The



surface types include five different SUPERPAVE mixtures, a 12.5-mm stone mastic asphalt (SMA), and a 12.5-mm open-graded friction course (OGFC). Additionally, the Smart Road has a Portland cement concrete (PCC) bridge in the middle and, at end of the asphalt sections, a continuously reinforced concrete pavement (CRCP) section with a texturized surface.

All four calculated parameters produced clear differences between all the different sections having different asphalt surface mix types, the concrete bridge, and the final continuously reinforced concrete section (de León et al. 2007). These empirical results demonstrated the applicability of the method, making it necessary to perform further verification to confirm if the system would distinguish possible nonuniformities present in otherwise homogenous paving segments. Real paving projects would permit the validity of this assumption to be tested.

## System Verification

The system was used to capture digital images at highway speeds along a series of recently paved projects in Virginia. Table 1 lists the sites visited and some of the results obtained. A total of 13 projects allowed the analysis of 18 continuous segments of recently paved road which allowed the refinement of the methodology and the development of the software needed to produce tables and plots that will be used by inspection personnel in the field. Two segments were visited on three different dates to study the effect of traffic on the results of the analysis. The following are some of the most important findings.

### *Continuous and Homogenous Road Segments*

To capture the video at night, the camera settings and input information were prepared outside of the actual road segment to be analyzed, usually in locations out of the traffic lane such as on the shoulder. This was done because it is very dangerous to stop the vehicle exactly at the beginning or at the end of the pavement section. Afterward, during data processing, the frames out of the segment to be analyzed are eliminated. If this had not been done, nonuniformity elements would have been introduced into the analysis of the data. To illustrate this, project 10 was processed and analyzed in its entirety and compared to the results obtained after the trimming process to analyze only continuous and homogenous road segments.

Figure 2a is Hotelling's  $T^2$  road profile plot obtained from the system after analyzing project 10 completely (431 images). The dotted lines represent the four different control limit values set for the  $T^2$  statistic obtained from the chi square ( $X^2$ ) distribution with  $p$  degrees of freedom, (in this case,  $p = 4$ ) and with  $\alpha$ -levels of 10%, 5%, 1%, and 0.5%, it yields  $T^2$  values of 7.78, 9.49, 13.28, and 14.86, respectively. Notice the very large values of  $T^2$  obtained at the beginning and end of the segment (old pavement sections), with other high values at locations in between.  $T^2$  values greater than 14.86 indicate very strong evidence ( $P < 0.005$ ) that these images are different, in other words, that they show nonuniformities. From the figure, this is especially obvious between the following locations: 20–80, 210–310, 690–710, 3,410–3,490, and 4,040–4,170 ft. Three of the largest values are found at locations 243, 826, and 4,091 ft with  $T^2$  values of 200, 46, and 130, respectively.

Figure 2b shows the results of the analysis when repeated to include only the newly paved section of the pavement located in between 320–3,390 ft. Table 2 shows in tabular form the results of the analysis of both sections. Notice that only six locations previously detected still demonstrate significance—428, 690, 700, 709, 826, and 1,321 ft—but with  $T^2$  values much greater than those computed when analyzing the whole section. Notice also that the total number

of significant nonuniformities detected (26 and 25) and the highest values detected (201 and 288) are similar. However, when the median values of  $T^2$  were used to analyze the overall variability between both analyses (to eliminate the effect of the high outlier values), these median values were found to be nearly twice as much for the whole section than for the newly paved section.

Figure 3 is a collection of six images of the pavement found at locations 243, 583, 826, and 4,091 ft. The image of location 583 ft is considered normal and is included for comparison purposes. The image at 826 ft clearly deserves very close inspection because it was consistently detected in both analyses with a very high  $T^2$ . Images of locations 243 and 4,091 ft were found to have the greatest  $T^2$  values outside the new section. As is to be expected, these images were found to be white pavement markings which contrasted very sharply with newly paved areas. This observation underlines the importance of strictly limiting the analysis inside the road segment with newly paved areas.

The image at 826 ft, however, upon further inspection during the day, was found to have moisture problems, as can be seen in the bottom two images of Figure 3. The high reflectivity that is emanated from the water spots creates the nonuniformity effect that separates it from the rest of the captured images for that road segment.

### ***Effect of Traffic***

As can be seen in Table 1, projects 8 and 9 illustrate an example of the effect of capturing the images after the pavement has been used by traffic over a period of time. There is a definite increasing trend in the number of nonuniformities that will appear, which would obviously increase the inspection task when reviewing a paved section.

Another example that made this fact more obvious was discovered after analyzing projects 12 and 13, two road segments that were identical and adjacent. The images were captured the same day project 13 was finished and only one day after project 12 was finished and opened to traffic. The images of project 12 showed many tire marks from vehicles that had dragged dirt onto the newly paved areas from the adjacent lots or residences on the side of the roads. Figure 4 shows some examples of this occurrence. Its potential effects on the visual analysis are obvious and can also be seen in Table 1, where the increases in all of the computed indicators of  $T^2$  for these two projects are very noticeable.

### ***Different Quality Control Procedures and the Dispersion of Nonuniformities***

Another very noticeable difference is found in the number of nonuniformities found in a pair of projects with similar lengths. These are projects 3 and 7, which are relatively long (10,950 and 12,167 ft) when compared with the others tested.

Project 3 shows a lower number of nonuniformities than project 7 (37 versus 83), but the relative dispersion of these nonuniformities is very different. To better explain this, a scatter for *both* projects was made and is included as Figure 5. This scatter plot is similar to the ones created by the system that plot the first two principal components after the PCA analysis had been performed. As explained before, the farther from the origin of the plot, the higher the probability that a point represents an image with nonuniformity.

Figure 5 has several interesting areas to analyze. First, two irregularly shaped polygons were created around the points that represent the locations with a very low probability ( $P > 10\%$ ) of having nonuniformities. It can be seen that the areas of the two polygons are similar, although the polygon for project 7 is more irregular in shape than the one for project 3. However, the outside rectangle that contains all the points for project 3 is smaller than that for project 7, and as

noted before, project 7 has more than twice the number of locations with a significant level of nonuniformity.

After considering these factors, a road profile for the  $T^2$  values was made for each project; Figures 6 shows both of these profiles. The specific location of the nonuniformities along both of these road segments is important for the inspection, but in these plots it is very evident that there is a long stretch of project 7 that is well beyond the 99.5% control limit value. This segment has 54 occurrences, 65% of the nonuniformities detected, and goes from location 6,044 to 6,569, a length of more than 525 ft. After analyzing the images captured by the system, it was found that the causes for these nonuniformities, some of which are shown in Figure 7, are mainly due to tire tread marks, dirt, and smeared asphalt blotches. Closer inspection during the day confirmed these causes, as shown in Figure 8. It was mainly the excess tack coat carried by the hauling trucks from the side road what caused the nonuniformities detected by the system. Although this is not a construction problem by itself, it represents an example of possible nonuniformities that would have warranted a closer inspection after the construction, just to make sure it would not be a problem. The system proved its capability to detect possible problems that would have alerted the inspection personnel reviewing the road segment, by allowing the identification of these locations.

### **Conclusions and Recommendations**

All of the projects evaluated confirmed that the digital imaging system developed has great potential to identify nonuniformities on recently completed road maintenance and construction road segments. The results suggest that the system can help the inspection process, especially immediately after the conclusion of paving operations during night operations. The system also creates a permanent record that allows the evaluation of pavement condition for comparison purposes during various stages of its service life.

It was found that it is very important to circumscribe the analysis to only the newly paved areas, as older or different pavement surfaces introduce nonuniformity into the analysis. It was found that traffic and other factors such as white lane markings, for example, alter the initial visual conditions and can modify the analysis. Further testing with different pavement mixes, construction methods, and equipment (like material transfer vehicles) is expected to produce a system that will help improve the paving methods in Virginia by better understanding how to avoid the introduction of sources of nonuniformities that can produce poor pavement performance. This system will be a valuable tool that has the potential to automate the construction inspection process, eliminate subjectivity, and improve quality-assurance procedures of HMA pavements.

## REFERENCES

1. Aparisi, F., and Haro, C. (2001). "Hotelling's T2 control chart with variable sampling intervals." *International Journal of Production Research*, 39(14), 3127-3140.
2. Asphalt Education Partnership. (2006) "Facts about asphalt." *Guides for Teachers*, <<http://www.beyondroads.com>> (Aug. 24, 2006).
3. de León, E., and Flintsch, G. W. (2006). "A non-contact system to detect and quantify segregation in hot mix asphalt pavements." *Proc., Application of Advanced Technology in Transportation*, ASCE, Chicago, Ill., 93-98.
4. de León, Flintsch, G.W., and Abbott, A. L. (2007) "Measuring the Uniformity of Hot-mix Asphalt Pavements with Digital Image Technology." Submitted for publication in the *Journal of the Transportation Research Board*, National Research Council, Washington, D.C., Paper No. 07-1613.
5. Duda, R., Hart, P., and Stork, D. (2001). *Pattern Classification*. Wiley & Sons, New York.
6. Flintsch, G.W., de León, E., McGhee, K.K., and Al-Qadi, I.L. (2003) "Pavement Surface Macrotecture: Measurement and Application." *Transportation Research Record: Journal of the Transportation Research Board*, No. 1860, National Research Council, Washington, D.C., 168-177.
7. Flintsch, G.W., McGhee, K.K., and de León, E. (2005) "Field Validation of Macrotecture-Based Hot Mix Asphalt Segregation Detection Methods." *Journal of Association of Asphalt Paving Technologists*, Volume 74, AAPT, St. Louis, Mo., 1-21.
8. Haralick, R., and Shapiro, L. (1992). *Computer and Robot Vision, Volume 1*. Addison-Wesley Publishing Company, Inc., Reading, Massachusetts.
9. Johnson, R., and Wichern, D. (2002). *Applied Multivariate Statistical Analysis*. Prentice Hall, New Jersey.
10. MATLAB Image Processing Toolbox. (2005). The Math Works, Inc., Natick, Massachusetts.
11. MATLAB Statistics Toolbox. (2005). The Math Works, Inc., Natick, Massachusetts.
12. Stroup-Gardiner, M., and Brown, E. R. (2000). *NCHRP Report 441, Segregation of Hot-Mix Asphalt Pavements*. TRB, National Research Council, Washington, DC.

**Table 1. Paving Sites Analyzed**

Project No.	Project ID	Date Taken	Date Paved	Total Frames Analyzed	Distance (feet)	Significant Non-Uniformities					Hotelling's $T^2$ Statistics per site		
						Total	Levels of Confidence				Sum <sup>1</sup> /100 <sup>2</sup>	Median <sup>3</sup>	
							99.5%	99%	95%	90%			
1	460-22	6/21		1,085	10,518	80	30	5	26	19	1,357	13	13
2	460-23	6/21		558	5,409	33	15	1	6	11	525	10	13
3	11-19	6/30		1,130	10,950	37	22	3	7	5	1,662	15	19
4	11-20	6/30		247	2,393	19	6	3	3	7	311	13	13
5	11-21A	6/30		518	5,017	25	11	3	3	8	778	16	14
	11-21B			370	3,580	16	12	0	2	2	550	15	32
	11-21C			194	1,873	14	11	0	2	1	480	26	24
	11-21D			240	2,319	19	10	1	5	3	596	26	18
	11-21E			258	2,494	22	10	1	8	3	628	25	13
	11-21F			949	9,199	50	22	2	12	14	1,411	15	13
6	11-46	6/22		444	4,490	27	15	1	7	4	729	16	15
7	11-47	6/22		1,255	12,167	83	34	7	22	20	2,255	19	13
8	RT 8S	5/22*	5/18	342	10,572	30	9	3	13	5	707	7	12
				1,097	10,637	97	40	7	32	18	1,477	14	13
				1,099	10,660	103	21	7	47	28	1,449	14	11
				1,098	10,648	117	29	18	38	32	1,523	14	12
9	RT 8N	5/22*	5/18	329	10,678	41	11	4	14	12	684	6	12
				1,104	10,710	64	34	5	14	11	1,876	18	16
				1,101	10,675	86	9	8	19	50	921	9	9
				1,101	10,676	98	16	5	39	38	1,108	10	10
10	SM E	7/24	7/18	317	3,070	25	11	1	10	3	671	22	14
				431	4,178	26	19	1	3	3	950	23	27
11	SM W	7/24	7/18	320	3,097	35	17	4	10	4	618	20	15
				376	3,642	17	11	0	5	1	881	24	22
12	RT 220S	8/16	8/15	213	2,059	18	10	0	5	3	510	25	16
13	RT 220N	8/16	8/16	213	2,067	22	8	1	2	11	305	15	10

\* The images captured on 5/22 were taken every 20 ft.

\*\* White balance was changed for the second image capture on 7/24

<sup>1</sup> This value represents the sum of all the values of the individual  $T^2$  “scores” for all significant non-uniformities in the project.

<sup>2</sup> This value represents sum value per every 100 feet in the project.

<sup>3</sup> This value represents the median value of all the  $T^2$  “scores” of all the significant non-uniformities in the project.

**Table 2.** Locations of significant visual difference

Project SM East all			Project SM East (new pavement only)		
Location (ft)	Hotelling's $T^2$	Confidence Level	Location (ft)	Hotelling's $T^2$	Confidence Level
19	35.6	99.5	321	15.5	99.5
29	37.2	99.5	330	15.0	99.5
49	35.5	99.5	428	23.7	99.5
58	47.7	99.5	437	18.0	99.5
68	33.1	99.5	466	14.6	99
78	15.8	99.5	476	12.3	95
214	8.5	90	690	26.8	99.5
<b>243</b>	<b>200.1</b>	99.5	700	24.2	99.5
272	10.5	95	709	34.2	99.5
281	13.7	99	719	11.4	95
291	11.1	95	<b>826</b>	<b>288.7</b>	99.5
310	35.2	99.5	933	8.5	90
428	7.8	90	1,263	10.1	95
690	17.4	99.5	1,321	12.3	95
700	15.7	99.5	1,389	11.6	95
709	17.9	99.5	1,409	10.1	95
<b>826</b>	<b>46.1</b>	99.5	1,419	8.3	90
1,321	8.5	90	1,438	10.2	95
3,410	22.9	99.5	1,739	7.8	90
3,420	36.1	99.5	1,759	11.1	95
3,430	25.0	99.5	2,002	15.9	99.5
3,440	10.6	95	2,011	12.3	95
3,488	53.3	99.5	2,021	10.4	95
4,042	29.0	99.5	2,720	16.6	99.5
<b>4,091</b>	<b>130.6</b>	99.5	2,778	40.9	99.5
4,168	45.6	99.5			



**Figure 1.** System framework and sample image

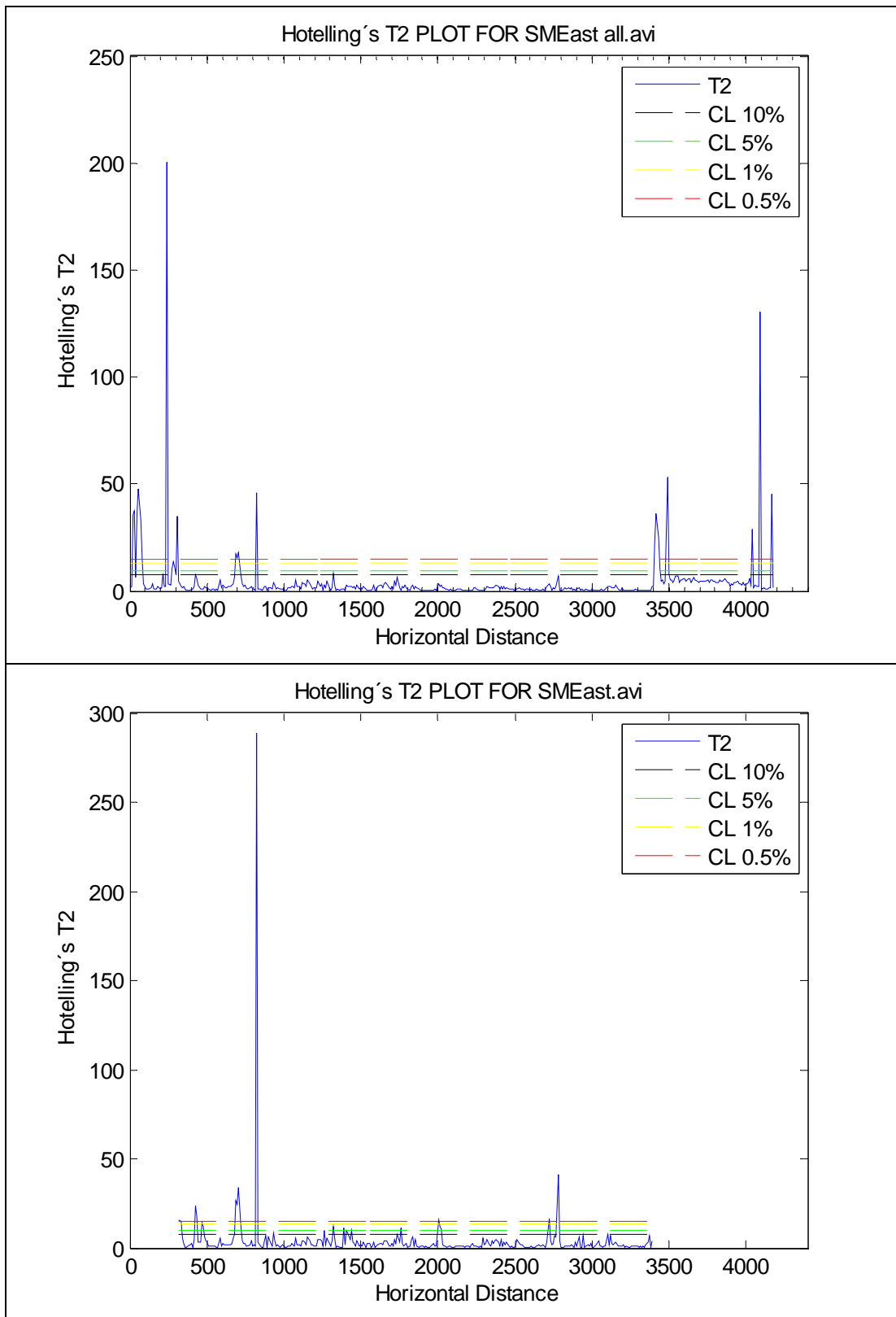


**Figure 2.** Hotelling's  $T^2$  plots for Project SM East a) complete and b) paved segment only



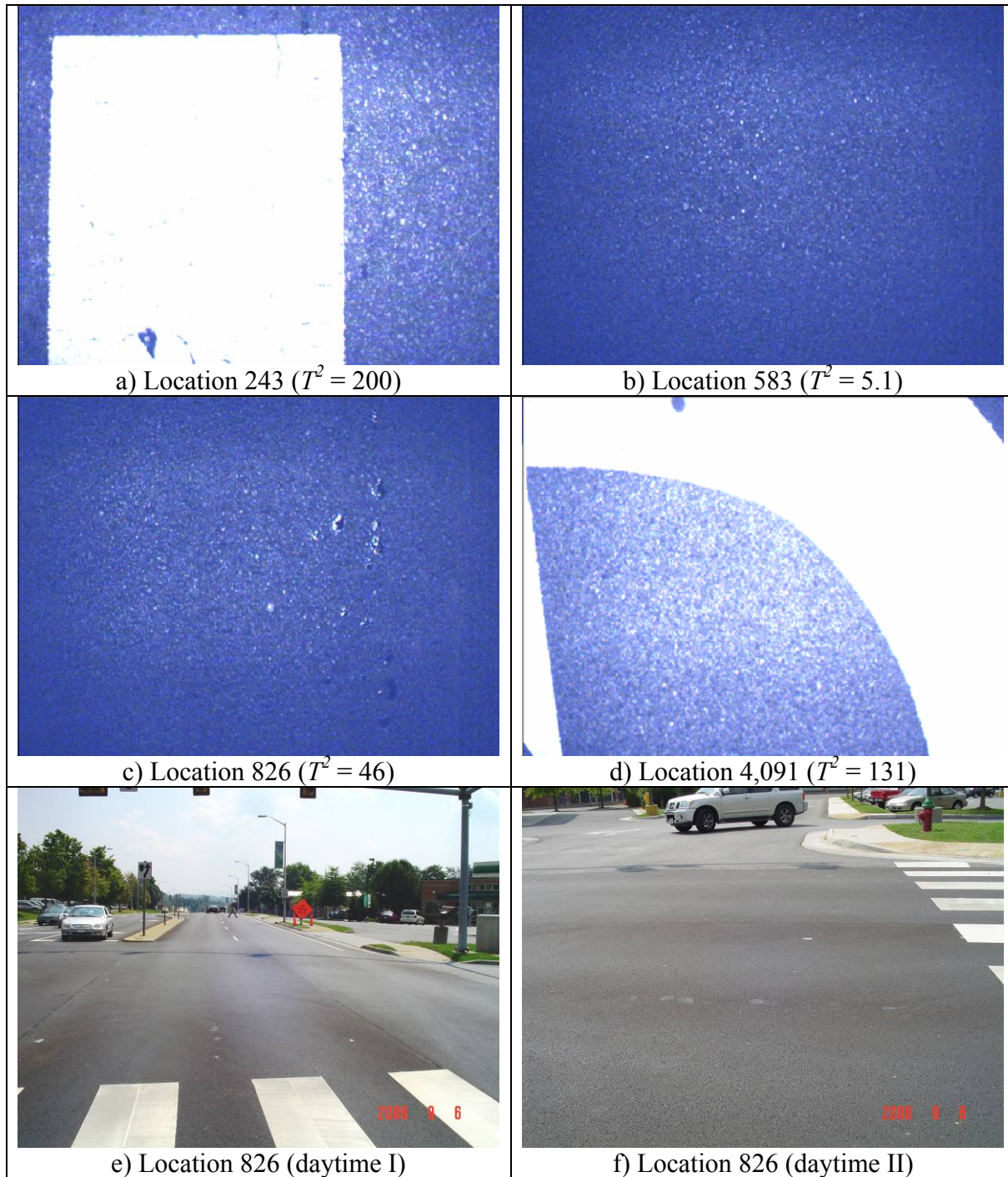


**Figure 3.** Highest  $T^2$  locations in SM East (all)



**Figure 4.** Images from intersections and adjacent dirt lots

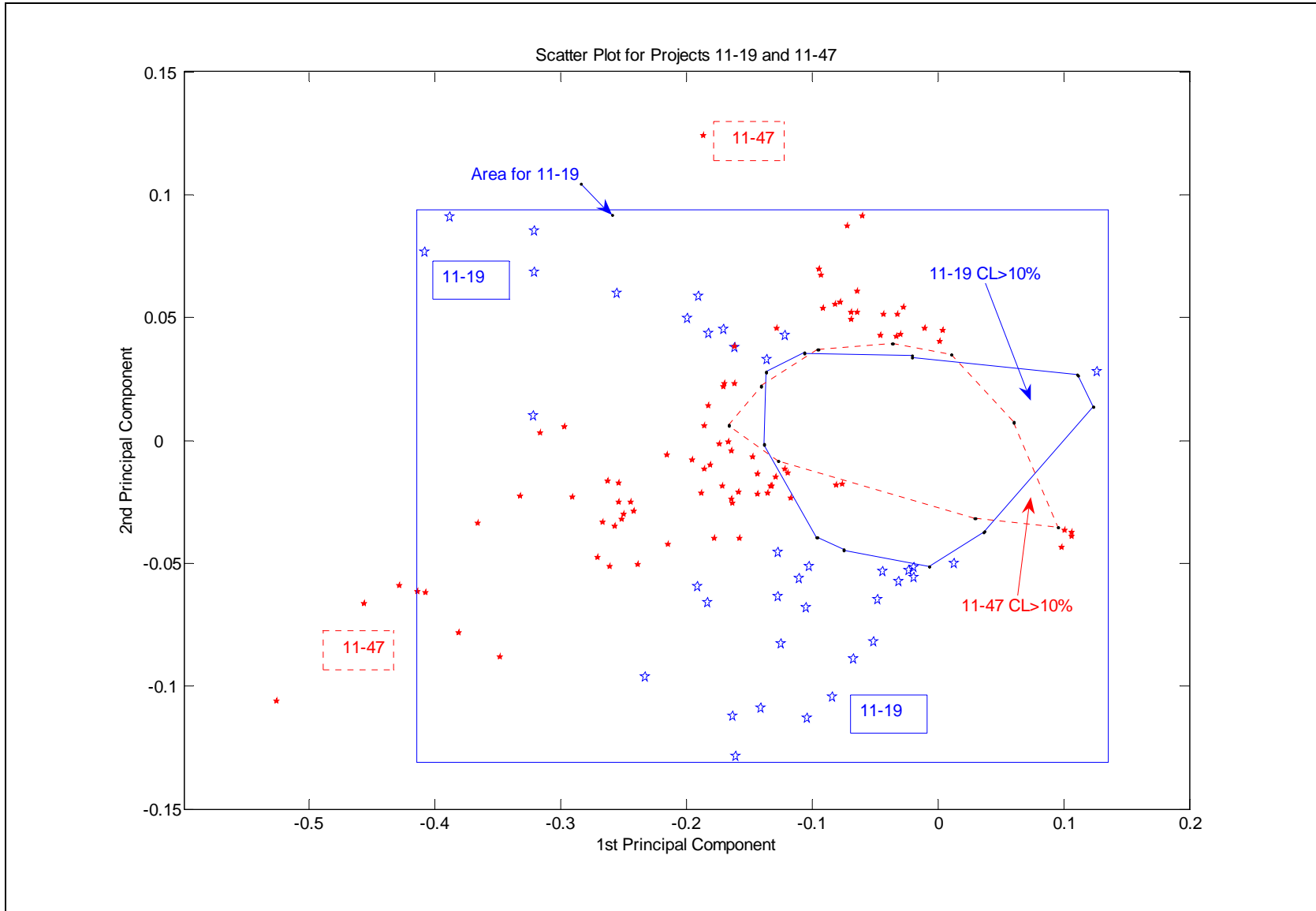


**Figure 5.** Combined scatter 2-D principal component plot for Projects 3 and 7

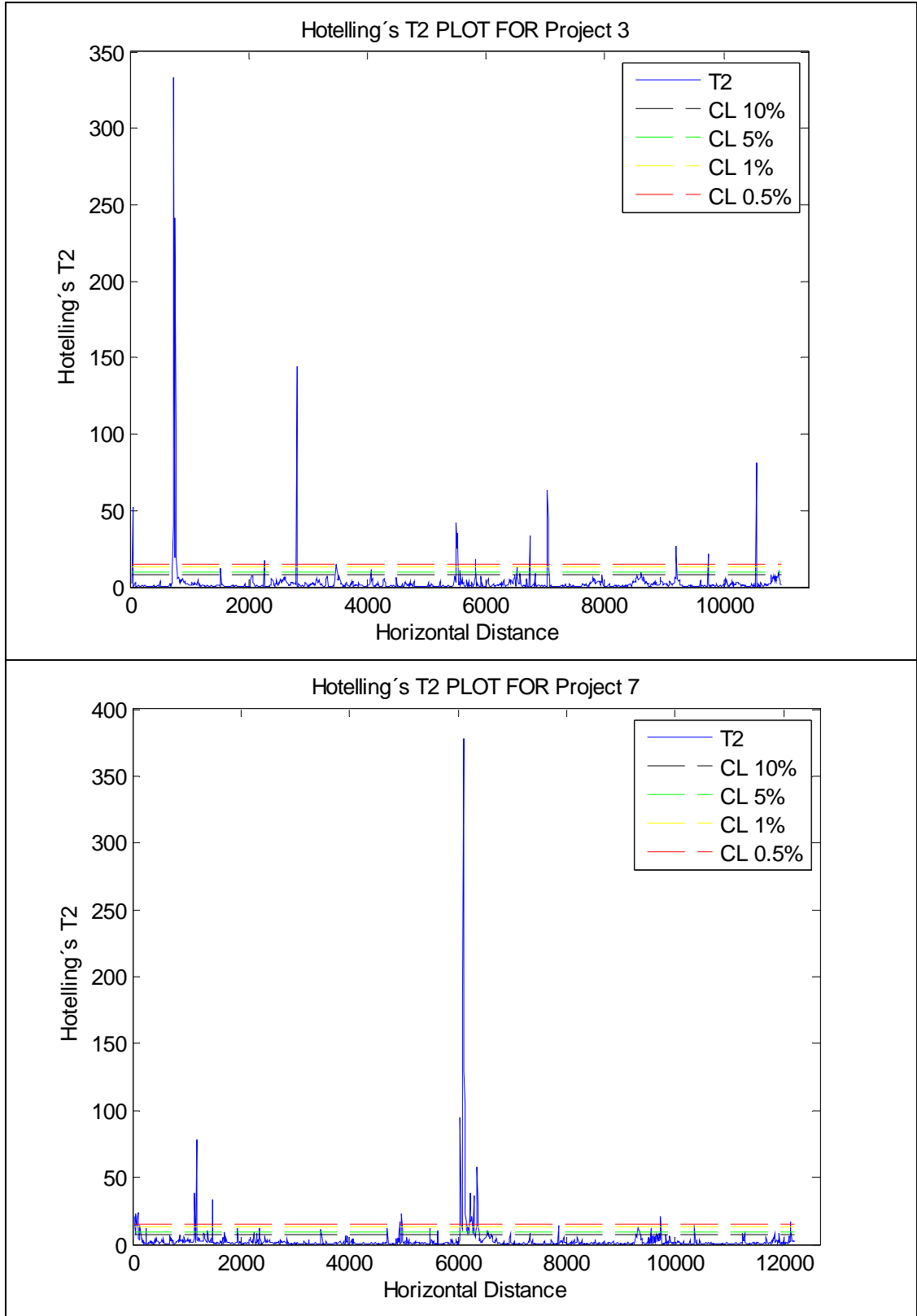


**Figure 6.** Hotelling's  $T^2$  plots for Projects 3 and 7

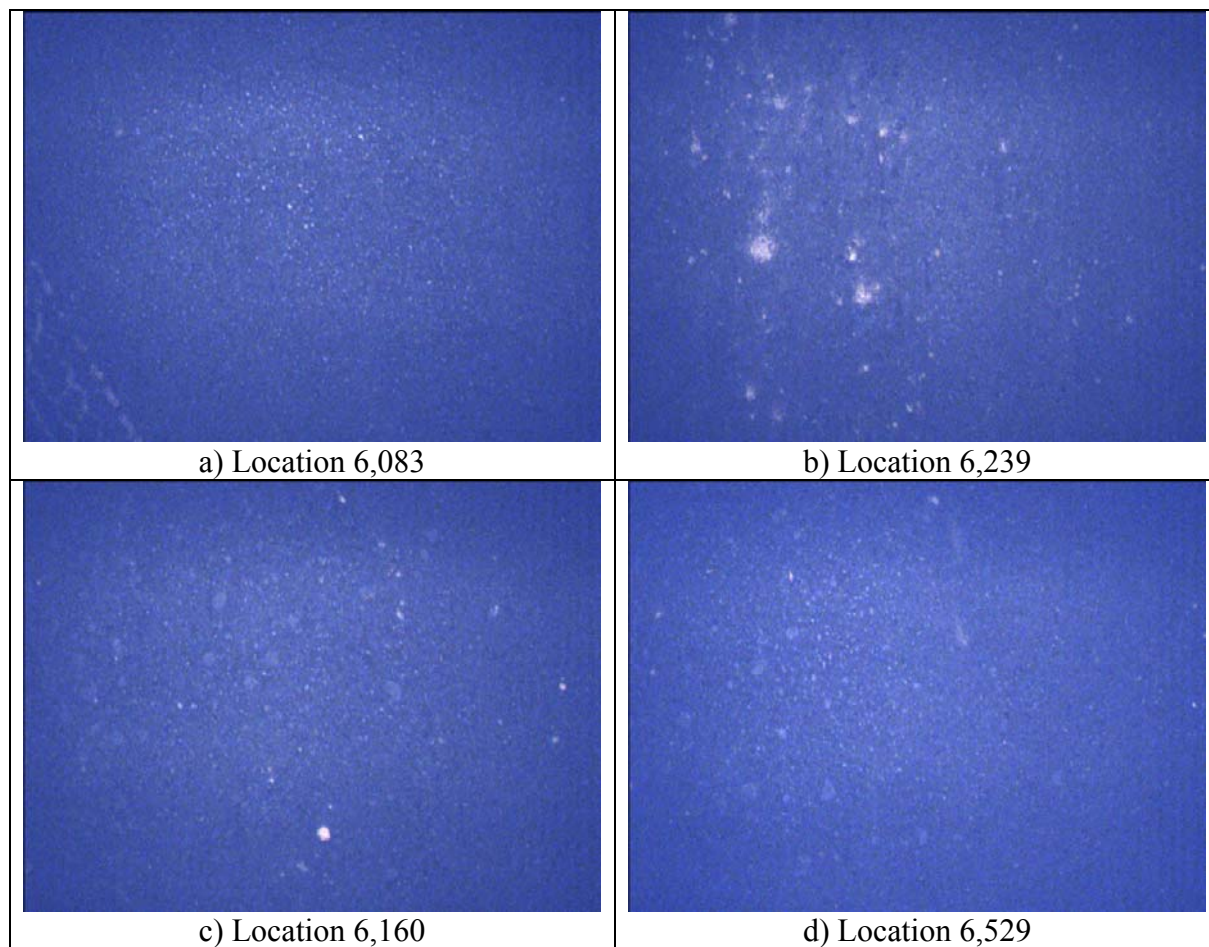


**Figure 7.** Examples of nonuniformities from Project 7 (nighttime)



**Figure 8.** Examples of nonuniformities from Project 7 (daytime)

## Summary, Findings, Conclusions and Recommendations for Future Research

Surface macrotexture measurements using high-speed laser profilers have been identified as a potentially promising tool to detect and quantify segregation for quality assurance purposes in the state of Virginia. However, field implementation work performed to test the uniformity of typical VDOT paving mixtures presented several problems. A recommendation was made to explore the use of an area based method such as digital image analysis. This dissertation focuses on the execution of this recommendation. Its main objective was to develop a non-contact system to detect segregated HMA areas and identify the locations of these areas along a road for HMA quality assurance purposes. The proposed system is relatively low cost and was developed using innovative image processing and analysis software.

The system computes the gray level co-occurrence matrix (GLCM) of images of newly constructed pavements to find various parameters that are commonly used in visual texture analysis. Using principal component analysis to integrate multivariable data into a single classifier, Hotelling's  $T^2$  statistic, the system creates a list of the location of possible nonuniformities that require closer inspection.

**Table 1.** Paving Sites Analyzed

Project No.	Project ID	Date Taken	Date Paved	Total Frames Analyzed	Distance (feet)	Significant Non-Uniformities				Hotelling's $T^2$ Statistics per site			
						Total	Levels of Confidence				Sum <sup>1</sup> /100 <sup>2</sup>	Median <sup>3</sup>	
							99.5%	99%	95%	90%			
1	460-22	6/21		1,085	10,518	80	30	5	26	19	1,357	13	13
2	460-23	6/21		558	5,409	33	15	1	6	11	525	10	13
3	11-19	6/30		1,130	10,950	37	22	3	7	5	1,662	15	19
4	11-20	6/30		247	2,393	19	6	3	3	7	311	13	13
5	11-21A	6/30		518	5,017	25	11	3	3	8	778	16	14
	11-21B			370	3,580	16	12	0	2	2	550	15	32
	11-21C			194	1,873	14	11	0	2	1	480	26	24
	11-21D			240	2,319	19	10	1	5	3	596	26	18
	11-21E			258	2,494	22	10	1	8	3	628	25	13
	11-21F			949	9,199	50	22	2	12	14	1,411	15	13
6	11-46	6/22		444	4,490	27	15	1	7	4	729	16	15
7	11-47	6/22		1,255	12,167	83	34	7	22	20	2,255	19	13
8	RT 8S	5/22*	5/18	342	10,572	30	9	3	13	5	707	7	12
		7/17		1,097	10,637	97	40	7	32	18	1,477	14	13
		7/24**		1,099	10,660	103	21	7	47	28	1,449	14	11
				1,098	10,648	117	29	18	38	32	1,523	14	12
9	RT 8N	5/22*	5/18	329	10,678	41	11	4	14	12	684	6	12
		7/17		1,104	10,710	64	34	5	14	11	1,876	18	16
		7/24**		1,101	10,675	86	9	8	19	50	921	9	9
				1,101	10,676	98	16	5	39	38	1,108	10	10
10	SM E	7/24	7/18	317	3,070	25	11	1	10	3	671	22	14
	SM E all			431	4,178	26	19	1	3	3	950	23	27
11	SM W	7/24	7/18	320	3,097	35	17	4	10	4	618	20	15
	SM W all			376	3,642	17	11	0	5	1	881	24	22
12	RT 220S	8/16	8/15	213	2,059	18	10	0	5	3	510	25	16
13	RT 220N	8/16	8/16	213	2,067	22	8	1	2	11	305	15	10

\*The images captured on 5/22 were taken every 20 ft.

\*\*White balance was changed for the second image capture on 7/24

<sup>1</sup> This value represents the sum of all the values of the individual  $T^2$  "scores" for all significant non-uniformities in the project.

<sup>2</sup> This value represents sum value per every 100 feet in the project.

<sup>3</sup> This value represents the median value of all the  $T^2$  "scores" of all the significant non-uniformities in the project.

A total of 18 continuous road segments of recently paved roads were analyzed with the system. These road segments allowed the refinement of the methodology and the software needed to produce tables and plots that will be used by inspection personnel in the field. The results demonstrated the capability of the system to detect potential nonuniformities of recently completed pavements. The system proved its potential as a useful tool in the final inspection process.

## **FINDINGS**

Each chapter of this dissertation represents a different stage of the research undertaken as described in the introduction. These are the major findings:

- Macrotexture measurements appear to be a practical means to detect and quantify segregation for quality assurance purposes. The use of this approach in a construction specification requires computing non-segregated estimated texture depth (ETD).
- Field verification experimental work further supported the hypothesis that high-speed macrotexture measurement has great promise as a tool for detecting and measuring HMA segregation. Correlations of texture with void level/density and asphalt content (traditional measures of segregation) are strong, especially for mixes with moderately-sized aggregates. However, because profilers measure very thin longitudinal lines, they may actually miss significant segregated areas.
- Testing with a digital imaging system developed at the Virginia Smart Road suggested that digital image analysis has the potential to identify different types of pavement surfaces better than the inertial laser profiler method tested previously.
- Experimentation with the system on road segments confirmed that it has great potential to identify non-uniformities on recently completed road maintenance and construction operations. The results suggest that the system can help the inspection process, especially immediately after the conclusion of paving operations during night operations.
- The system also created a permanent record that will allow maintaining the means to evaluate the condition of the pavement, for comparison purposes, during its service life after the initial work.

## **CONCLUSIONS**

A new system was developed with digital visible-light image technology to detect non-uniformities in HMA. Areas having different texture characteristics in pavement surfaces can be discriminated using different parameters that characterize surface texture (contrast, correlation, energy, and homogeneity). This allows identifying areas along a road where segregation is suspected.

Field testing suggested that the system identifies different types of pavement surfaces better than the available inertial laser profiler. This system can automate the HMA construction inspection process and reduce subjectivity. Furthermore, if segregation can be detected properly, the use of such a system will help improve the quality assurance inspection process, especially during night operations.



Therefore, the system has the potential to increase pavement service life and reduce down time from repair work. The system also has the advantage of creating a permanent record that will allow pavement evaluations, for comparison purposes, during its service life.

## **RECOMMENDATIONS AND SUGGESTIONS FOR FUTURE RESEARCH**

From an operational point of view, when using any digital imaging system, it is strongly recommended that all image acquisition be done as soon as possible after the construction operations are finished. It was observed that in some cases, traffic, dirt, or other factors, such as lane markings, can alter the visual analysis indicating nonuniformities that clearly do not affect the pavement's performance.

Future research should include testing the system with different pavement mixes and construction conditions. This would be beneficial to determine what can be done to the paving operations to eliminate some of the non-uniformities that have the potential to become areas with bad pavement performance. A complete new study with different pavement mixes, construction methods, and equipment (like material transfer vehicles) is recommended to help improve the paving methods in Virginia by better understanding how to avoid the introduction of sources of nonuniformities that can produce poor pavement performance.

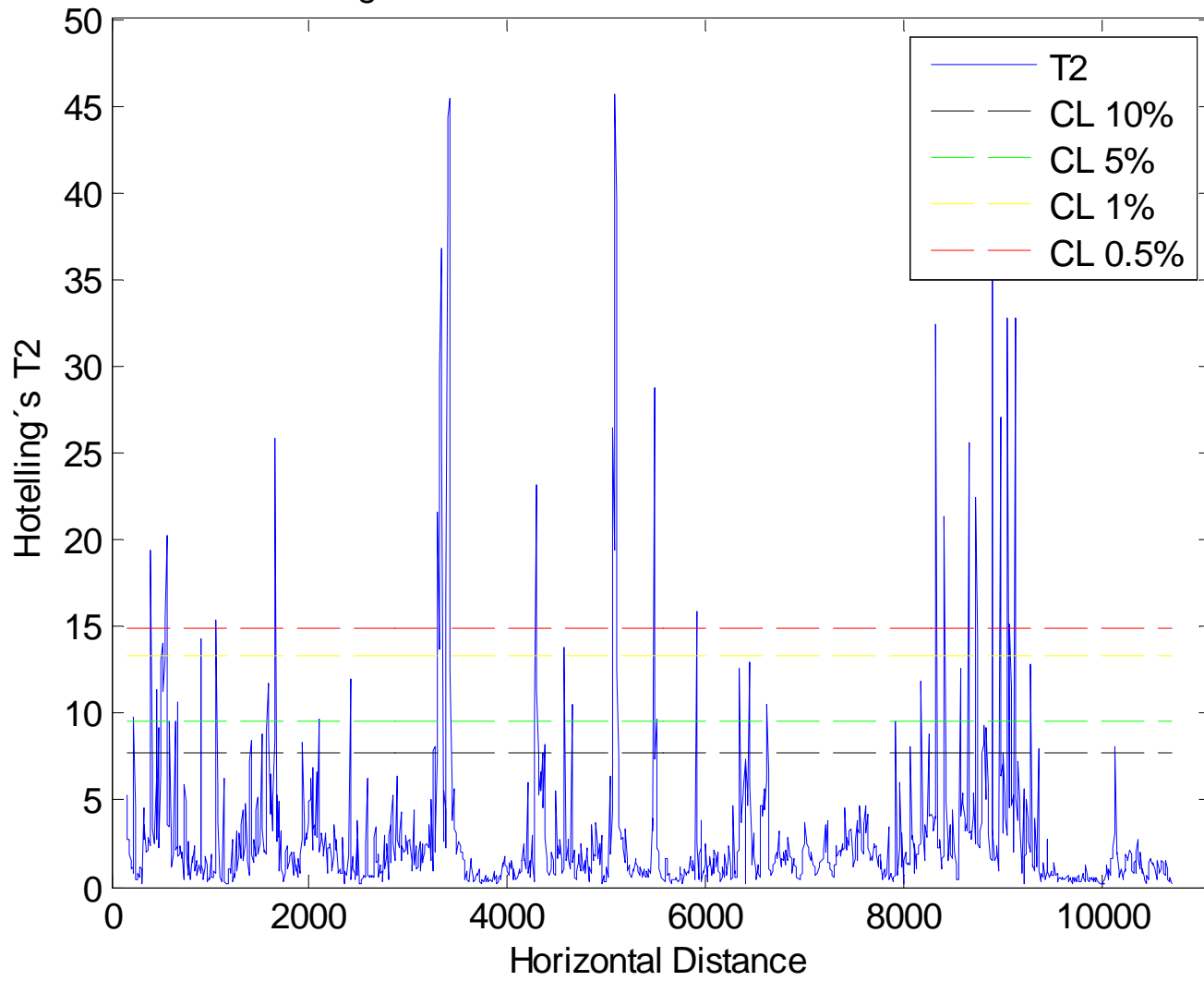
As any novel approach, this system is susceptible to improvements. Arrangements for wider area illumination are recommended to cover larger sections of pavement surface with each pass. Updating the software and hardware are recommended to enable the use of the camera's full capabilities and avoid unnecessary processing of the data.

Finally, it is recommended to explore the benefits of combining laser and digital visual-light image technologies for detecting and quantifying segregation in recently paved pavements for quality assurance purposes. A combined system would ideally use the laser-based measurements to provide precision and the digital imaging technology to enhance the coverage.

# Appendix A

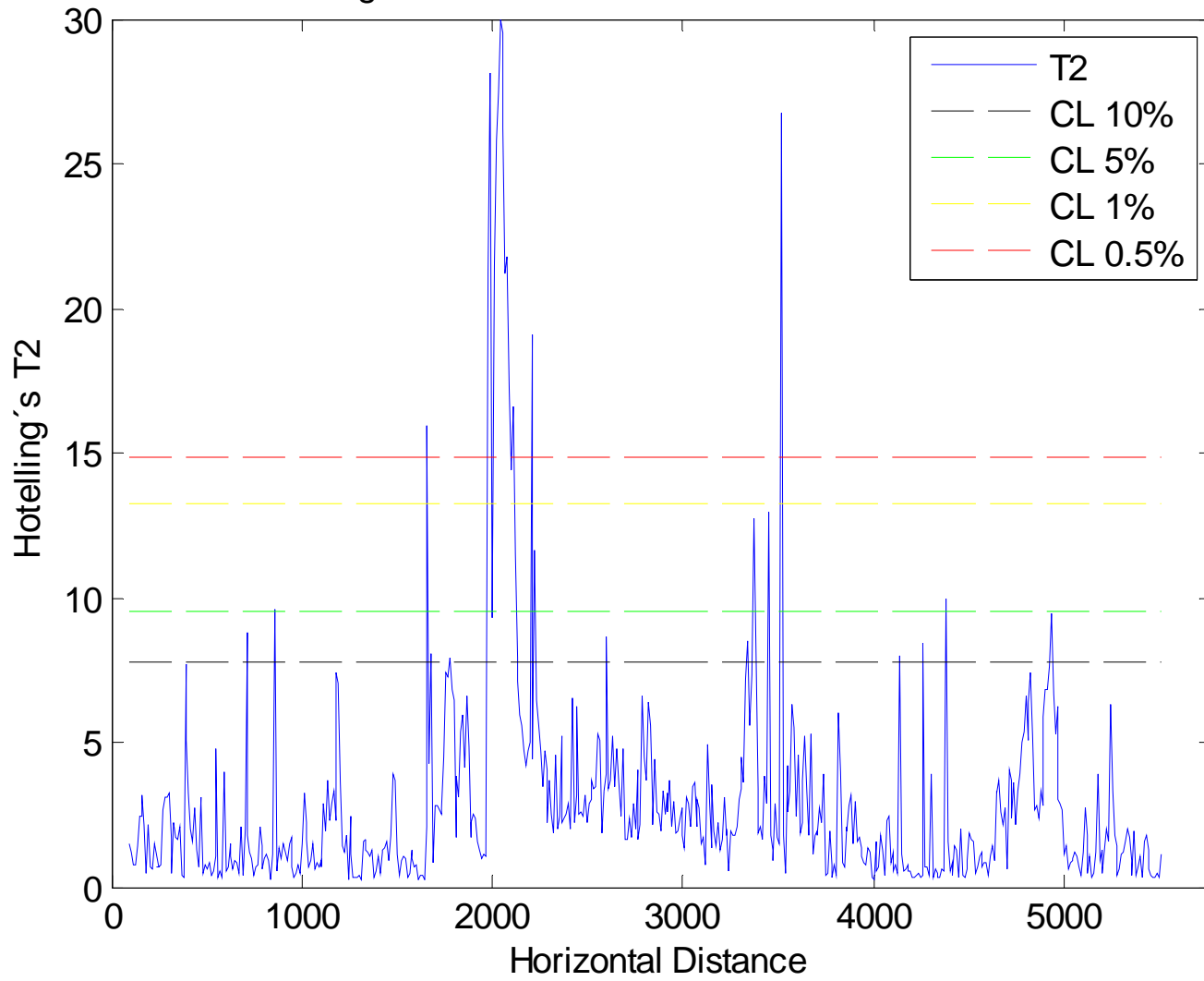
Hotelling's  $T^2$  Plots

Hotelling's T2 PLOT FOR 460-06-22-@10-12.5mm.avi



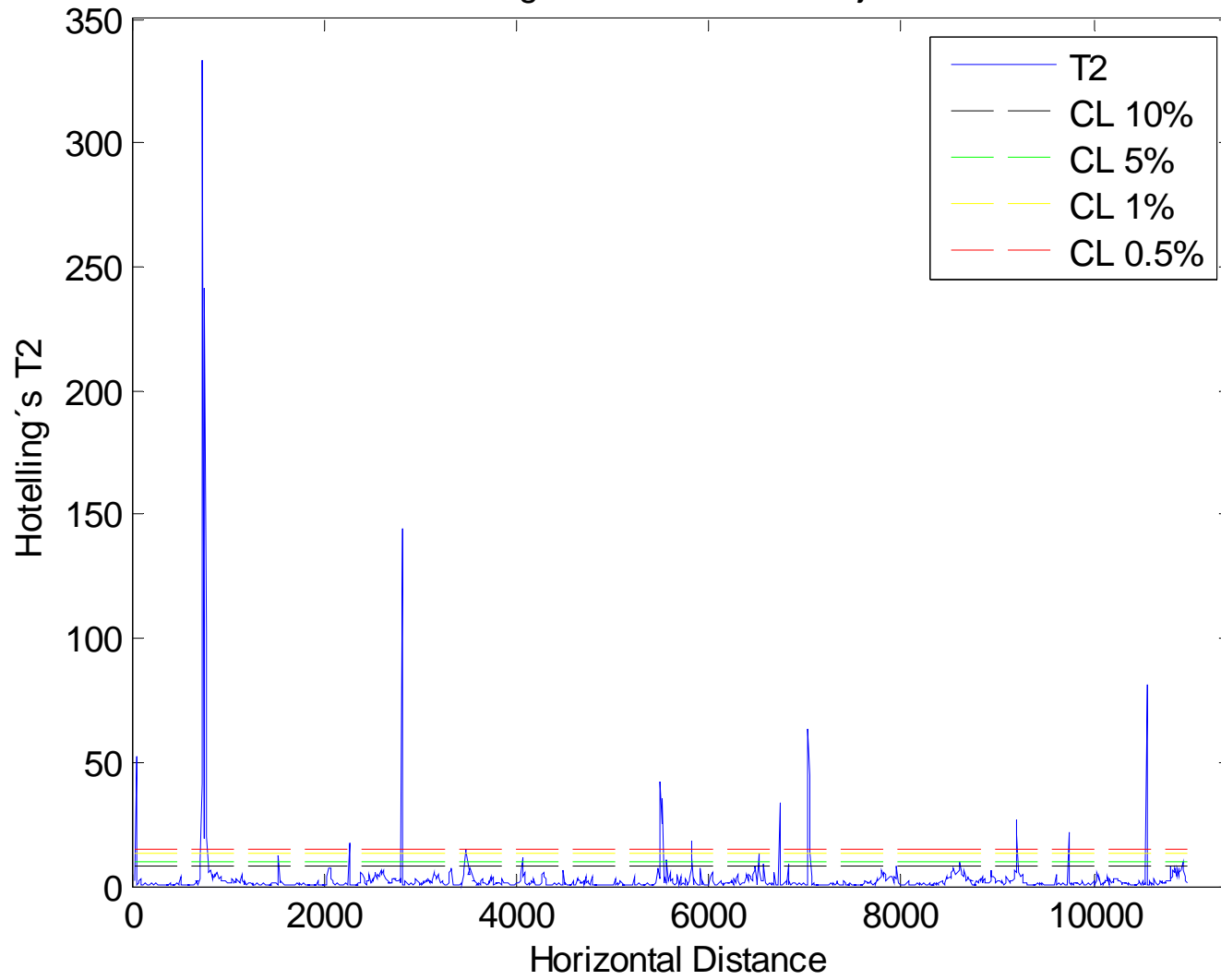
Hotelling's T2 Plot for project #1: 460-22

Hotelling's T2 PLOT FOR 460-06-23-@10-12.5mm.avi



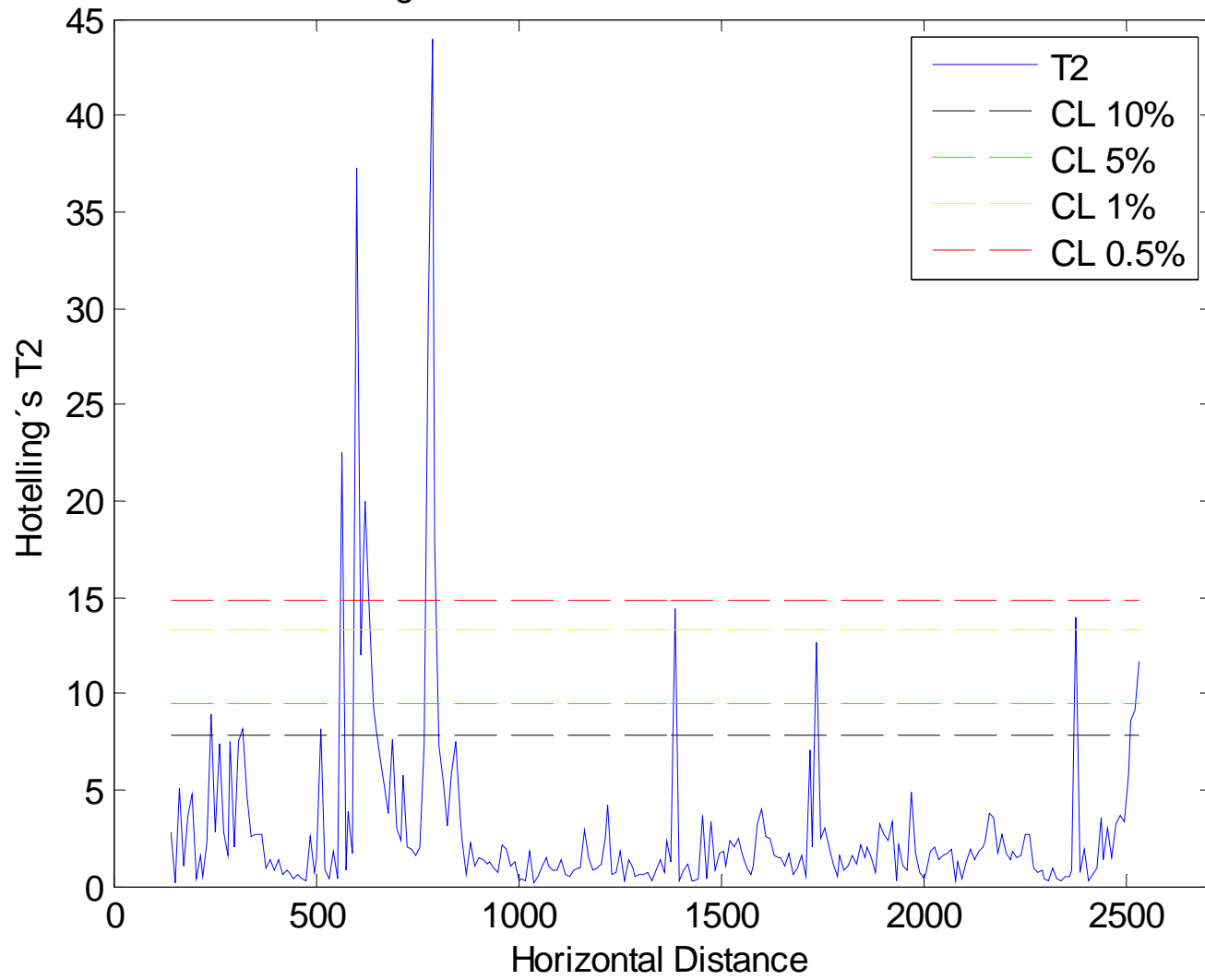
Hotelling's T2 Plot for project #2: 460-23

Hotelling's T2 PLOT FOR Project 3

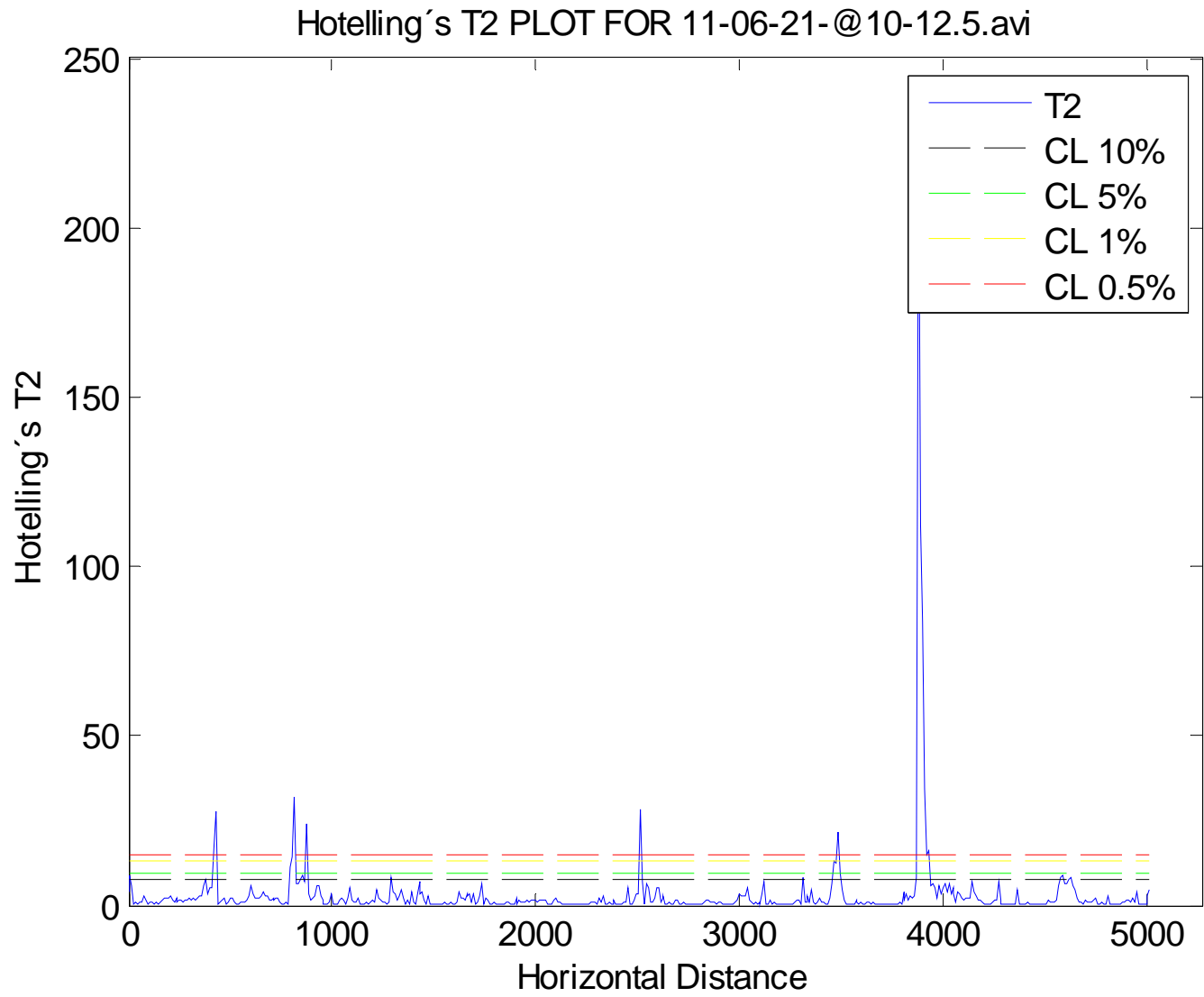


Hotelling's T2 Plot for project #3: 11-19

Hotelling's T2 PLOT FOR 11-06-20-@10-12.5.avi

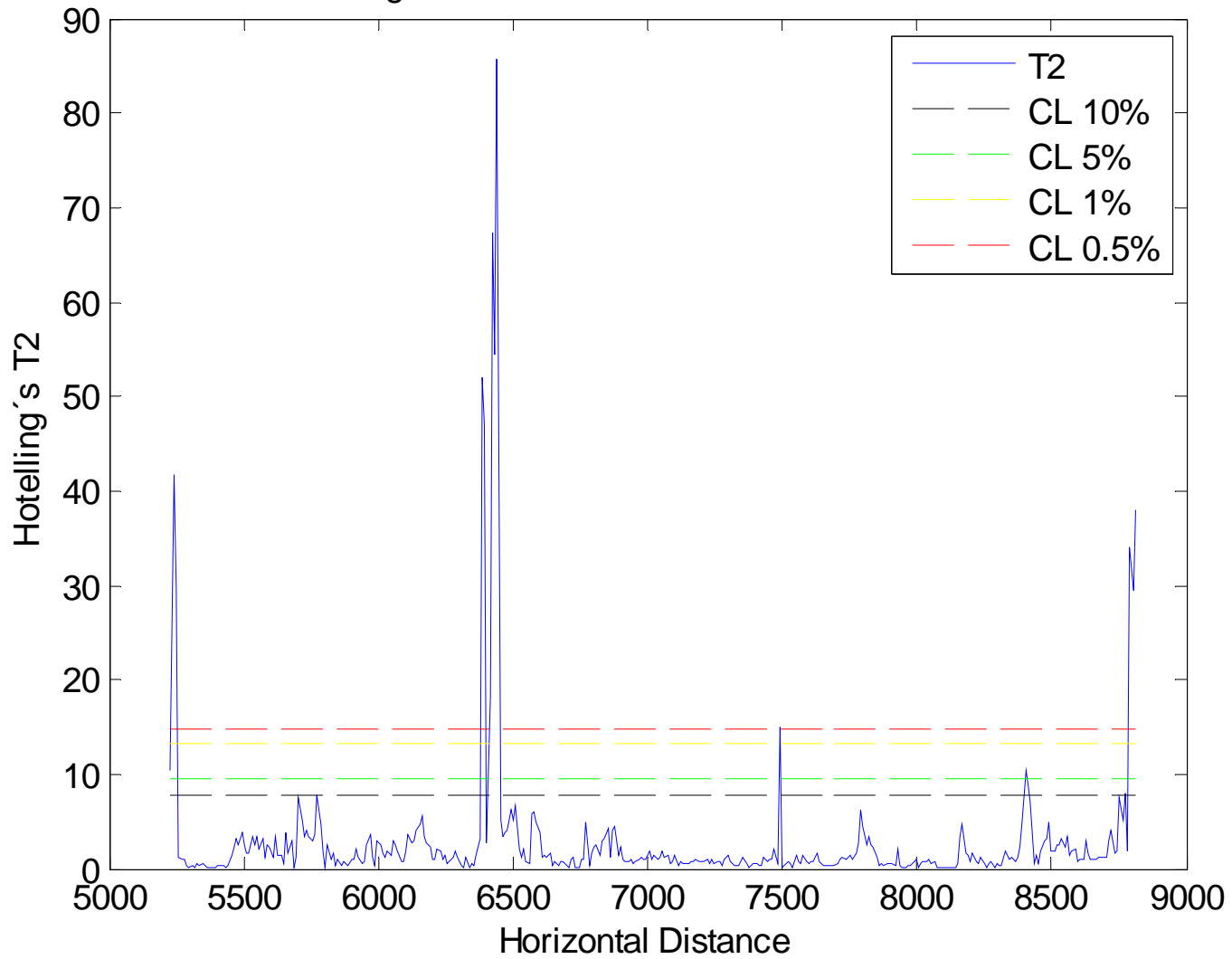


Hotelling's T2 Plot for project #4: 11-20



Hotelling's T2 Plot for project #5a: 11-21A

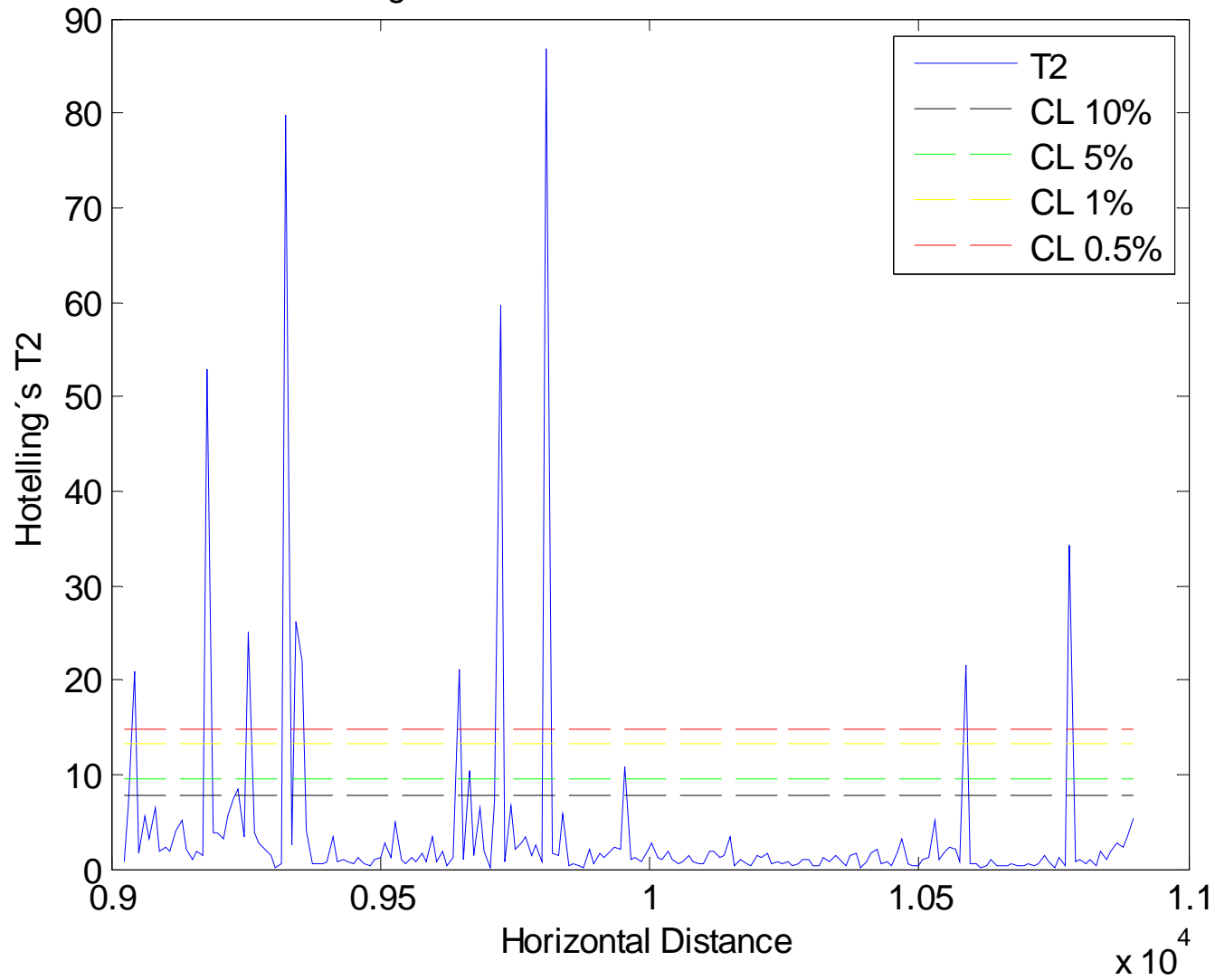
Hotelling's T2 PLOT FOR 11-06-21-@10-12.5.avi



Hotelling's T2 Plot for project #5b: 11-21B

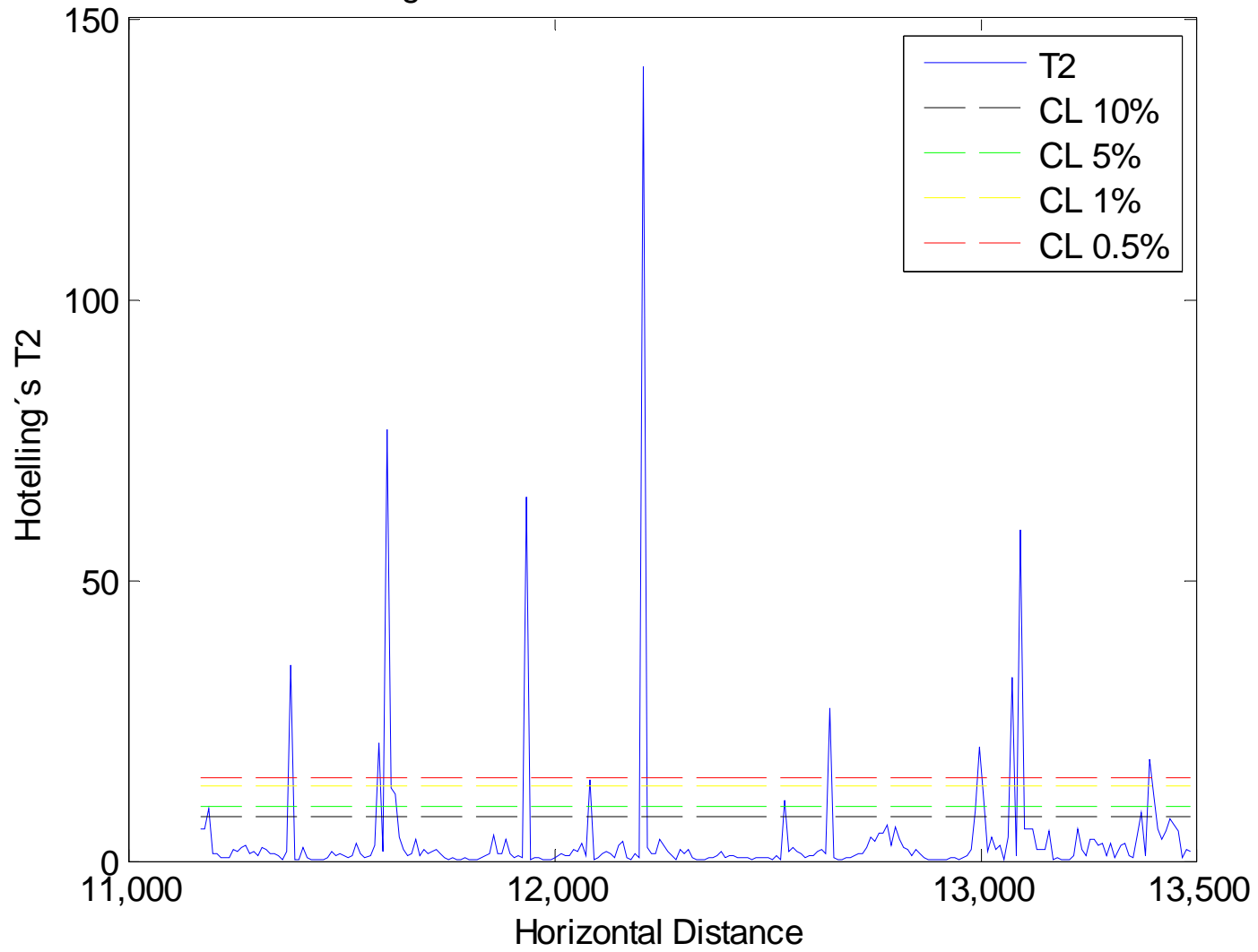


Hotelling's T2 PLOT FOR 11-06-21-@10-12.5.avi

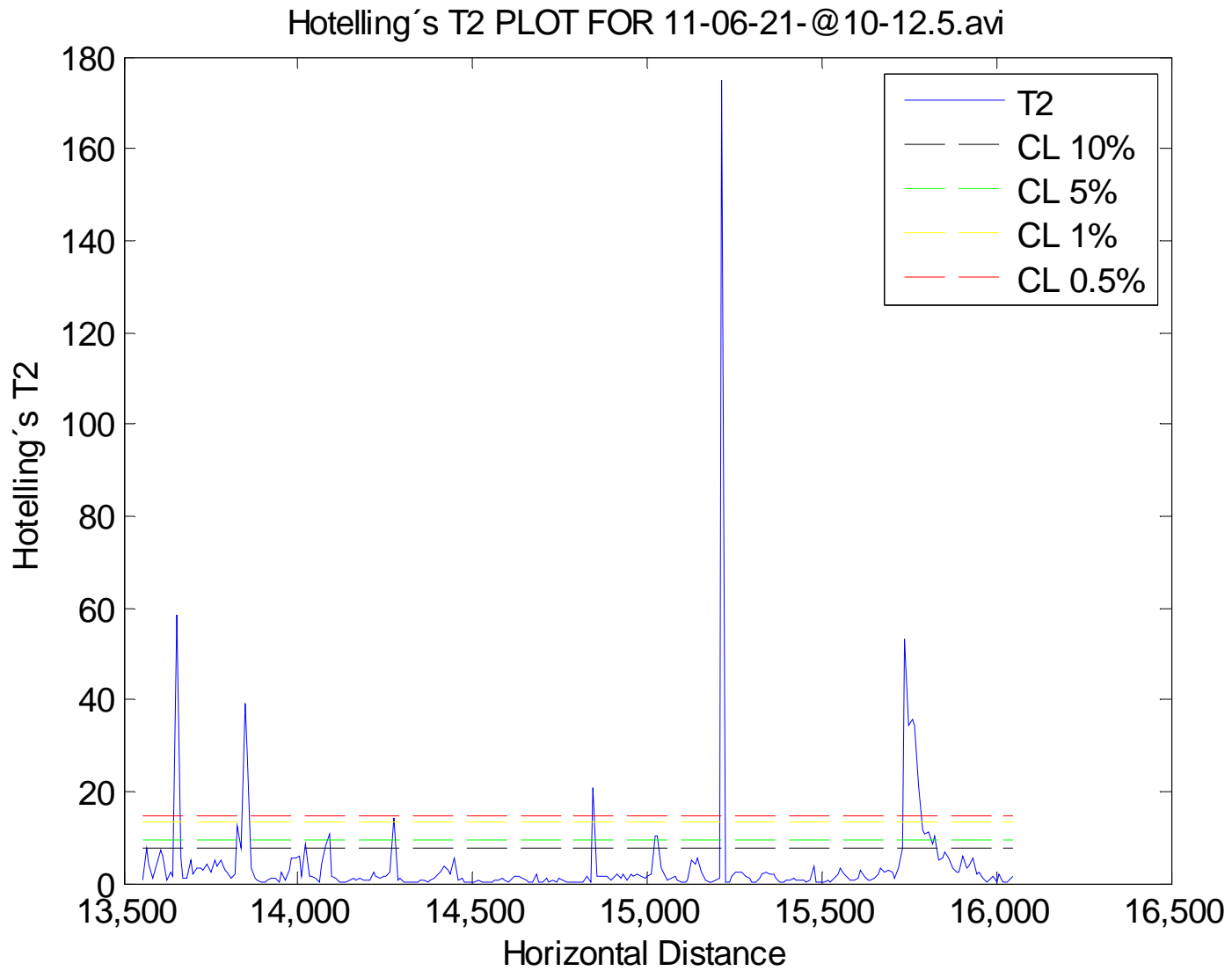


Hotelling's T2 Plot for project #5c: 11-21C

Hotelling's T2 PLOT FOR 11-06-21-@10-12.5.avi

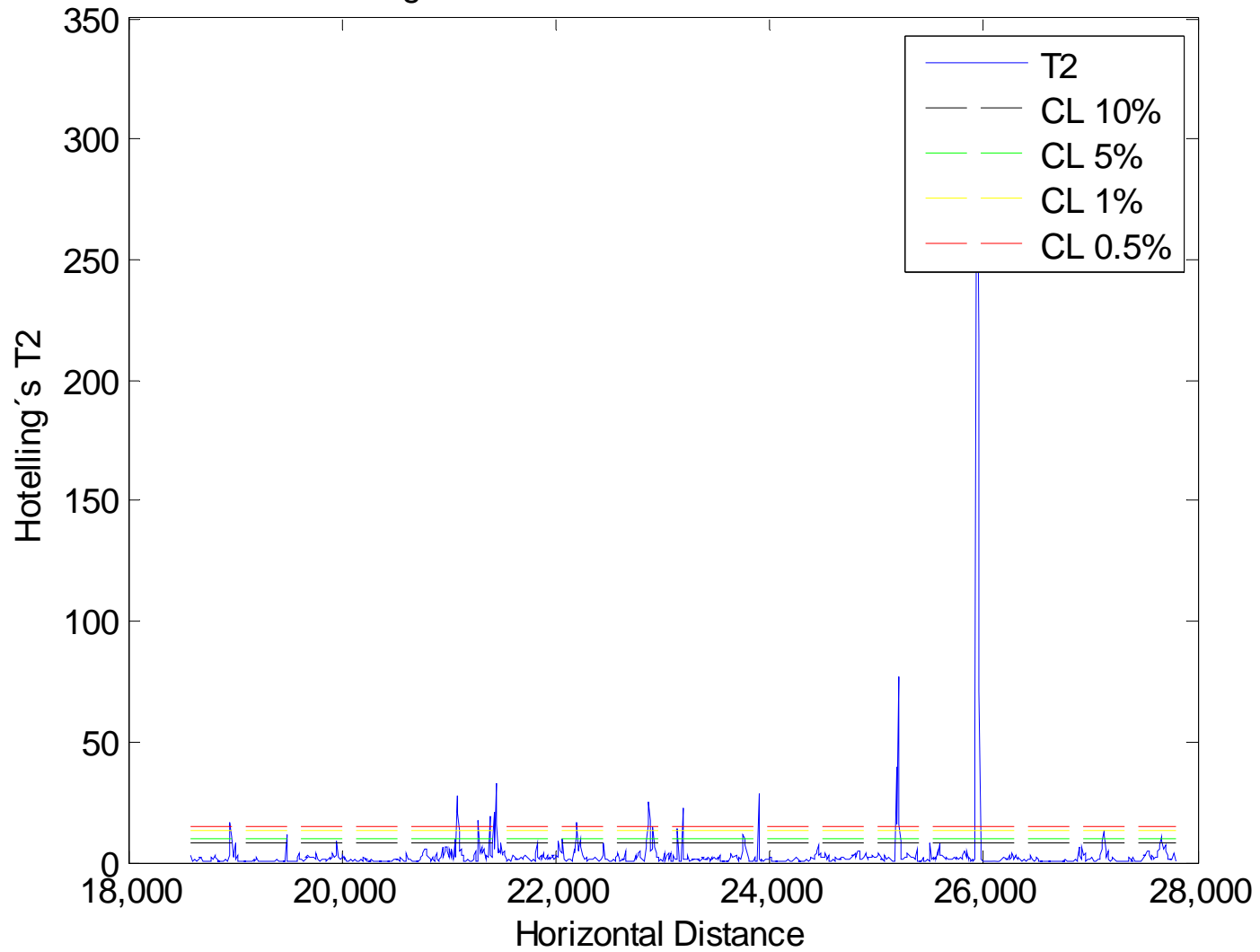


Hotelling's T2 Plot for project #5d: 11-21D



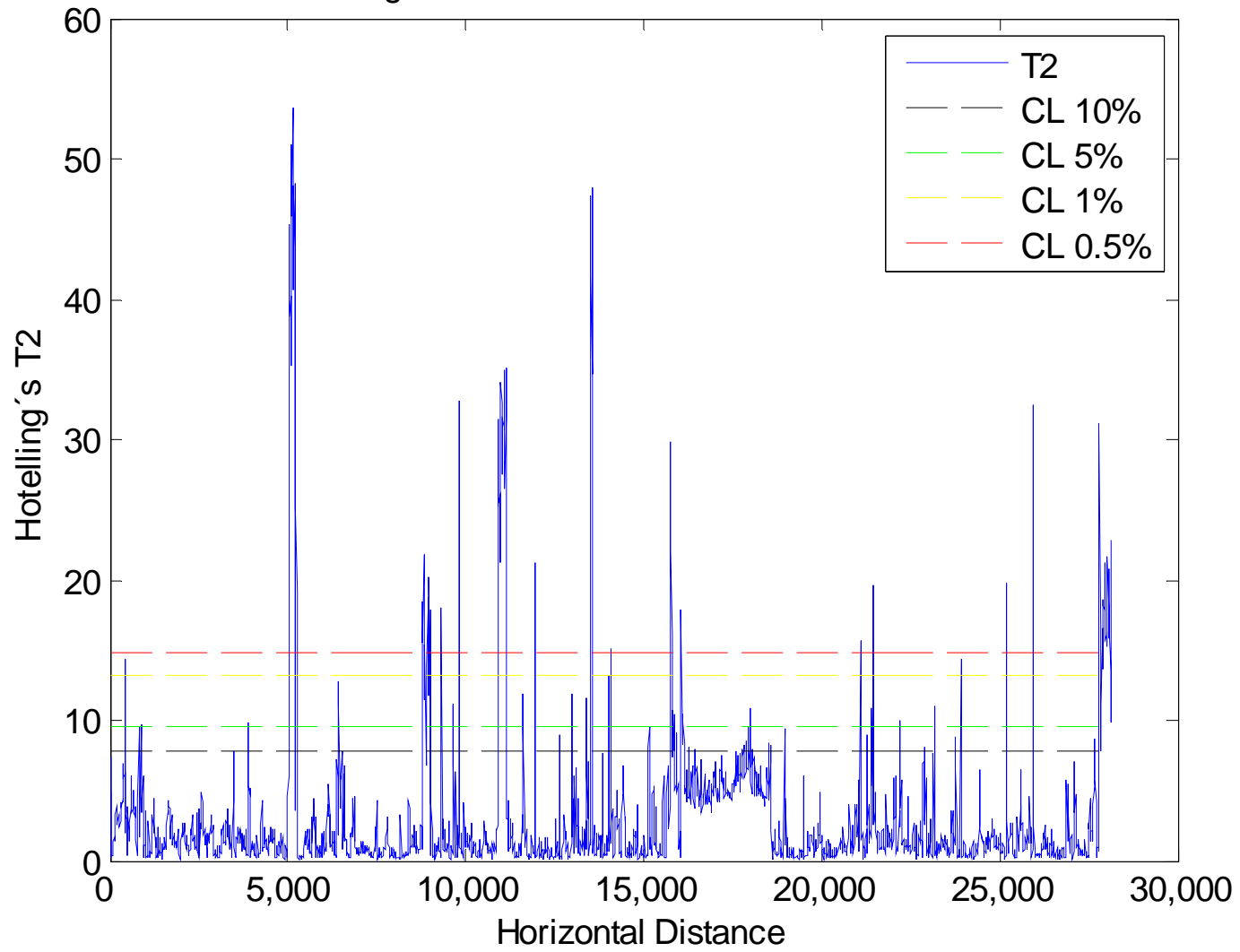
Hotelling's T2 Plot for project #5e: 11-21E

Hotelling's T2 PLOT FOR 11-06-21-@10-12.5.avi

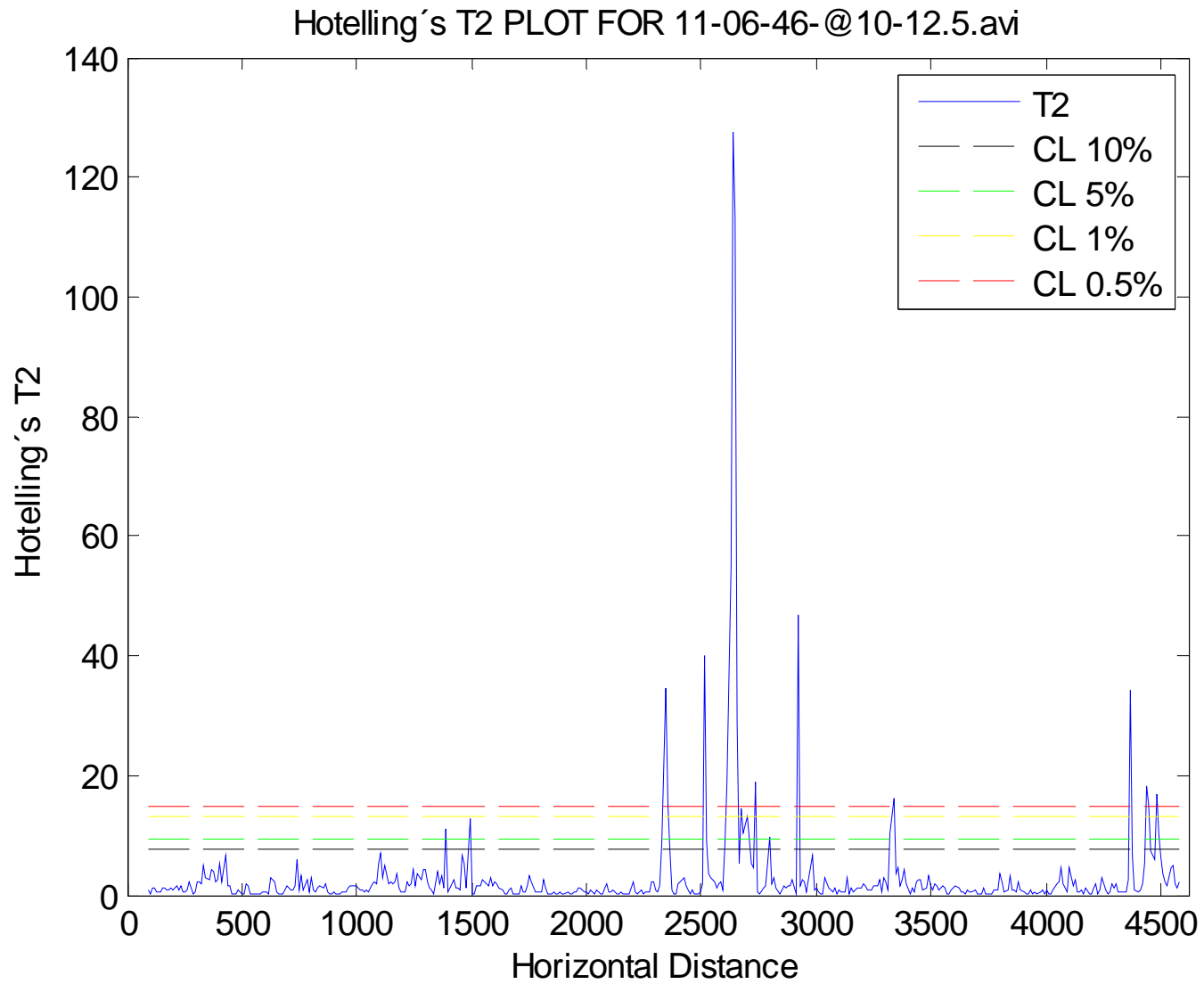


Hotelling's T2 Plot for project #5f: 11-21F

Hotelling's T2 PLOT FOR 11-06-21-@10-12.5.avi

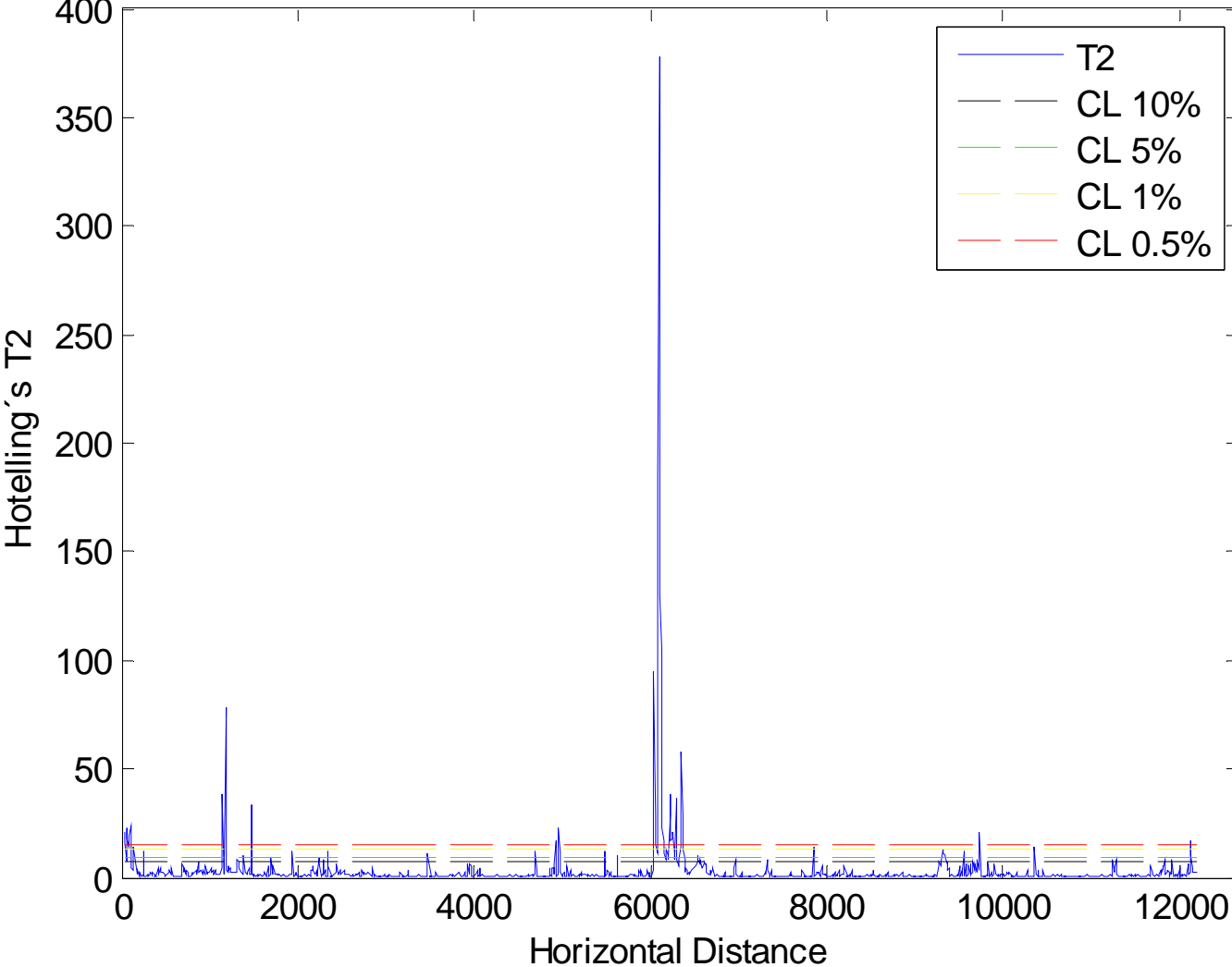


Hotelling's T2 Plot for project #5all: 11-21 all



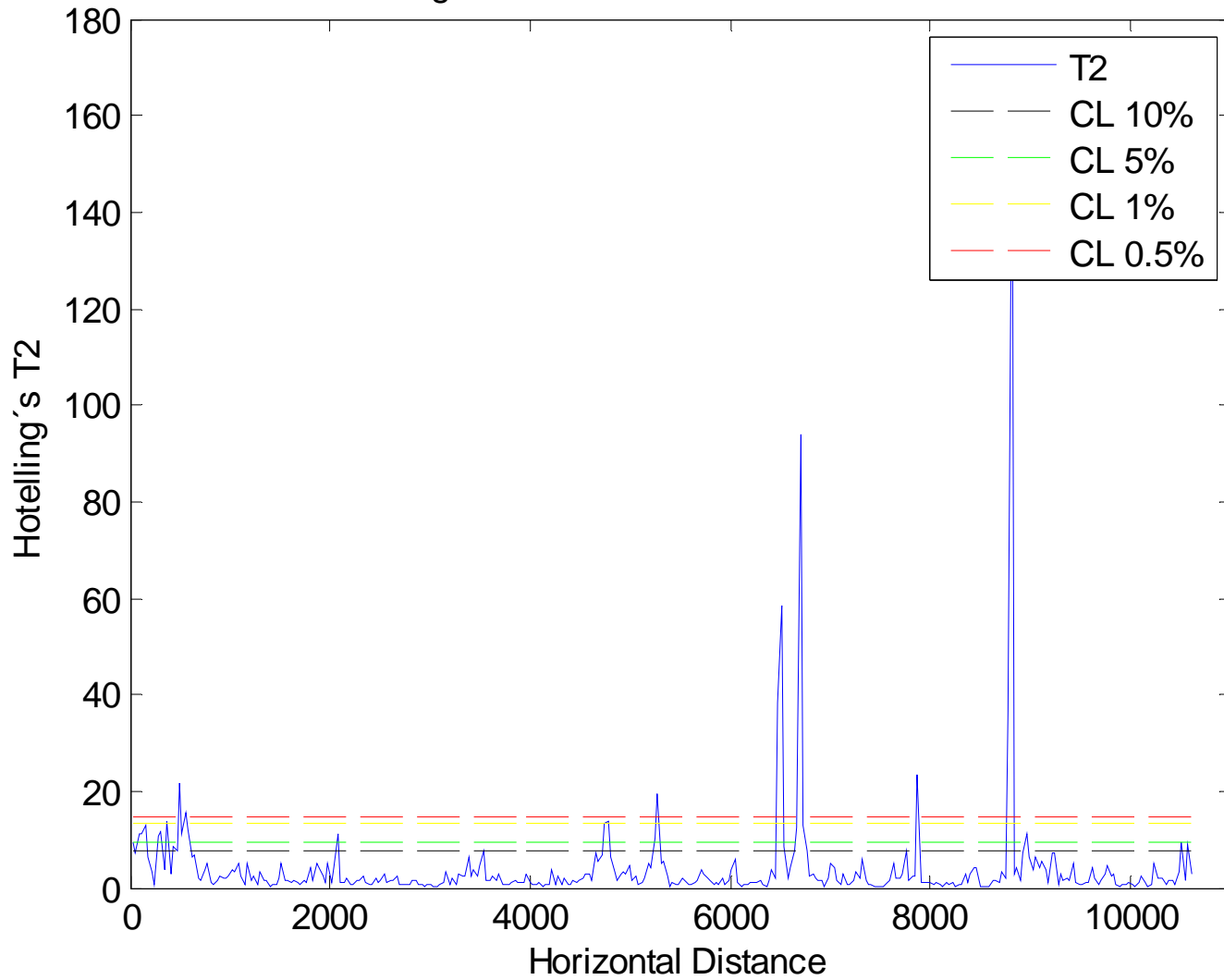
Hotelling's T2 Plot for project #6: 11-46

Hotelling's T2 PLOT FOR Project 7



Hotelling's T2 Plot for project #7: 11-47

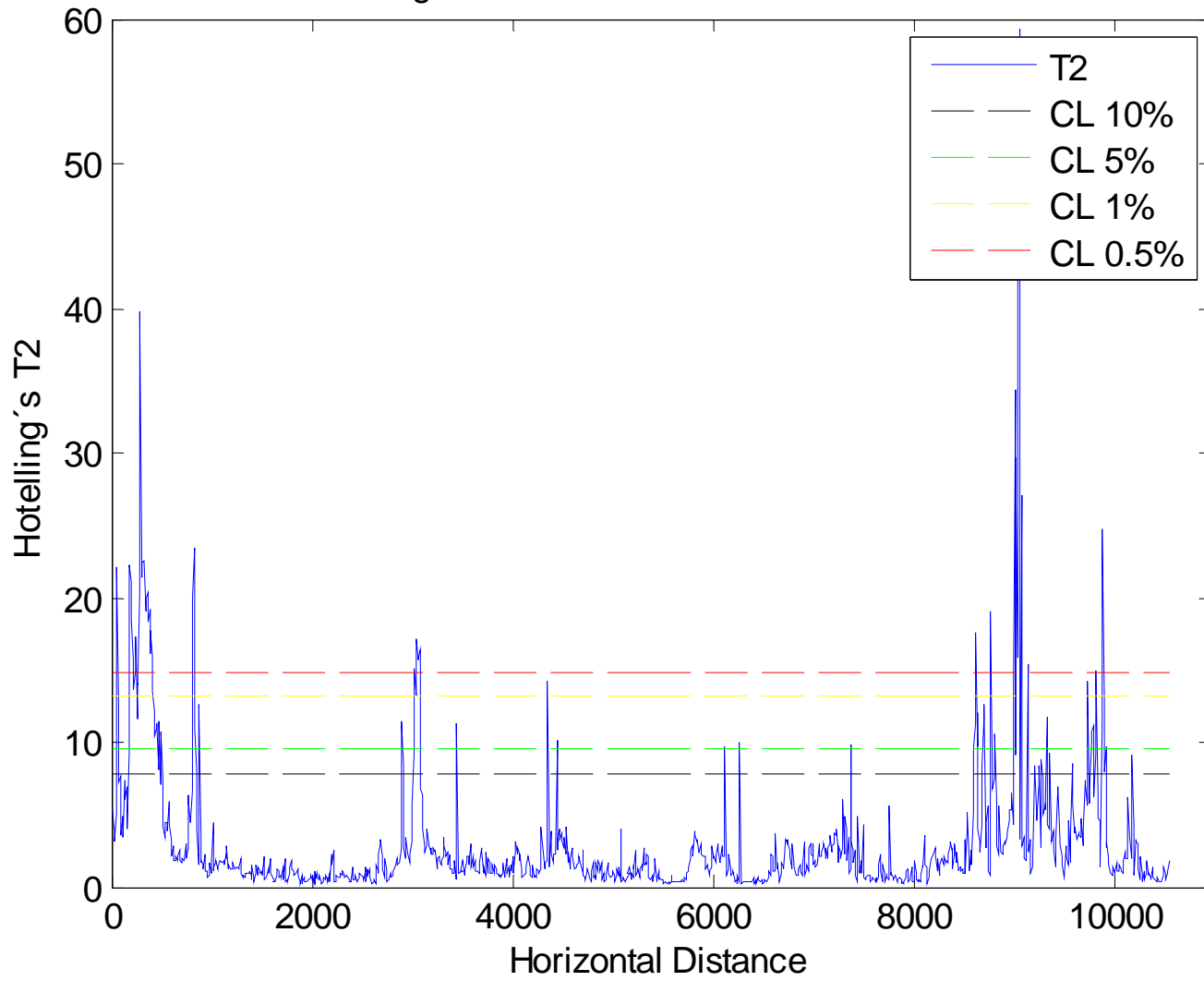
Hotelling's T2 PLOT FOR Rt 8 South 12.5-1.avi



Hotelling's T2 Plot for project #8a: RT 8S-1

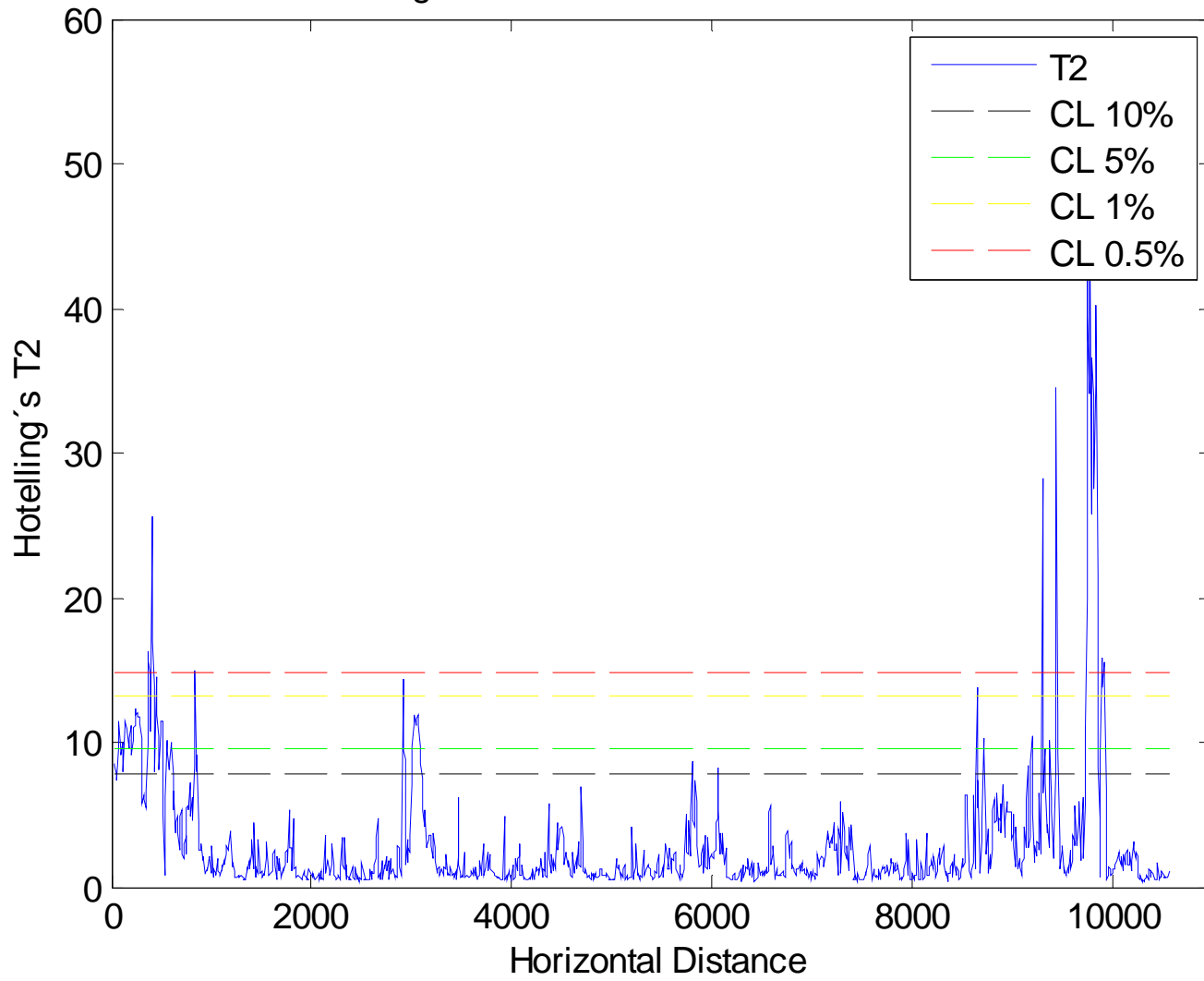


Hotelling's T2 PLOT FOR Rt 8 South 12.5-2.avi



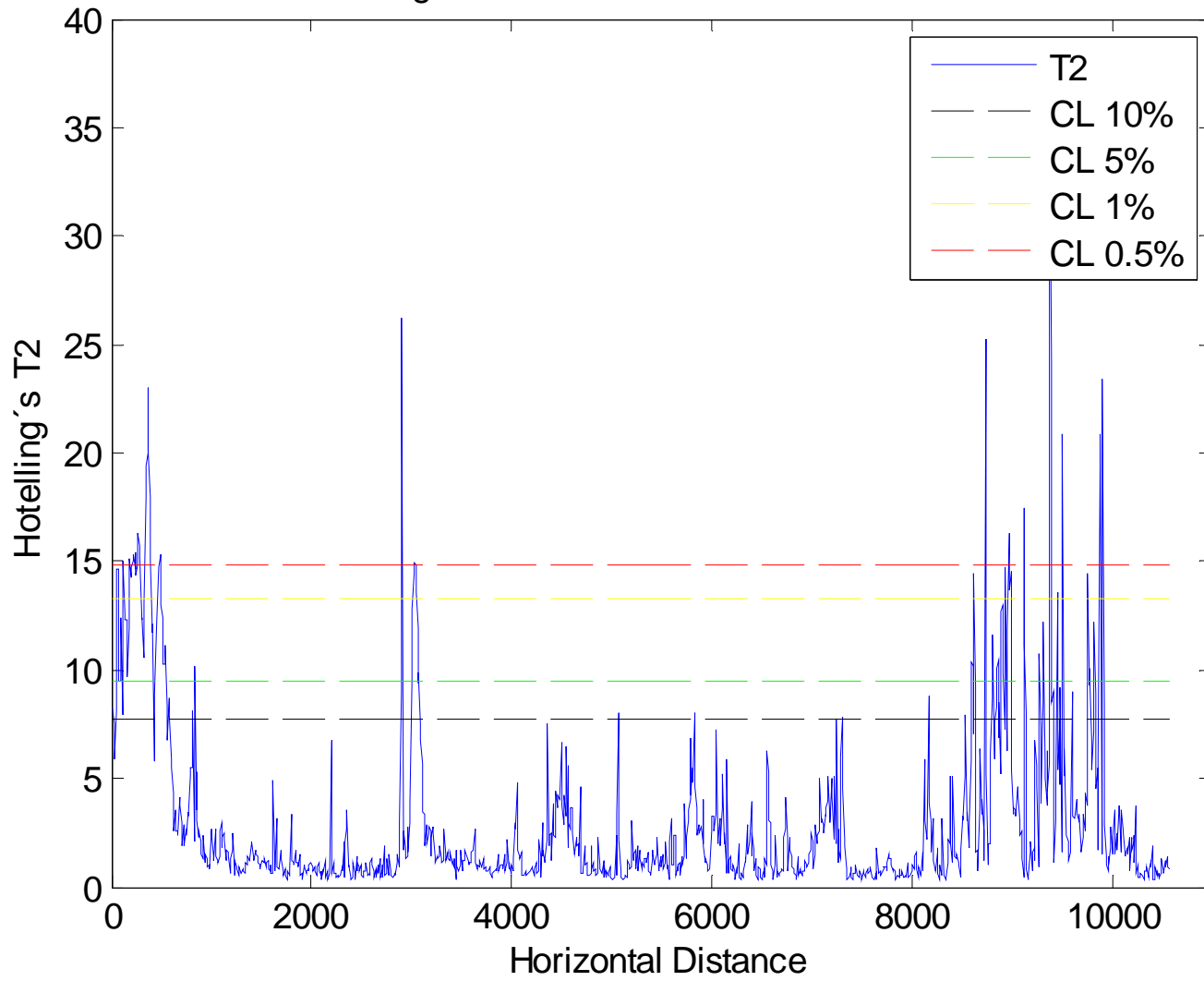
Hotelling's T2 Plot for project #8b: RT 8S-2

Hotelling's T2 PLOT FOR Rt 8 South 12.5-3.avi

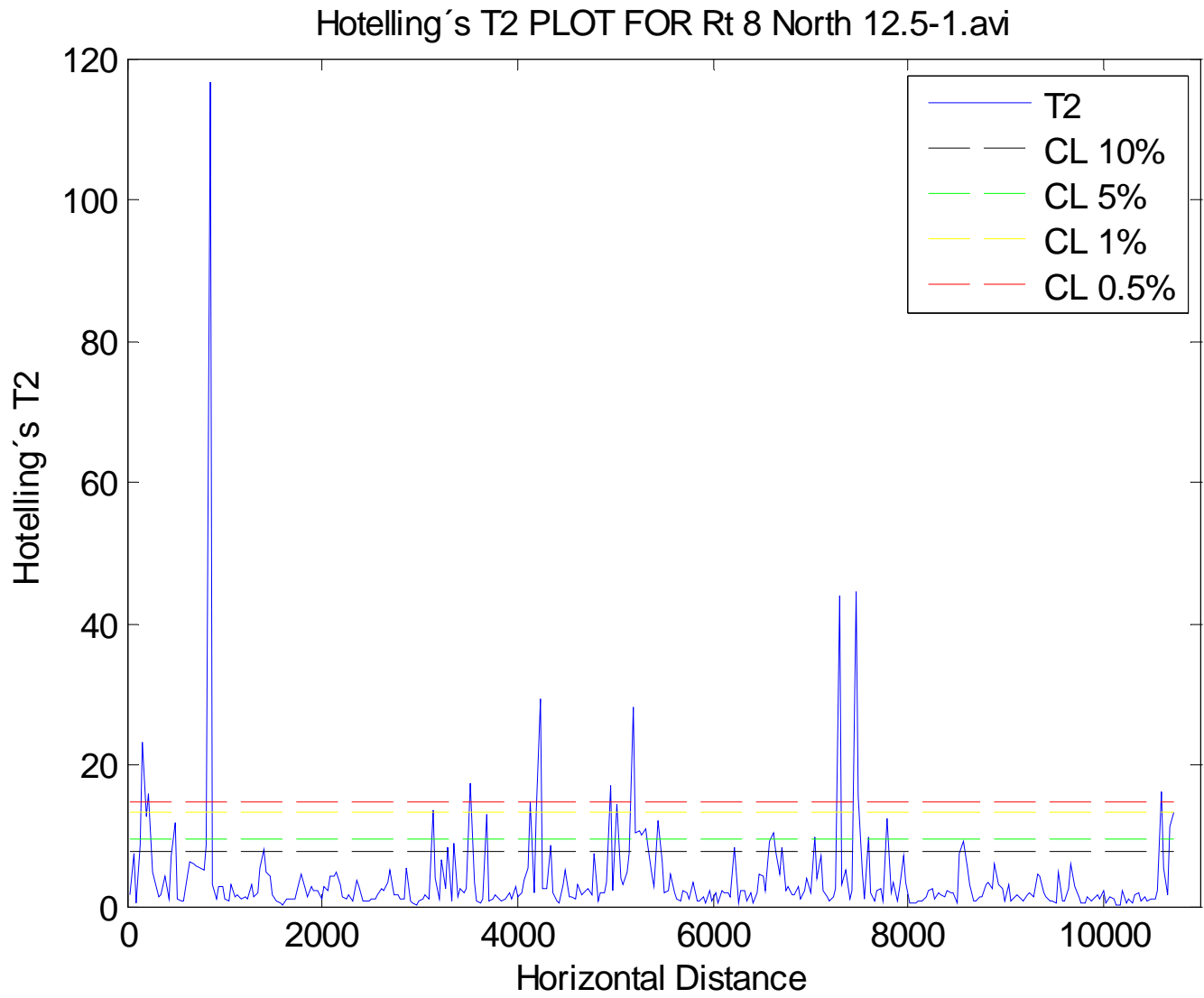


Hotelling's T2 Plot for project #8c: RT 8S-3

Hotelling's T2 PLOT FOR Rt 8 South 12.5-4.avi

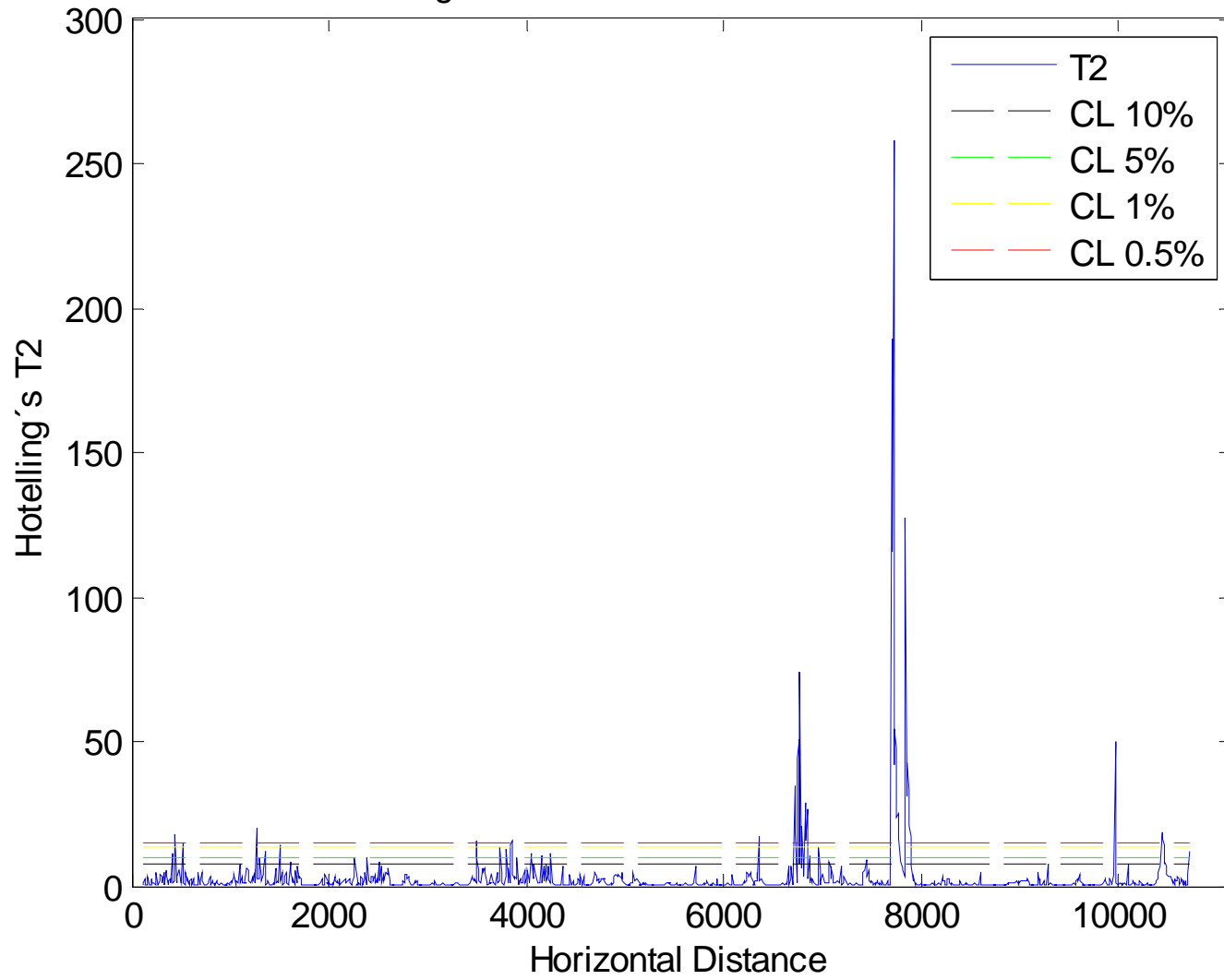


Hotelling's T2 Plot for project #8d: RT 8S-4



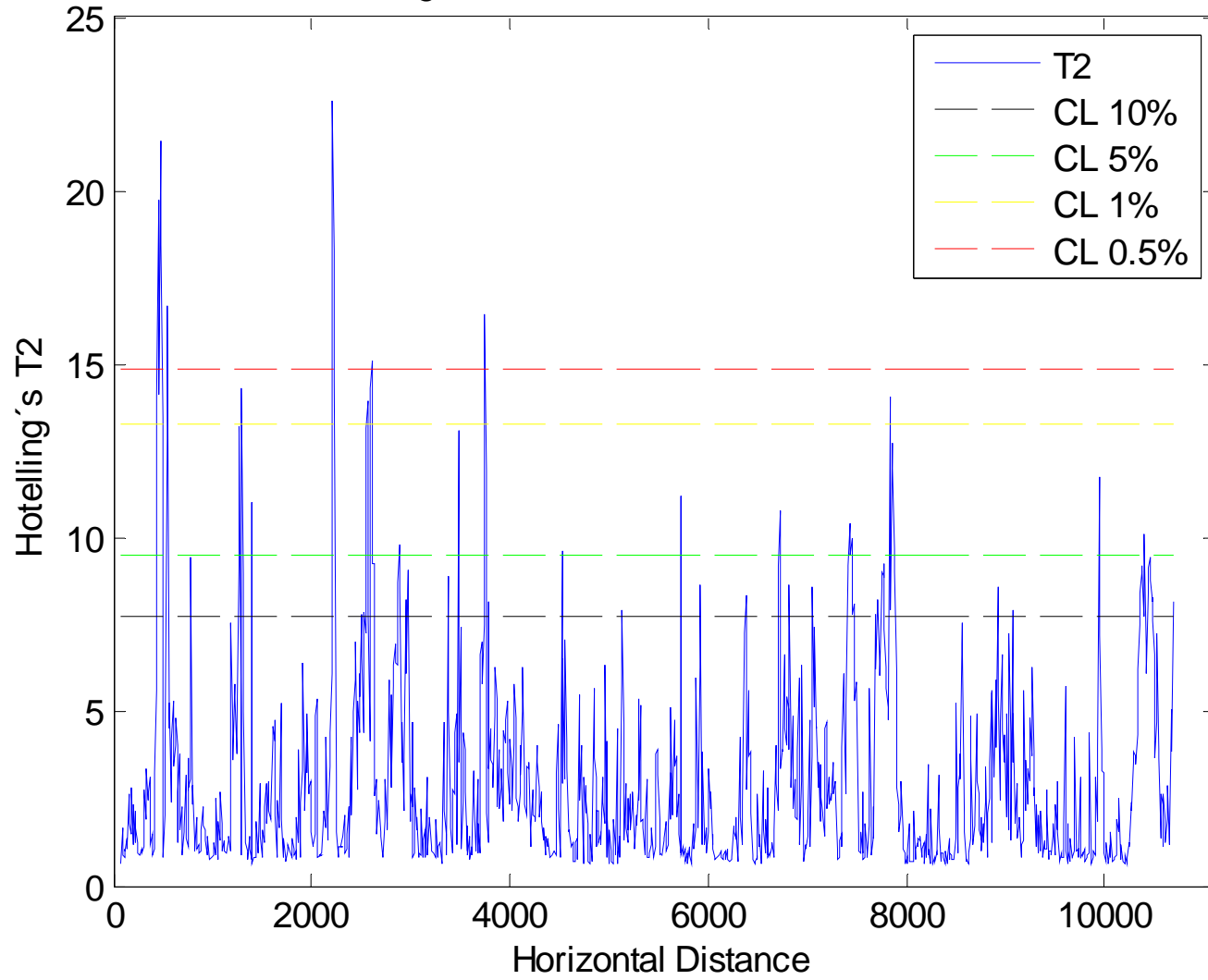
Hotelling's T2 Plot for project #9a: RT 8N-1

Hotelling's T2 PLOT FOR Rt 8 North 12.5-2.avi



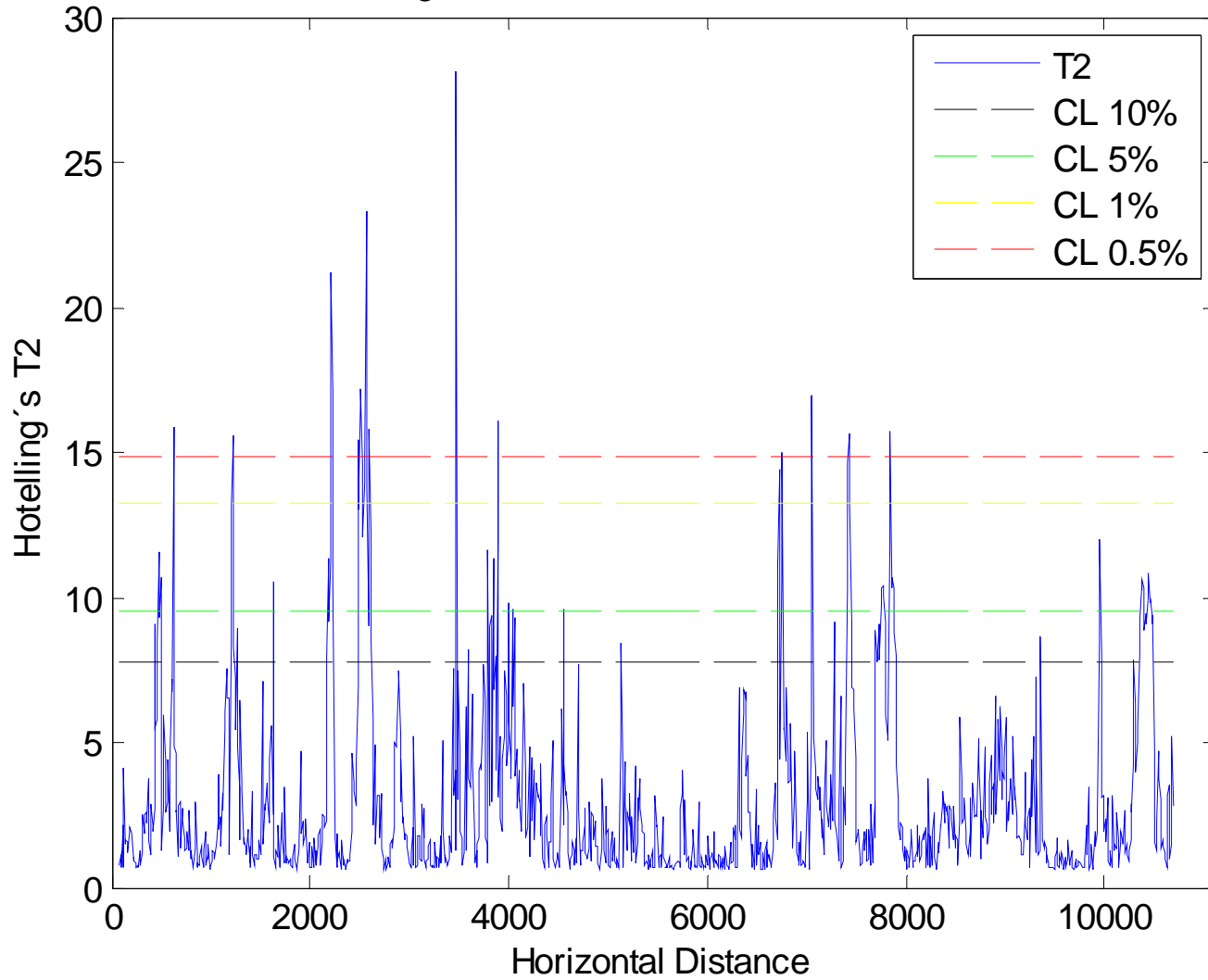
Hotelling's T2 Plot for project #9b: RT 8N-2

Hotelling's T2 PLOT FOR Rt 8 North 12.5-3.avi

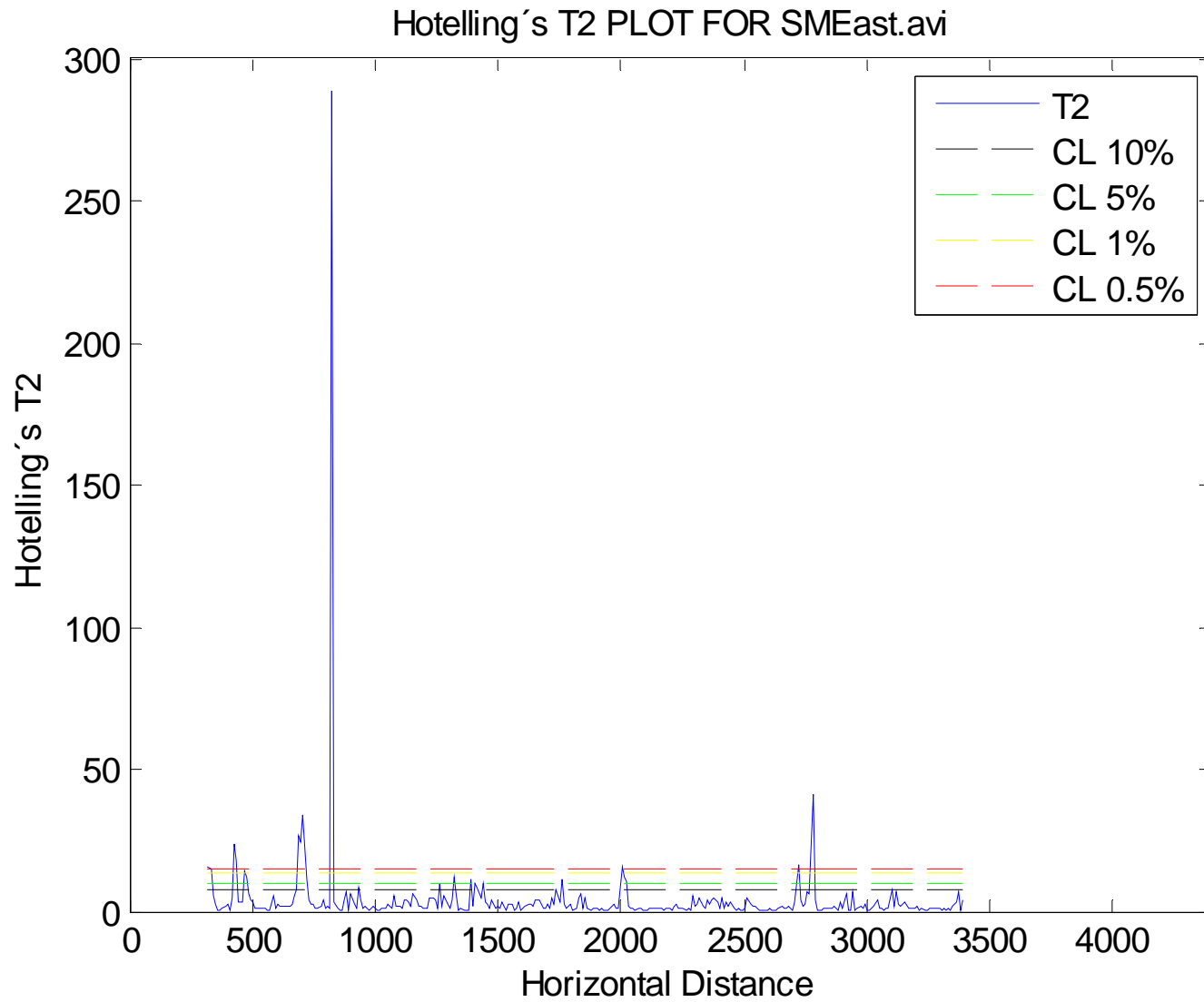


Hotelling's T2 Plot for project #9c: RT 8N-3

Hotelling's T2 PLOT FOR Rt 8 North 12.5-4.avi

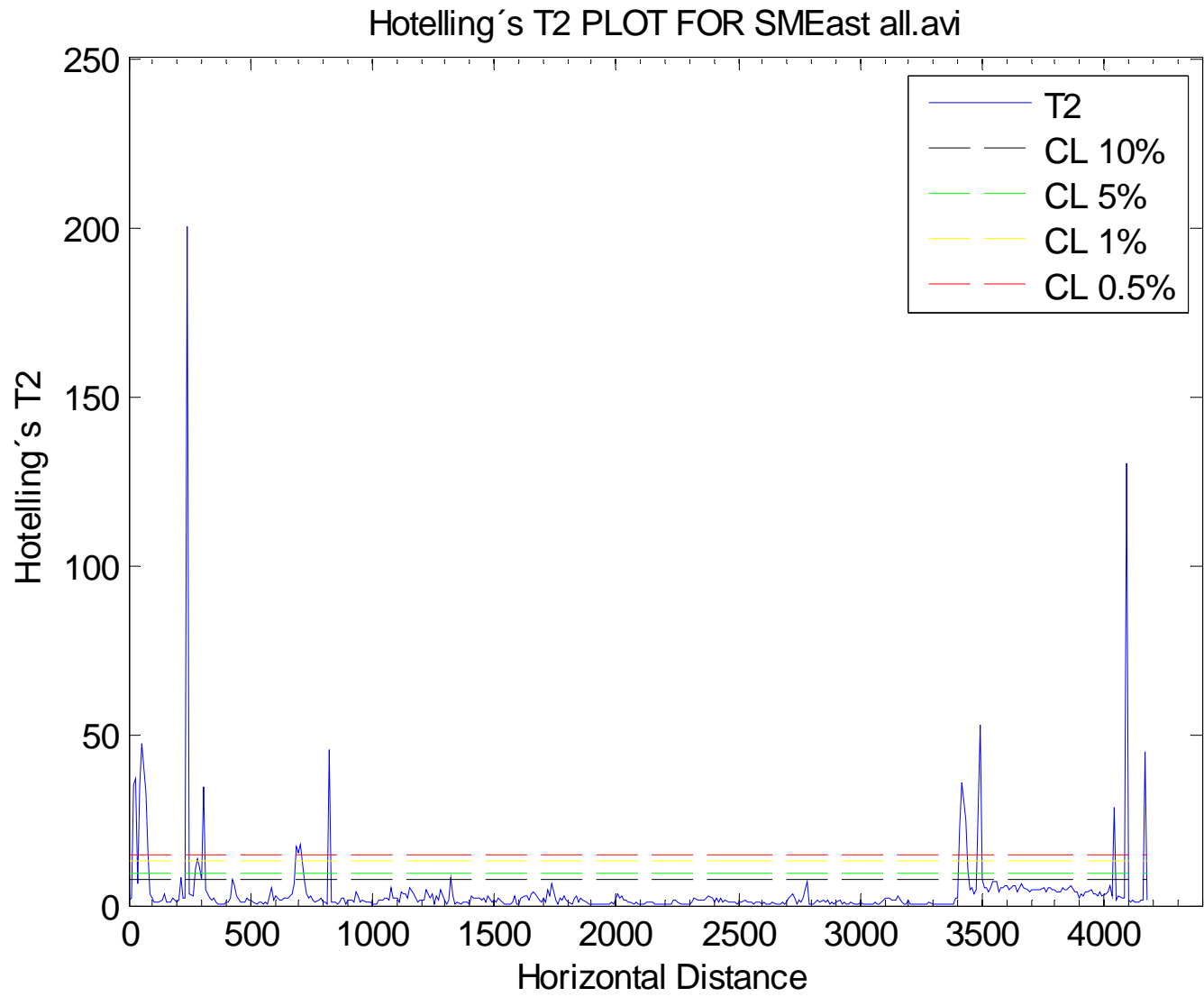


Hotelling's T2 Plot for project #9d: RT 8N-4



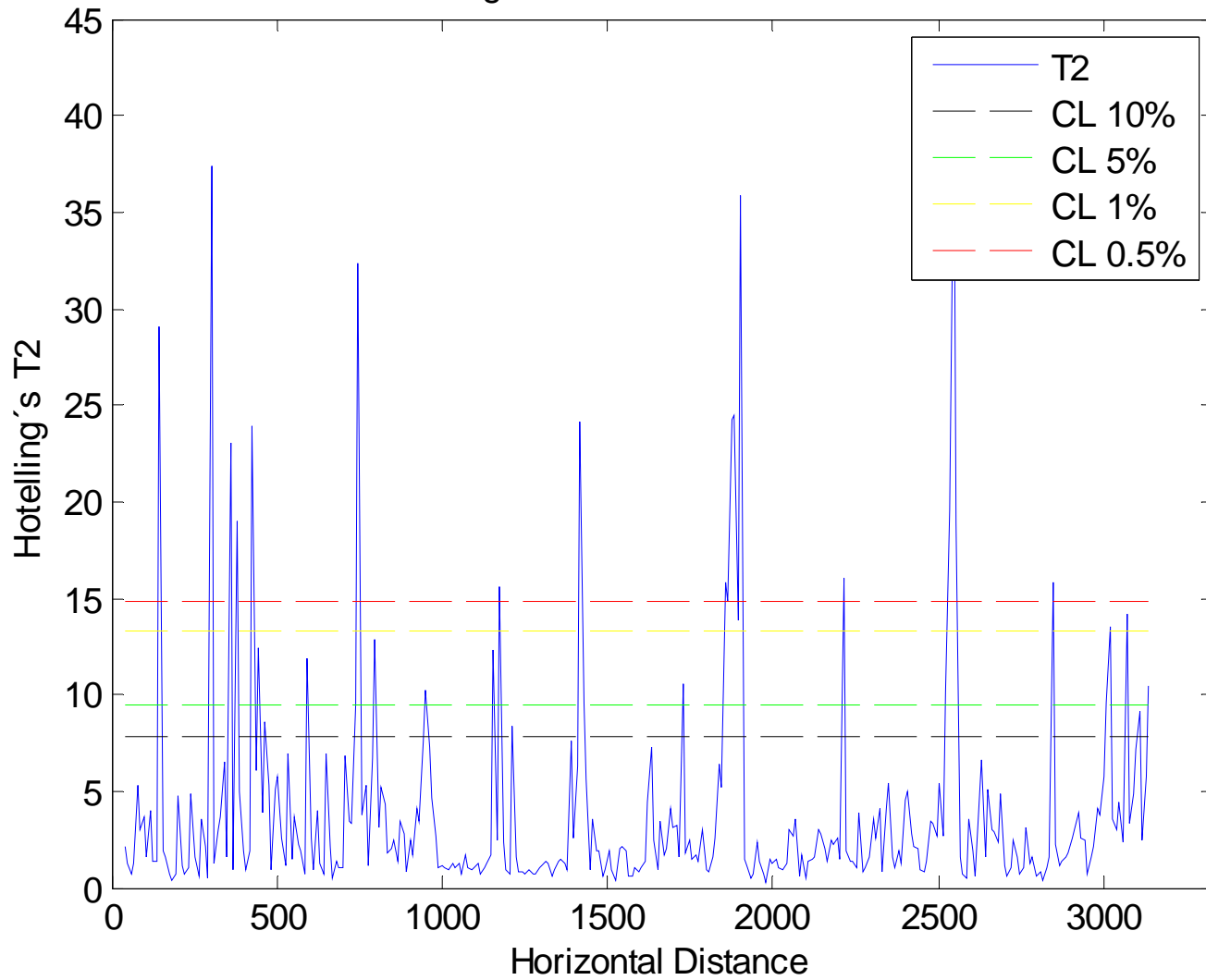
Hotelling's T2 Plot for project #10a: SM E



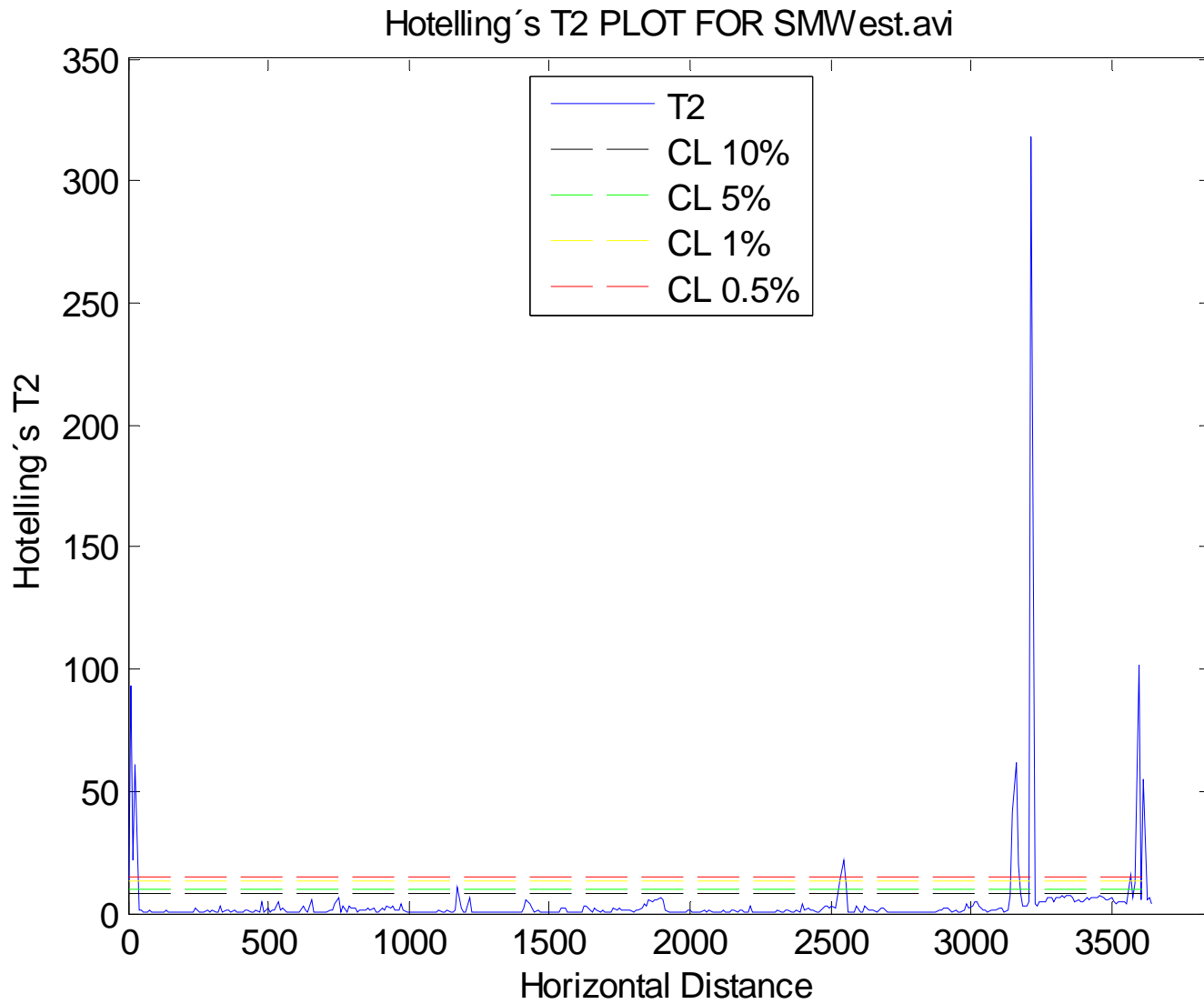


Hotelling's T2 Plot for project #10b: SM E all

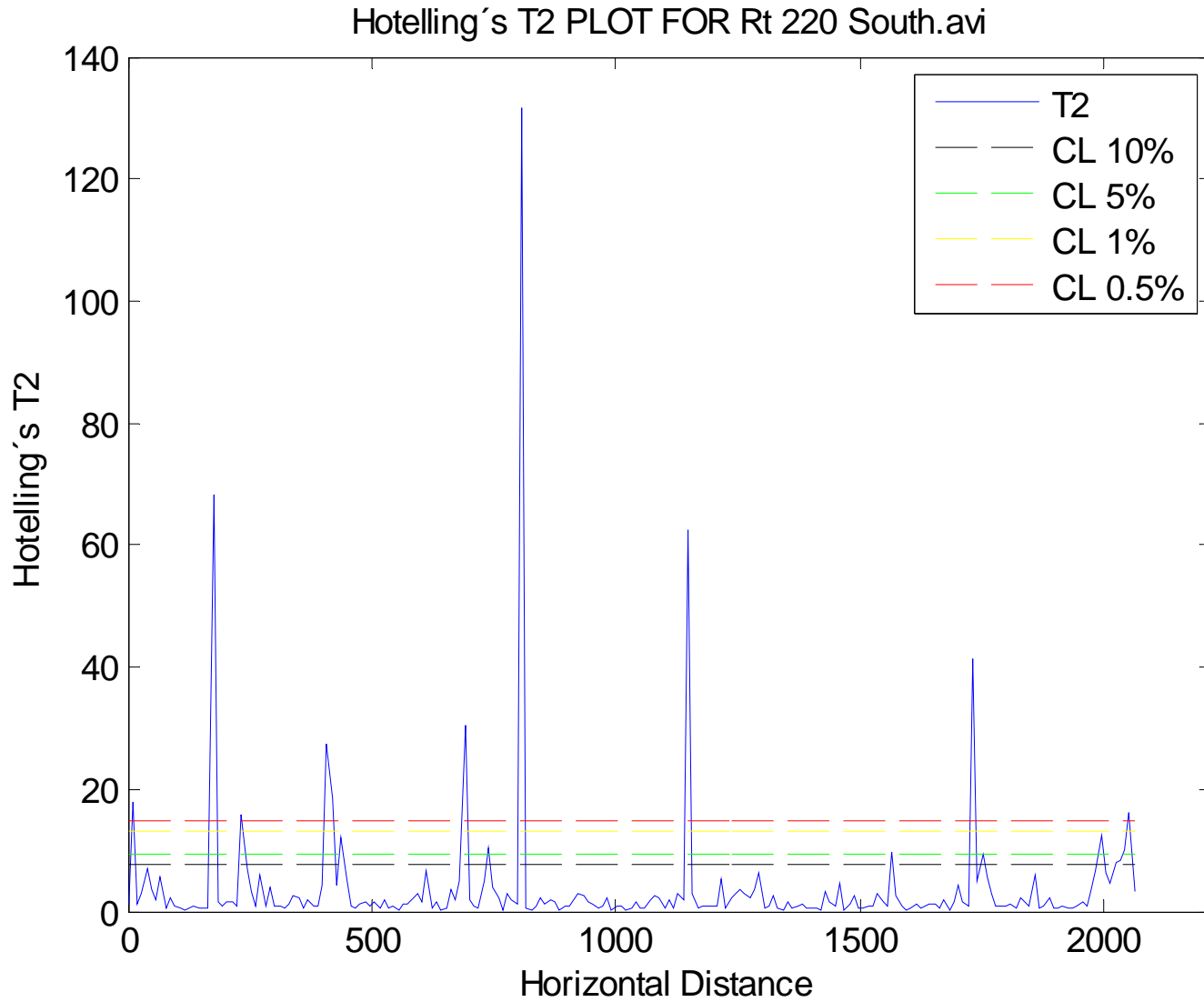
Hotelling's T2 PLOT FOR SMWest.avi



Hotelling's T2 Plot for project #11a: SM W

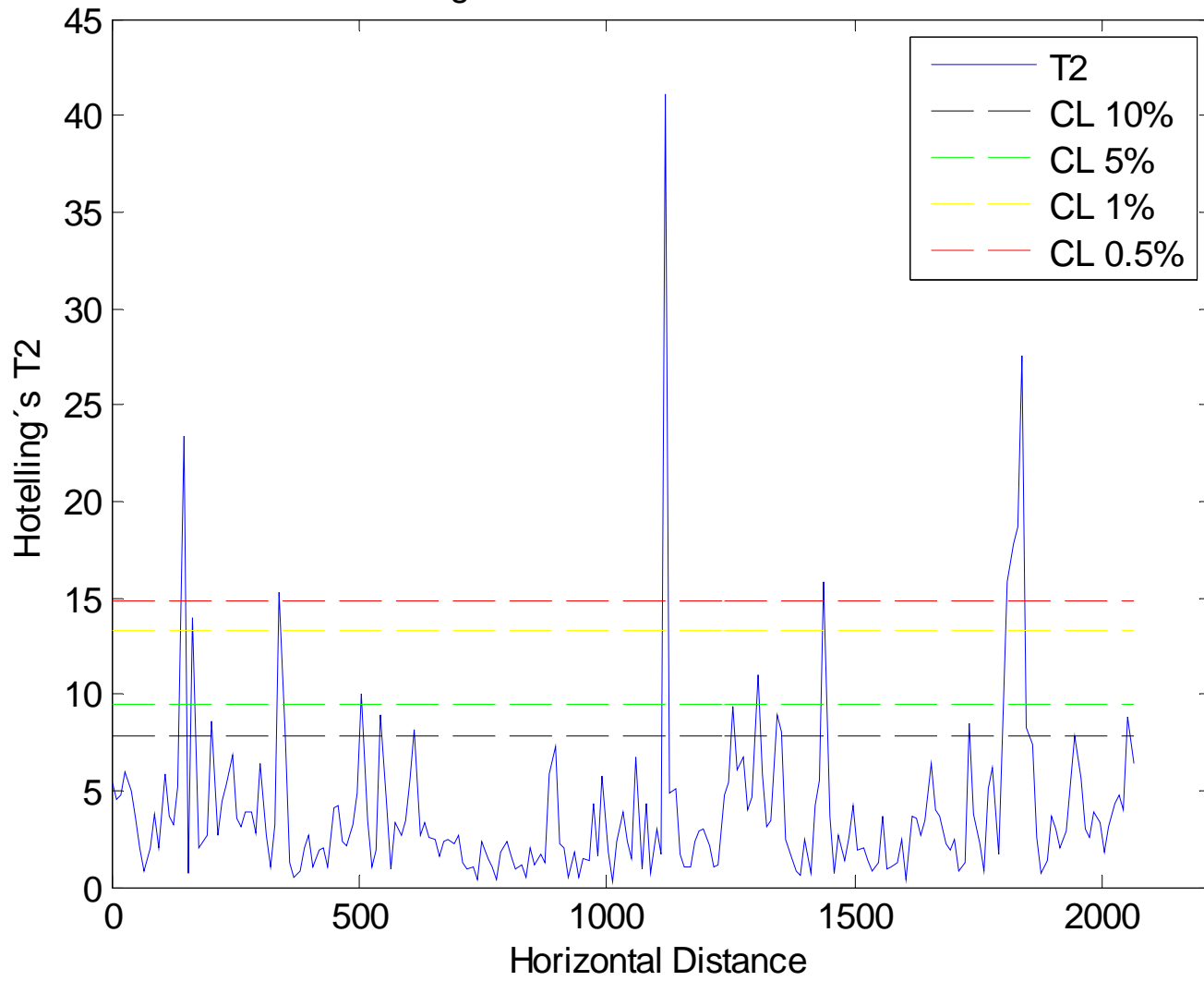


Hotelling's T2 Plot for project #11b: SM W all



Hotelling's T2 Plot for project #12: RT 220S

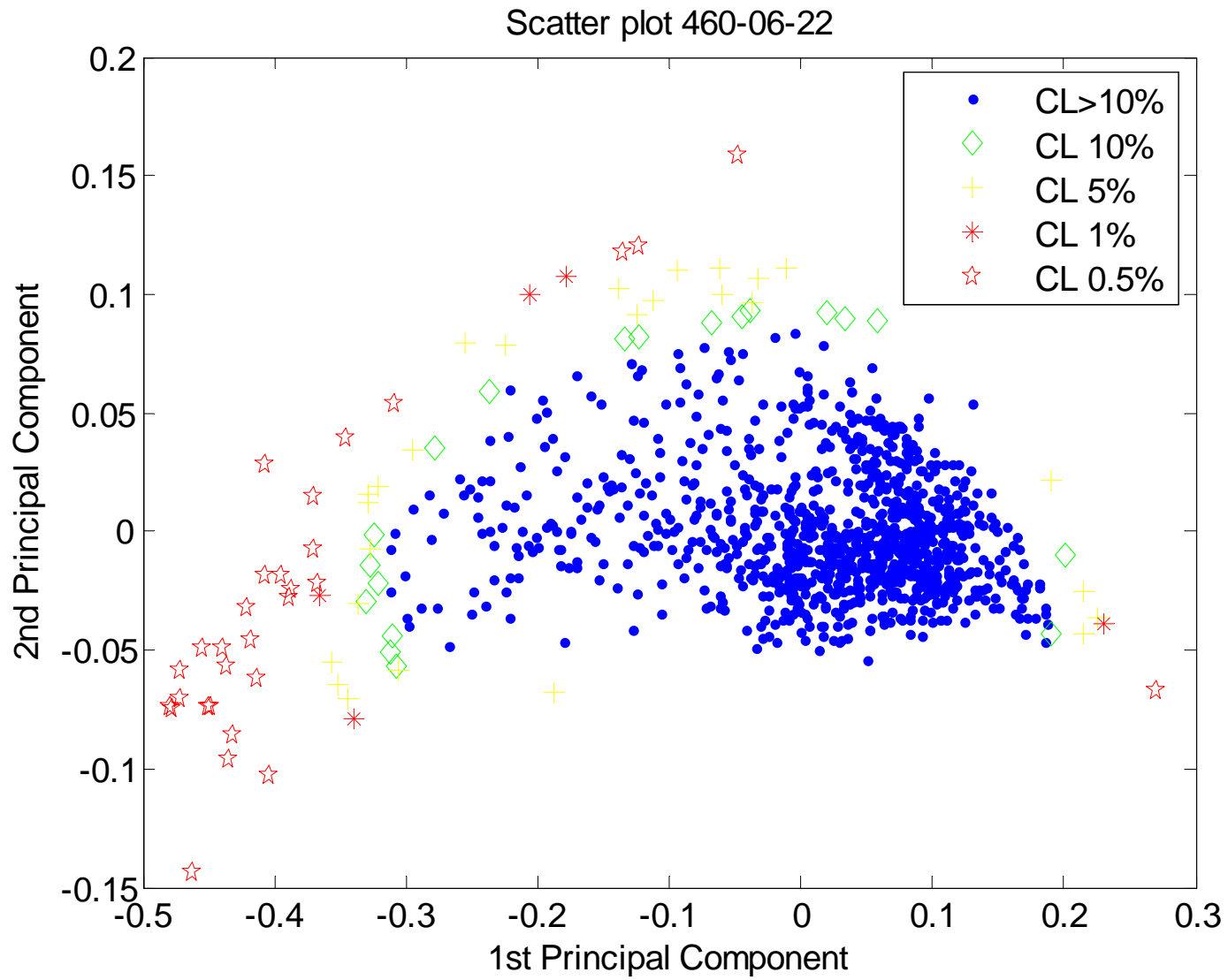
Hotelling's T2 PLOT FOR Rt 220 North.avi



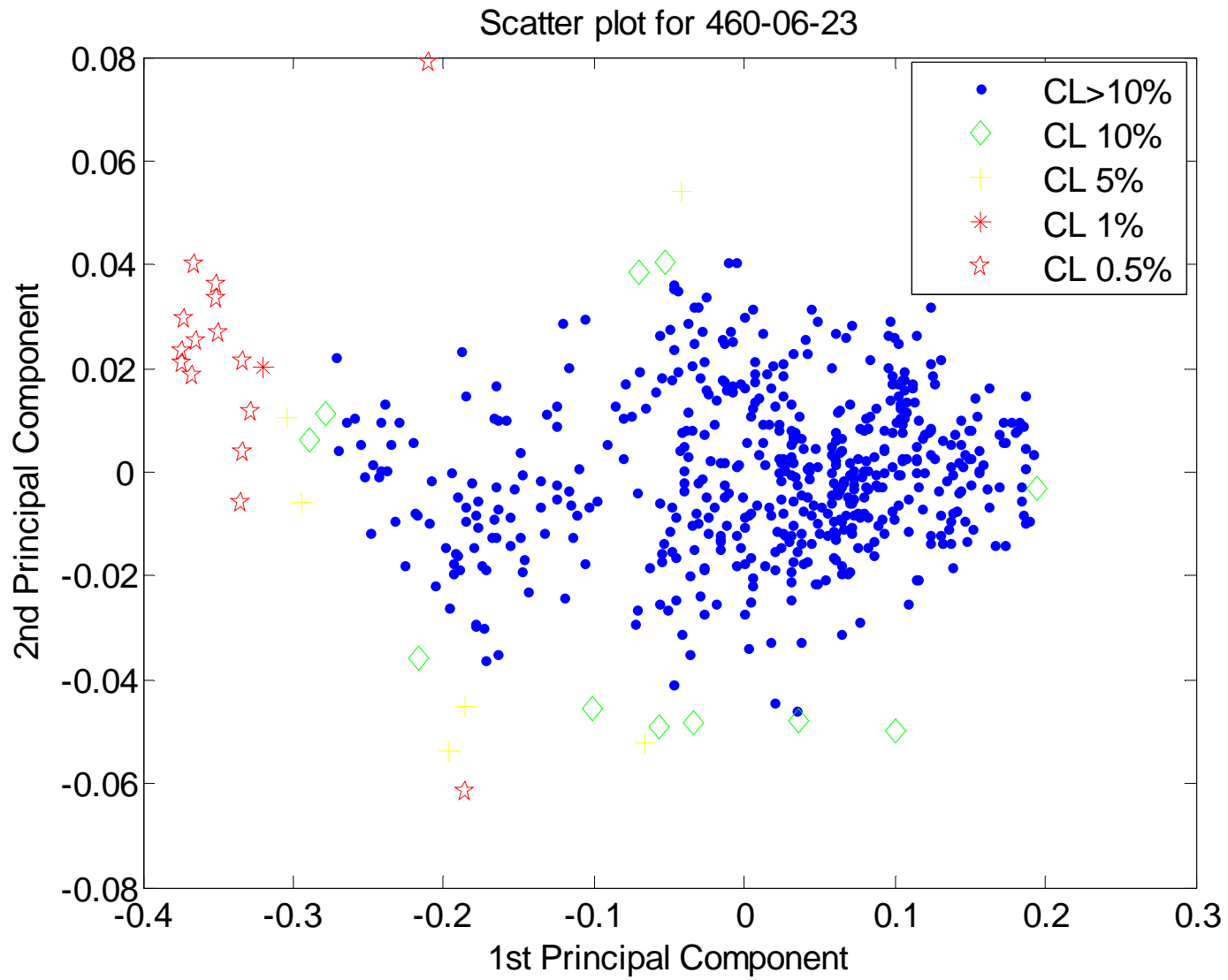
Hotelling's T2 Plot for project #13: RT 220N

# Appendix B

Scatter Plots of PCA components in 2-D

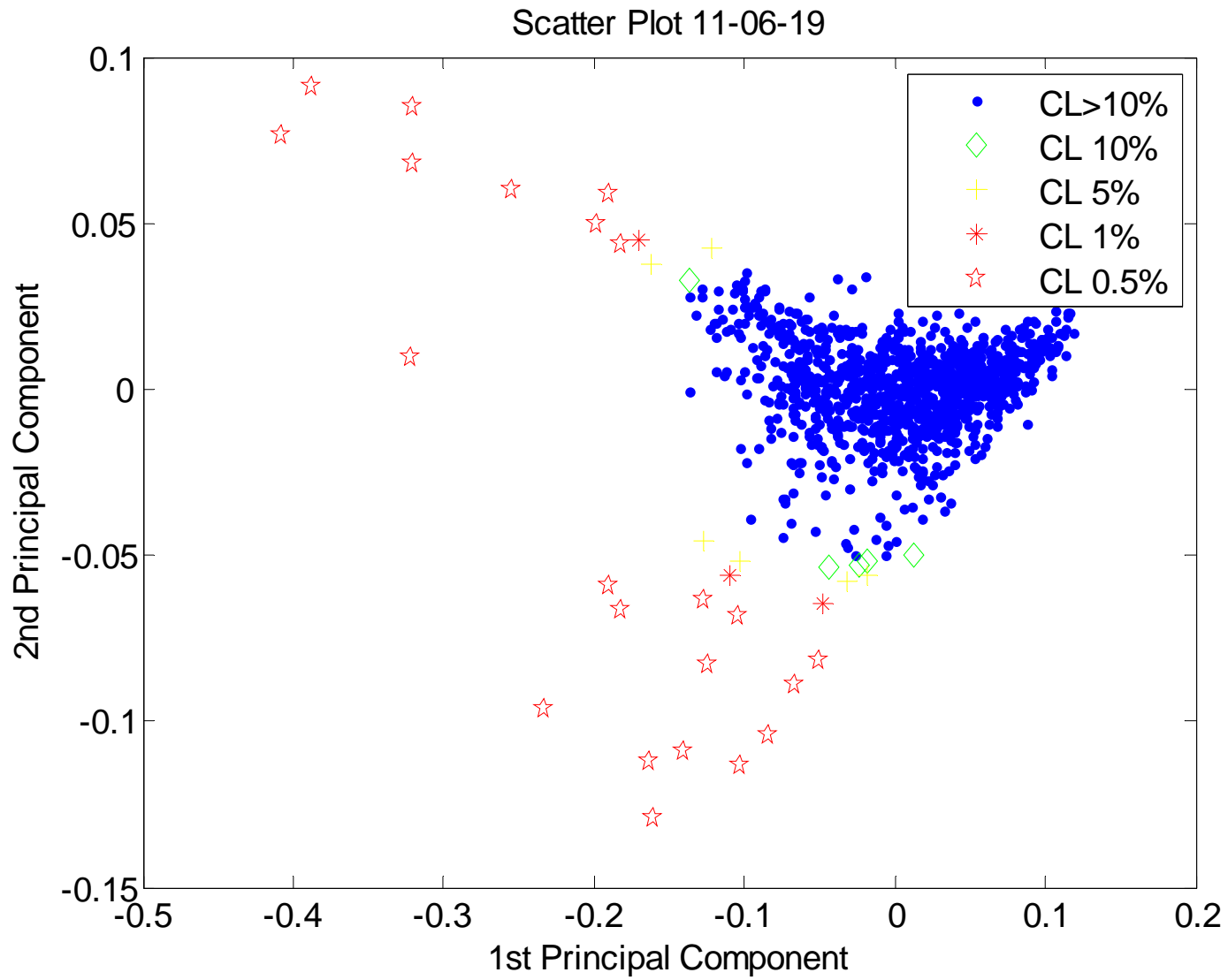


Principal Component Analysis 2-D Scatter Plot for project #1: 460-22

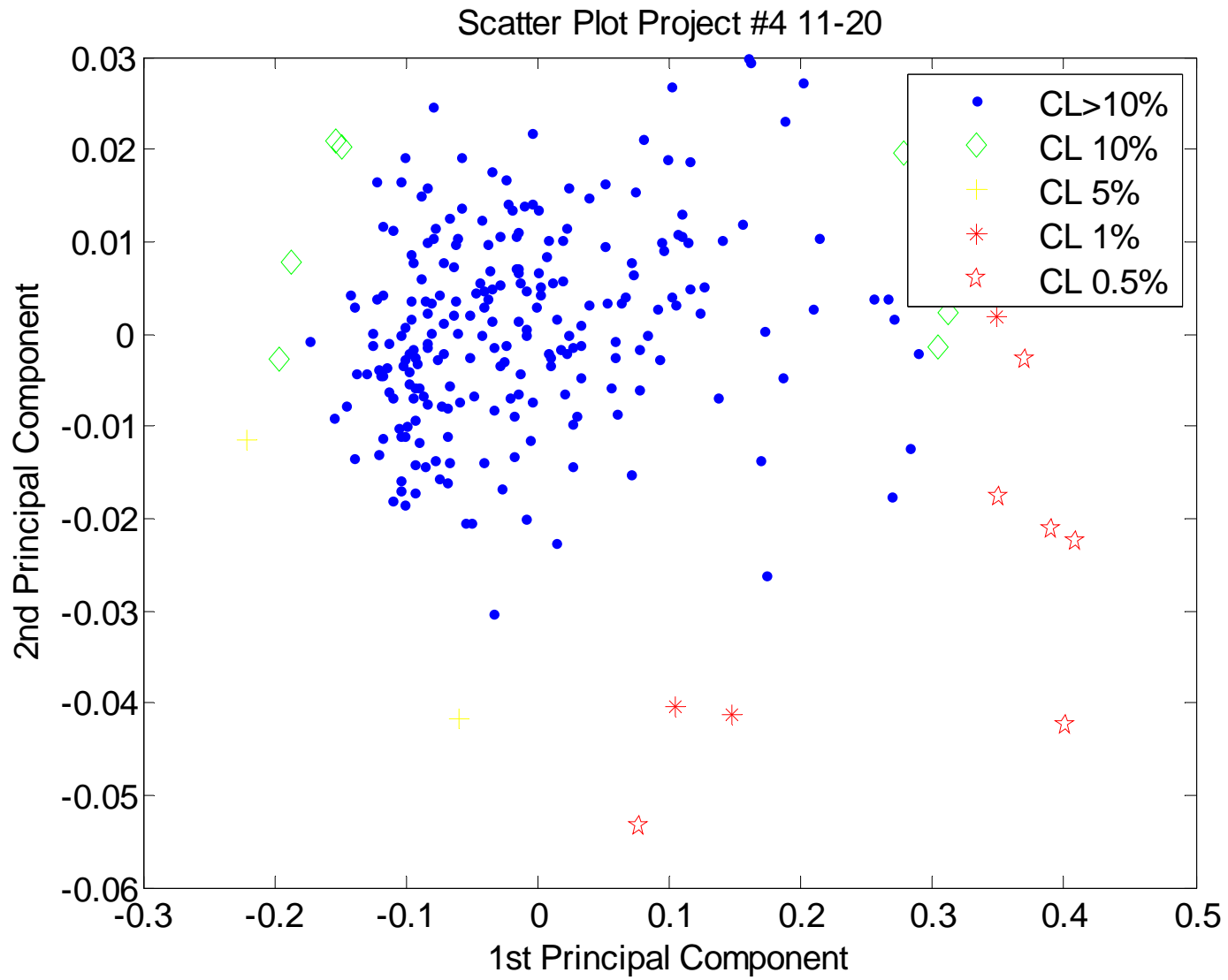


Principal Component Analysis 2-D Scatter Plot for project #2: 460-23

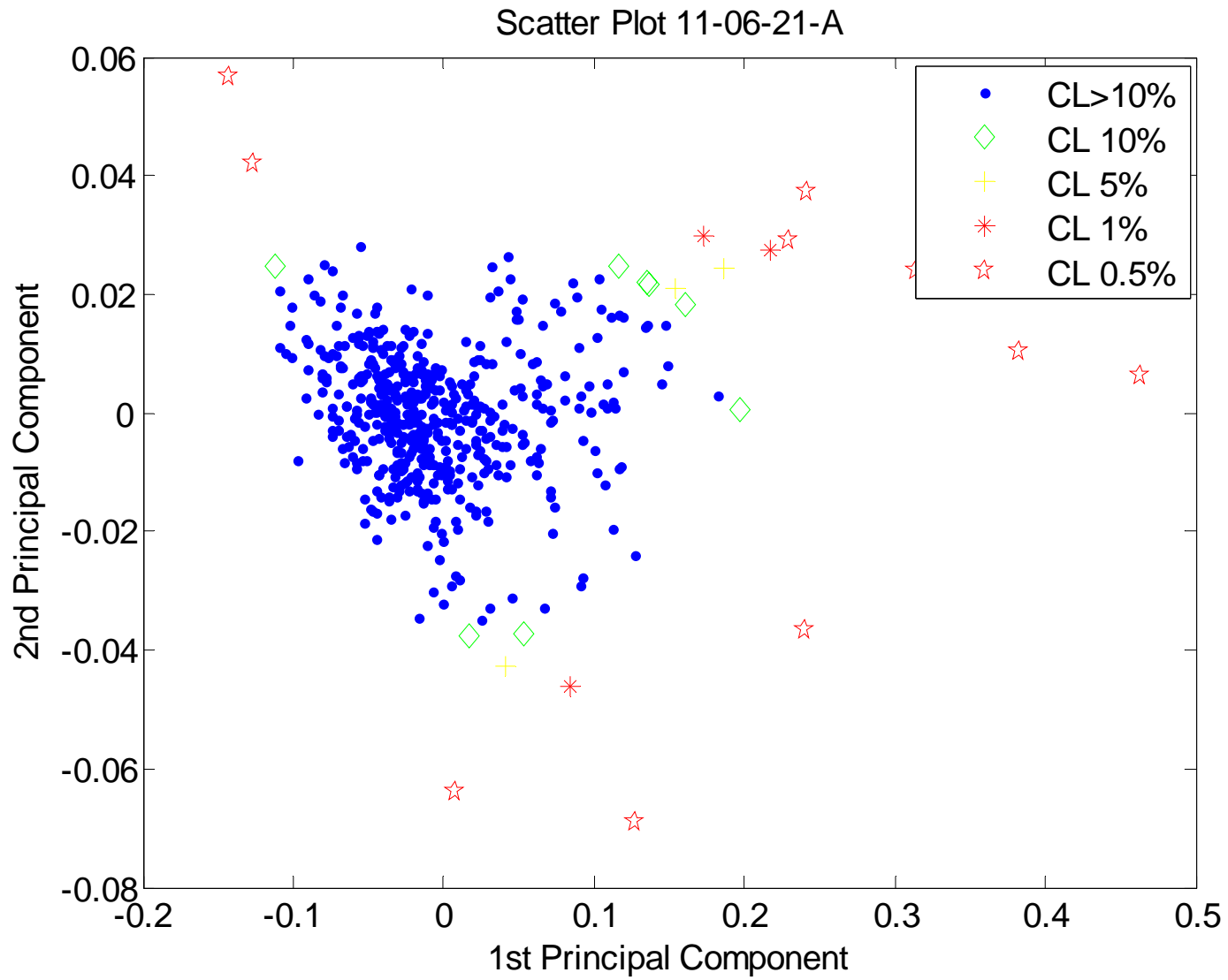




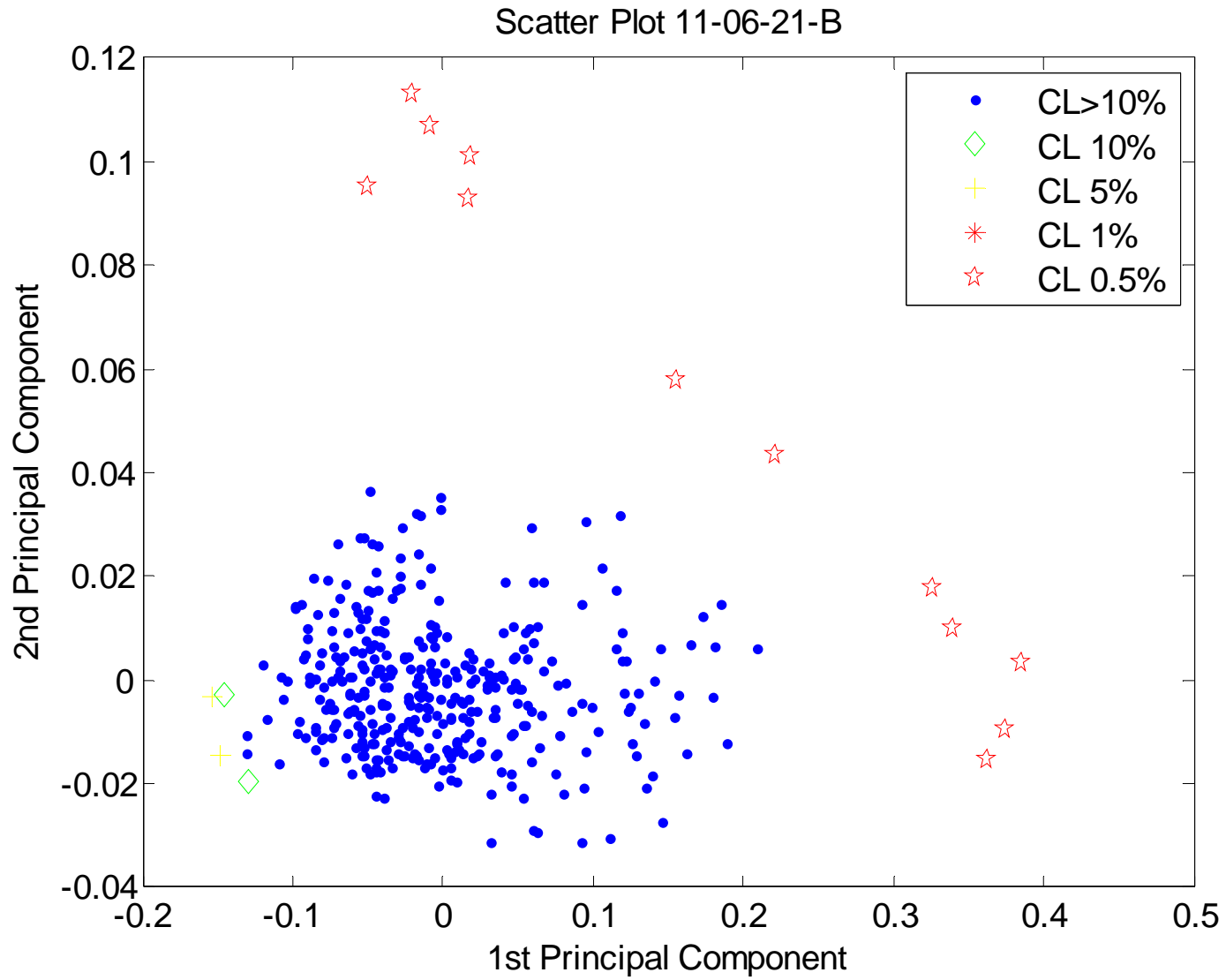
Principal Component Analysis 2-D Scatter Plot for project #3: 11-19



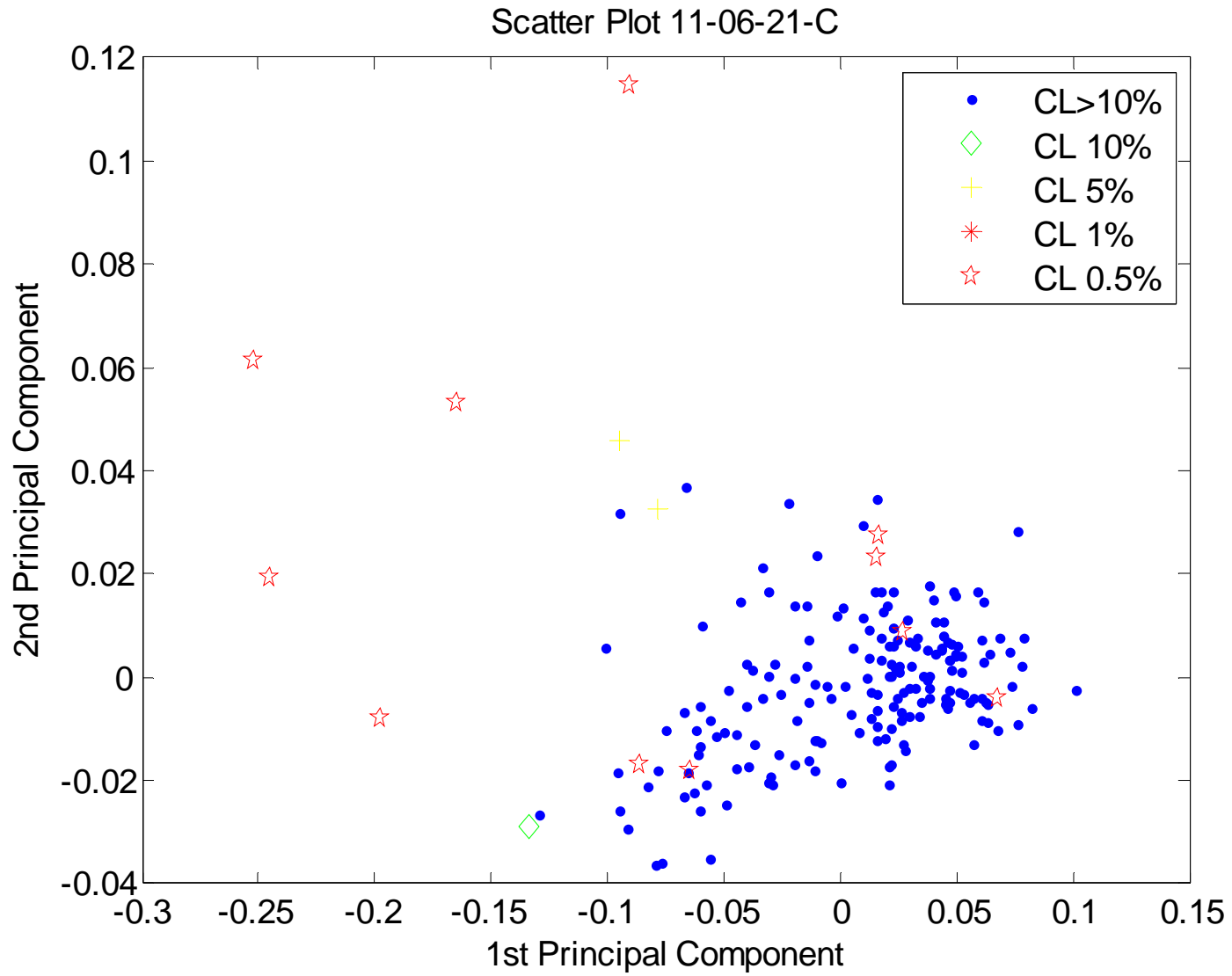
Principal Component Analysis 2-D Scatter Plot for project #4: 11-20



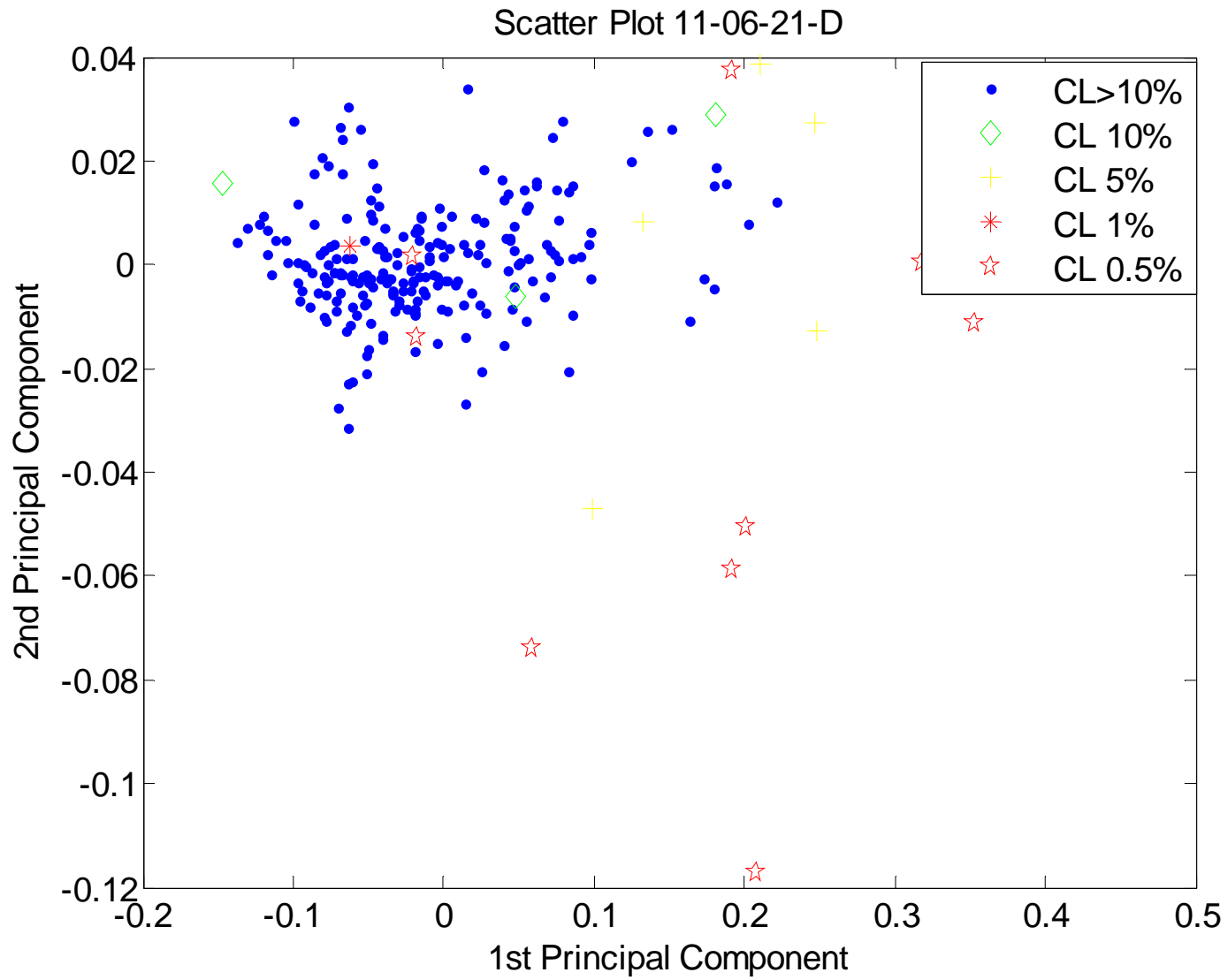
Principal Component Analysis 2-D Scatter Plot for project #5a: 11-21A



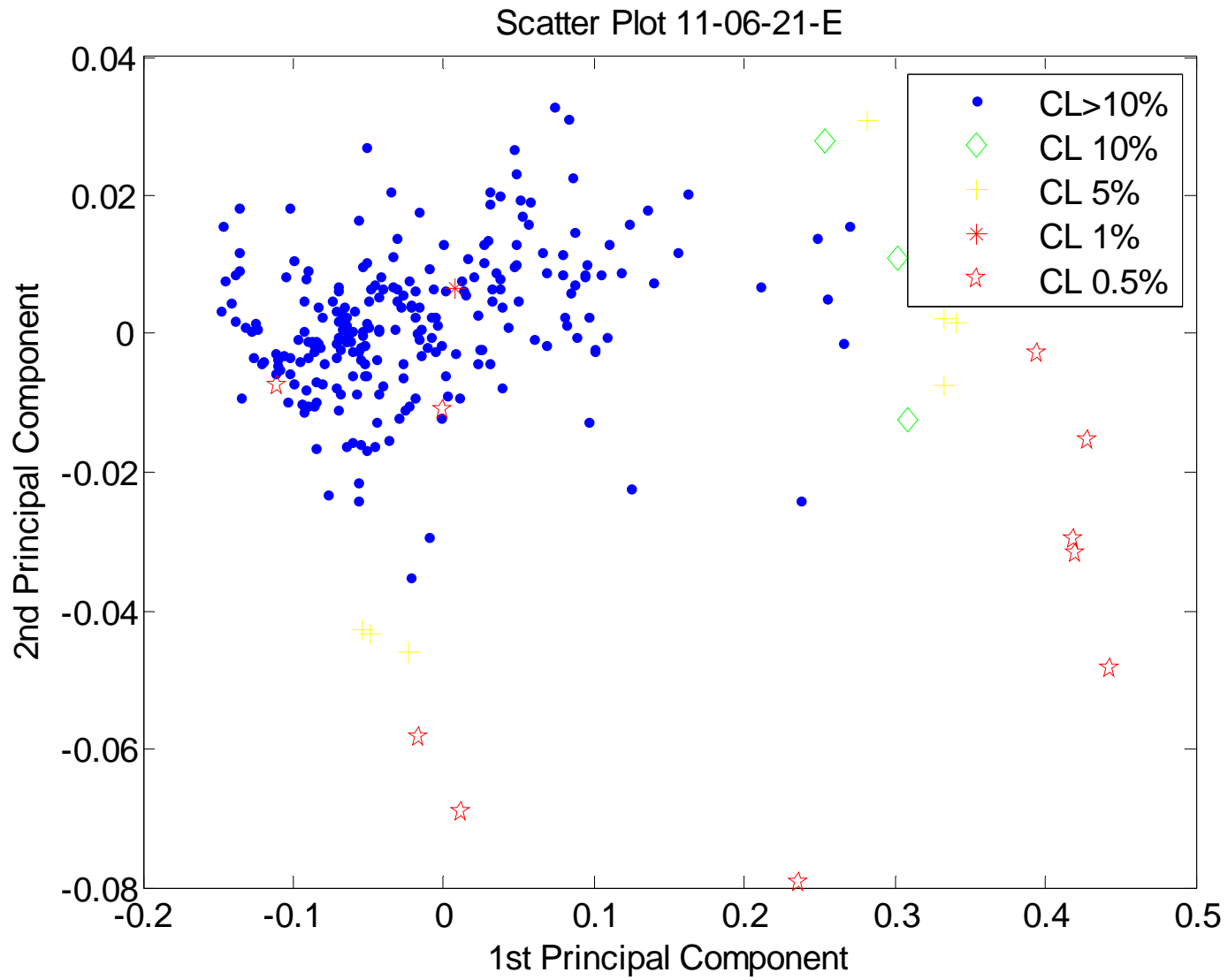
Principal Component Analysis 2-D Scatter Plot for project #5b: 11-21B



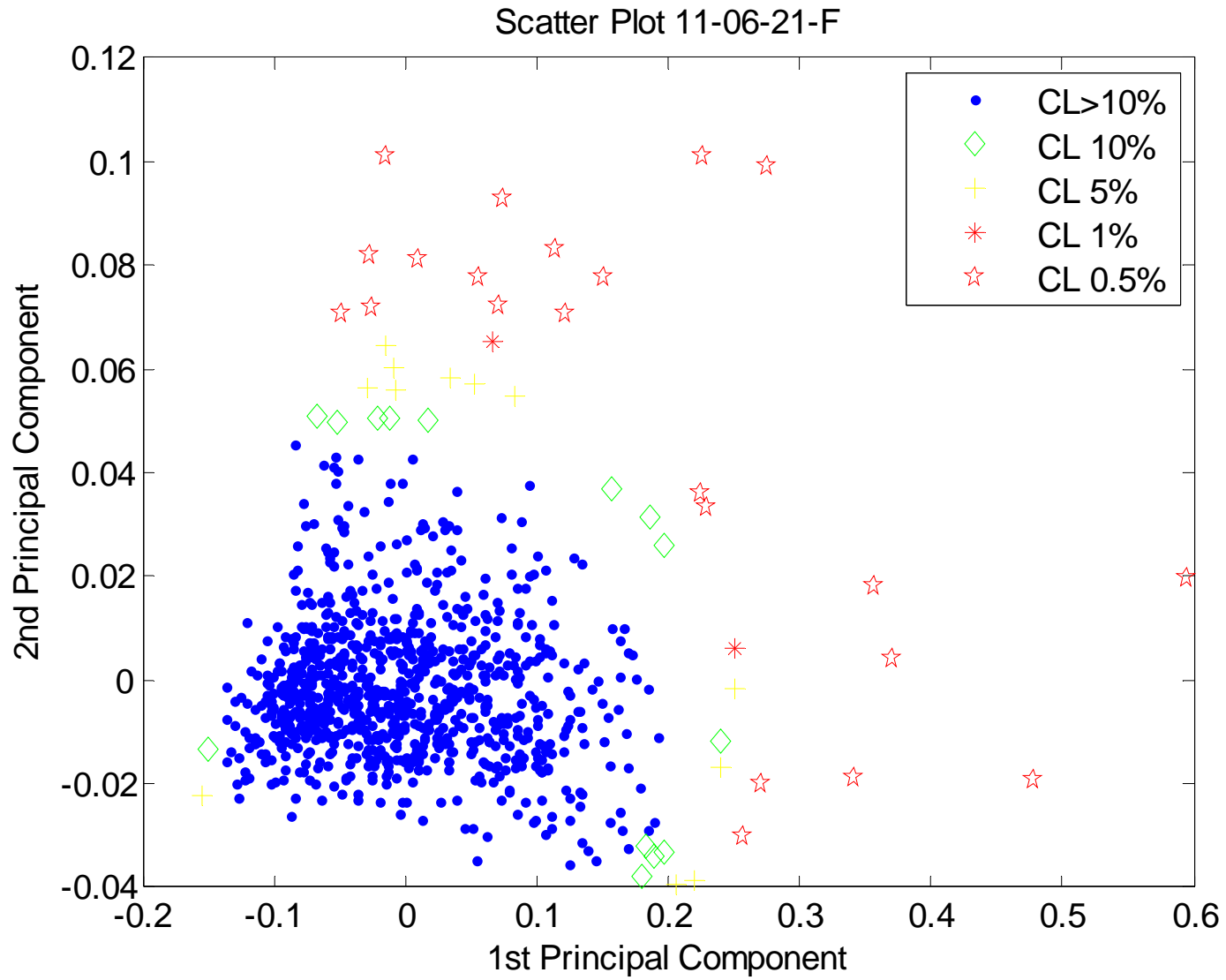
Principal Component Analysis 2-D Scatter Plot for project #5c: 11-21C



Principal Component Analysis 2-D Scatter Plot for project #5d: 11-21D

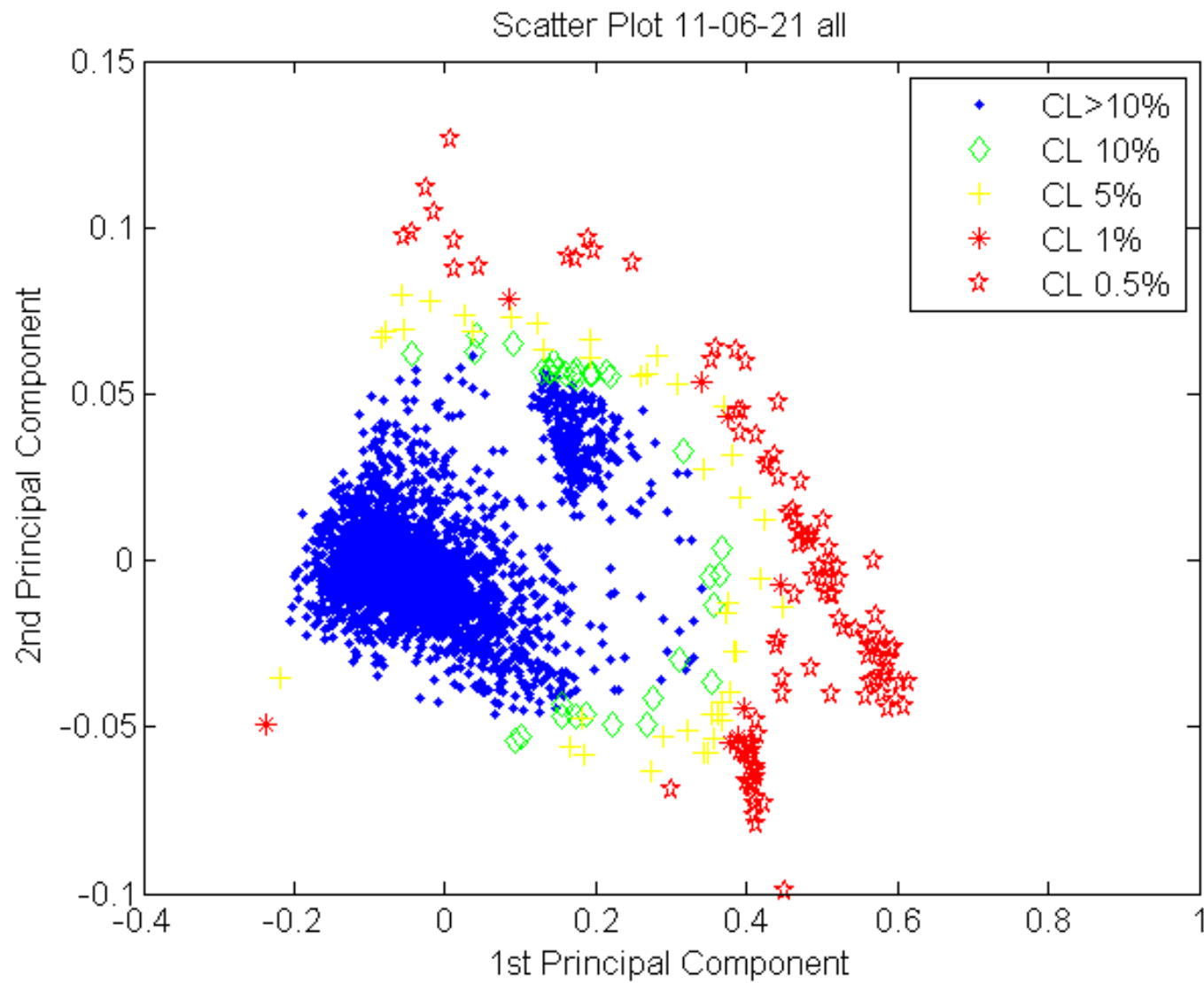


Principal Component Analysis 2-D Scatter Plot for project #5e: 11-21E

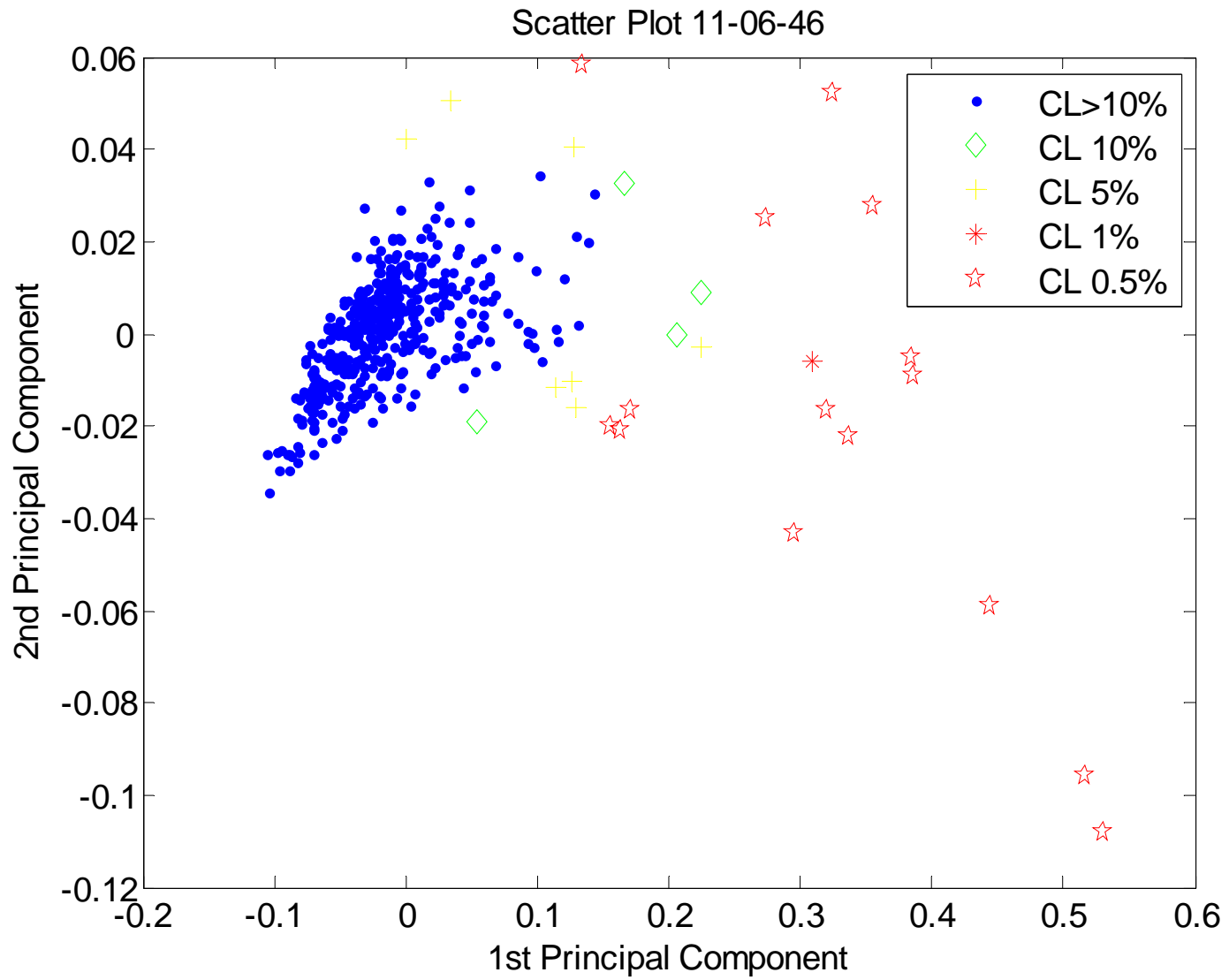


Principal Component Analysis 2-D Scatter Plot for project #5f: 11-21F

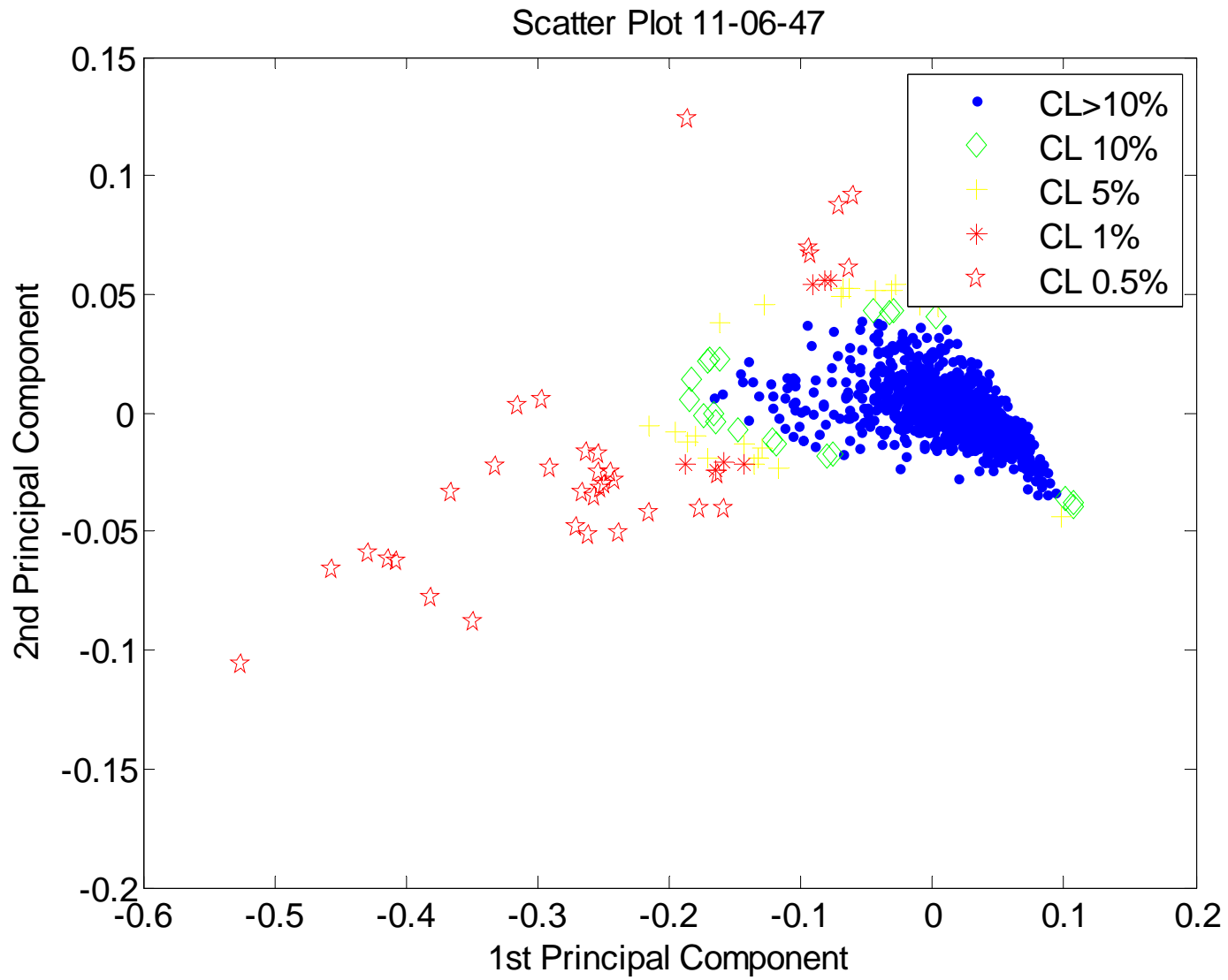




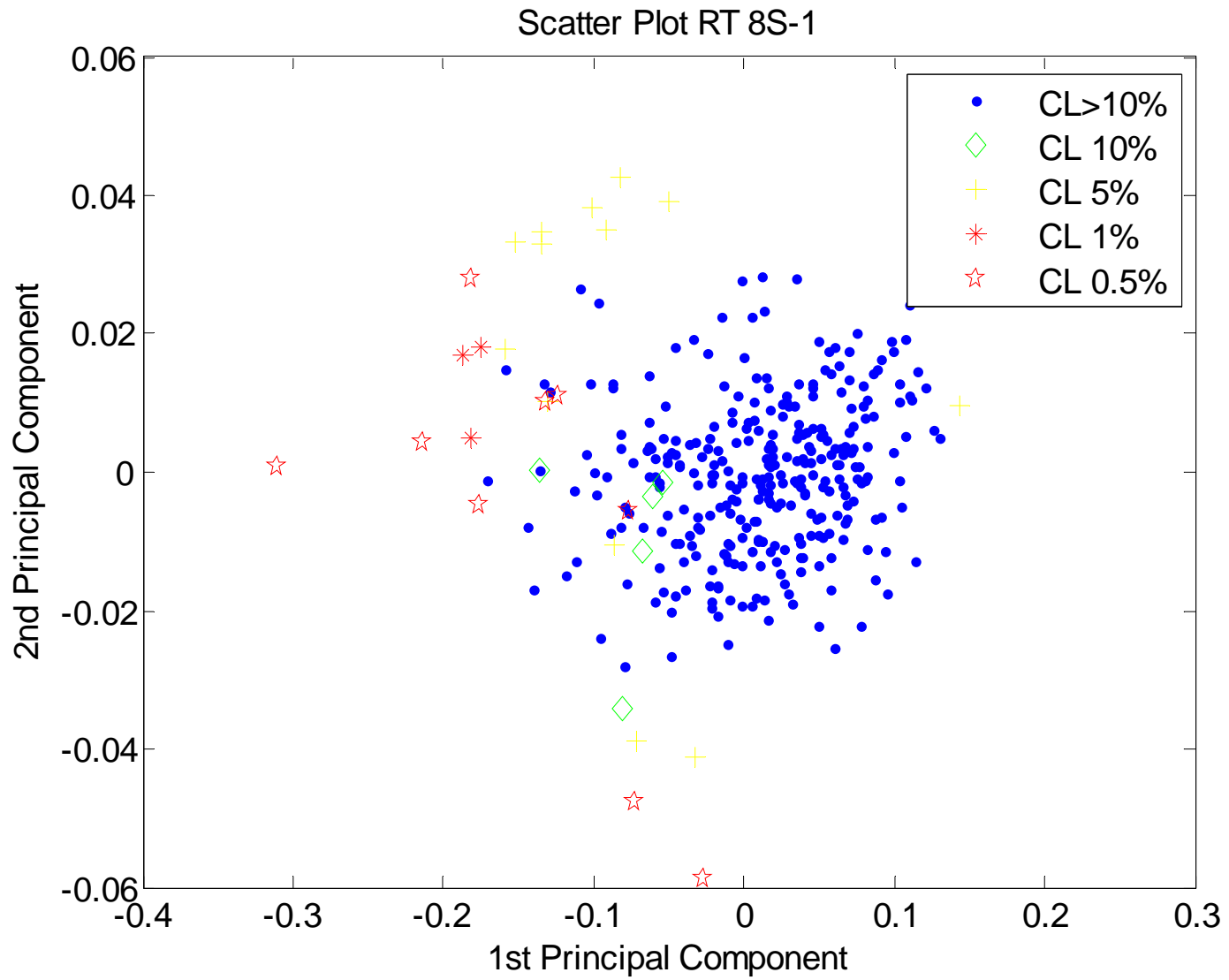
Principal Component Analysis 2-D Scatter Plot for project #5all: 11-21 all



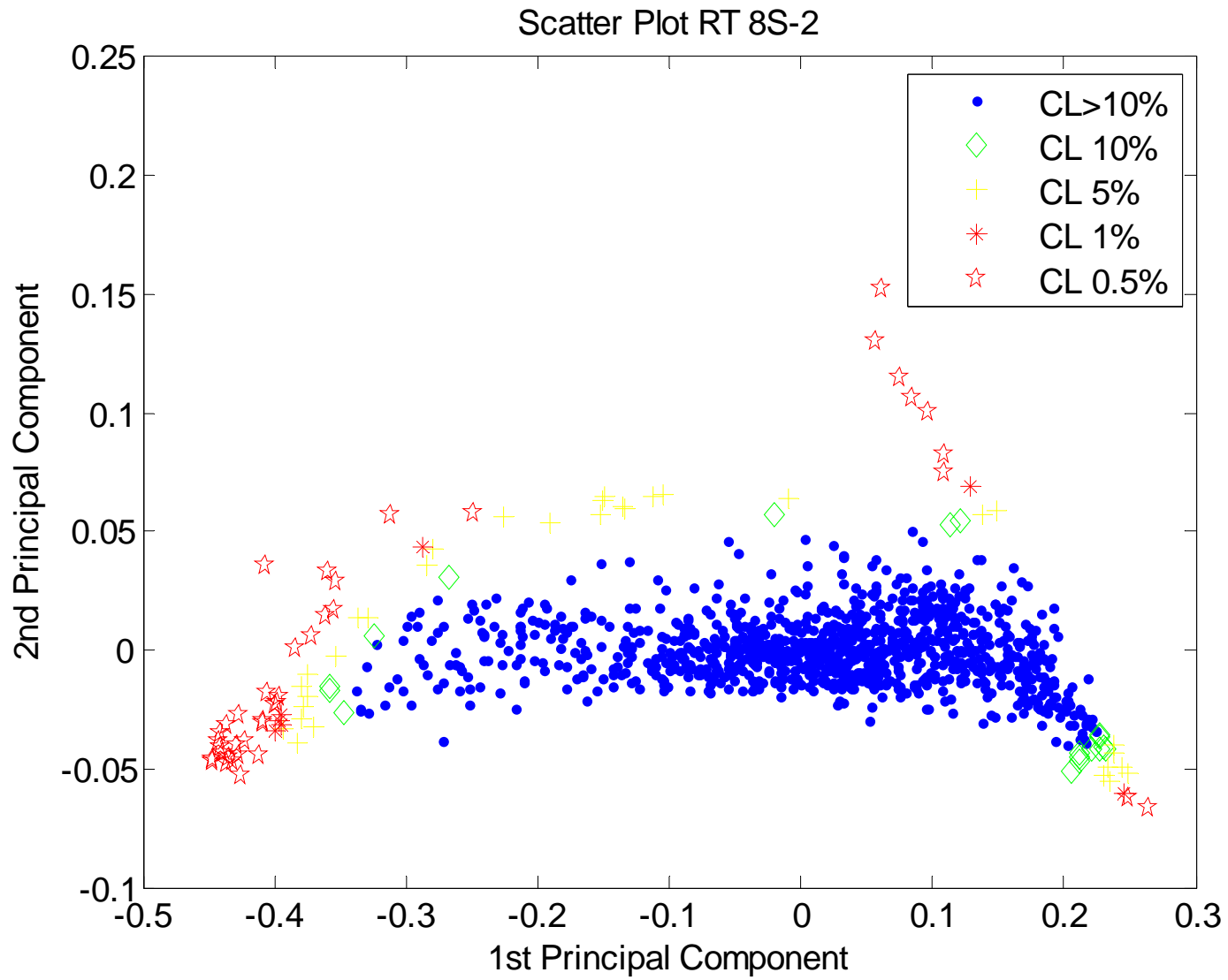
Principal Component Analysis 2-D Scatter Plot for project #6: 11-46



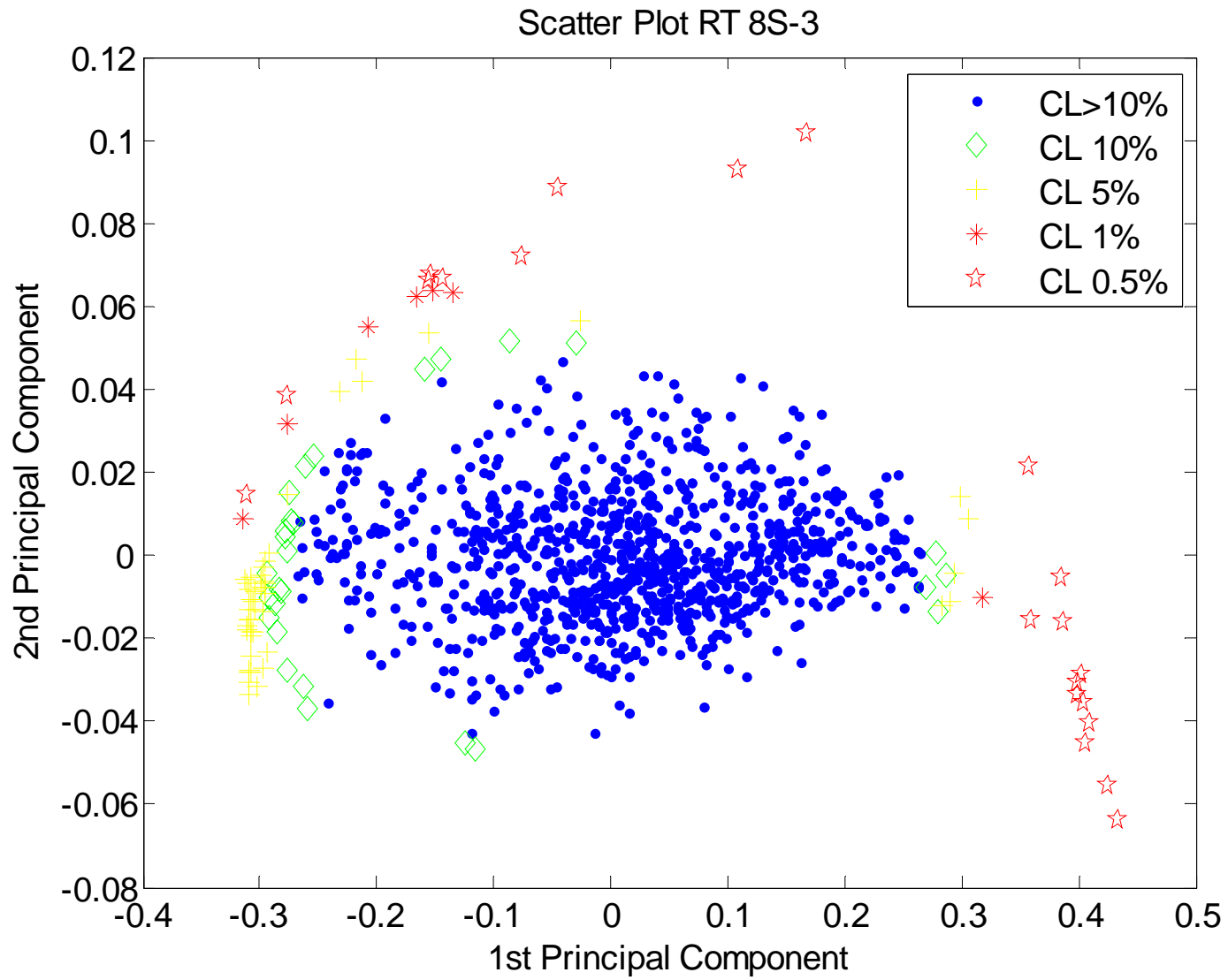
Principal Component Analysis 2-D Scatter Plot for project #7: 11-47



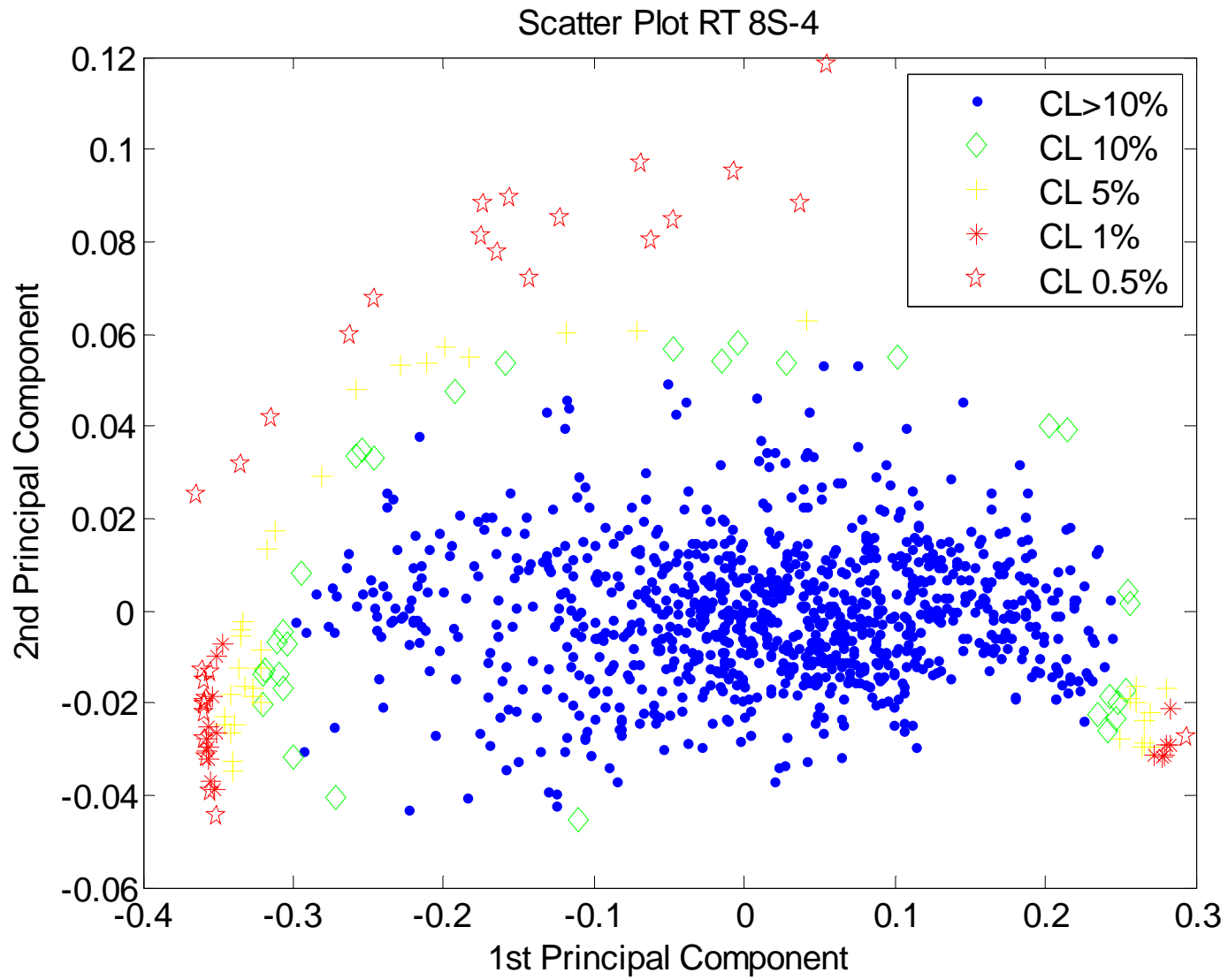
Principal Component Analysis 2-D Scatter Plot for project #8a: RT 8S-1



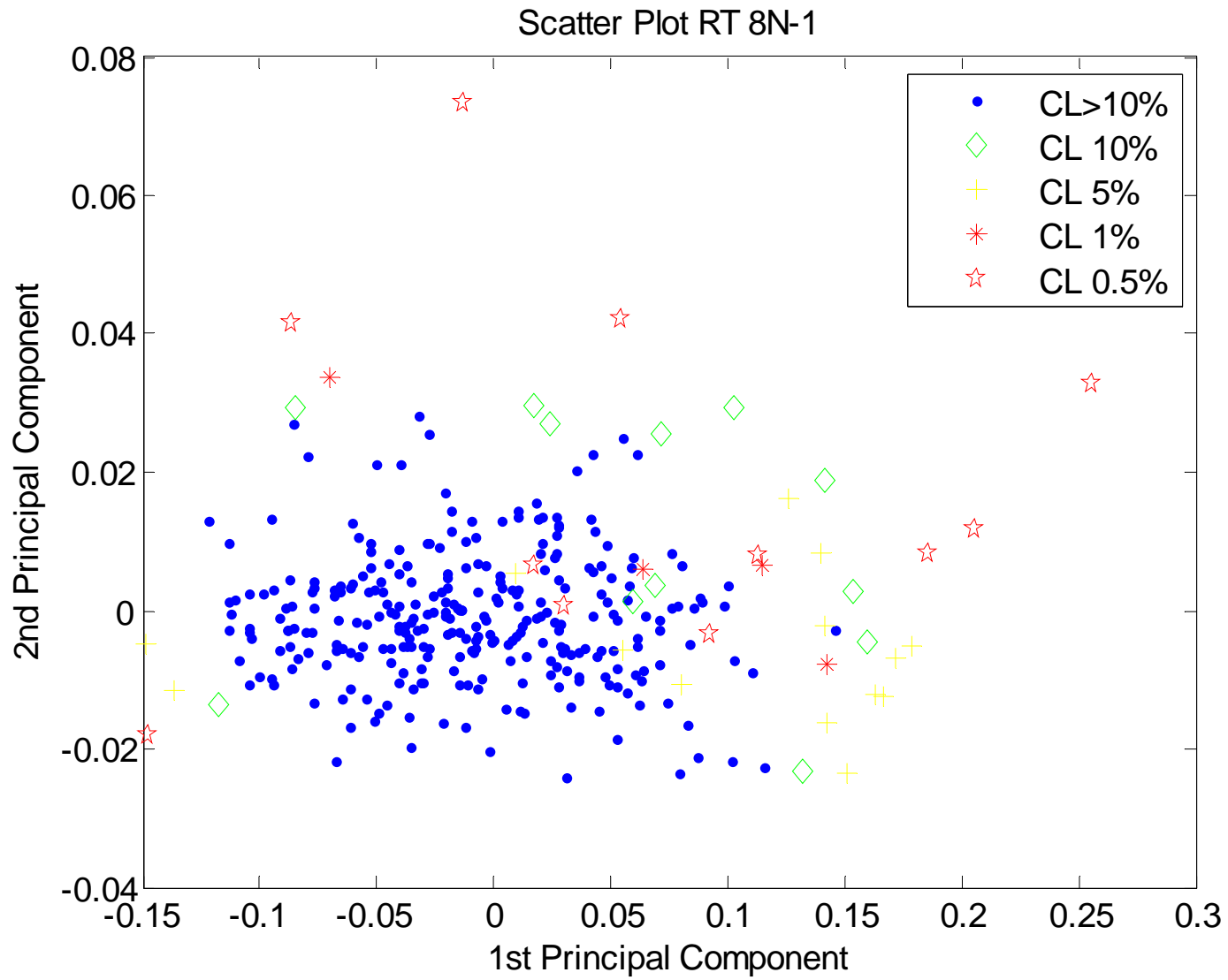
Principal Component Analysis 2-D Scatter Plot for project #8b: RT 8S-2



Principal Component Analysis 2-D Scatter Plot for project #8c: RT 8S-3

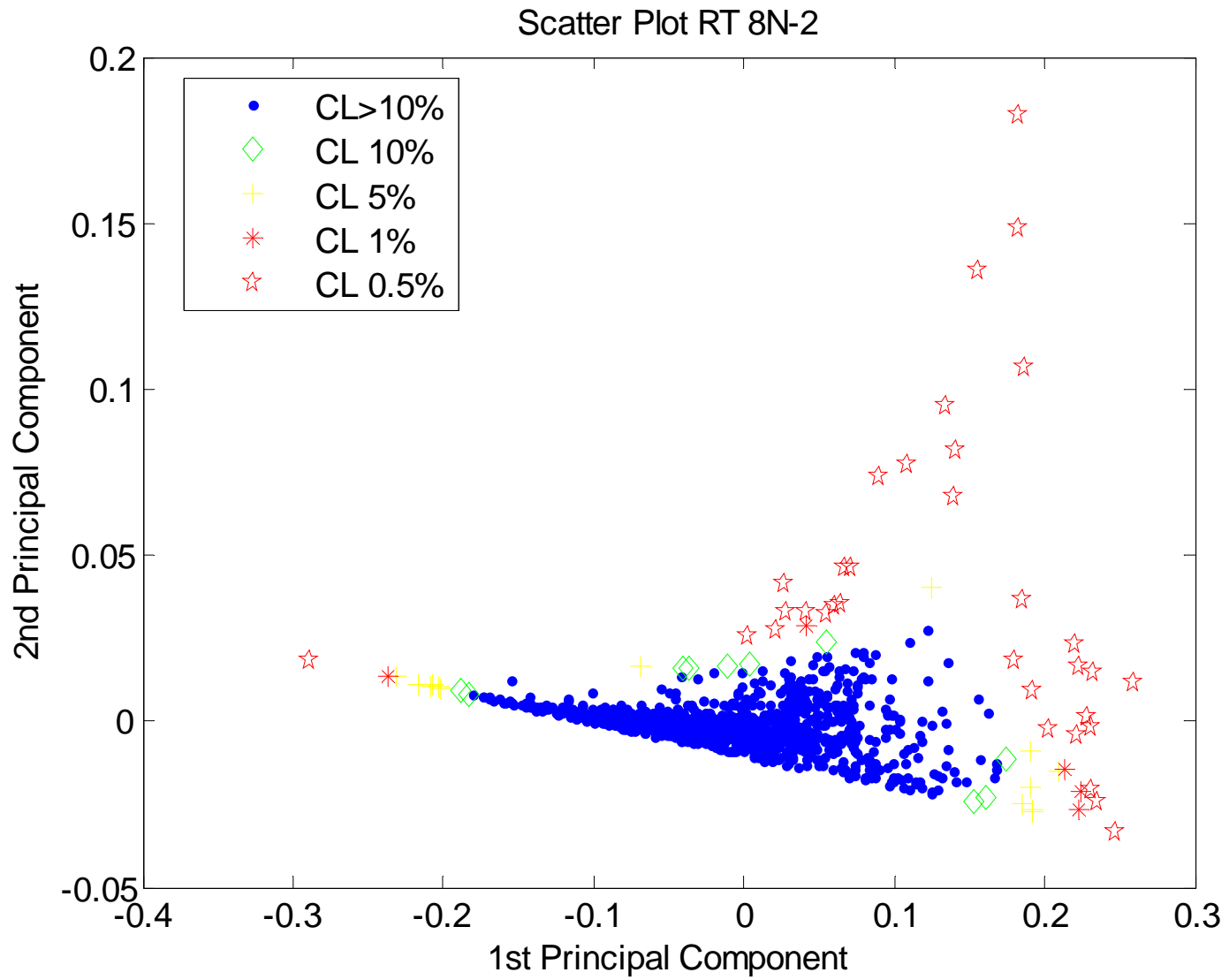


Principal Component Analysis 2-D Scatter Plot for project #8d: RT 8S-4

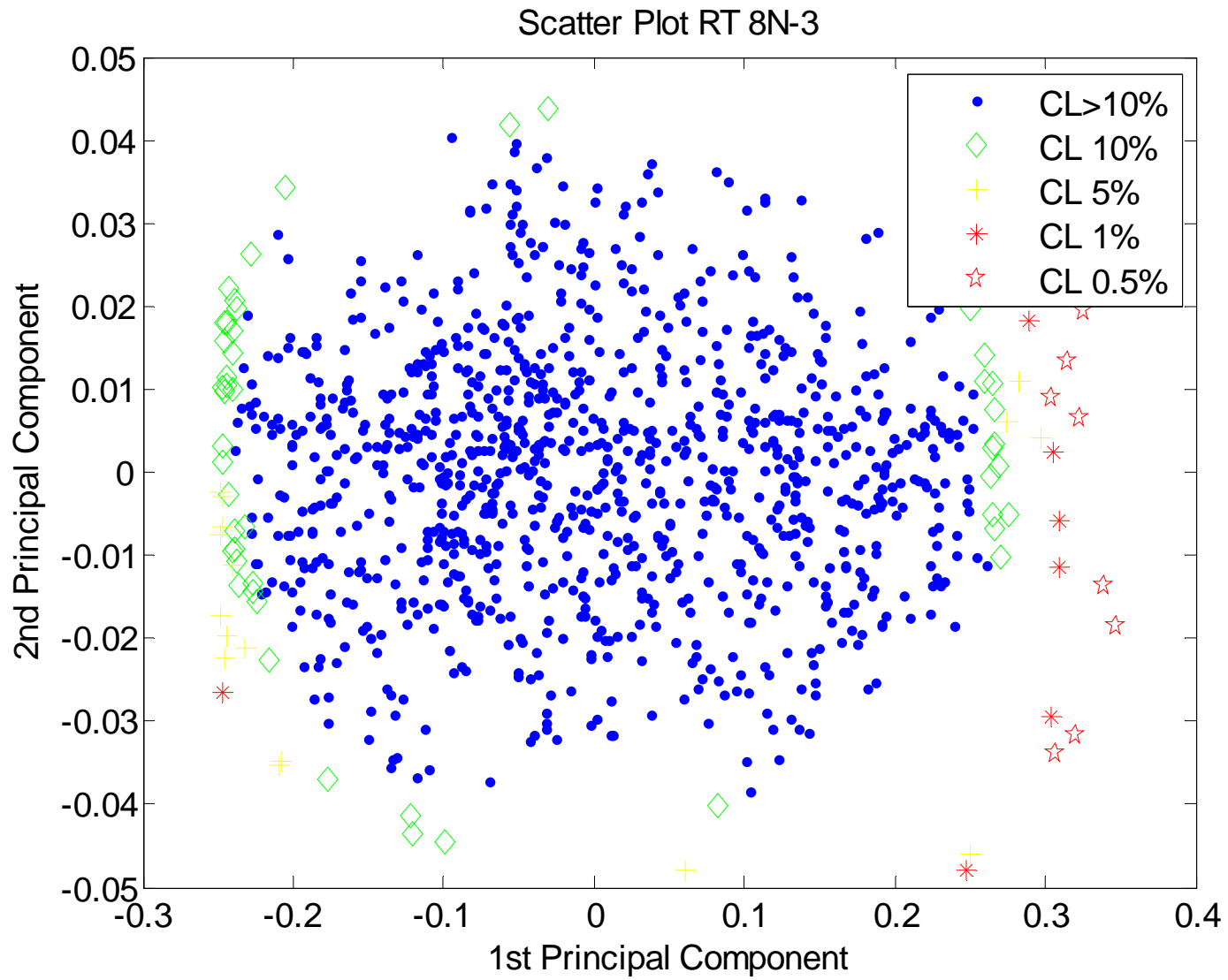


Principal Component Analysis 2-D Scatter Plot for project #9a: RT 8N-1

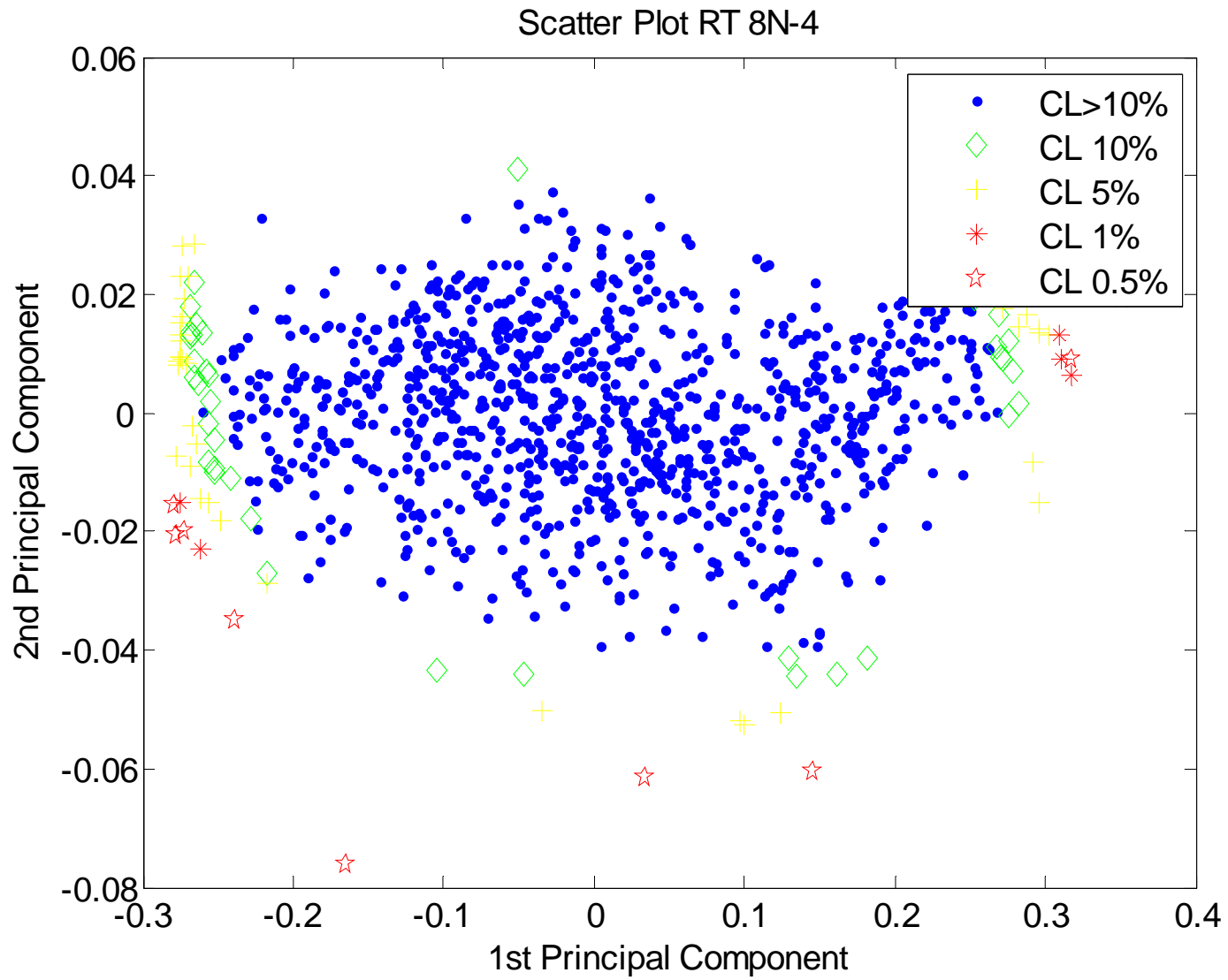




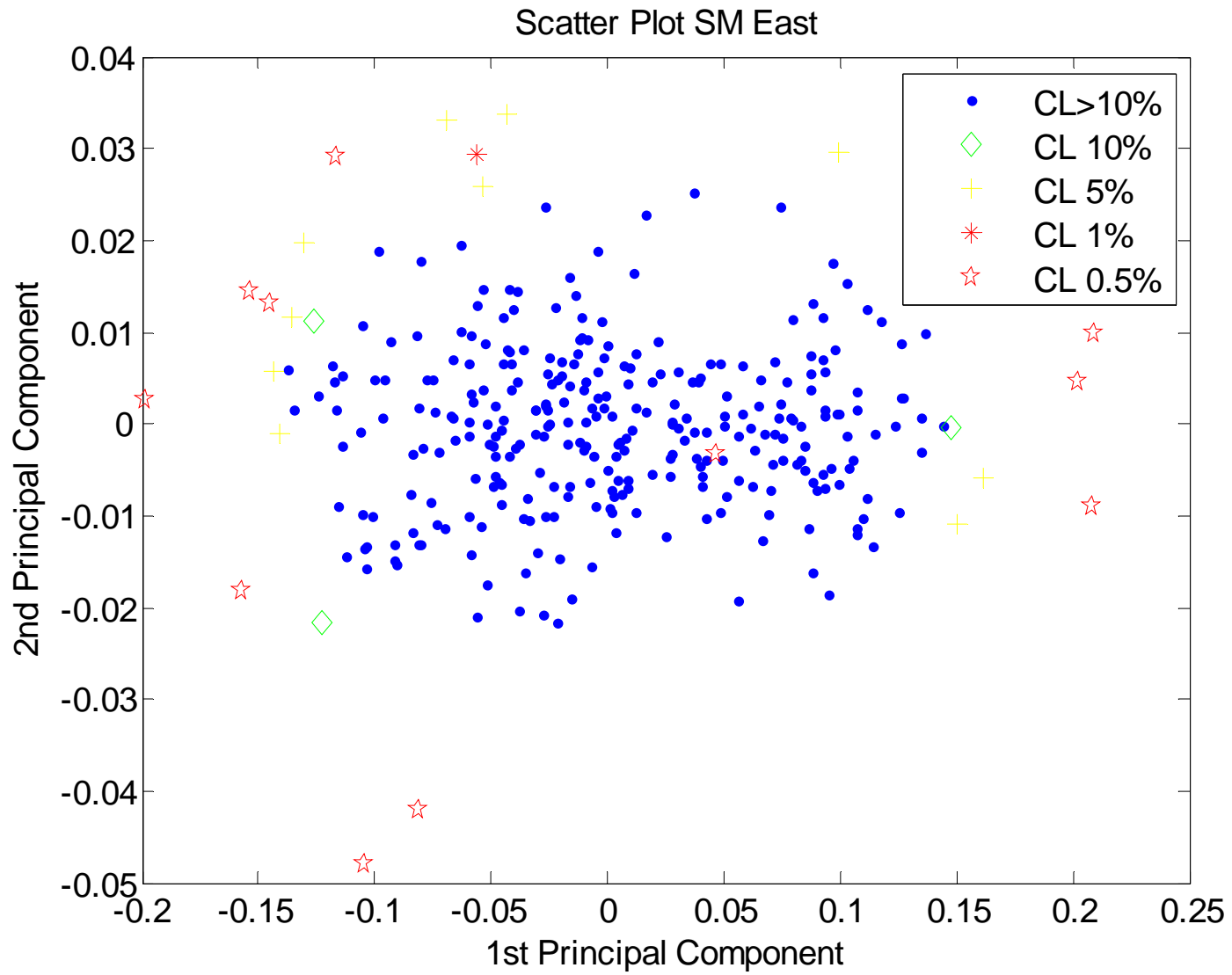
Principal Component Analysis 2-D Scatter Plot for project #9b: RT 8N-2



Principal Component Analysis 2-D Scatter Plot for project #9c: RT 8N-3

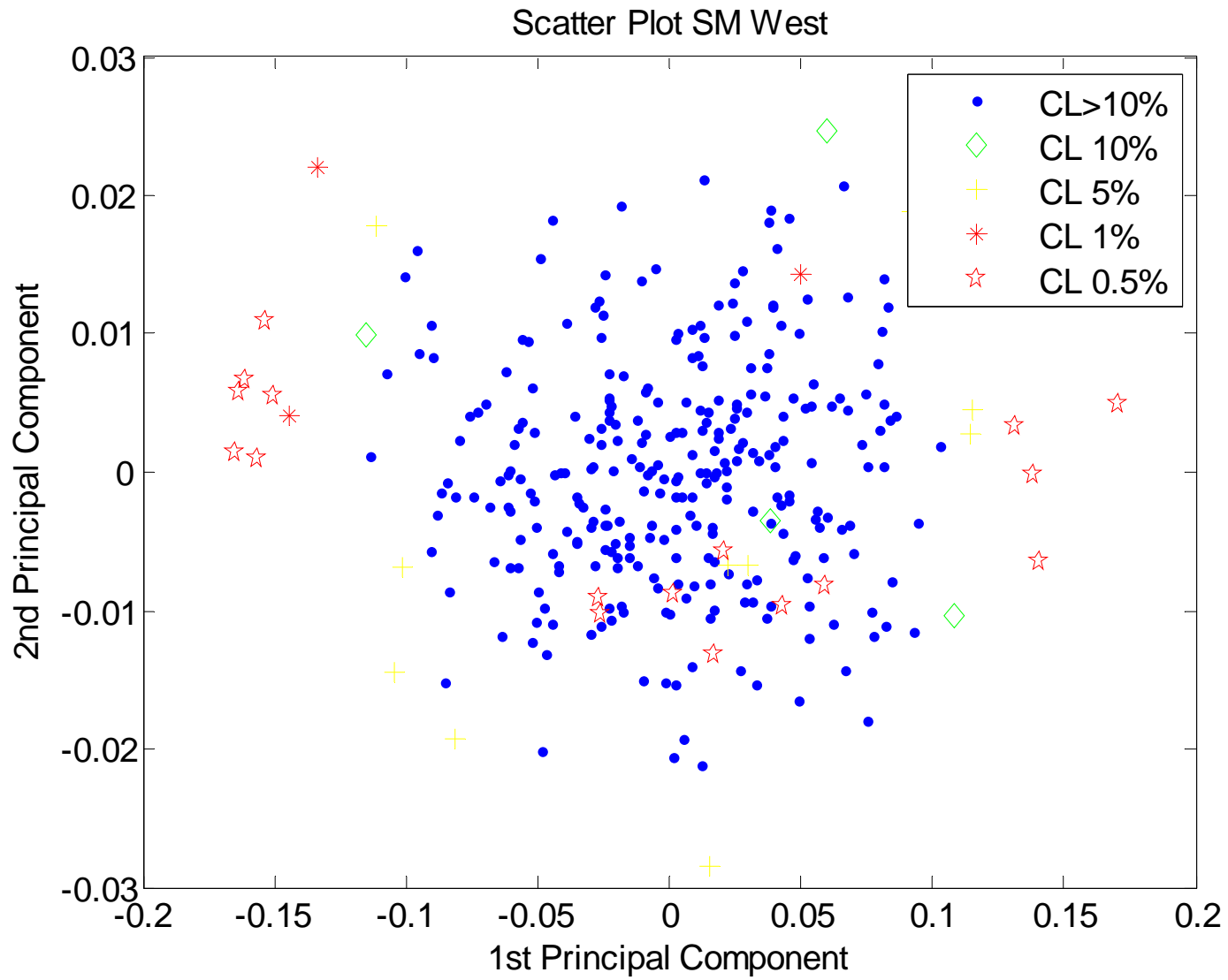


Principal Component Analysis 2-D Scatter Plot for project #9d: RT 8N-4

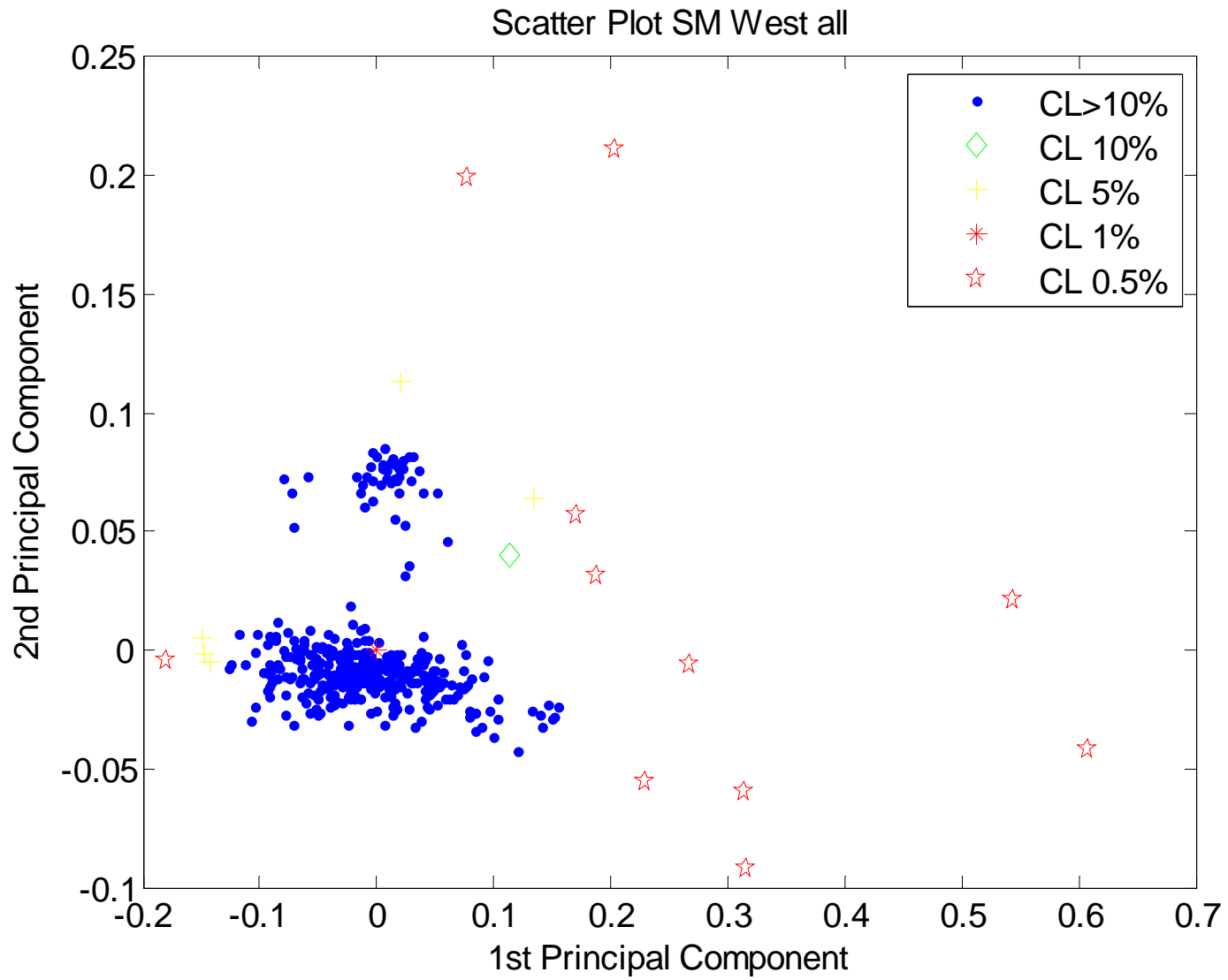


Principal Component Analysis 2-D Scatter Plot for project #10a: SM E

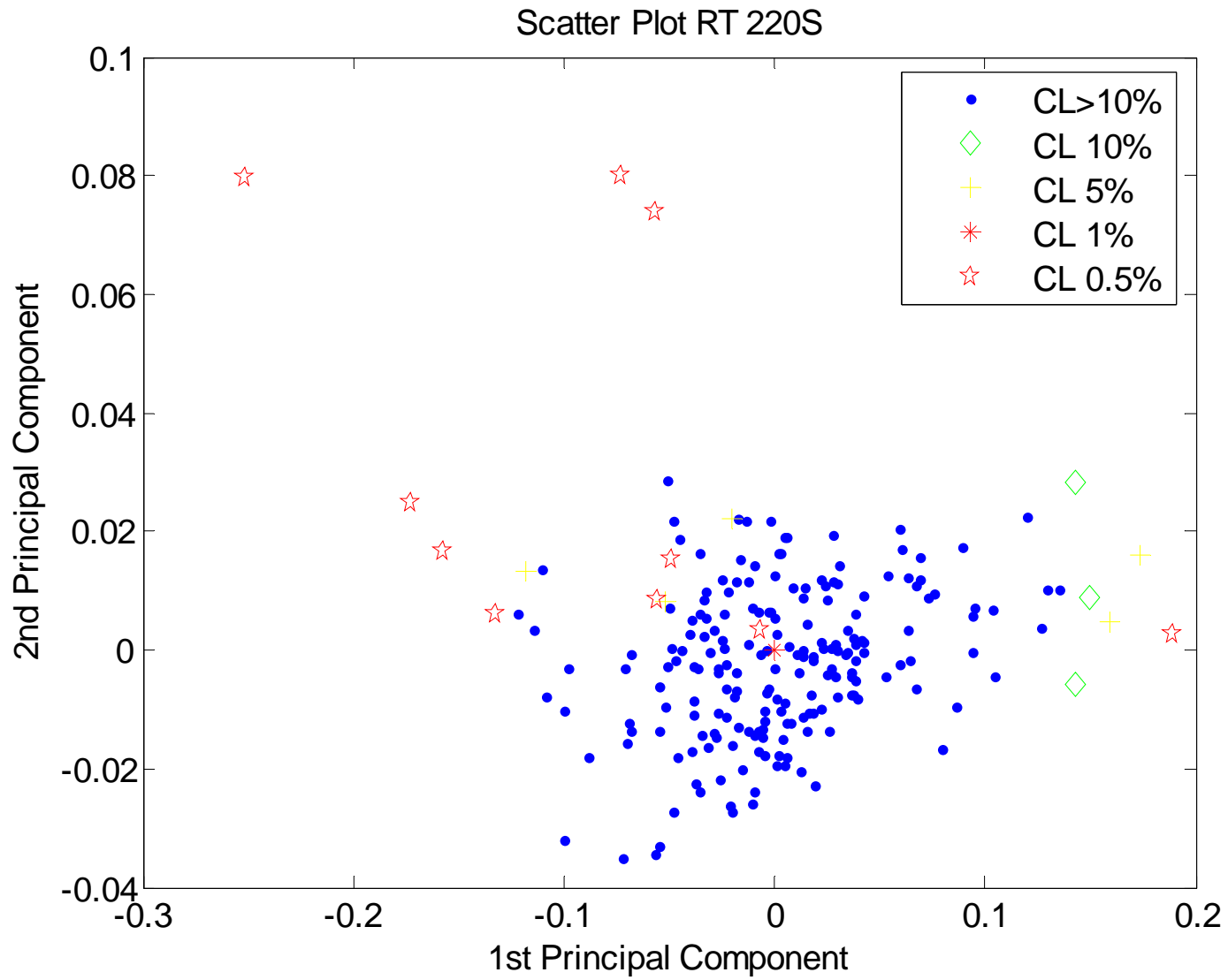




Principal Component Analysis 2-D Scatter Plot for project #11a: SM W

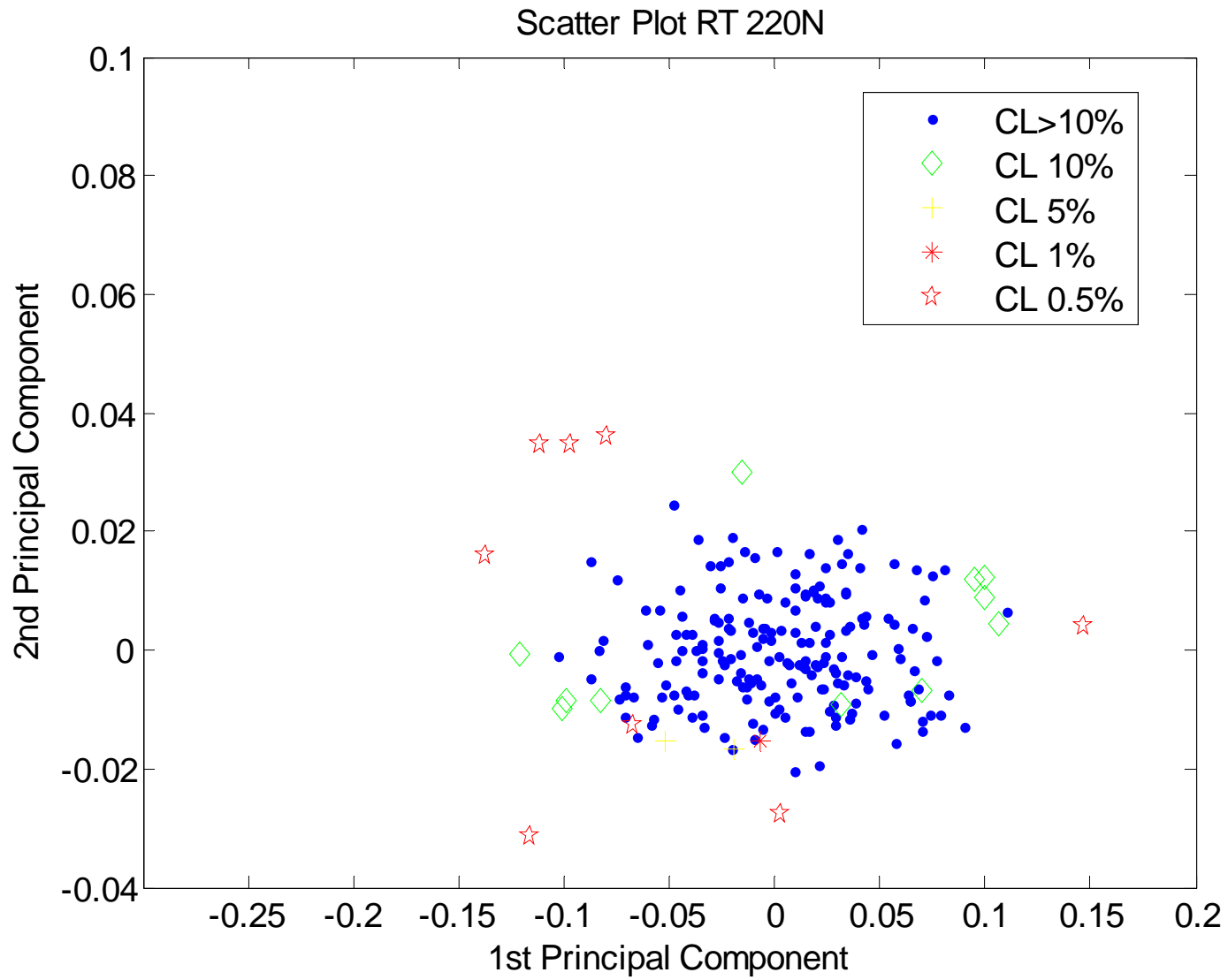


Principal Component Analysis 2-D Scatter Plot for project #11b: SM W all



Principal Component Analysis 2-D Scatter Plot for project #12: RT 220S





Principal Component Analysis 2-D Scatter Plot for project #13: RT 220N